



# Engineering and Optimisation of Mini-dystrophin Constructs for Duchenne Muscular Dystrophy Gene Therapy

**Mojgan Reza**

Thesis submitted for the degree of Doctor of Philosophy

Newcastle University

Faculty of Medical Sciences

Institute of Genetic Medicine

November 2014

## **Abstract**

Muscular dystrophies (MDs) are inherited disorders characterised by muscle weakness and atrophy. One of the most severe forms is Duchenne muscular dystrophy (DMD) which together with the milder allelic form Becker muscular dystrophy (BMD) are known as the dystrophinopathies and result from defects in the X-linked gene encoding dystrophin. Dystrophin is a structural protein of the muscle that connects the internal cytoskeleton of muscle fibres to the extracellular matrix. DMD is also amongst the most common forms of muscular dystrophy, affecting ~1 in 4000 live male birth and manifests as rapidly progressive muscle degeneration leading to loss of ambulation and death in the second or third decade from respiratory or cardiac failure. Currently, there is no cure for this devastating disease. Clinical management of symptoms and complications is limited to stabilising the condition, slowing deterioration over time and palliative care. Since discovery of the DMD gene in 1986, researchers have dedicated substantial effort into vector technologies, facilitating the use of gene therapy to reintroduce a functional copy of the dystrophin gene into muscle fibres, a potential approach to treat DMD patients. However, this approach poses additional challenges relative to many gene therapy approaches since the full-length dystrophin cDNA is ~14 kb, exceeding the packaging capacity of most viral vectors. A number of large internal in-frame dystrophin deletions have been identified in patients that produce a relatively mild phenotype with later age of onset and a slower rate of disease progression than classical DMD. This observation has inspired the construction of internally truncated, but largely functional versions of dystrophin suitable for gene transfer using viral vectors. So far the most widely used miniaturised dystrophin transgenes have been tested in AAV-mediated gene delivery which has identified several limitations indicating the use of more favourable transgenes that have smaller deletions, yet carrying more functional parts of dystrophin. In this study human mini-dystrophin constructs of 4.3-7.7 kb in size were designed that retain key functional elements of dystrophin molecule and their relative functionality investigated in mdx mice. The ultimate aim of this study is the characterisation and optimisation of these mini-dystrophin constructs for gene delivery studies via viral vectors as a therapeutic tool for treatment of Duchenne muscular dystrophy.

*“Our aspirations are our possibilities”*

Samuel Johnson (1709-1784)

***Dedicated to Duchenne patients and their families***

## **Acknowledgements**

I would like to express my deepest appreciation to my supervisors Professor Hanns Lochmüller and Dr Steve Laval for their expert guidance, supervision, generosity in sharing their scientific knowledge and for helping me to develop my academic career. I am unutterably grateful to Hanns for giving me this precious opportunity to carry out this demanding and interesting study. My special gratitude is dedicated to Steve for his everyday approachability to answer questions and particularly his thoughtful suggestions, while proof reading this thesis. I would also like to thank all my colleagues in the muscle group, especially Dan Cox for always being a real team worker; without his help in the Biobank, this work would not have been accomplished. Thanks to Morten Ritso for his steady helpfulness whenever it is needed, Jon Ingledew for his support with lentiviral work, Elizabeth Greally for her hard work maintaining the animal supply, Dr Alison Blain and Dr Rita Barresi for all useful discussions and sharing their expertise, Stephanie Carr for her aid with one of the constructs and to everyone else in the team who make our everyday work life so pleasant. I am grateful for collaboration with Professor Francesco Muntoni, Professor Jenny Morgan and their team for all motivating discussions and input during this study. I am indescribably thankful to my parents, brother, sisters, nieces, nephews and the rest of my family all over the world for their love throughout my life and for always being there for me despite the difficult, unusual and bizarre circumstances in our life. I am especially grateful to my beloved father who always believed in me and who I am missing so much. My special appreciation and thanks is given to Homayun for always being a supportive friend, in spite of hard times that we went through together. I would also like to thank my life time friends back home in Germany who have always been as loving as my own family, especially Erika and Hubert. Immeasurable thanks to Missagh, Sulamita, Robin and Daniel, the source of my love, hope and happiness, for filling my life with joy and for making me such a blessed and lucky mum. I am deeply grateful to the clinical staff at the Queen Elizabeth Hospital who have been taking care of my dearest Robin, for helping him to hopefully cure and come back home soon, for giving me trust and faith which enabled me to complete this thesis. And finally, boundless thanks to Ralf for his continuous encouragement to carry out this study and for supporting me with his profound knowledge throughout this project. For always standing by my side in happiness und during difficult times; for giving me abundant love and inspiration in every moment of my life, despite hundreds miles distance between us.

## Declaration

I, Mojgan Reza declare that the presented work in this thesis is a result of my own original research. I confirm that the work done by others is clearly acknowledged and any published work is clearly attributed and the source is always given. I certify that this thesis contain no material that has been submitted for any other academic degree and has not been published previously before submission.

## Selected Publications

Deficiency of the exosomal core protein EXOSC8 disrupts mRNA metabolism and results in severe infantile leukodystrophy.

Veronika Boczonadi, [...] **Mojgan Reza**, [...] et al. JCI: **2014** 75270-RG -1

Mutation of the human mitochondrial phenylalanine-tRNA synthetase causes infantile-onset epilepsy and cytochrome c oxidase deficiency.

Abdulraheem Almalki, [...] **Mojgan Reza**, [...] et al. Biochim Biophys Acta. **2014** Jan; 1842(1):56-64.

Mitochondrial DNA deletions in muscle satellite cells: implications for therapies.

Sally Spendiff, **Mojgan Reza**, [...] et al. Hum Mol Genet. **2013** Dec 1; 22(23):4739-47.

Two new protocols to enhance the production and isolation of human induced pluripotent stem cell lines.

Dick E, [...], **Reza M** [...] et al. Stem Cell Res. **2011** Mar; 6(2):158-67.

## Table of Contents

Abstract.....	i
Dedication.....	ii
Acknowledgments.....	iii
Declaration.....	iv
Selected Publications.....	iv
List of Tables .....	ix
List of Figures.....	x
List of Abbreviations.....	xii
<b>Chapter 1 Introduction.....</b>	<b>1</b>
1.1 Skeletal muscle structure and function .....	1
1.2 The dystrophin-associated glycoprotein complex (DGC) .....	4
1.3 Muscular dystrophy.....	5
1.3.1 Dystrophinopathies.....	7
1.4 Dystrophin gene ( <i>DMD</i> ) and protein .....	9
1.4.1 Chromosomal organisation, protein isoforms and tissue distribution of dystrophin .....	9
1.4.2 Protein structure and domain composition of muscle specific dystrophin protein (Dp427m).....	11
1.4.3 Mutations in muscle specific dystrophin Dp427m .....	12
1.5 Animal models of DMD .....	13
1.6 Therapeutic approaches for DMD.....	15
1.6.1 Non-viral gene transfer.....	15
1.6.2 Upregulation of a dystrophin-related protein or other genes.....	16
1.6.3 Cell-based therapy .....	16
1.6.4 Stop codon readthrough (small molecule therapy) .....	17
1.6.5 Exon skipping .....	18
1.6.6 Viral vector-mediated gene therapy .....	19
1.6.7 Mini- and micro-dystrophin functional domains.....	20
1.6.8 Clinical trials and current status of DMD gene transfer therapy.....	24
1.7 Statement of aims .....	25
<b>Chapter 2 Materials and Methods.....</b>	<b>26</b>
2.1 Standard molecular biology techniques .....	26
2.1.1 Polymerase chain reaction (PCR).....	26
2.1.2 Agarose gel electrophoresis.....	26
2.1.3 DNA purification by gel extraction .....	27
2.1.4 Digestion of DNA using restriction endonucleases .....	27
2.1.5 DNA measurement.....	27

2.1.6	PCR or restriction digest purification .....	27
2.1.7	DNA sequencing.....	27
2.2	Splicing by overlap extension polymerase chain reaction (SOE-PCR) .....	28
2.3	Cloning .....	29
2.3.1	Ligation .....	29
2.3.2	Transformation into chemically competent E. coli cells.....	29
2.3.3	Purification of plasmid DNA.....	29
2.4	Cell culture .....	30
2.4.1	Cells.....	30
2.4.2	Cell expansion .....	30
2.4.3	Standard cell culture conditions for immorto myoblasts.....	31
2.4.4	Immorto myoblast differentiation into myotubes.....	31
2.4.5	Thawing and recovery of frozen cells.....	31
2.4.6	Freezing of living cells for long-term storage .....	32
2.4.7	Cell counting.....	32
2.4.8	E6E7 expressing retrovirus supernatant production .....	33
2.4.9	Establishment of an immortalised human DMD cell line.....	33
2.4.10	Enrichment of myoblasts in culture .....	33
2.4.11	Cell transfection using lipofection .....	34
2.4.12	Cell transfection using electroporation.....	34
2.4.13	Harvesting cells.....	34
2.4.14	Stable transfection of mdx-immorto myoblasts .....	35
2.4.15	Cells and G418 titration .....	35
2.5	Protein electrophoresis and Western blotting .....	36
2.6	Immunofluorescence and histology .....	37
2.6.1	Cryosectioning of muscle tissue.....	37
2.6.2	Haematoxylin-Eosin (H&E) staining .....	37
2.6.3	Immunofluorescent labelling of cultured cells .....	38
2.6.4	Immunofluorescence labelling of muscle tissue.....	38
2.6.5	Direct antibody labelling for immunofluorescence.....	39
2.6.6	Production of VSV-G lentivirus.....	39
2.7	Image analysis .....	40
2.7.1	Morphometric parameters .....	40
2.7.2	Fluorescence intensity quantification .....	40
2.8	Image analysis .....	40
2.9	<i>In vivo</i> experiments .....	41
2.9.1	Animal care and husbandry.....	41
2.9.2	<i>In vivo</i> electroporation .....	41
2.10	Computational analysis.....	42

2.10.1	Primer design .....	42
2.10.2	Sequence alignments .....	42
2.10.3	BLAST searches .....	42
2.10.4	Cloning analysis using PlasmaDNA.....	42
2.10.5	Image composite editor.....	42
2.10.6	ImageJ .....	43
2.10.7	Statistics.....	43
<b>Chapter 3 Design, construction and characterisation of mini-dystrophin constructs..</b>		<b>46</b>
3.1	Introduction .....	46
3.2	Aims .....	47
3.3	Characterisation of a human full-length dystrophin plasmid as the initial clone .....	48
3.3.1	Restriction analysis of full-length dystrophin clones.....	48
3.3.2	Amplification of the complete dystrophin coding sequence .....	49
3.3.3	Primer walking and sequencing of clone 5.....	50
3.4	Construction of mini-dystrophin constructs .....	52
3.4.1	Rational definition of mini-dystrophins .....	52
3.4.2	Construction of mini-dystrophin C2/ $\Delta$ H2-R19 .....	54
3.4.3	SOE-PCR of mini-dystrophin C2/ $\Delta$ H2-R19 .....	55
3.4.4	Introducing SOE-PCR product into pRSVDysFL .....	56
3.5	Characterisation of the mini-dystrophin constructs.....	57
3.5.1	Verification of the C2/ $\Delta$ H2-R19 insert and vector by digestion .....	57
3.5.2	Verification of the deletion in C2/ $\Delta$ H2-R19 by PCR .....	58
3.5.3	Verification of the insert C2/ $\Delta$ H2-R19 and sequencing results .....	59
3.5.4	Verification of the reading frame of C2/ $\Delta$ H2-R19.....	60
3.5.5	Subcloning of C2/ $\Delta$ H2-R19 into expression vector pCMV-Tag2 .....	61
3.5.6	Summary of C1/ $\Delta$ R3-R13 construction and characterisation .....	63
3.5.7	Summary of C7/ $\Delta$ H2-R23 construction and characterisation .....	65
3.5.8	Summary of C9/ $\Delta$ R1-R10 construction and characterisation .....	67
3.6	Cell transfection and protein expression of mini-dystrophin constructs.....	70
3.6.1	Transfection into HeLa cells and Western blotting.....	70
3.7	Discussion.....	71
<b>Chapter 4 <i>In vitro</i> characterisation and assessment of mini-dystrophin constructs ....</b>		<b>73</b>
4.1	Introduction .....	73
4.2	Aims .....	74
4.3	Transient transfection of mini-dystrophins and their cellular localisation.....	75
4.3.1	Stable transfection of mdx-immorto myoblasts with mini-dystrophin constructs...	76
4.3.2	Differentiation ability of stably transfected myoblasts .....	77

4.4	Establishment of an immortalised DMD human myoblast line.....	78
4.4.1	Comparison of transfection efficiency in mouse and human cell lines.....	79
4.4.2	FACS analysis of transfection in different cell lines .....	81
4.4.3	Choice of the best transfection method and transfectants .....	83
4.5	Immunofluorescence results .....	85
4.5.1	Transient transfection of DMD human myoblasts .....	85
4.6	Improving gene transfer efficiency using viral transduction .....	86
4.6.1	Introduction to design of replication incompetent lentiviral vectors .....	86
4.7	Lentiviral transduction .....	88
4.7.1	Subcloning of selected constructs into a lentiviral vector.....	88
4.7.2	Generation of lentivirus containing mini-dystrophin constructs driven by desmin promoter .....	89
4.8	Production of VSV-G lentivirus .....	93
4.9	Myoblasts transduction .....	95
4.9.1	GFP transduction and expression results .....	95
4.9.2	Staining results of DMD human myoblasts after transduction with viral particles carrying mini-dystrophins .....	95
4.10	Discussion.....	97
<b>Chapter 5</b>	<b>Expression of mini-dystrophin constructs in mdx mouse muscle .....</b>	<b>101</b>
5.1	Introduction .....	101
5.2	Aims .....	102
5.3	Intramuscular injection and electroporation of mini-dystrophins into mdx mouse muscle .....	103
5.4	Analysis of mini-dystrophin expression and localisation in electroporated mdx muscles .....	104
5.5	Analysis of dystrophin expression intensity .....	107
5.6	Correlation between dystrophin expression, internal nuclei and myofibre size .....	110
5.6.1	Evaluation of internal nuclei .....	110
5.6.2	Quantitative determination of myofibre size .....	116
5.7	Effect of mini-dystrophin constructs on DGC proteins .....	123
5.7.1	Gamma-sarcoglycan restoration .....	123
5.7.2	nNOS stabilisation at the sarcolemma .....	125
5.8	Discussion .....	127
<b>Chapter 6</b>	<b>General discussion and future directions .....</b>	<b>136</b>
<b>References</b> .....		<b>154</b>

## Appendices

Appendix A Sequences of the oligonucleotides used for cDNA synthesis and PCR.....	146
Appendix B Primers for mini-dystrophin constructs and vectors.....	147
Appendix C Antibodies used in this project.....	148
Appendix D The entire coding sequence from C2/ $\Delta$ H2-R19 as an example.....	149

## List of Tables

Table 2.1 Reagents and buffers used in this project.....	44
Table 2.2 Cell culture media used in this project.....	45
Table 3.1 Summary of the mini-dystrophin constructs.....	69
Table 5.1 Median percentage of dystrophin positive fibres and proportion of internal nuclei in electroperated muscles.....	113
Table 5.2 Descriptive statistics of muscle fibre size distribution (area) .....	120
Table 5.3 Descriptive statistics of muscle fibre size distribution (minimal Feret).....	121

## List of Figures

Figure 1.1 Structural organisation of a muscle fibre and the sarcomere .....	2
Figure 1.2 Dystrophin-associated glycoprotein complex .....	5
Figure 1.3 Genomic organisation of the dystrophin gene .....	10
Figure 1.4 Dystrophin protein (Dp427m) and its domains .....	11
Figure 2.1 Schematic of SOE-PCR principle .....	28
Figure 3.1 Restriction analysis of full-length dystrophin clones .....	48
Figure 3.2 Amplification of the complete coding sequence of full-length dystrophin by PCR ....	49
Figure 3.3 Creation of a full-length dystrophin contig .....	50
Figure 3.4 Characterisation of the full-length dystrophin (pRSVDysFL).....	51
Figure 3.5 Summary of mini-dystrophin constructs .....	53
Figure 3.6 Design of the mini-dystrophin construct C2/ $\Delta$ H2-R19 .....	54
Figure 3.7 PCR amplification of the construct C2/ $\Delta$ H2-R19 .....	55
Figure 3.8 Double digest of full-length dystrophin plasmid by <i>Cla</i> I and <i>Ngo</i> MIV and SOE-PCR fragment .....	56
Figure 3.9 Digestion of C2/ $\Delta$ H2-R19 compared to the full-length dystrophin .....	57
Figure 3.10 PCR amplification of C2/ $\Delta$ H2-R19 dystrophin fragments .....	58
Figure 3.11 Sequencing results for C2/ $\Delta$ H2-R19.....	59
Figure 3.12 Protein alignment for C2/ $\Delta$ H2-R19 .....	60
Figure 3.13 Subcloning of mini-dystrophin C2/ $\Delta$ H2-R19 into expression vector pCMV-Tag2 ...	62
Figure 3.14 Summary of construct C1/ $\Delta$ R3-R13 .....	64
Figure 3.15 Summary of construct C7/ $\Delta$ H2-R23 .....	66
Figure 3.16 Summary of construct C9/ $\Delta$ R1-R10 .....	68
Figure 3.17 Illustration of the mini-dystrophin protein expression by Western blot .....	70
Figure 4.1 Transient expression of GFP and mini-dystrophin construct C1/ $\Delta$ R3-R13 in mdx- immorto myoblasts .....	75
Figure 4.2 Transfected mini-dystrophin clones selected with G418 .....	76
Figure 4.3 Comparison of differentiation ability of stably transfected mdx-immorto cells with untreated controls .....	77
Figure 4.4 Desmin staining on immortalised DMD human cell line .....	78
Figure 4.5 Comparison of transfection efficiency in different myoblast lines .....	80
Figure 4.6 Flow cytometric results of mouse and human myoblasts transfected with a GFP control construct following Amaxa nucleofection .....	82
Figure 4.7 Comparison of transfection efficiency of several lipofection reagents with nucleofection on DMD human myoblasts in cell culture .....	84
Figure 4.8 DMD human myoblasts after transfection and staining with anti-dystrophin antibody Mandra1 .....	85
Figure 4.9 Schematic drawing of the four constructs required to build VSV-pseudotyped third generation HIV-1 derived lentiviral vectors .....	87
Figure 4.10 First cloning step for generation of lentiviral vector containing mini-dystrophin constructs driven by desmin promoter .....	89

Figure 4.11 Second cloning step for generation of lentiviral vector containing mini-dystrophin constructs driven by desmin promoter .....	90
Figure 4.12 Third cloning step for generation of lentiviral vector containing mini-dystrophin constructs driven by desmin promoter .....	91
Figure 4.13 Fourth cloning step for generation of lentiviral vector containing mini-dystrophin constructs driven by desmin promoter .....	92
Figure 4.14 Diagram of the viral production procedure .....	94
Figure 4.15 Myoblast transduction using lentivirus .....	95
Figure 4.16 Immunofluorescence following transduction of DMD human myoblasts with lentivirus carrying mini-dystrophins .....	96
Figure 5.1 Transcutaneous electroporation of skeletal muscle after injection of mini-dystrophin constructs .....	103
Figure 5.2 Dystrophin expression in mdx mouse muscles electroporated with mini-dystrophin constructs .....	105
Figure 5.3 Statistical analysis of dystrophin positive fibres.....	106
Figure 5.4 Semi-quantitative measurement of dystrophin expression intensity .....	108
Figure 5.5 Statistical analysis of dystrophin expression intensity .....	109
Figure 5.6 Analysis of internalised nuclei in muscle fibres .....	111
Figure 5.7 Determination of internal nuclei in mini-dystrophin expressing fibres .....	114
Figure 5.8 Distribution of internal nuclei in mini-dystrophin positive electroporated fibres .....	115
Figure 5.9 Correlation between muscle fibre geometric parameters.....	117
Figure 5.10 Morphometric quantification of muscle fibre size and statistical analysis of transfected fibres.....	119
Figure 5.11 Frequency distribution of muscle fibre size using cross-sectional area .....	122
Figure 5.12 Dystrophin and $\gamma$ -sarcoglycan expression in electroporated muscle.....	124
Figure 5.13 Dystrophin and nNOS expression in electroporated muscle.....	126

## List of Abbreviations

AA	Amino acid
AAV	Adeno-associated virus
ABD	Actin-binding domain
AD	Autosomal dominant
AON	Antisense oligonucleotide
Ad	Adenovirus
Amp	Ampicillin
AR	Autosomal recessive
BMD	Becker muscular dystrophy
cDNA	Complementary DNA
CK	Creatine kinase
CMD	Congenital muscular dystrophy
CMV	Cytomegalovirus
CXMD	Canine X-linked muscular dystrophy
DAPC	Dystrophin-associated protein complex
DGC	Dystrophin-associated glycoprotein complex
dNTP	Deoxyribonucleotide triphosphate
DMD	Duchenne muscular dystrophy
DNA	Deoxyribonucleic acid
Dys	Dystrophin
ECM	Extracellular matrix
EDTA	Ethylenediaminetetra-acetic acid
ESC	Embryonic stem cell
GRMD	Golden retriever muscular dystrophy
HSV	Herpes simplex virus
iPSC	Induced pluripotent stem cell
kb	Kilo bases
kDa	Kilo Daltons
LB	Luria Bertani
LGMD	Limb-girdle muscular dystrophy
Mbp	Mega base pairs
MEB	Muscle-eye-brain
MD	Muscular dystrophy
mdx	Murine dystrophy X-linked
MRI	Magnetic resonance imaging
mRNA	Messenger RNA
nNOS	Neuronal nitric oxide synthase
ns	Not significant
nt	Nucleotide
OMIM	Online Mendelian Inheritance in Man

PAGE	Polyacrylamide gel electrophoresis
PCR	Polymerase chain reaction
Pen/strep	Penicillin/streptomycin
rAAV	Recombinant adeno-associated virus
RNA	Ribonucleic acid
SOC	Super optimal broth with catabolite repression
SOE-PCR	Splicing by overlapping extension PCR
SR	Sarcoplasmic Reticulum
TA	Tibialis anterior
TAE	Tris-acetate-EDTA
TBST	Tris-buffered saline with Tween 20
UTR	Untranslated region
WWS	Walker Warburg syndrome

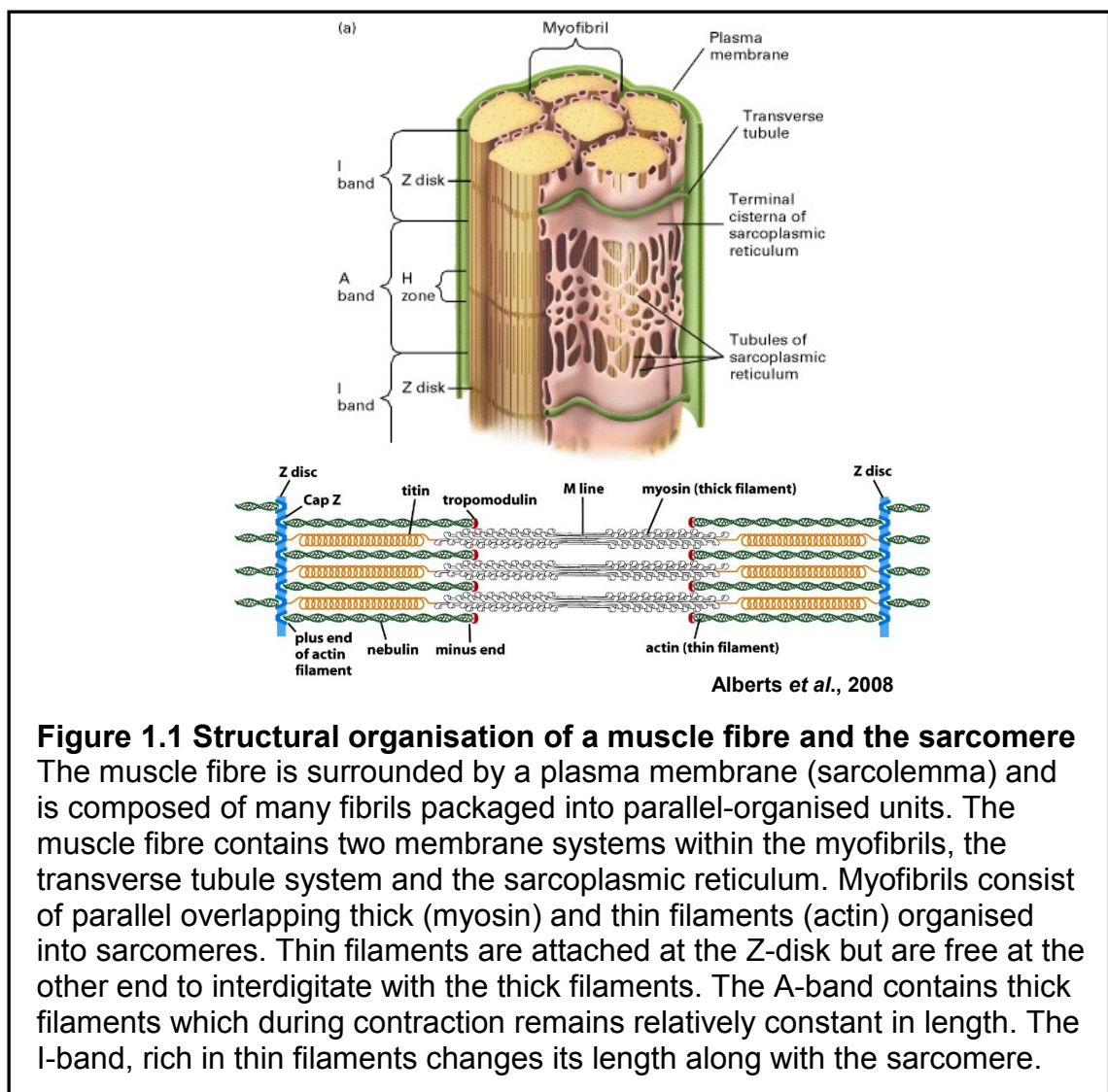
# Chapter 1 Introduction

## 1.1 Skeletal muscle structure and function

There are three types of muscle, skeletal muscle (striated), smooth muscle and cardiac muscle, that all are responsible for contraction but vary in origin, development, structure and function. Cardiac and smooth muscle cells are responsible for involuntary movement, while skeletal muscle cells react to conscious and voluntary control. In an adult human skeletal muscle, cells (muscle fibres) can be 2-3 cm long and 100  $\mu\text{m}$  in diameter (Alberts *et al.*, 2008). Muscle is enclosed by a strong sheath of extracellular matrix (ECM) known as epimysium. Whole muscle consists of many subunits called fascicles. Each fascicle is surrounded by connective tissue called perimysium. Fascicles are composed of bundles of highly differentiated and elongated muscle fibres with a cytoplasm containing an organised filament system based on the contractile proteins actin and myosin which are enveloped by a sheath called the endomysium. Approximately 10-50 muscle fibres are joined together in a bundle which are attached at both ends to tendons or connective tissue and have multiple nuclei that are generally located peripherally within the fibre (Hagen *et al.*, 1998). The number of nuclei is approximately 50 -100 per millimetre of muscle fibre length (Ishikawa, 1983).

Muscle fibres consist of bundles of parallel-oriented myofibrils and these form myofilaments. Myofibrils count for 75-85 percent of the fibre volume. Myofibrils consist of regularly consecutive 2-3  $\mu\text{m}$  long sections and parallel overlapping thick and thin filaments known as sarcomeres (Bagshaw, 1982) which are the basic units of force generation (Loeb, 1986). Organelles such as mitochondria and sarcoplasmic reticulum (SR) are found in the muscle fibre cytoplasm (sarcoplasm). The sarcoplasmic reticulum is essential for storage of calcium that is released after stimulation of muscle and triggers contraction. The typical red colour of muscle is caused by the muscle pigment myoglobin, an iron- and oxygen-binding protein that is responsible for storage and transfer of oxygen (Schiebler *et al.*, 1999). Thick and thin filaments are responsible for force generation and are predominantly composed of the proteins myosin and actin respectively. The myosin molecule consists of two heavy chains and four light

chains while thin filaments are composed of actin, tropomyosin and troponin. Globular actin molecules polymerise to build actin filaments (Bagshow, 1982). A myofibril volume contains 55% myosin and 25% actin. Using specific dyes, some regions of a muscle fibre appear darker than other areas, because dense protein bands are stained stronger. These bands are known as A-bands and the weaker areas with less protein density are labelled as I-bands. Within the I-band there is a dense protein zone known as Z-line or Z-disk (Eisenberg, 1985). Within the A-band is a dense protein area called the H-zone. In the middle of the H-zone is an area known as the M-line. The M-line consists of a network of proteins that binds the thick filaments and the Z-disk, and is composed of a protein complex that binds to the thin filaments. Thin filaments are attached at the Z-disk but are free at the other end to interlock to the thick filaments. During muscle contraction the sarcomere I-band and H-zone become shorter while the A-band length remains constant (Bagshow, 1982).



The muscle fibre contains two specialised membrane systems within the myofibrils. One is the transverse tubule system and the other the sarcoplasmic reticulum, both separate from each other but responsible for conveying the external stimulus provided by the motor neuron to the centre of the fibre (Peachey, 1985). There are two different types of skeletal muscle fibres based on functional, histological and morphological differences which relate to the proportion of myofibrils to sarcoplasm and mitochondria. Type I fibres, the so-called slow-twitch fibres, are red in appearance due to the higher content of oxygen-binding protein myoglobin. They are thin and contain a high number of mitochondria and sarcoplasm and are specialised to generate slow and sustained contraction. Type II fibres are known as fast-twitch fibres or white fibres due to their lower myoglobin content. They are thicker and contain relatively small number of mitochondria, have a high number of myofibrils and pronounced sarcoplasmic reticulum. These fibres are characterised by the ability for strong but short-term performance (Schiebler *et al.*, 1999). Muscle fibres have a complex membrane network.

The muscle fibre is entirely enclosed by the plasma membrane which is known as the sarcolemma. The sarcolemma is divided into three layers, the plasma membrane (plasmalemma) which is a lipid bilayer, basal lamina and thin collagen fibrils. The sarcolemma is tightly attached to the basal lamina, which consists of extracellular matrix (ECM) proteins (Voermans *et al.*, 2008). Disruptions of this connection are the cause of numerous forms of muscular dystrophy (Rahimov and Kunkel, 2013a).

Satellite cells, the adult muscle stem cells, are usually located between the basal lamina and the plasma membrane (Moyle and Zammit, 2014). These cells are involved in forming new fibres after muscle injury. The precursors of skeletal muscle fibres are called myoblasts. Myoblast development depends on two different regulatory pathways, embryonic specification by the paired box genes Pax3 and Pax7, and the MyoD cascade of transcription factors which regulate the expression of genes that are involved in myoblast maturation. Nuclei are initially in the centre of myotubes, however they move to periphery later following fusion and the maturation of myofibres (Folker and Baylies, 2013). After a period of proliferation, the myoblasts stop dividing and start to express

muscle specific genes that are required for their final differentiation. In this process they fuse and form differentiated, highly specialised and multinucleated muscle fibres. After differentiation muscle fibres grow and mature, the nuclei do not replicate their DNA and the fibre never divides again (Charge and Rudnicki, 2004). In adult life, new skeletal muscle fibres are not generated, however the existing muscle fibres have the ability to grow if renewal is required. This process can be initiated after stimulation or exercise-induced injury and is regulated by activation of quiescent mononuclear satellite cells lying within the basal lamina (Ceafalan *et al.*, 2014). Upon activation, satellite cells can proliferate, differentiate and fuse to the existing muscle fibres. Satellite cells divide asymmetrically, producing myoblasts and replenishing the pool of stem cells (Kuang *et al.*, 2007). This self-renewal capability of satellite cells becomes limited in some forms of muscular dystrophy. For instance, in Duchenne muscular dystrophy, differentiated muscle fibres are progressively damaged due to loss of dystrophin. Satellite cells are activated to repair the damaged fibres. This regenerative process is exhausted over time leading to loss of capability to repair and eventually fibres are irreversibly replaced by connective tissue and fat (Sacco *et al.*, 2010).

## **1.2 The dystrophin-associated glycoprotein complex (DGC)**

The DGC is a protein network which links the actin cytoskeleton to the extracellular matrix (ECM) surrounding the muscle fibre (Poon *et al.*, 2002) and stabilises the sarcolemma, protecting the muscle from contraction-induced damage and necrosis (Straub *et al.*, 1997; Culligan *et al.*, 1998; Hoffman and Dressman, 2001). The DGC comprises at least ten different proteins. This complex may also be involved in transmembrane signal transfer (Rando, 2001). The DGC consists of cytoplasmic, transmembrane and extracellular proteins including dystrophin, sarcoglycans, dystroglycan, caveolin-3, syntrophins, dystrobrevins, sarcospan and neuronal nitric oxide synthase (Lapidos *et al.*, 2004). Dystrophin binds F-actin intracellularly which directly connects the DGC with the contractile elements of the muscle (Rybakova *et al.*, 1996). In the absence of dystrophin, the entire DGC is destabilised at the sarcolemma (Thomas *et al.*, 1998). Studies have implicated components of this complex in a

wide range of muscular dystrophies. Furthermore, disruption of the DGC is also involved in many forms of acquired diseases (Townsend, 2014).

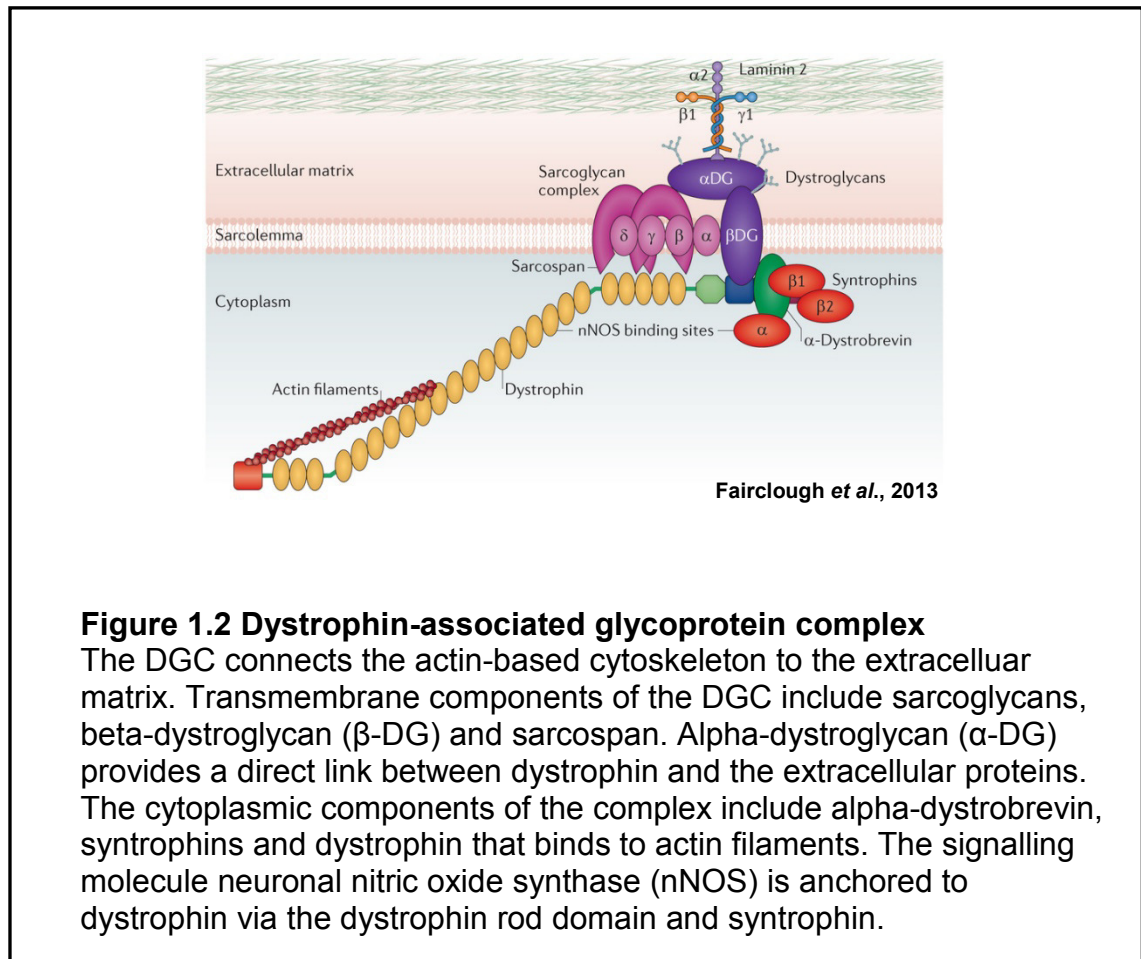


### Figure 1.2 Dystrophin-associated glycoprotein complex

The DGC connects the actin-based cytoskeleton to the extracellular matrix. Transmembrane components of the DGC include sarcoglycans, beta-dystroglycan ( $\beta$ -DG) and sarcospan. Alpha-dystroglycan ( $\alpha$ -DG) provides a direct link between dystrophin and the extracellular proteins. The cytoplasmic components of the complex include alpha-dystrobrevin, syntrophins and dystrophin that binds to actin filaments. The signalling molecule neuronal nitric oxide synthase (nNOS) is anchored to dystrophin via the dystrophin rod domain and syntrophin.

## 1.3 Muscular dystrophy

Muscular dystrophies (MDs) are a heterogeneous group of over 40 inherited diseases characterised by progressive muscle atrophy and weakness (Emery, 2002b; Muir and Chamberlain, 2009). These conditions arise as a consequence of muscle fibre degeneration leading to irreversible fatty infiltration and fibrosis (Kornegay *et al.*, 2012). Although muscular dystrophies show similarities in dystrophic changes on muscle biopsy, their underlying genetic causes vary widely with different forms of the disease affecting different muscle groups (Mercuri and Muntoni, 2013). The various forms of muscular dystrophy differ in their mode of inheritance, the underlying genetic causation, the affected muscle groups, age of onset and the disease course (Emery, 2002b). A number of muscular dystrophies can affect cardiac and respiratory function and result in premature death (Rando, 2001; Heydemann and McNally, 2007). In rare forms of muscular dystrophies other organs or tissues are involved such as skin, eye,

brain and inner ear. Muscular dystrophy is classified into different forms, based on underlying molecular and cellular mechanisms (Rahimov and Kunkel, 2013a). Several muscular dystrophies result from mutations leading to disruption of the dystrophin-associated glycoprotein complex (DGC) (Ibraghimov-Beskrovnaya *et al.*, 1992).

Duchenne muscular dystrophy is caused by frame-shifting mutations resulting in complete loss of dystrophin protein in muscle fibres, whereas mutations causing BMD are mainly in-frame and produce reduced levels and partially functional dystrophin. Both forms result in disruption of cytoskeletal and ECM connection (Koenig *et al.*, 1988; Monaco, 1989).

The sarcoglycan complex in muscle consists of four transmembrane proteins,  $\alpha$ -,  $\beta$ -,  $\gamma$ - and  $\delta$ -sarcoglycans and mutations in this complex are associated with autosomal recessive limb-girdle muscular dystrophies (LGMDs) which generally present as childhood forms of LGMD (Lim and Campbell, 1998; Nigro, 2003; Sandona and Betto, 2009). Defects in any of the sarcoglycan subunits generally result in reduction or absence of the entire protein complex and destabilisation of the sarcolemma (Rahimov and Kunkel, 2013a).

The dystroglycan complex is the core element between cytoskeleton and ECM (Moore and Winder, 2010). The dystroglycan complex is encoded by a single gene *DAG1* and consists of  $\alpha$ - and  $\beta$ -dystroglycan, both produced from a single transcript through post-translational proteolytic cleavage and subsequently forming a stable complex. Dystrophin binds to  $\beta$ -dystroglycan on the cytoplasmic side of the cell. By contrast,  $\alpha$ -dystroglycan is localised on the extracellular side and binds laminin in the ECM (Ibraghimov-Beskrovnaya *et al.*, 1992).

A large number of muscle and brain disorders result from mutations in genes that are involved in glycosylation of  $\alpha$ -dystroglycan, one of the major mechanisms leading to LGMDs and congenital muscular dystrophy (CMDs) (Johnson *et al.*, 2013). Hypoglycosylation of  $\alpha$ -dystroglycan results in reduced binding capacity to laminin in the ECM (Zhang *et al.*, 2011). There is also secondary loss of laminin- $\alpha$ 2 which is caused by mutations in other genes

(Brockington *et al.*, 2001). The main CMD subtypes are classified by gene involved and clinical phenotype including severe forms such as muscle-eye-brain disease (MEB), Walker-Warburg syndrome (WWS) and Fukuyama CMD which are known as dystroglycanopathy type A (MDDGA) (Moore *et al.*, 2002) and are caused by mutations in *POMT1*, *POMT2*, *FKTN*, *FKRP*, *LARGE*, *POMGNT1*, *ISPD*, the *LMNA*-related CMD and the *SEPN1*-related CMD (Muntoni and Voit, 2004). There are two other forms including a less severe form called as MDDGB and the mildest form known as MDDGC (Rahimov and Kunkel, 2013a). These disorders are known as secondary dystroglycanopathies because they are caused by insufficient glycosylation of  $\alpha$ -dystroglycan, and not by mutations in the dystroglycan gene itself (Rahimov and Kunkel, 2013a).

The ECM is a network of extracellular glycoproteins that provides structural support to myofibres. Mutations in these proteins generally cause congenital muscular dystrophy (CMD) (Rahimov and Kunkel, 2013b). The most common form is caused by the deficiency of laminin- $\alpha$ 2 (*LAMA2*) and is known as merosin-deficient or type 1A (*MDC1A*) (Helbling-Leclerc *et al.*, 1995). There are many other forms of muscular dystrophies with different underlying defects and clinical manifestation (Mercuri and Muntoni, 2013).

### **1.3.1 *Dystrophinopathies***

Duchenne muscular dystrophy (DMD; OMIM 310200) is the most common childhood form of muscular dystrophy with an incidence of ~1 in 4000 newborn males (Mendell *et al.*, 2012; van Ruiten *et al.*, 2014). The first reported clinical observations are from the 19<sup>th</sup> century by Edward Meryon (1852) and some years later by Guillaume Duchenne de Boulogne (1861) who described clinical manifestations and muscle histology of the disease in detail (Becker and Kiener, 1955; Kunkel *et al.*, 1989). Becker and Kiener described the less frequent and milder allelic form Becker muscular dystrophy (BMD; OMIM 300376) with an incidence of ~1 in 17000 (Becker and Kiener, 1955). DMD and BMD are both X-linked, inherited disorders of muscle caused by mutations in the *DMD* gene, the largest known human gene which encodes dystrophin (Kingston *et al.*, 1984). Mutations in the *DMD* gene lead to absence (in DMD) or alteration in protein structure and reduced expression (in BMD) of the dystrophin protein, resulting

in muscle degeneration (Hoffman *et al.*, 1987b). In about two thirds of cases inherit the mutation from their mother who is a carrier of the defective gene. *De novo* mutations occur in one third of cases (Lane *et al.*, 1983). The onset of Duchenne muscular dystrophy is in infancy (Manzur *et al.*, 2008; van Ruiten *et al.*, 2014). Affected individuals are clinically normal at birth, although creatine kinase levels in serum may be elevated if checked. Motor delay may be the first symptom of DMD between 2-5 years of age, and then patients present difficulties in running and climbing stairs (Dubowitz, 1978; Emery, 2002a), followed by rapid disease progression and loss of ambulation by 13 years of age (Bushby *et al.*, 2010b). About 20% of affected boys have mental impairment with an IQ of less than 70 (Bushby *et al.*, 1995). Most affected individuals develop respiratory complications due to diaphragmatic and intercostal muscle weakness and die in their twenties or early thirties from respiratory failure unless mechanically ventilated (Bushby *et al.*, 2010a). Cardiac dysfunction and cardiomyopathy are also part of the dystrophinopathy phenotype and can also result in early death (Emery, 1993). Becker muscular dystrophy is similar to Duchenne muscular dystrophy in the distribution of muscle wasting but the course of the disease is milder, the onset of symptoms later and the rate of progression slower (Romitti *et al.*, 2009). The age of onset is very variable and some individuals have no symptoms until adult life. Loss of ambulation may occur, but later than in DMD. Life expectancy is higher than in DMD and mortality is often associated with cardiac symptoms. Differing disease severity of these forms depends on the type of mutation and the resulting dystrophin expression. BMD patients also display dilated cardiomyopathy and respiratory and skeletal muscle weakness (Monaco *et al.*, 1988; Bushby *et al.*, 2010a). Most patients are diagnosed based on a combination of phenotypical manifestation and genetic analysis (Annexstad *et al.*, 2014). Independent of family history, DMD diagnosis is made by observation of aberrant muscle function in male infants (Bushby *et al.*, 2010a). DMD is generally diagnosed when the child is around 5 years old but due to delayed developmental milestones the diagnosis might be much earlier. Clinical symptoms include delay in walking and speaking, waddling gait, toe walking, difficulty with running or climbing stairs and frequent falls. Gower's sign (a characteristic manoeuvre for standing from a prone position) in a male infant usually leads to diagnostic investigations (Bushby *et al.*, 2010a). Alongside the clinical presentation, testing

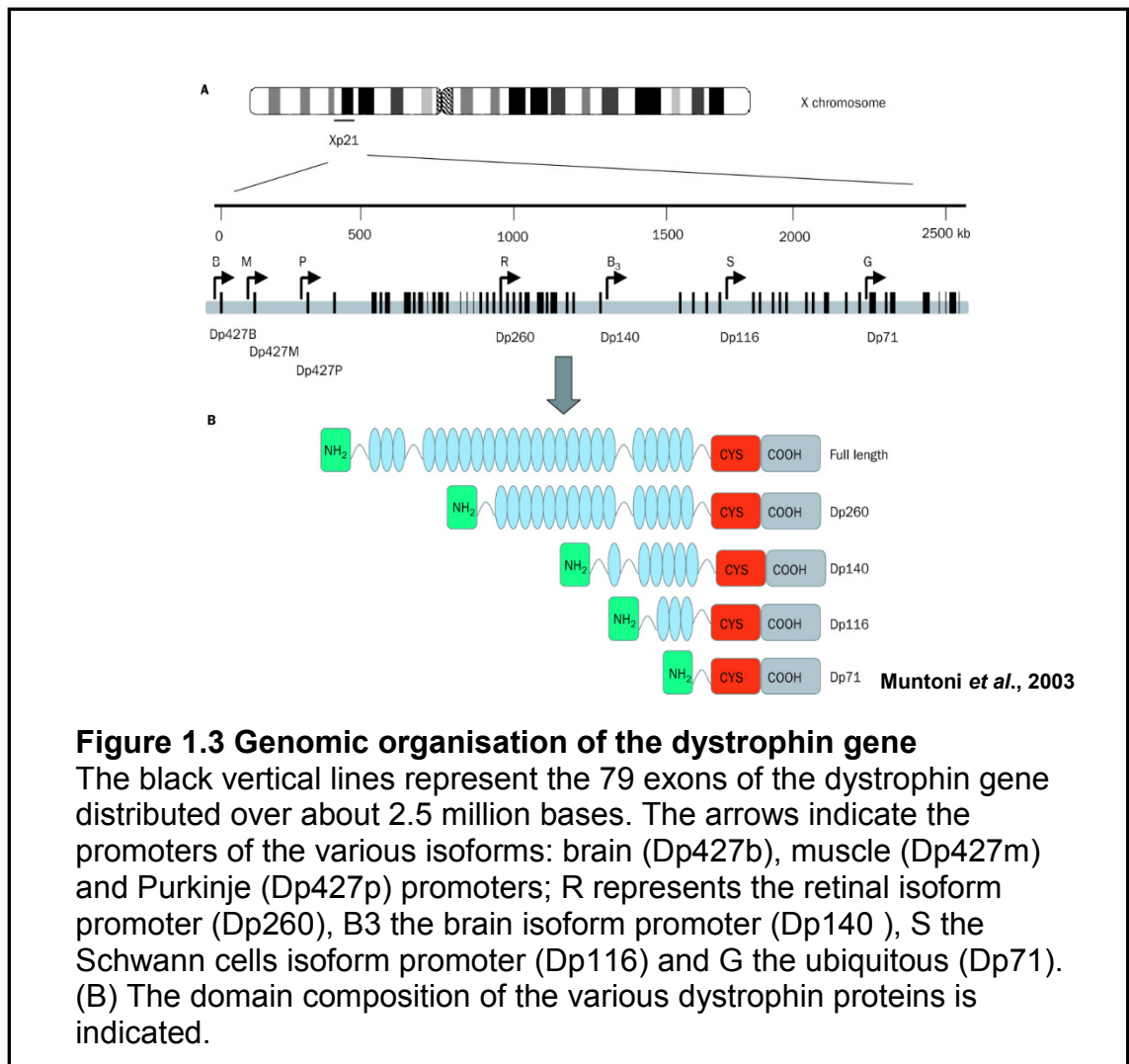
for a *DMD* mutation in a blood sample is essential, since the results are required for prenatal diagnosis and feasibility of currently available mutation-specific clinical trials (Bushby *et al.*, 2010a). Genetic tests include multiplex PCR (Prior and Bridgeman, 2005) multiplex ligation-dependent probe amplification (Lalic *et al.*, 2005) multiplex amplifiable probe hybridisation (Dent *et al.*, 2005) and single-condition amplification/deletion (Flanigan *et al.*, 2003). No further testing is required if one of these tests leads to the confirmation of a *DMD* mutation. If a *DMD* mutation has not been identified in genetic testing, signs or symptoms consistent with DMD are present and CK level is persistently elevated, full sequencing of the dystrophin gene and/or a muscle biopsy may be necessary. Depending on availability of genetic testing, a muscle biopsy could be considered for determination of the level of dystrophin expression to distinguish DMD from the milder BMD (Bushby *et al.*, 2010a). Two reviews from an international group of experts in DMD management provide multidisciplinary guidelines for DMD diagnosis and comprehensive recommendations for pharmacological and psychosocial management and optimal care (Bushby *et al.*, 2010a; Bushby *et al.*, 2010b).

## **1.4 Dystrophin gene (*DMD*) and protein**

### **1.4.1 *Chromosomal organisation, protein isoforms and tissue distribution of dystrophin***

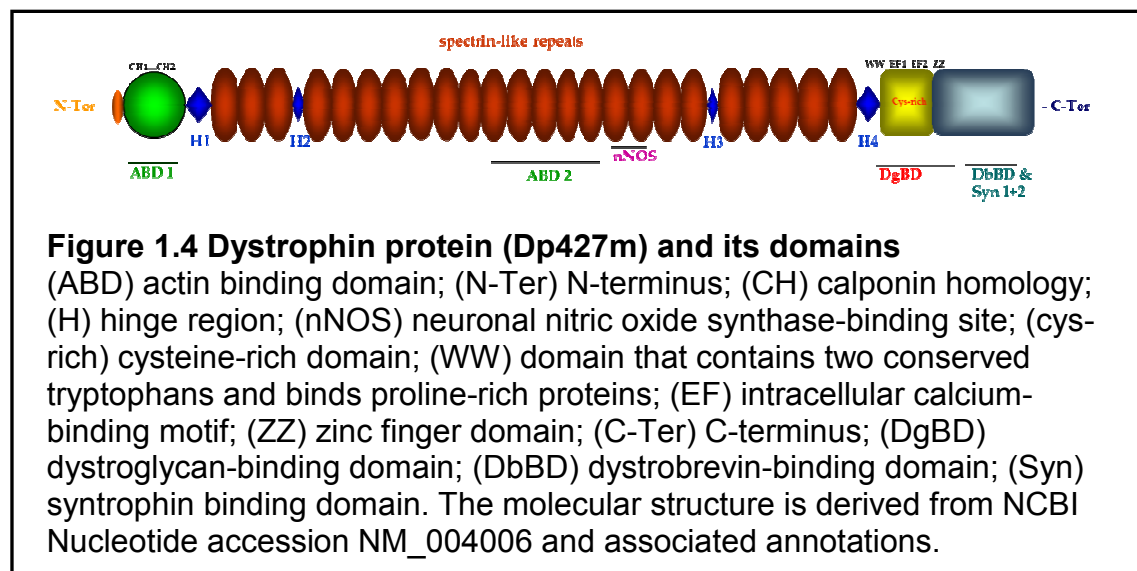
The X-linked dystrophin gene is the largest gene in human genome (van Essen *et al.*, 1992). The genomic sequence covers more than 2.5 million base pairs, representing approximately 0.1% of the entire human genome. The coding sequence of 79 exons comprises 1% of the genomic locus, while 99% of the gene consists of intronic sequences (Lander *et al.*, 2001). The complete ~14 kb messenger RNA of full-length dystrophin encodes 3685 amino acids and is primarily expressed in skeletal and cardiac muscle and at lower levels in the brain (Lambert *et al.*, 1993). There are three full-length isoforms, Dp427b (brain), Dp427m (muscle) and Dp427p (Purkinje), and several smaller isoforms (Sadoulet-Puccio and Kunkel, 1996; Muntoni *et al.*, 2003) (Figure 1.3). The three full-length isoforms have the same number of exons, but differ in their respective promoters and unique first exons (Muntoni *et al.*, 2003). The brain

promoter drives expression in the hippocampus of the brain and in cortical neurons (Lederfein *et al.*, 1992), the Purkinje promoter in Purkinje cells and the muscle promoter in skeletal muscle and cardiomyocytes (Bies *et al.*, 1992). Due to alternative internal promoters and splicing, a range of shorter dystrophin isoforms are generated producing the protein products Dp260 in retina, Dp140 in brain, retina and kidney, Dp116 in Schwann cells and Dp71 with ubiquitous expression in most non-muscle tissues (Muntoni *et al.*, 2003). This splice variant is also detected in cardiac but not in skeletal muscle (Tennyson *et al.*, 1996).



### 1.4.2 Protein structure and domain composition of muscle specific dystrophin protein (Dp427m)

The muscle specific dystrophin transcript encodes Dp427m, a 427 kDa protein (Figure 1.4) which is a member of the beta-spectrin and alpha-actinin family (Blake *et al.*, 2002). Dystrophin is a cytoplasmic protein and located at the inner surface of the muscle fibre membrane (sarcolemma). It is a vital part of the dystrophin-associated glycoprotein complex (DGC) which connects the cytoskeleton of muscle fibres to the surrounding extracellular matrix through the sarcolemma. The lack of this structural protein results in sarcolemmal instability and reduces the resistance of the muscle fibres to contraction-induced injury (Durbeej and Campbell, 2002).



The dystrophin molecule contains a number of distinct protein domains. The N-terminal actin-binding domain (ABD), containing two calponin homology motifs, a central coil-coiled, triple-helical rod domain which is characterised by 24 spectrin-like repeats separated into three subregions by 4 hinges and including a second ABD and the binding site for neuronal nitric oxide synthase (nNOS), a cysteine-rich region responsible for binding to  $\beta$ -dystroglycan (composed of a WW domain, two EF hands and a zinc-finger domain). The C-terminus binds to  $\alpha$ - and  $\beta$ -syntrophin and dystrobrevin (Koenig *et al.*, 1988). Although the elements of the dystrophin molecule have been identified and studies in transgenic mdx mice have explored the importance of a number of these structural domains, the functional requirement for many parts of the protein

remains unclear (van der Plas *et al.*, 2006). The N-terminal domain is one of the regions in the gene with a high rate of deletions. Mutations in this region encoding ABD1 have shown to be associated with reduced dystrophin resulting in a severe BMD phenotype. In contrast a deletion of ABD2 domain but maintaining ABD1 leads to a mild phenotype in transgenic mdx muscle (Banks *et al.*, 2007). The loss of the C-terminus which contains the cysteine-rich domain and is associated with the other proteins of DGC complex leads to disruption of the whole complex (Sweeney and Barton, 2000).

### **1.4.3 Mutations in muscle specific dystrophin Dp427m**

The dystrophin gene has a high mutation rate relative to other human genes. This is due to the large size and the internally repetitive structure of the gene which makes it vulnerable to non-homologous recombination events (Lapidos *et al.*, 2004). Deletions and duplications account for more than two thirds of the mutations that cause DMD or BMD (Den Dunnen *et al.*, 1989; Koenig *et al.*, 1989a). Approximately 65% of mutations in both diseases are intragenic deletions of one or more exons. There is no direct relationship between the location and extent of the deletion and the severity of the clinical presentation. The phenotype depends more directly on the effect that these mutations have on the translational reading frame (Muntoni *et al.*, 2003). Frame-shifting deletions of a single exon or nonsense mutations can lead to the severe clinical phenotype of DMD, whereas in-frame deletions of up to 50% of the dystrophin coding sequence can lead to a mild BMD phenotype, with a shorter but partially functional dystrophin and a reduced expression level (England *et al.*, 1990; Love *et al.*, 1991b). However there are exceptions to this reading frame rule with DMD patients carrying in-frame deletions or duplications and patients with frame-shift mutations presenting with a BMD phenotype (Muntoni *et al.*, 2003). Deletions can occur anywhere in the dystrophin gene but there are two regions with a high incidence: the most commonly mutated region is between exons 45-55 and there is a minor 5' end hot-spot including exons 2-19 (Koenig *et al.*, 1989b). 5-10% of DMD and BMD mutations are duplications in the dystrophin gene (Love *et al.*, 1991b; Muntoni *et al.*, 2003). Another form of *DMD* mutation is point mutation which accounts for 20% to 35% of cases and most of the point mutations identified in DMD patients are nonsense mutations (Roberts *et al.*,

1994). DMD/BMD phenotypes and their corresponding mutations are catalogued in the Leiden muscular dystrophy database (<http://www.dmd.nl/>).

## 1.5 Animal models of DMD

There are two naturally occurring animal models for DMD with defects in dystrophin: X-linked muscular dystrophy mice (mdx) (Bulfield *et al.*, 1984), and X-linked muscular dystrophy dogs (cxmd) (Valentine *et al.*, 1988). The mdx mouse was identified in 1984 on the C57BL/10 strain while screening for biochemical variants in CK and carries a nonsense point mutation in exon 23 of dystrophin gene (Bulfield *et al.*, 1984). The mouse is the most widely used animal model for DMD due to the ease of breeding and relatively low cost of housing (Sicinski *et al.*, 1989). Although DMD patients and mdx mice are both dystrophin deficient, the muscle pathology of mdx mice progresses more slowly, displaying a milder phenotype compared to DMD patients. Mdx mice show only a 20% reduction in life span (Chamberlain *et al.*, 2007). There are other alleles at the mouse *DMD* locus including exon 52 knockout mice (mdx52) (Araki *et al.*, 1997) and mdx<sup>3cv</sup> which both have a more severe phenotype. Other researchers have described the double knockout mice (dko) lacking both dystrophin and utrophin which develop a disease with a much more severe pathology than mice missing dystrophin alone (Deconinck *et al.*, 1997) and display a more severe dystrophic phenotype than DMD patients. Although there are genetic and phenotypic differences between dko mice and humans, these mouse models, provide a valuable experimental model to monitor the efficacy of therapeutic interventions (Isaac *et al.*, 2013).

Dystrophin-deficient dog models (cxmd) for DMD were first identified in 1988 in the dystrophic golden retriever (Valentine *et al.*, 1988) which may be the most promising animal model for testing therapeutic interventions due to closer clinical similarity with human DMD in terms of disease severity compared to dystrophic mouse models (Shimatsu *et al.*, 2003). However the high cost for maintenance, daily care and difficult breeding of dystrophic dogs has limited their use for experimental and preclinical testing (Grounds *et al.*, 2008). Furthermore the most widely used golden retriever model (GRMD) shows a wide variability in the phenotype making the functional assessment difficult

(Brinkmeyer-Langford and Kornegay, 2013). It has been reported that dystrophic dogs treated with corticosteroids displayed impairment of some measures of muscle function showing a larger number of necrotic fibres which is in contrast to the beneficial effects of steroid use in human patients (Hollinger *et al.*, 2014). Other breeds include Rottweiler (Collins and Morgan, 2003) and German shorthaired pointers (Schatzberg *et al.*, 1999). A Beagle model has also been produced by crossing beagles with dystrophic golden retriever (Shimatsu *et al.*, 2003).

Hypertrophic Feline Muscular Dystrophy (FHMD) is a feline model for dystrophin deficiency (Vos *et al.*, 1986). The characteristic features of these dystrophic cats are their distinct hypertrophic muscles but the disease symptoms and progression are different from human DMD or other mammalian models. Therefore they have not been used due to the pathological dissimilarities with DMD (Nakamura and Takeda, 2011).

Recently, pig models have been described as being more similar to humans in terms of genetics and physiology. A DMD pig model with a deletion in exon 52 may have potential for use in experimental studies, in particular exon skipping research, since exon 52 is a frequent deletion in DMD patients (Klymiuk *et al.*, 2013). This model exhibits progressive and dystrophic features in skeletal muscle, including cycles of degeneration-regeneration, inflammation, fibrosis, impaired ambulation, elevated creatine kinase and muscle weakness with a short life expectancy of 3 months due to respiratory failure (Klymiuk *et al.*, 2013). A pig model has also been identified as a novel animal model for BMD. Dystrophin insufficiency causes selective muscle histopathology and loss of dystrophin-glycoprotein complex assembly in pig skeletal muscle (Hollinger *et al.*, 2014). Currently, pig models are being used in experimental studies in a variety of human diseases including cancer, diabetes, cystic fibrosis, Huntington's disease, kidney disease and cardiovascular disease (Flisikowska *et al.*, 2014).

The homozygous dystrophin-deficient zebrafish (*dmd*<sup>ta222ta/ta222ta</sup>) shows similarities with many aspects of the human disease including fibrosis, inflammation and dystrophic histopathology in muscle sections and has been

suggested as a model system for analysis of muscle fibre loss and *in vivo* drug screening (Berger *et al.*, 2010).

## **1.6 Therapeutic approaches for DMD**

Currently, the only available therapies for DMD are conventional, such as use of glucocorticoids, respiratory support through mechanical ventilation, cardiac support using beta-blockers and ACE inhibitors, and orthopaedic or surgical interventions (Bushby *et al.*, 2010a). However, there have been promising experimental approaches developed in mammalian models for therapeutic applications, leading to human clinical trials (Bushby *et al.*, 2010a). Since the discovery of the genetic defect in DMD (Monaco *et al.*, 1986), various molecular strategies have been proposed to either replace the defective dystrophin gene through introduction of a functional copy or restore the translational reading frame (Chamberlain, 2002). Although recent advances in transgene engineering, AAV serotype analysis and vector delivery to muscle have shown promising results in animal models of DMD, there are still hurdles that limit attempts for a successful gene transfer strategy. Major obstacles associated with viral vectors include limited packaging capacity, loss of therapeutic gene expression and immune response (Dunant *et al.*, 2003). Alternative therapeutic approaches are exon skipping, readthrough of stop codons, transplantation of muscle stem cells or other stem cells, utrophin upregulation, the use of surrogate genes to increase muscle mass such as follistatin and combined cell- and gene approaches (Cossu and Sampaolesi, 2007).

### **1.6.1 *Non-viral gene transfer***

Plasmid DNA containing a dystrophin insert can be engineered and amplified in large amounts and injected into skeletal muscle of mdx mice (Park and Oh, 2010). Researchers have observed dystrophin expression in up to 10% of the muscle fibres as a result of naked plasmid injection into mdx mouse muscle and a decrease in internally nucleated fibres without development of an immune response (Acsadi *et al.*, 1991). However preclinical studies have not shown this method to be efficient enough to be considered as a treatment for DMD (Muir and Chamberlain, 2009). This approach in combination with electroporation is a

useful tool for measuring local effects of transgenes in animal models but not for systemic transgene delivery which would be required to achieve whole body muscle targeting in patients (Wells *et al.*, 2003).

### **1.6.2 *Upregulation of a dystrophin-related protein or other genes***

A possible alternative therapy is to compensate for the missing dystrophin using dystrophin-related proteins such as utrophin, a protein with a high degree of structural and functional similarity to dystrophin (Tinsley *et al.*, 1992). Utrophin can also associate with dystrophin-associated proteins and act as a link between F-actin and extracellular matrix (Khurana *et al.*, 1991). Although utrophin is primarily expressed at the neuromuscular junctions in adult muscle, a number of studies have demonstrated that utrophin overexpression can lead to an amelioration of the dystrophic phenotype (Tinsley *et al.*, 1996). Using this method could also avoid the negative effect of the immune response against exogenous dystrophin, since utrophin is normally expressed in mdx and DMD muscles (Chakkalakal *et al.*, 2005). However utrophin binds actin only via the N-terminal domain and lacks sequence corresponding to spectrin-like repeats 15-19 of dystrophin and therefore cannot stabilise nNOS at the membrane (Lai *et al.*, 2013). In addition to utrophin, the rAAV-mediated gene delivery of other genes such as the muscle-building follistatin in combination with a micro-dystrophin has shown improved resistance to eccentric contraction-induced injury and force restoration in mdx mice (Rodino-Klapac *et al.*, 2013).

### **1.6.3 *Cell-based therapy***

Another potential therapeutic option is cellular therapy aiming to reconstitute the satellite cell niche. The transplanted cells must possess the ability to fuse with existing myofibres and express the missing dystrophin (Muir and Chamberlain, 2009). There are two different cell transplantation options: allogeneic (donor-derived) and autologous (patient-derived). Autologous grafts are less prone to immunological rejection, but require genetic manipulation to restore the genetic defect before cells can be reintroduced into skeletal muscle, whereas cell transplantation from a donor involves the risk of immune rejection (Price *et al.*, 2007). Allogeneic satellite cells from a wild type donor have been widely used

as stem cells for a cell-based therapy option. The drawback of this method is the limited distribution of cells, massive cell death after injection and immune rejection (Skuk *et al.*, 2007). Autologous transplantation of isolated satellite cells could circumvent the immunological response, however the limited amount of isolated myogenic progenitors and reduced myogenicity following their expansion in culture reduces their transplantation capacity (Webster and Blau, 1990). Other cell types suggested for a cell-based therapy include bone marrow-derived progenitors capable of being expanded quickly *in vitro* and migration and engraftment in muscle (Ferrari *et al.*, 1998), and muscle-derived progenitor cells, isolated based on expression of specific markers such as CD133 and CD34. Autologous transplantation of muscle-derived CD133<sup>+</sup> cells (Torrente *et al.*, 2007) and mesoangioblasts derived from pericytes (Dellavalle *et al.*, 2007; Meng *et al.*, 2012) have also been suggested as candidates with regenerative capacity in skeletal muscle. Alternative prospective cell types are embryonic stem cells (ESCs) and patient-specific induced pluripotent stem cells (iPSCs) which can be reprogrammed from patient fibroblasts and expanded in culture (Perlingeiro *et al.*, 2008; Dick *et al.*, 2011). Use of patient-derived iPSCs may overcome many limitations of cell therapy such as immune rejection of the transplanted cells and expansion of the cells to a therapeutically useful number. However, significant problems remain, such as targeted differentiation of the cells into a myogenic lineage without resort to viral vectors expressing myogenic factors (Yoshida and Yamanaka, 2010).

#### **1.6.4 Stop codon readthrough (small molecule therapy)**

Approximately 10% of DMD mutations are nonsense mutations introducing a premature termination codon into the dystrophin mRNA resulting in termination of protein translation and absence of dystrophin at the cell membrane (Wilschanski *et al.*, 2011). Aminoglycoside antibiotics such as gentamicin can cause the translational apparatus to ignore stop codons (Malik *et al.*, 2010). Treatment of cultured mdx cells with gentamicin has shown the presence of dystrophin in the sarcolemma and functional protection against muscle injury (Barton-Davis *et al.*, 1999). However, high toxicity in clinical trials precluded the use of this agent in patients (Welch *et al.*, 2007). The identification that PTC124 (ataluren) had more efficacy in premature stop codon readthrough than

gentamicin has led to a phase I preclinical safety trial using ataluren administration. Phase II trials involved 5-20 year old DMD and BMD patients over 48 weeks. Patients receiving a low dose treatment showed slower disease progression, whereas treatment with high dose ataluren demonstrated a similar outcome as in placebo group. A phase III study using ataluren was started in March 2013 to determine the efficacy of low-dose ataluren (Seto *et al.*, 2014). The encouraging results from this study suggest ataluren as an important advance in treatment of nonsense mutations in dystrophinopathies in terms of safety and efficacy (Bushby *et al.*, 2014).

### **1.6.5 Exon skipping**

Exon skipping provides an alternative approach to restore the reading frame of the dystrophin transcript by modulating the splicing machinery with antisense oligonucleotides (AON), skipping mutated exon(s) and resulting in production of a truncated but partially functional dystrophin protein (Yin *et al.*, 2008). AONs are synthetic single-strand nucleic acids which bind to a complementary sequence at the mRNA level (Mann *et al.*, 2001). One of the limitations of exon skipping is that due to the genetic heterogeneity of DMD, only small cohorts with specific mutations may benefit from any given AON drug (Mitrpant *et al.*, 2009). However, since the majority of deletions occur between exon 43 and 53, skipping of a subset of exons could be applicable to a substantial cohort of affected individuals. For example a treatment targeted at skipping exon 51 could be effective in 13% of DMD patients (Aartsma-Rus *et al.*, 2006). Two different compounds, drisapersen (2-O-methylAONs-Pro051-GSK-2402968) developed by Prosensa and GSK, and eteplirsen (morpholino AON-AVI4658) by Sarepta Therapeutics have been tested in clinical trials to skip exon 51 in dystrophin pre-mRNA and restore the mRNA reading frame. Drisapersen is composed of a 2-O-methyl phosphorothioate backbone (Flanigan *et al.*, 2014). Eteplirsen is composed of a phosphorodiamidate morpholino backbone (Mendell *et al.*, 2013). Both compounds have been used in clinical trials in patients with confirmed mutations for DMD. However after treatment the primary outcome measure (6-minute walk test) in the largest trial did not show any significant improvement over placebo. Several side effects including low platelet

counts and kidney toxicity was reported in some patients with higher drug doses (Flanigan *et al.*, 2014).

### **1.6.6 Viral vector-mediated gene therapy**

Gene delivery of dystrophin using viral vectors requires truncated versions of dystrophin, since the full-length dystrophin cDNA (~14 kb) is too large to be accommodated into most conventional viral vectors (Wang *et al.*, 2000). The idea for generation of mini- and micro-dystrophin constructs has arisen following observation of some BMD patients carrying large intragenic dystrophin deletions but displaying a mild phenotype (England *et al.*, 1990; Love *et al.*, 1991a). For example, large in-frame deletions involving almost 66% of the coding region have been reported in patients with mild BMD (Passos-Bueno *et al.*, 1994). These findings suggested that it would be possible to convert a severe DMD caused by a frame-shift mutation into a milder, BMD-like form by expressing an internally truncated dystrophin gene (Wang *et al.*, 2009).

Over recent years, several viral vectors have been used in preclinical studies to facilitate gene therapy for DMD. Adenovirus (Ad), recombinant adeno-associated virus (rAAV) and retroviruses carrying dystrophin constructs have been widely used and have shown improvement in disease pathology in animal models of DMD (Gregorevic *et al.*, 2004). Adenoviral vectors have a large cloning capacity and are able to transduce dividing and non-dividing cells. These vectors have high transduction level in regenerating muscles and a large cloning capacity, capable of expressing a full-length dystrophin protein in the patient cells. However, use of adenoviral vectors remains problematic due to the limited persistence of transgene expression and immunological reactions against viral products in animal models (Ghosh *et al.*, 2006).

Adeno-associated viral vectors have shown encouraging results in a number of genetic disorders including muscular dystrophies and gene transfer of mini- and micro-dystrophins (Warrington and Herzog, 2006). Wild type AAV is a non-pathogenic virus in humans (Carter, 2005), has high transduction efficiency and displays long-term stable expression of the transgene in mdx muscle (Goyenvalle *et al.*, 2011). AAV has a major drawback which is the limited

packaging capacity of approximately 5 kb and is therefore unable to transfer the full-length dystrophin to skeletal muscle (Blankinship *et al.*, 2006). However the development of mini- and micro-dystrophins has to some extent overcome these constraints (Muir and Chamberlain, 2009).

Retroviral vectors derived from lentivirus such as HIV are one of the most promising viral vectors for gene transfer strategies, due to their ability to integrate into host chromosomes of dividing and non-dividing cells leading to long-term integration in the host genome (Naldini *et al.*, 1996). They have up to ~11 kb insert capacity and display low toxicity (Sinn *et al.*, 2005). A major concern of using these vectors is the risk of activation of nearby genes and insertional mutagenesis which might be carcinogenic (Wang *et al.*, 2009).

#### **1.6.7 *Mini- and micro-dystrophin functional domains***

Gene replacement studies have shown that dystrophin expression can be restored to the sarcolemma by introducing mini- or micro-dystrophin where the C-terminal region and part of the internal rod domain had been removed, provided the essential dystroglycan-binding domain and parts of N-terminal actin-binding regions remain unaffected (Banks *et al.*, 2007). Chamberlain and colleagues at the University of Washington-Seattle and other groups have conducted extensive work on mini- and micro-dystrophins in gene therapy experiments leading to improvement of dystrophic muscle in mdx mice (Harper *et al.*, 2002; Scott *et al.*, 2002; Friedrich *et al.*, 2004; Banks *et al.*, 2007; Park and Oh, 2010; Nakamura and Takeda, 2011).

Studies in transgenic mice have also shown that expression of truncated dystrophin molecules missing large sequences of the dystrophin rod domain prevented a wide range of functional characteristics of dystrophic pathology (Harper *et al.*, 2002). Research has shown that dystrophin lacking the middle portion of the protein can correct underlying pathology as long as the N-terminal actin-binding domain and C-terminal domain are intact (Banks *et al.*, 2007). Other studies have postulated that cysteine-rich and C-terminal domains are crucial for stabilising the DGC and are required for a fully functional dystrophin protein due to binding properties of these regions to other integral proteins (Bies

*et al.*, 1992) and the absence of the C-terminus in dystrophin of mdx has been suggested to lead to loss of DGC as a whole (Sweeney and Barton, 2000). While the cysteine-rich domain which binds to the dystroglycan-sarcoglycan complex has been reported to be critical for function (Corrado *et al.*, 1996; Rafael *et al.*, 1996) and disruptions in this region result in a severe phenotype in patients (Suzuki *et al.*, 1992; Ervasti, 2007), the C-terminal domain has been suggested to be at least partially redundant and can be removed without severely compromising dystrophin function (Harper *et al.*, 2002; Yatsenko *et al.*, 2009).

For identification of the minimal regions of the rod domain required for a functional protein, smaller constructs retaining one to six repeats in dystrophin were generated (Harper *et al.*, 2002; Jorgensen *et al.*, 2009). Although some of these micro-dystrophin constructs showed efficacy in preventing progressive muscle damage, the treated mdx muscles were slightly weaker than controls suggesting that gene therapy using micro-dystrophins might prevent development of dystrophy, but do not fully restore muscle strength (Blankinship *et al.*, 2006).

A biophysical scan of the rod domain targeting 24 individual spectrin-like repeats assessed thermodynamic stability and resistance to proteolysis of repeats found that individual repeats considerably vary in their behaviour, suggesting that the architecture of the rod domain and its biological function is more complex than a repetitive structure (Mirza *et al.*, 2010). These data suggest that individual repeats are not simply interchangeable and therefore care should be taken when designing mini-dystrophin constructs (Banks *et al.*, 2010).

Reviewing the literature, much attention has been paid to the role of the rod domain in binding to signalling molecules including nNOS. nNOS restoration should be considered as a criterion for selecting a truncated version of dystrophin molecule for DMD gene therapy (Akbar *et al.*, 2003; Lai *et al.*, 2009; Thomas *et al.*, 2009; Li *et al.*, 2010b; Jarmin *et al.*, 2014). In skeletal muscle, nNOS is produced by endothelial cells and by muscle fibres and expressed at the sarcolemma (Thomas *et al.*, 2003). The muscle-specific isoform of neuronal

nitric oxide synthase (nNOS) has been identified as a component of the DGC (Chang *et al.*, 1996), is expressed in skeletal muscles of all mammals (Akbar *et al.*, 2003) and has been reported to have a significant impact on many processes in skeletal muscle including regulation of the blood flow, force production, glucose uptake and myotube differentiation (Thomas *et al.*, 2003). Therefore the absence of nNOS may negatively influence clinical features of dystrophinopathies (Stamler and Meissner, 2001). In normal skeletal muscle, nNOS is located at the cytosolic surface of the sarcolemma and is activated during contraction to transport nitric oxide (NO) to the muscle vasculature, causing the dilation of blood vessels that is needed for the increased metabolism of contracting muscle (Sander *et al.*, 2000). Incorrect nNOS localisation impairs dilation of blood vessels during muscle contraction leading to muscle ischemia and necrosis (Thomas *et al.*, 1998). Although nNOS function depends on its location in the muscle fibre membrane (Nawrotzki *et al.*, 1998), the nNOS knockout mouse displays no muscle pathology (Huang *et al.*, 1993; Chao *et al.*, 1998) and removing nNOS from mdx mouse does not lead to a more severe phenotype (Crosbie *et al.*, 1998). However, in dystrophin-deficient muscle, the sarcolemmal nNOS is reduced and incorrectly localised to the cytosol (Brenman *et al.*, 1995; Li *et al.*, 2011b).

Initial studies indicated that nNOS indirectly anchors to the C-terminal domain of dystrophin via syntrophin (Brenman *et al.*, 1995; Chang *et al.*, 1996). Systematic research on the rod domain nNOS-binding site has shown that the presence of repeats 16 and 17 is required for binding nNOS at the sarcolemma and that the presence of syntrophin alone does not result in sarcolemmal nNOS expression. Based on this model, it was suggested that localisation of nNOS depends on two distinct interactions, one between the syntrophin and nNOS PDZ domains and the other between spectrin-like repeats 16 and 17 in the dystrophin rod region and the nNOS PDZ domain (Lai *et al.*, 2009). According to these findings utrophin that lacks both repeats 16 and 17 and some of the dystrophin mini-genes will not localise nNOS to the sarcolemma (Lai *et al.*, 2013). These observations suggest that mini-dystrophin design could significantly impact nNOS restoration to the sarcolemma in order to reduce the disease pathology.

Recently the same group has reported that only the expression of naturally phased repeats 16 and 17 is sufficient to restore nNOS to the sarcolemma in mouse muscle, since the presence of  $\alpha 2$  and  $\alpha 3$  helices of dystrophin repeats 16 and 17 form a domain in the  $\alpha 1$  helix of dystrophin repeat 17 that is responsible for nNOS binding to dystrophin (Lai *et al.*, 2013). However, despite extensive research in the last decade, the mechanism of dystrophin and nNOS interaction is not completely understood and requires further research (Li *et al.*, 2011a).

Several studies have explored the correlation between deletion of different hinges with disease severity (Carsana *et al.*, 2005; Banks *et al.*, 2010). The presence of hinge 2 or hinge 3 affects flexibility of the rod domain (Banks *et al.*, 2010). Hinges separate the nested spectrin-like repeats, allowing more flexibility in the rod domain. Experiments using several mini- and micro-dystrophins have shown that replacing hinge 2 with hinge 3 led to improvement in the dystrophic phenotype of the mdx mouse. The inclusion of the polyproline site in hinge 2 with a large deletion in the hinge 3 region led to ringed and small myofibres, disruption of myotendinous and abnormal neuromuscular junctions in mdx gastrocnemius muscles. In contrast, replacing hinge 2 (exon17) with hinge 3 significantly prevented muscle degeneration and improved muscle function (Harper *et al.*, 2002). Both hinges contain six prolines which disrupt the alpha-helical structures. Prolines in hinge 3 are evenly spaced but five of the six prolines in hinge 2 are grouped together. It has been proposed that the location of this polyproline sequence within the truncated rod domain is associated with a severe structural disruption affecting the connection between F-actin and  $\beta$ -dystroglycan. In contrast, the presence of hinge 2 in full-length dystrophin, containing a larger number of spectrin-like repeats between the hinge and the  $\beta$ -dystroglycan binding domain, allows greater flexibility in the dystrophin structure. This led to the suggestion that the rigid alpha-helical structure of the polyproline site significantly reduces the flexibility of truncated dystrophins which is required for connection between the cytoskeleton and extracellular matrix (Banks *et al.*, 2010). These data suggest that the polyproline site is not a necessary component of dystrophin and that the consequences of removing or retaining hinges might also depend on the size of deletions and the number of spectrin-like repeats.

The phasing of the repeats and hinges are another important factor for a functional dystrophin (Harper *et al.*, 2002). Constructs which had repeats and hinges joined in ways that did not significantly differ from the natural pattern of these units in dystrophin have proved to be more functional. A construct ( $\Delta$ H2–R19) carrying precisely eight sequential rod domain repeats displayed significant functional improvement in mdx mouse compared to a similar construct ( $\Delta$ exon 17-48) containing 1 partial and 8 repeats as a result of deletion of the relevant exons (Harper *et al.*, 2002).

To sum up, large in-frame deletions in the rod domain do not severely disrupt the muscle function as long as the reading frame is preserved. However, the rod domain cannot be completely deleted or their domains replaced by homologous domains from other proteins and the precise order and phasing of the retained domains is crucial (Harper *et al.*, 2002; Carsana *et al.*, 2005).

### **1.6.8 *Clinical trials and current status of DMD gene transfer therapy***

Although efficient gene transfer of truncated versions of dystrophin has been reported in various mouse models, there are still several issues that need to be addressed when using viral vectors in larger animal models or patients. One of the major hurdles in viral vector-mediated gene therapy remains the host immune response (Odom *et al.*, 2007). The only human trial with rAAV mediated mini-dystrophin gene delivery resulted in transgene-specific T-cell immune reaction. Six boys with frame-shifting deletions participated in this study which started in March 2006 and completed in April 2009. The AAV used for this trial was produced by Asklepios Biopharmaceutical (Mendell *et al.*, 2010). rAAV-mediated micro-dystrophin  $\Delta$ D3990 was injected into patient's biceps. Some of patients displayed increased T-cell immune response against the viral vector. At least one patient showed mini-dystrophin specific T-cell immune response 15 days post treatment. None of the treated patients showed significant dystrophin levels. The T-cell reaction against the transgene was thought to be as a result of a low level of dystrophin expression in revertant fibres that are found in DMD patients (Mendell *et al.*, 2010). A recent study involving 70 DMD patients has shown anti-dystrophin T-cell immune response in ~28% of patients (Flanigan *et al.*, 2013). In a different study, it has been

shown that transient immunosuppression prevented T-cell activity in the dystrophic dog model (Gregorevic *et al.*, 2009).

A major issue for a gene replacement therapy is that a successful transgene delivery depends on the disease progression, the degree of fibrotic tissue and the level of intact dystrophin fibres. A combination of gene replacement therapy with cell therapy may have more efficacy for patients in later stages of the disease (Seto *et al.*, 2014).

## **1.7 Statement of aims**

Design and production of truncated miniaturised versions of dystrophin encoding specific domains to investigate the structural and functional benefits gained from these domains, whilst maintaining a size capable of being packaged into lentiviral vectors.

*In vivo* gene transfer of the mini-dystrophins in mdx mouse muscle using intramuscular injection and electroporation; evaluation of the expression and subcellular localisation of mini-dystrophins.

Analysis of the level of dystrophin expression and the number of transfected fibres; evaluation of morphological changes including internal nuclei and myofibre size distribution.

Investigating the ability of mini-dystrophins to restore DGC proteins such as the sarcoglycan complex and nNOS.

Determination of the overall suitability of different constructs for preclinical studies including cloning into lentiviral vectors for stem cell transduction into dystrophin-deficient skeletal muscle.

Identification of key elements of the dystrophin molecule required for optimal functionality following gene transfer.

## Chapter 2 Materials and Methods

### 2.1 Standard molecular biology techniques

#### 2.1.1 *Polymerase chain reaction (PCR)*

PCR amplification was conducted using a thermal cycler (SensoQuest, Labcycler 48). The amplification parameters depended on the template and primers. Primer sets used in this project are listed in appendix A and B. Usually the PCR reaction was prepared in a 50  $\mu$ l reaction mixture as listed below:

Component	Volume (50 $\mu$ l)
5x Phusion Buffer	10 $\mu$ l
dNTPs (10 mM)	1 $\mu$ l
Forward primer (5 $\mu$ M)	2 $\mu$ l
Reverse primer (5 $\mu$ M)	2 $\mu$ l
DNA (50 ng/ $\mu$ l)	2 $\mu$ l
Phusion DNA Polymerase	0.5 $\mu$ l
Nuclease-Free Water	32.5 $\mu$ l

PCR reactions were run using the following program:

1. Initial denaturation: 94 °C for 5 minutes
  2. Denaturation: 94 °C for 30 seconds
  3. Annealing: 60 °C for 30 seconds
  4. Extension: 72 °C for (30 seconds-3 minutes, depending on the fragment size)
  5. Last extension: 72 °C for 5 minutes
- 30-35 cycles for steps 2-4. Hold at 4 °C

#### 2.1.2 *Agarose gel electrophoresis*

0.8-1.5 % agarose gels (Lonza) were prepared (Table 2.1). 1-5  $\mu$ l of samples and 1-2  $\mu$ l of 6x Loading Dye (New England BioLabs) were loaded and gels run at 5 V/cm in 1x TAE buffer for 60-90 minutes until optimal migration was obtained. DNA was visualised under UV light, using GelDoc-it 310 Imaging System (UVP). Size of DNA fragments were determined relative to 1 kb DNA

Ladder (New England BioLabs) 100 bp DNA Ladder (New England BioLabs) or Lambda DNA *Hind*III Digest (New England BioLabs).

### **2.1.3 *DNA purification by gel extraction***

For the isolation and purification of a single DNA band, the desired product was excised, extracted and purified from the agarose gel using QIAquick Gel Extraction Kit (Qiagen) according to manufacturer's recommendations.

### **2.1.4 *Digestion of DNA using restriction endonucleases***

Reactions were prepared by pipetting DNA, buffer and water together, vortexing the mixture and adding the enzymes. Samples were incubated according to manufacturer's recommendations under optimal conditions for the enzyme. Digested products were run on an agarose gel for quantification or isolation of particular bands. In the case of double or triple digestion, simultaneous digestion was performed according to manufacturer's instructions.

### **2.1.5 *DNA measurement***

DNA concentrations were determined using NanoDrop spectrophotometer (Thermo Scientific, NanoDrop 2000).

### **2.1.6 *PCR or restriction digest purification***

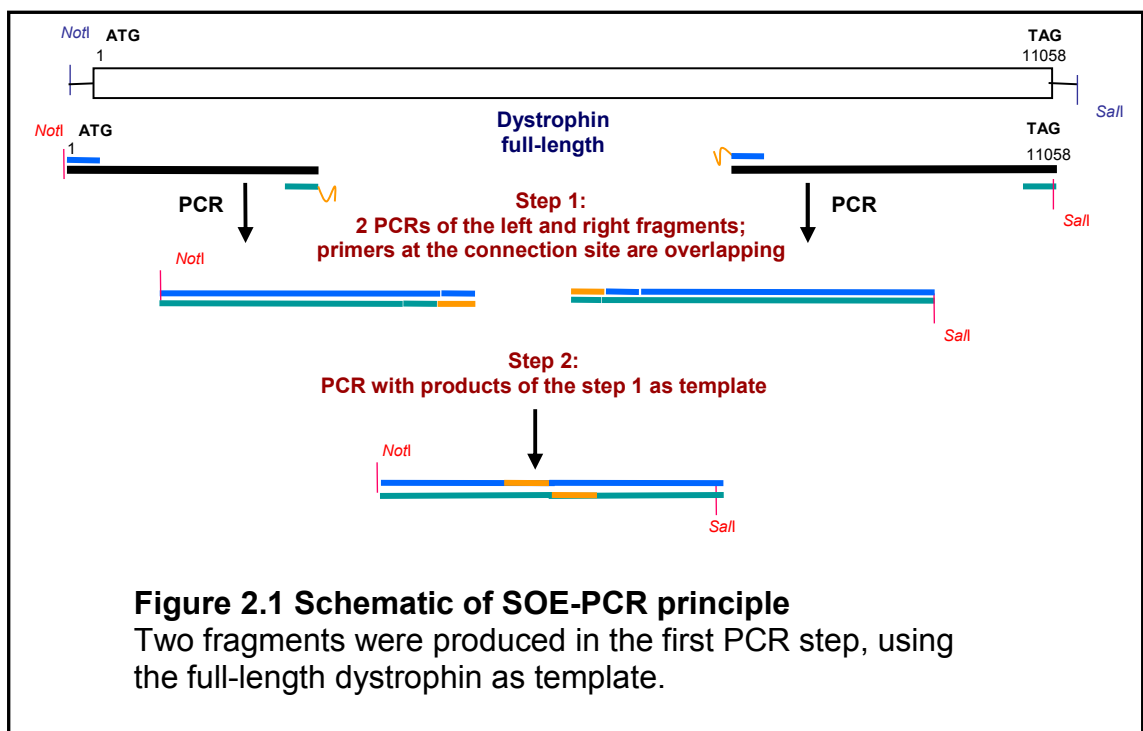
PCR fragments or digestion products were purified with the QIAquick PCR Purification Kit (Qiagen). The procedure was performed using a microcentrifuge (Eppendorf 5417R), according to manufacturer's recommendations.

### **2.1.7 *DNA sequencing***

Sequencing was carried out by sequencing service MWG Biotech in Ebersberg, Germany. 15 µl of purified plasmid DNA or PCR products at a concentration of 50 ng/µl were sent with 15 µl of the appropriate primer at 5 pmol/µl.

## 2.2 Splicing by overlap extension polymerase chain reaction (SOE-PCR)

SOE-PCR was used to create defined deletions in cDNA clones which included two different PCR steps. Primers were designed for two gene fragments flanking the region to be deleted. The reverse primer of the left fragment contained an overhang sequence complementary to the forward primer of the right fragment. The forward primer of the left fragment and the reverse primer of the right fragment contained an endogenous or engineered unique restriction enzyme site. In the first PCR reaction the fragments were amplified using the standard PCR protocol. Upon a successful PCR at the expected sizes for each of the two PCR products, the resulting products were purified using QIAquick PCR Purification Kit (Qiagen) and 5 µl of each template was added to a PCR tube. If one PCR product was judged to be in a lesser amount, the reaction was compensated by adding another 1-5 µl of it. No primers were added in this step as the templates primed each other. 15 PCR cycles were used for amplification. The products were run on an agarose gel to isolate the combined product of the individual fragments and the new products were gel extracted using QIAquick Gel Extraction Kit (Qiagen) and digested for cloning. The principle of the SOE-PCR is illustrated in figure 2.1.



## **2.3 Cloning**

### **2.3.1 Ligation**

The concentration of vector and insert DNA were determined either using the NanoDrop spectrophotometer or by agarose gel against a known amount of standard marker. DNA ligation reactions were prepared using T4 DNA Ligase and T4 DNA Ligase Buffer (New England BioLabs). The reactions were incubated in a total reaction volume of 20  $\mu$ l at room temperature for 10 minutes and heat inactivated at 65 °C for a further 10 minutes. The reaction mixture was used directly for bacterial transformation without further purification.

### **2.3.2 Transformation into chemically competent *E. coli* cells**

XL10-Gold Chemically Ultracompetent Cells (Stratagene), or Methyltransferase Deficient Chemically Competent C2925 *E. coli* Cells (New England BioLabs) suitable for growth of plasmids free of Dam and Dcm methylation, were used for transformation of plasmids. The competent cells were thawed on ice.

100 pg - 1 ng of plasmid or ligation mixture was mixed with the cells. After a short incubation on ice for 15-30 minutes, heat shock was carried out at 42 °C for 45 seconds and samples were immediately placed back on ice for 2 minutes. SOC medium (Table 2.1) was added and the transformed cells were shaken horizontally at 37 °C in a rotating incubator at 200 rpm for 1 hour. Cells were plated out on prewarmed selective medium containing LB medium and Agar (Table 2.1), and 50  $\mu$ g/ml Ampicillin (Sigma) or Kanamycin (Sigma). Plates were incubated at 37 °C overnight.

### **2.3.3 Purification of plasmid DNA**

For clean-up of plasmid DNA, single colonies of transformed bacteria were inoculated in 5 ml of LB medium containing selective antibiotic (Ampicillin or Kanamycin at 50  $\mu$ g/ml), incubated at 37 °C in a shaking incubator for 12-16 hours overnight. The cells were harvested and plasmid DNA was prepared, using QIAprep Spin Miniprep Kit (Qiagen). For larger scale plasmid preparation 50-500 ml of bacterial culture was grown and plasmid extracted with either

EndoFree Plasmid Maxi Kit (Qiagen) or EndoFree Plasmid Mega Kit (Qiagen) following the manufacturer's instructions.

## **2.4 Cell culture**

### **2.4.1 Cells**

Cell culture work carried out for this study varied for each specific cell type including HeLa cells, HEK-293T, C2C12, mdx-immorto and C57BL/10-immorto myoblasts (Jat *et al.*, 1991) (all provided by Morten Ritso, Institute of Genetic Medicine, Newcastle University) and human myoblasts (MRC-CNMD Biobank). In order to keep adherent cells healthy and actively growing it was necessary to subculture them at regular intervals. Apart from C57BL/10-immorto and mdx-immorto lines (incubated and grown at 33 °C), cells were grown at 37 °C and 5% CO<sub>2</sub>, fed every other day and passaged when they reached a seeding density of ~70% and until consistent growth rate and appropriate yield was achieved.

### **2.4.2 Cell expansion**

Generally when cells attained ~70% confluence, they were split into 5x 10 cm<sup>2</sup> petri dishes. To do this the supernatant was removed and the cells washed with 5 ml of sterile 1x PBS (Dulbecco's Phosphate Buffer Saline, Sigma). For splitting, 1 ml of 0.05% Trypsin-EDTA 1x (Life Technologies) was used and incubated for 2-3 minutes at 37 °C and 4 ml of growth medium was added to inactivate the Trypsin-EDTA. The cell suspension was transferred into a 15 ml tube and centrifuged at 450 g for 5 minutes. The supernatant was discarded and cells resuspended in 5 ml growth medium. 1 ml of the cell suspension was dispensed into each of the 10 cm<sup>2</sup> petri dishes and 9 ml of growth medium was added to each petri dish and returned to the incubator. When the cells reached ~70% confluence, cells were ready for freezing and storage.

### **2.4.3 Standard cell culture conditions for immorto myoblasts**

The most used cell lines for this study were mouse mdx-immorto and mouse C57BL/10-immorto myoblasts (Jat *et al.*, 1991). Both cell lines were derived from mdx and C57BL/10 mice that were crossed with transgenic immorto mouse CBA; B10-Tg (*H-2K<sup>b</sup>-tsA58*) carrying the Simian Virus 40 (SV40) thermo-labile large tumor antigen (Jat *et al.*, 1991), a conditional immortalising gene, under the control of the mouse *H-2K<sup>b</sup>* gene promoter. The tsA58TA<sub>g</sub> gene product is expressed in the presence of IFN $\gamma$  and temperature of 33°C. Cells were grown in 75 cm<sup>2</sup> collagen-coated flasks at 33 °C in 5% CO<sub>2</sub> using immorto growth medium (Table 2.2) supplemented with mouse recombinant IFN $\gamma$  (Life Technologies) and allowed to reach ~70% confluence. Cells were detached using trypsin and split as previously described.

### **2.4.4 Immorto myoblast differentiation into myotubes**

After several passaging steps, immorto myoblasts were seeded into collagen-coated flasks or 6-well plates, depending on the experiment. Myotube formation was induced by reducing the serum concentration to 5%. Cells were allowed to grow in immorto growth medium at 33 °C in 5% CO<sub>2</sub> until they reached ~70% density. From this point on medium was replaced by differentiation medium supplemented with 2% Horse Serum (Life Technologies) and temperature was raised from 33 °C to 37 °C to induce myotube formation. The differentiation medium was replenished every other day until cells were fused into myotubes over a period of 2-8 days.

### **2.4.5 Thawing and recovery of frozen cells**

This process was performed very quickly to minimise cell death. Prewarmed medium was prepared in advance. Frozen cryovials were taken from liquid nitrogen and immediately placed in a water bath at 37 °C. The vial was disinfected with 70% ethanol as soon as the ice became detached from the wall of the tube. The content was poured into a 10 cm<sup>2</sup> petri dish containing 8 ml of appropriate growth medium. The plate was shaken and placed in the incubator. After 3-4 hours incubation and cell attachment the medium was changed with 8

ml fresh medium to remove freezing solution and any DMSO residue from the culture.

#### **2.4.6 Freezing of living cells for long-term storage**

Ideally cells were frozen from cultures at low passage number. When cells reached the appropriate density, medium was removed from the flasks/dishes, washed and cells detached using trypsin as described previously. Once cells were detached, 5-10 ml washing medium (Table 2.2) was added to each flask/dish, the cell suspensions were then collected and transferred into a 50 ml centrifuge tube and centrifuged at 350 g and 4 °C for 5 minutes. After centrifugation the supernatant was aspirated with a sterile glass pipette, the pellet resuspended in 5 ml of cold freezing medium (Table 2.2) and quickly dispensed in 5 aliquots into cryotubes placed on ice. The cryotubes were placed in a box and stored at -80 °C for a minimum of 48 hours, before they were transferred to liquid nitrogen for long-term storage.

#### **2.4.7 Cell counting**

When cell number was required, cells were counted using a hemocytometer. Cells were trypsinised as described previously and a uniform cell suspension was obtained and placed in a conical centrifuge tube. The cell suspension was pipetted up and down in the tube 7-10 times. 100 µl of the cell suspension was placed into a new Eppendorf tube and 100 µl Trypan Blue (Sigma) was added and mixed gently. Four corner squares of the hemocytometer were selected and using a hand tally counter, the number of cells in this area of 16 squares was counted and the average was calculated. The total number of cells was determined using the 10x objective of the microscope Motic AE20. The live cells (unstained by Trypan Blue) were counted and dead cells (stained blue) could be counted separately for estimating viability. The number of cells per ml was calculated following this formula: Cells/ml = number of cells counted/number of squares counted x 10<sup>4</sup> x dilution factor. Total cells = cells/ml x vol. of original suspension. The percentage of viable cells was calculated as: % viability = (number of viable cells counted/total number of cells counted) x 100.

#### **2.4.8 E6E7 expressing retrovirus supernatant production**

This work and all other viral work was performed at containment level 2, according to the institutional guidelines (Newcastle University, BioCOSH regulations for Microbiological Hazards and Genetic Modification, GM Ref.: 28/10a). A vial of E6E7 virus producing cells was provided by Dr Rolf Stucka (Friedrich Baur Institute, Munich, Germany). Cells were thawed in a 25 cm<sup>2</sup> flask in virus culture medium (DMEM supplemented with 10% FBS) with 0.2 mg/ml G418 Selection Marker (Geneticin, Life Technologies) and cultured for at least two passages, so that the cells proliferated well after thawing and reached ~70% confluence. At this time the medium was replaced with antibiotic-free medium. The supernatant was collected after 24 hours and filtered through a 0.45 µm filter. Aliquots were prepared and stored at -80 °C for long-term storage. For cell transduction including immortalisation 500 µl of the supernatant was used along with medium containing 4 µg/ml Hexadimethrine bromide (Polybrene, Sigma) to infect cells.

#### **2.4.9 Establishment of an immortalised human DMD cell line**

A muscle biopsy with informed consent was obtained in the course of a clinical trial from a Duchenne muscular dystrophy patient (aged 10 years at biopsy) with a deletion in exon 52 which was processed in the MRC-CNMD Biobank. Immortalisation was performed according to the procedure described in the published protocol (Lochmuller *et al.*, 1999). The isolated myoblasts were infected with a retrovirus expressing the E6E7 gene region from human papillomavirus type 16 and the integration of the virus was confirmed by selection of G418-resistant cells for 14 days. Cells were grown in standard skeletal muscle growth medium (Table 2.2) and allowed to reach ~30-50% confluence.

#### **2.4.10 Enrichment of myoblasts in culture**

During the first several passages of the primary cultures, myoblast growth was enhanced by preplating in order to eliminate fibroblasts from the culture. During each subculturing step, the cell suspension was incubated for 20 minutes which

allowed the fibroblasts to settle onto the plastic surface. The supernatant containing a cell population enriched for myoblasts was plated into a new 25 cm<sup>2</sup> flask. At the end of culturing the purity of myoblasts was tested using the early myogenesis marker Desmin (Dako) and expression was visualised using immunohistochemistry as described elsewhere.

#### **2.4.11 Cell transfection using lipofection**

Cells were cultured in the appropriate growth medium for each cell type and seeded into 6-well plates 24 hours before transfection to be approximately 70% confluent upon transfection. For transfection, growth medium was replaced with transfection medium (Table 2.2). Cells were transfected with the mini-dystrophin constructs, using the Lipofectamine 2000 Transfection Reagent (Life Technologies) as per the manufacturer's instructions. Cells were incubated for a further 24-48 hours before harvesting. For each experiment a GFP control was used to evaluate the transfection efficiency and GFP positive cells were visualised using an Axioplan M200 inverted microscope (Zeiss).

#### **2.4.12 Cell transfection using electroporation**

For difficult-to-transfect cells such as myoblasts, cells were transfected by electroporation using Amaxa Nucleofector II (Amaxa Biosystems) and Amaxa Cell Line Nucleofector Kit (Lonza). Cells were grown in 6-well plates and medium was replaced every other day and passaged at least 3 times before electroporation. Cells were seeded at  $1.5 \times 10^5$ – $1 \times 10^6$  viable cells per well. A higher confluence was avoided for the optimal transfection efficiency. Cells were transfected using transfection medium (Table 2.2) and the cell type specific Nucleofector Kit, according to manufacturer's recommendations and analysed 24-48 hours after transfection using light and fluorescence microscopy.

#### **2.4.13 Harvesting cells**

The growth medium was removed from the cells and they were washed in 1x PBS to remove residual serum. For 6-well plates, cells were washed with 1 ml 1x PBS and 250  $\mu$ l of 0.05% Trypsin-EDTA was added to allow removal of the

cells from the flasks before harvesting. Alternatively a cell scraper was used to detach the cells from the plastic surface. The cell suspension was collected and centrifuged at 1300 g for 2 minutes. Cell pellets were washed with 1x PBS, centrifuged again, the supernatant removed and frozen at -80 °C.

#### **2.4.14 Stable transfection of mdx-immorto myoblasts**

Transfection of mdx-immorto myoblasts with mini-dystrophin constructs using Lipofectamine 2000 was performed as previously described. The following day, the standard medium was replaced with medium containing 0.2 mg/ml G418. The G418 concentration and the optimal cell density was determined using titration in 96-well plates as described in the next section. Un-transfected cells were used as a negative control in each experiment to ensure that only cells expressing neomycin (present in mini-dystrophin plasmids) were able to survive. The G418 treatment was continued for 10-12 days and medium changed every other day. 24-well plates with 1 ml media in each well were prepared and stable transfected cells imaged under an inverted microscope (Motic AE20) to select the resistant colonies. A circle was drawn around the positive colonies on the underside of the wells. Cells were washed with 1x PBS, a glass cloning cylinder (Sigma) was placed on the circle and 20 µl of 0.05% Trypsin-EDTA was added on the marked area. A pipette with a sterile tip was lowered to the surface of the colony of interest and the cells transferred to a well in the 24-well plate. In 1-2 days, when cells were confluent, they were split and expanded. Selection of G418-resistant cells was continued for at least 14 days and grown until cell colonies were ready for long-term storage. Different clones were then screened for dystrophin expression by Western blot.

#### **2.4.15 Cells and G418 titration**

A combined titration of the cell numbers and the G418 concentration determined the plating density and the amount of G418. 100 µl medium was preplated into a 96-well plate. 100 µl of cell suspension containing 4000 cells per well was added in the first column and 100 µl from the first column was carried over to the next well, diluting cells in a ratio of 1:2 for each consecutive well (12 wells). 100 µl of the cell suspension in the last well was discarded. The

amount of G418 required was determined by titration of a range between 0.2-1.4 mg/ml by adding 1.4 mg/ml in the first row and decreasing concentrations for the following rows in 0.2 µl steps. The last row was used as control without G418. Cells were incubated in standard conditions, medium was changed every other day and the treatment with G418 continued for 10 days. The G418 concentration was defined as just above the concentration with complete cell death.

## **2.5 Protein electrophoresis and Western blotting**

Cell pellets were lysed in 1% SDS (Sodium Dodecyl Sulfate, Sigma) in 1x PBS. The volume of the buffer depended on the size of the pellet. The cells were lysed by pipetting up and down and placed in a heat block for 5 minutes. For snap-frozen muscle samples and cryostat sections, proteins were prepared in lysis buffer (Table 2.1). 40 mg tissue was placed in a 50 ml Falcon tube and homogenised in 400 µl lysis buffer using a tissue raptor (Qiagen). Triton X-100 was added to a final concentration of 1% and the tubes were placed on ice for 30 minutes. The lysate was centrifuged briefly and transferred to Eppendorf tubes and spun at 700 g and 4 °C for 10 minutes. The supernatant was transferred into a clean Eppendorf tube and spun down at full speed for 30 minutes. The resulting pellet containing membrane protein was lysed in 50 µl lysis buffer. Protein concentration was measured using the BCA Assay (Bicinchoninic Acid Assay, Sigma), according to the manufacturer's recommendations. 25 µg of protein in a final volume of 20 µl was placed in an Eppendorf tube. 7.5 µl NuPAGE LDS Sample Buffer 4x (Life Technologies) and 3 µl NuPAGE Reducing Agent 10x (Life Technologies) were added to the sample which was put onto a heat block for denaturation at 95 °C for 5 minutes. 10 µl SeeBlue Protein Ladder (Life Technologies) and the total volume of samples (30 µl) were loaded on Novex NuPAGE 3–8% Tris–Acetate Gels (Life Technologies) and the tank (Life Technologies, Novex Mini-Cell) was filled with Tris–Acetate running buffer. The gel was run at 150 V for 2 hours. Proteins were transferred onto PVDF membranes (GE Healthcare) in a transfer tank (Mini Trans-Blot Electrophoresis Transfer Cell, BIO-RAD), containing chilled 1x transfer buffer (Table 2.1) and surrounded by ice at 350 mA for 1.5 hours. Immediately after transfer the membrane was blocked in 5% milk powder in 1x

TBST (Table 2.1) on a shaker for 1 hour. The milk solution was drained and the membrane placed in a plastic bag. Primary antibody Anti-Dystrophin Mandra1 (abcam), 1:1000 or NCL-DYS3 1:125 (Novocastra), diluted in 5% milk in 1x TBST solution was added to the membrane and incubated in the sealed bag in the cold room on a shaker overnight. The next day primary antibody was drained off and membrane rinsed three times in 1x TBST for 10 minutes. Anti-Mouse IgG Horseradish Peroxidase-Conjugated Secondary Antibody (Dako, 1:1000), diluted in 5% milk powder in TBST was added to the membrane and incubated at room temperature on a shaker for 1 hour. The washing steps used for the primary antibody were applied and the protein bands were detected in dark room using ECL Prime Western Blotting Detection Reagent (GE Healthcare) on photographic film or visualised using a Multi Spectral Imaging System (UVP).

## **2.6 Immunofluorescence and histology**

### **2.6.1 *Cryosectioning of muscle tissue***

8 µm serial sections of frozen muscles were cut with a cryotome (MICROME HM560, Zeiss) and mounted on Superfrost Plus Slides (VWR) along the entire TA muscle, separated by intervals of about 100 µm between the sets of serial sections. Intervening sections were collected in Eppendorf tubes for protein extraction. Slides were stained immediately or wrapped in cling film and stored at -80 °C.

### **2.6.2 *Haematoxylin-Eosin (H&E) staining***

Slides were air-dried for 30 minutes and stained with Haematoxylin Harris (VWR) for 3 minutes. After a wash step in running tap water for 2 minutes they were dipped in 1% HCl (Hydrochloric Acid, Fluka; diluted in 70% ethanol) for 5 seconds and rinsed in tap water for 30 seconds. For staining of the cytoplasm Eosin (1% AQUEOUS, VWR) was applied for 30 seconds followed by rinsing the slides under running tap water for a further 30 seconds. Slides were dipped in an ascending alcohol series of 70%, 90% and 100% for 5 seconds each and placed in HistoClear (National Diagnostics) twice for 3 minutes each. The slides

were then mounted with DPX Mounting Medium (LAMB) and allowed to dry overnight. Images were captured using an Axioplan2 Imaging Microscope (Zeiss).

### **2.6.3 *Immunofluorescent labelling of cultured cells***

Cells were seeded either onto coated 8-well chamber slides (Lab-Tek) or in 6-well plates containing cover slips inside the wells and allowed to reach the appropriate growth, depending on the cell type. Medium was aspirated, cells were washed with 1x PBS and then fixed in 4% PFA (Paraformaldehyde, Sigma) at room temperature for 10 minutes before washing in 1x PBS. 0.25% Triton X-100 (Sigma) was applied for permeabilisation of cell membranes. The cells were then blocked with 4% BSA (Bovine Serum Albumin, Sigma) or 10% Goat Serum (abcam) in 1x PBS for 1 hour. Primary antibody was diluted in the same blocking solution, added to cells and incubated at room temperature for 1 hour. Cells were then washed three times in 1x PBS for 15 minutes and incubated with a secondary antibody diluted in blocking buffer at room temperature for 1 hour and washed as previously described. Slides were mounted and nuclei were stained with DAPI Mounting Media Vectashield (Vector Laboratories). Cells were visualised with an AxioImager.Z1 (Zeiss).

### **2.6.4 *Immunofluorescence labelling of muscle tissue***

Slides were allowed to equilibrate to room temperature. Sections were circled with a Water-Repellent Barrier Pen (Vector Laboratories) and washed in 1x PBS for 15 minutes. For each experiment secondary-only antibody controls, wild type (C57BL/10) tissue sections and dystrophic sections (mdx) were included as controls alongside the mini-dystrophin transfected muscle sections. Slides were blocked in blocking solution (4% BSA in 1x PBS) for 30 minutes. If a secondary goat antibody was used, the samples were blocked in a 20% goat serum in 1x PBS. Primary antibodies were diluted in blocking medium. Sections were then incubated at room temperature for 1 hour following three washing steps in 1x PBS for 10 minutes each. Sections were incubated with secondary antibodies (diluted in blocking medium), washed as previously described, mounted in Vectashield with DAPI and visualised under an Axioimager.Z.1

Microscope (Zeiss). A list of primary antibodies and dilutions used in this project is shown in this work (Appendix C).

### **2.6.5 *Direct antibody labelling for immunofluorescence***

This method was performed for staining of mouse tissue using mouse antibodies. The direct labelling was conducted by Zenon Alexa Fluor 488 Mouse IgG1 Labelling Kit (Life Technologies). 1 µg of antibody was prepared in a maximum volume of 20 µl. 5 µl of component A was added to the antibody and incubated for 5 minutes at room temperature followed by addition of 5 µl of component B to the mixture and incubation for 5 minutes at room temperature. The antibody complex was diluted using standard protocol for the primary antibody and applied for staining.

### **2.6.6 *Production of VSV-G lentivirus***

Lentivirus with a VSV-G envelope can infect most mammalian cells; therefore all work was performed at containment level 2, according to the institutional guidelines (Newcastle University, BioCOSHH regulations for Microbiological Hazards and Genetic Modification, GM Ref.: 28/10a). Four plasmids including the envelope plasmid (pMD2-VSV-G), the core packaging plasmid (pMDLg/pRRE), the plasmid expressing REV protein (pRSV-REV) and the transfer vector plasmid (pCCL.sin.PPT.prom.EGFP.EWpre), subcloned with mini-dystrophins were transfected into the packaging cell line HEK-293T to create the infectious viral particles. The transfer constructs carried the mini-dystrophins C1/ΔR3-R13 and C2/ΔH2-R19 driven by the desmin promoter or GFP under control of the CMV promoter which was used as a control. GFP transfected cells were examined using an Axioplan M200 inverted microscope (Zeiss). The virus supernatant was collected 20, 30 and 48 hours after transfection.

## **2.7 Image analysis**

### **2.7.1 *Morphometric parameters***

Digital images of the electroporated muscle sections and controls were used to analyse the pathology-relevant morphometric parameters including percentage of internal nuclei and variability in muscle fibre size. Sections stained for dystrophin, laminin and DAPI were imaged using an AxioImager.Z1 at 20x magnification and analysed with ImageJ software. For assessment of internal nuclei myofibre boundaries were defined. The number of fibres with internal nuclei was given as a percentage relative to all fibres. Fibres were measured by the software including muscle fibre area, Feret's diameter and minimal Feret's diameter. The original scale was converted from pixel to  $\mu\text{m}^2$  using a user-defined setting in the software. The corresponding results were saved and statistics delivered using GraphPad Prism as described in chapter 5.

### **2.7.2 *Fluorescence intensity quantification***

Sections from the electroporated muscles were immunolabelled for dystrophin and laminin and images acquired as previously described. Control muscle sections, expressing dystrophin at normal levels and mdx, were labelled simultaneously. Using ImageJ analysis software the images were split for dystrophin and laminin. Subsequently, a threshold was set to create a mask for measurement of the region of interest. Each region where intensity values were measured covered the entire membrane and background was subtracted from the entire image. The channel for dystrophin was measured and the same region was selected to measure the intensity of the same region as a normalisation value. The ratio of dystrophin and laminin in selected regions was calculated by dividing dystrophin and laminin intensity (median intensity of green divided by median intensity of red). Values were presented in box plots.

## **2.8 Image analysis**

An AxioImager.Z1 Microscope (Zeiss) with an AxioCam HRm Camera was used to capture images. Wild type sections or cells were used to set exposure times

and unstained controls were used to confirm minimal background. A minimum of five pictures were taken of each section. Living cells were viewed with a Motic AE20 or an Axiovert 200M Inverted Microscope (Zeiss) and the images were captured on an AxioCam HRc Digital Camera. An AxioPlan2 Imaging Microscope (Zeiss) was used for H&E staining.

## **2.9 *In vivo* experiments**

### **2.9.1 *Animal care and husbandry***

Wild type *C57BL/10* (BL/10) and *C57BL/10ScSn-Dmd<sup>mdx</sup>* (mdx) mice for this study were bred in the animal facility at the Institute of Genetic Medicine (Elizabeth Greally, Institute of Genetic Medicine, Newcastle University). The mdx colony was maintained homozygously. Breeders were housed as pairs of one male and one female. Animals were maintained according to the standards set by the Functional Genomics Unit (FGU, Institute of Genetic Medicine, Newcastle University). All procedures were approved by the Home Office and were carried out under Animals Scientific Procedures Act of 1986 under the licence number PPL 60/4137.

### **2.9.2 *In vivo* electroporation**

12 week old mdx mice were weighed and anaesthetised with Isoflurane. Pain relief Carprofen or Metacam (at 50 mg/kg or 1 mg/kg respectively; provided by FGU) were administered subcutaneously. Both hind legs were completely shaved and *tibialis anterior* (TA) muscles were injected perpendicularly, first with Hyaluronidase (0.4 U/ $\mu$ l in 25  $\mu$ l of normal Saline, Sigma) then with 50  $\mu$ g of plasmid (1  $\mu$ g/ $\mu$ l – total vol. 50  $\mu$ l) in the central portion of the muscle (0.5 ml insulin needle 3 mm deep). After injecting the second leg, ECG Gel (Camcare Gels) was applied to the first leg and electroporated transcutaneously (settings: 8x 20 ms pulses of 200 V/cm with intervals of 250 ms applied through 2x 1.5 cm<sup>2</sup> stainless steel plate electrodes placed on each side of the leg). Electroporation was performed using BTX ECM 830 electroporation device firstly on the right, followed by the left leg. The plates were placed in such a manner that they did not restrict movement of the leg but were close enough to

form a circuit using the gel. Mice were placed into an incubator for recovery. Mice were euthanised by cervical dislocation, 14 days post injection at an age of 14 weeks and TA muscles were harvested and embedded in 10% Tragant (Gum Tragacanth, Sigma) on labelled cork discs and frozen by immersion in Isopentane (Sigma) cooled in liquid nitrogen for cryosectioning.

## **2.10 Computational analysis**

### **2.10.1 *Primer design***

Primers were designed using Primer3 software, available at <http://primer3.ut.ee>

### **2.10.2 *Sequence alignments***

Sequence alignments were carried out using ClustalW2 at <http://www.ebi.ac.uk/Tools/msa/clustalw2/>, DNAMAN software, Chromas and CodonCode Aligner at <http://www.codoncode.com/aligner/>.

### **2.10.3 *BLAST searches***

Searching regions of similarity between sequences were performed using BLAST (Basic Local Alignment Search Tool). BLAST is available online at <http://blast.ncbi.nlm.nih.gov/Blast.cgi>.

### **2.10.4 *Cloning analysis using PlasmaDNA***

PlasmaDNA program was used for building a visual map of the dystrophin full-length and mini-dystrophin constructs after sequencing of the entire plasmids. This program allows *in silico* simulation of the cloning experiment. The program is freely available for download at <http://research.med.helsinki.fi/plasmadna>.

### **2.10.5 *Image composite editor***

This software was used for creation of the entire muscle cross sections by stitching and combining overlapping images to a single image. This software is

free available at [http://download.cnet.com/Image-Composite-Editor/3000-2192\\_4-10973746.html](http://download.cnet.com/Image-Composite-Editor/3000-2192_4-10973746.html).

### **2.10.6 *ImageJ***

Image Analysis Software ImageJ was used for light microscope image processing and analysis including muscle fibre cross sectional area, Feret's diameter calculation, assessment of pathological internal nuclei within myofibres and pixel value statistics of dystrophin expression density of defined selections. ImageJ can be downloaded from <http://imagej.nih.gov/ij/download.html>.

### **2.10.7 *Statistics***

Statistical analyses were carried out using statistical software GraphPad Prism. Data were first checked for normality of distribution by the D'Agostino & Pearson omnibus normality algorithms, followed by a Bonferroni post-hoc analysis of median between groups. For non-normally distributed data a non-parametric ANOVA (Kruskal-Wallis Analysis of Variance) was performed. Adjusted P-values were determined by multiple comparisons using Tukey's or Dunn's multiple testing. P-Values were given as \*\*\*\*P < 0.0001; \*\*\*P < 0.001; \*\*P < 0.01; \*P < 0.05. The data were summarised showing the median and standard deviation for muscle fibre size, percentage of internal nuclei and expression intensity for each construct in transfected muscles. The resulting data were used to determine a correlation between improvements of transfected muscles among different constructs.

Reagent	Application	Recipe	Supplier
Agarose	Gel electrophoresis	1x Tris-Acetate-EDTA (see below for details), 0.8%-2% agarose and Safe View	Safe View Nucleic Acid Stain (NBS Biologicals), all other components from Sigma
Agar/LB	Transformation/cloning	LB broth + 15 g agar/l	Agar (Fisher Scientific); See SOC medium
LB medium	Transformation/cloning	LB broth (10 g Bacto-Tryptone, 5 g Yeast Extract, 10 g NaCl, dissolved in 1 litre distilled or deionised water, and sterilised by autoclaving)	See SOC medium
Lysis buffer	Homogenisation of tissue	10 mM tris, protease inhibitor (1 tablet/10 ml) and PMSF (10 mg/ml in 98% Ethanol; 5 µl/10 ml added just before use)	Protease inhibitor (Roche), PMSF (Roche)
Running buffer	Western blot	700 ml distilled water and 35 ml 1x NuPAGE Tris-Acetate SDS Running Buffer 20x	(Life Technologies)
SOC medium	Transformation/cloning	0.5% Yeast Extract, 2% Bacto-Tryptone, 10 mM NaCl, 2.5 mM KCl, 10 mM MgCl <sub>2</sub> , 10 mM MgSO <sub>4</sub> and 20 mM Glucose, dissolved in 1 litre distilled or deionised water sterilised by autoclaving; 50 µg/ml Ampicillin just before use	Yeast Extract (Fisher Scientific), Bacto-Tryptone (Fisher Scientific), NaCl (Sigma), KCl (Sigma), MgCl <sub>2</sub> (Sigma), MgSO <sub>4</sub> (Sigma), Glucose (Sigma), Ampicillin (Sigma)
TAE	Gel electrophoresis	1x Tris-Acetate-EDTA (1x TAE= 0.04 M Tris Base, 0.04 M Sodium Acetate and 1 mM EDTA)	All chemicals from Sigma
TBST	Western blot	1x TBST (Tris Buffered Saline with Tween 20, 10x TBST= 87.66 g/l NaCl, 250 ml/l of 2 M Tris, pH 7.8, 5 ml/l Tween 20, in ultrapure water to 1 litre)	All chemicals from Sigma
Transfer buffer	Western blot	1x transfer buffer (10x transfer buffer= 30.3 g/l Tris Base, 144 g/l Glycine)	All chemicals from Sigma

**Table 2.1 Reagents and buffers used in this project**

<b>Media</b>	<b>Applications</b>	<b>Recipes</b>	<b>Supplier</b>
Collagen solution	Coating culture flasks/plates	179 ml dH <sub>2</sub> O, 1 ml Ethanoic Acid (EtOOH, 100% sterilised by filtering with a 0.2 µm filter, solution stored at 4 °C)	EtOOH, 100% (Sigma), Collagen (Sigma)
Differentiation medium	Human and mouse myoblasts	Dulbecco's Modified Eagle's medium (DMEM) + 2% Horse Serum + 1% Penicillin/Streptomycin (Pen/Strep)	DMEM (Life Technologies), Horse Serum (Life Technologies), Pen/Strep 100x (Life Technologies)
Freezing medium	Fibroblasts, HEK293T cells, HeLa cells and myoblasts	70% DMEM, 20% Foetal Bovine Serum (FBS), 10% Dimethyl Sulphoxide (DMSO)	FBS (Sera Laboratories International), DMSO (Sigma)
Immorto growth medium	Mouse immorto cells	DMEM + 20% FBS + 1% Pen/Strep + 15 µg IFN <sub>γ</sub> in 500 ml DMEM	IFN <sub>γ</sub> (Life Technologies)
Skeletal muscle growth medium	Human myoblasts	Skeletal Muscle Growth Medium (SMGM) + supplement mix + 10% FBS + 1.5% Glutamax + 0.3 % Gentamicin	SMGM (Promocell), Glutamax (Life Technologies), Gentamicin (Life Technologies)
Standard growth medium	Fibroblasts, HEK293T cells and HeLa cells	DMEM + 10% FBS + 1% Pen/Strep	See above for details
Transfection medium	HEK293T cells, HeLa cells and myoblasts	OptiMEM + 10% FBS, without antibiotics	OptiMEM (Life Technologies)
Virus culture medium	Viral transduction, immortalisation	DMEM + 10% FBS + 4 µg/ml Hexadimethrine Bromide (Polybrene)	Polybrene (Sigma)
Washing medium	Fibroblasts, HEK293T cells, HeLa cells and myoblasts	DMEM + 10% FBS + 0.4% Gentamicin or 1% Pen/Strep	See above for details

**Table 2.2 Cell culture media used in this project**

## Chapter 3 Design, construction and characterisation of mini-dystrophin constructs

### 3.1 Introduction

Gene replacement therapy is considered as a promising approach for treatment of Duchenne muscular dystrophy. One of the major challenges of this method is the large size of the dystrophin cDNA of ~14 kb, exceeding the packaging capacity of conventional viral vectors. Therefore smaller versions of the gene are needed to facilitate dystrophin gene therapy via viral vectors. The idea of generating smaller versions of dystrophin is based on studies in Becker muscular dystrophy patients with large in-frame deletions who present with a mild phenotype and prolonged life expectancy relative to Duchenne muscular dystrophy patients. Reports on transgenic mice expressing mini- and micro-dystrophins and by deleting coding sequences for different parts in the cDNA have identified regions dispensable for dystrophin function (Dickson *et al.*, 2002; Harper *et al.*, 2002; Lai *et al.*, 2009a; Lai *et al.*, 2013). These miniaturised genes can be introduced into viral vectors including AAV and lentiviral vectors. This chapter aims to construct highly functional dystrophin mini-genes following consideration of several factors required for rod domain functionality such as the number of repeats, presence or absence of internal hinge domains, and retention of specific domains such as the nNOS binding site, the second actin-binding domain and the C-terminus with focus on constructs within the packaging capacity of lentiviral vectors with the aim that these could be introduced into muscle stem cells. It was hypothesised that engineering smaller deletions in the rod domain including various regions to form constructs as close to the full-length as possible would lead to functional improvement of the mini-genes and might enable us to explore how the deletion of individual repeat units or other domains affects the overall gene function. Particularly, it was planned to include some constructs capable of restoring nNOS to the sarcolemma. In this chapter construction and characterisation of mini-dystrophin constructs is demonstrated.

## **3.2 Aims**

Rational definition and design of mini-dystrophin constructs that retain key functional elements of dystrophin at the protein level.

Provision of a standard method and protocol for construction of truncated mini-genes that can be applied to introduce deletions in any part of the dystrophin molecule.

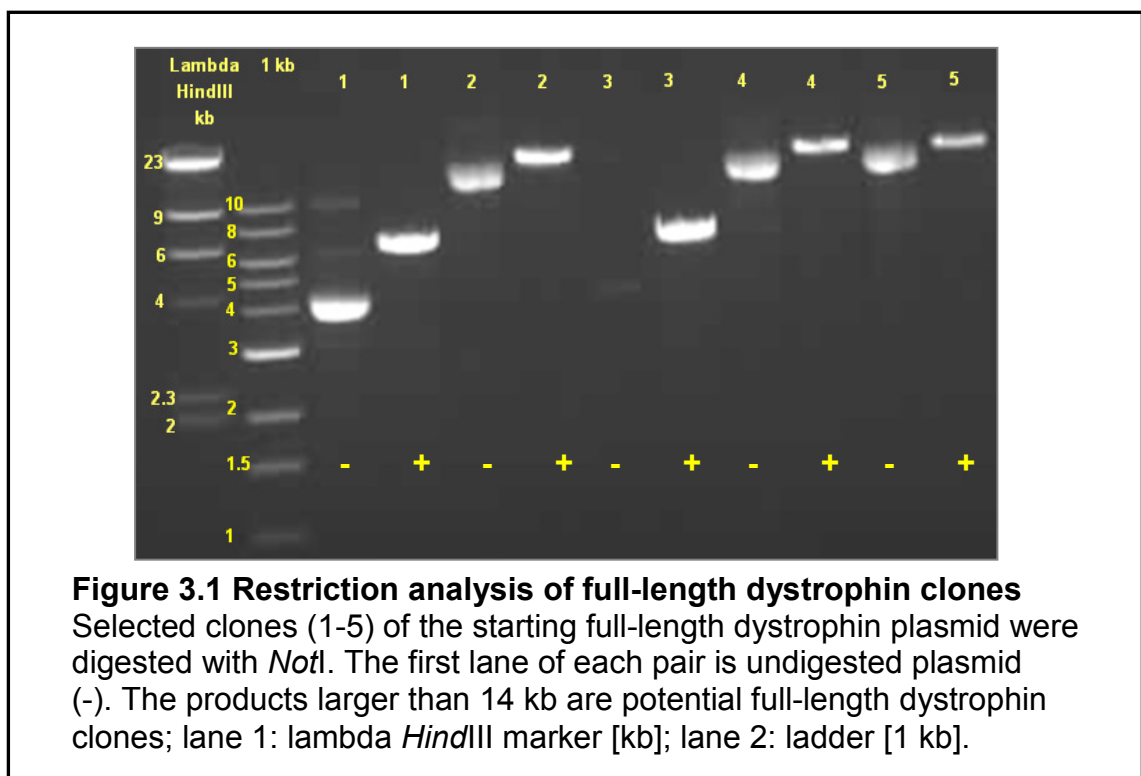
Characterisation of the mini-dystrophin constructs and verification of the translational reading frame.

Investigation of the construct expression after transfection into HeLa cells to confirm expression levels and sizes of the expressed mini-dystrophins.

### 3.3 Characterisation of a human full-length dystrophin plasmid as the initial clone

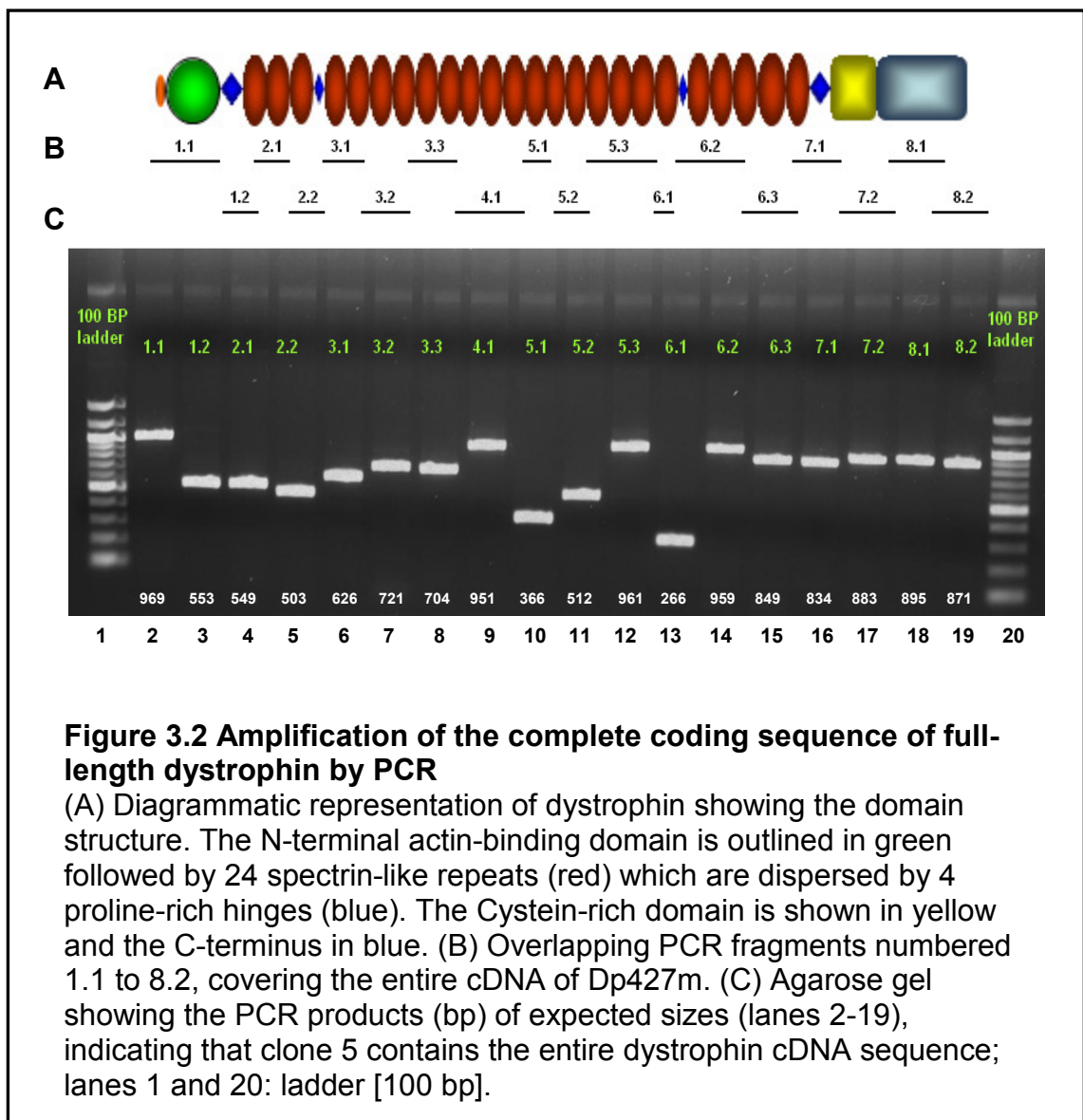
#### 3.3.1 Restriction analysis of full-length dystrophin clones

A plasmid containing the entire human coding sequence for the Dp427m isoform of dystrophin (the major isoform in muscle) was kindly provided by Rolf Stucka, Friedrich-Baur Institute, Munich, Germany. The sequence and a map of this plasmid were not available. Therefore a classical plasmid characterisation procedure was carried out. The plasmid was transformed into XL1-Blue competent cells. Colonies were selected, purified and digested with *NotI* and separated on an agarose gel. The resulting bands and their different sizes (Figure 3.1) indicated a mixture of various plasmids in the initial sample. Given the expected cDNA size of approximately 14 kb, the plasmid size was expected to be larger than 14 kb. Based on these assumptions, clones 2, 4 and 5 (Figure 3.1) seemed to have the correct size. Clone 5 was selected for further characterisation.



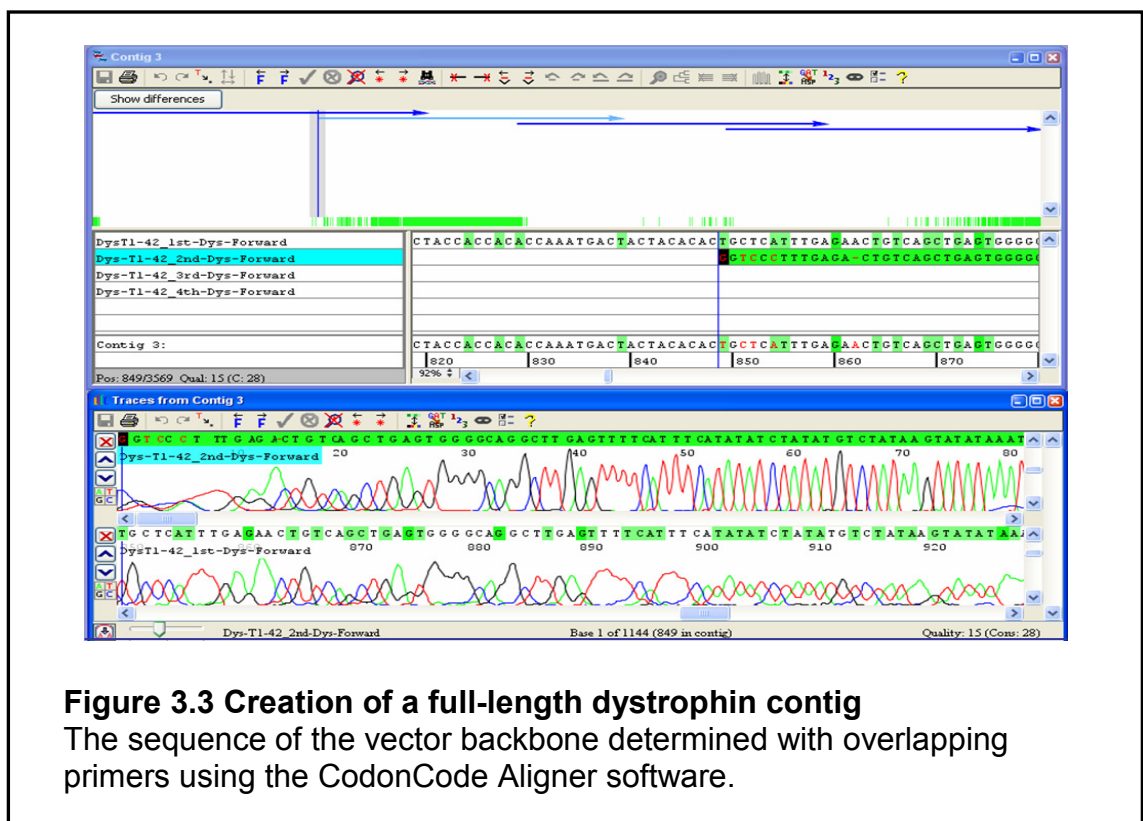
### 3.3.2 Amplification of the complete dystrophin coding sequence

In order to characterise the insert of clone 5, PCR amplification of the entire human dystrophin cDNA was performed using 18 overlapping primer pairs (primers kindly provided by Ralf Herrmann, Clinic for Paediatrics I, University Hospital, Essen, Germany). A table of these primers is attached as appendix A. The amplification resulted in 18 fragments of the expected sizes as published by Rinninsland *et al.*, 1992, indicating that this clone contained a complete dystrophin cDNA sequence (Figure 3.2).

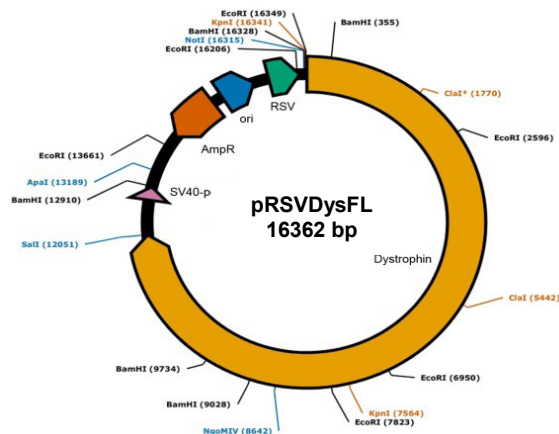


### 3.3.3 Primer walking and sequencing of clone 5

Since no detailed sequence information of the dystrophin vector or the multiple cloning sites and the adjacent regions of insert and vector were available, a complete sequence analysis for the clone 5 was performed to verify its properties. Sequencing started from the known sequence of the dystrophin insert, using cDNA primer 1.1R for the 5' and 8.2F for the 3' regions into the vector. The sequencing results were used as templates for the design of the next overlapping primers and this procedure was repeated four times until the entire vector backbone was sequenced. A contig of the vector was created using the sequencing data and the CodonCode Aligner software (Figure 3.3; <http://www.codoncode.com/>). The sequencing results revealed that the complete full-length dystrophin plasmid contained 16362 bp consisting of 4314 bp of vector and 12048 bp of coding and non-coding sequence of dystrophin cDNA (Figure 3.4).



**A**



**B**

Bp	Elements
1–155	Dystrophin 5'-UTR
156–11213	Dystrophin coding sequence (ATG–TAG)
11214–12048	Dystrophin 3'-UTR
12049–16363	Vector
12666–12900	SV40 polyadenylation signal
14730–13871	AmpR (counter-clockwise)
14902–15480	Origin pBR322
15732–16243	RSV promoter
16296–16362	MCS

**C**

**Multiple cloning site**

*HindIII*    *BglII*    *NotI*    *BamHI*    *KpnI*    *EcoRI*  
 ...AGCTTCTAGAGATCTGAGCGGCCGCTCTAGAEGATCCCGGGTACCAGGCTCGAATTC...  
**5'-UTR (Dystrophin)**  
 CGGAGAAAAACGAATAGGAAAACTGAAGTGTACTTTTTTTAAAGCTGCTGAAGTTTGTTG  
 GTTCTCATTGTTTTTAAGCCTACTGGAGCAATAAAGTTTGAAGAAGTTTACCAGTTTTT  
 TTTATCGCTGCCTTGATATACACTTTTCAAATGCTTTGGTGGGAAGAAGTAGAGGACTGTT  
 ATGAAAGAGAAGATGTTCAAAGAAAACATTCACAAAATGGGTAAATGCACAATTTTCT...  
**3'-UTR**  
 ...GTCCGACAGCAGTCAGCCTATGCTGCTCCGAGTGGTTGGCAGTCAAACCTCGGACTCCATG  
 GGTGAGGAAGATCTTCTCAGTCTCCCGAGGACACAAGCACAGGGTTAGAGGAGGTGATGGA  
 GCAACTCAACAACCTTCCCTAGTTCAAGAGGAAGAAATACCCCTGGAAAGCCAATGAGAG  
 AGGACACAATGTAGGAAGTCTTTTCCACATGGCAGATGATTTGGGCAGAGCGATGGAGTCC  
 TAGTATCAGTCATGACAGATGAAGAAGGAGCAGAATAAATGTTTTACAACCTCC

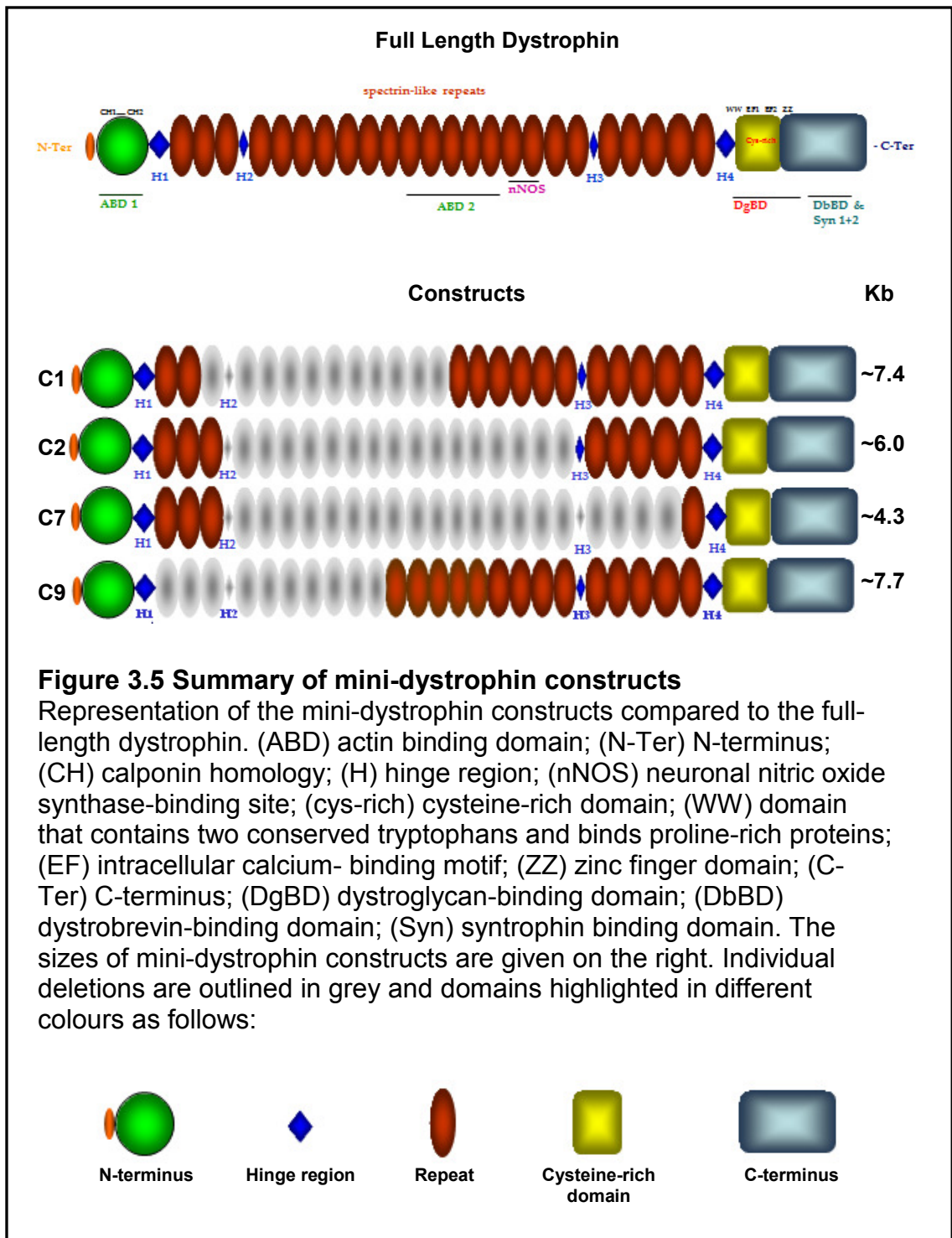
**Figure 3.4 Characterisation of the full-length dystrophin (pRSVDysFL)**

(A) Map of the full-length dystrophin (pRSVDysFL) showing the restriction enzymes used in this project and the multiple cloning site. The map of the full-length dystrophin is annotated using the PlasmaDNA program (<http://research.med.helsinki.fi/plasmadna>). (B) Identification of vector elements; the vector backbone and the structural elements were identified by BLAST searches and different components defined by the alignment of the published sequences to these elements. Abbreviations: SV40-PolyA (Simian Virus 40 Polyadenylation Sequence), AmpR (Ampicillin Resistance), Ori (Origin of Replication), RSV (Rous Sarcoma Virus Promoter). (C) Multiple cloning site and the start codon at the 5' end and the region showing the stop codon. The dystrophin cDNA is cloned via *NotI* at the 5' end and *Sall* at the 3' end (not shown). The untranslated regions in this construct are 155 bp at the 5' and 836 bp at the 3' ends derived from the wild type human sequence.

### **3.4 Construction of mini-dystrophin constructs**

#### **3.4.1 *Rational definition of mini-dystrophins***

Four truncated mini-dystrophin constructs were engineered from the full-length human dystrophin cDNA. Individual domains were defined according to the reference sequence (accession number NP\_003997) obtained from the National Centre for Biotechnology Information (NCBI). The dystrophin mini-genes were of a size to allow them to be packaged within conventional lentiviral vectors. Several factors important in the design of mini-dystrophins were identified including the preservation of the entire N- and C-terminal regions, cysteine-rich domain, four or more spectrin-like repeats and two or more hinge regions. Two of these mini-genes maintain repeats 16 and 17 among the retained repeats of the rod domain. All constructs contain hinge 1 and hinge 4. The construct C9/ $\Delta$ R1-R10 retains the second actin-binding domain (ABD2; repeats 11-15) and was generated under my supervision with the technical help of Stephanie Carr (undergraduate student, School of Biology, Newcastle University), during her bachelor degree in Cellular and Molecular Biology. A summary of all constructs is highlighted in this section (Figure 3.5; Table 3.1) and detailed descriptions of individual constructs will be given in the relevant sections.



### 3.4.2 Construction of mini-dystrophin C2/ $\Delta$ H2-R19

To illustrate the design, construction and characterisation of mini-dystrophin constructs, C2/ $\Delta$ H2-R19 will be used as an example including splicing by overlap extension polymerase chain reaction (SOE-PCR), subcloning of the construct into an expression vector, overlap-PCR of the entire coding sequence, sequencing and confirmation of the reading frame. Construct C2/ $\Delta$ H2-R19 has a deletion in the central rod domain relative to wild type dystrophin including hinge 2 and repeats 4-19 (16 repeats), resulting in a truncated dystrophin protein predicted to be 222 kDa. The corresponding truncation at the transcript level is 5106 bases between nucleotide 1993 and 7098, connecting glutamine at position 664 directly to glutamic acid at position 2367 in the protein (Figure 3.6A).

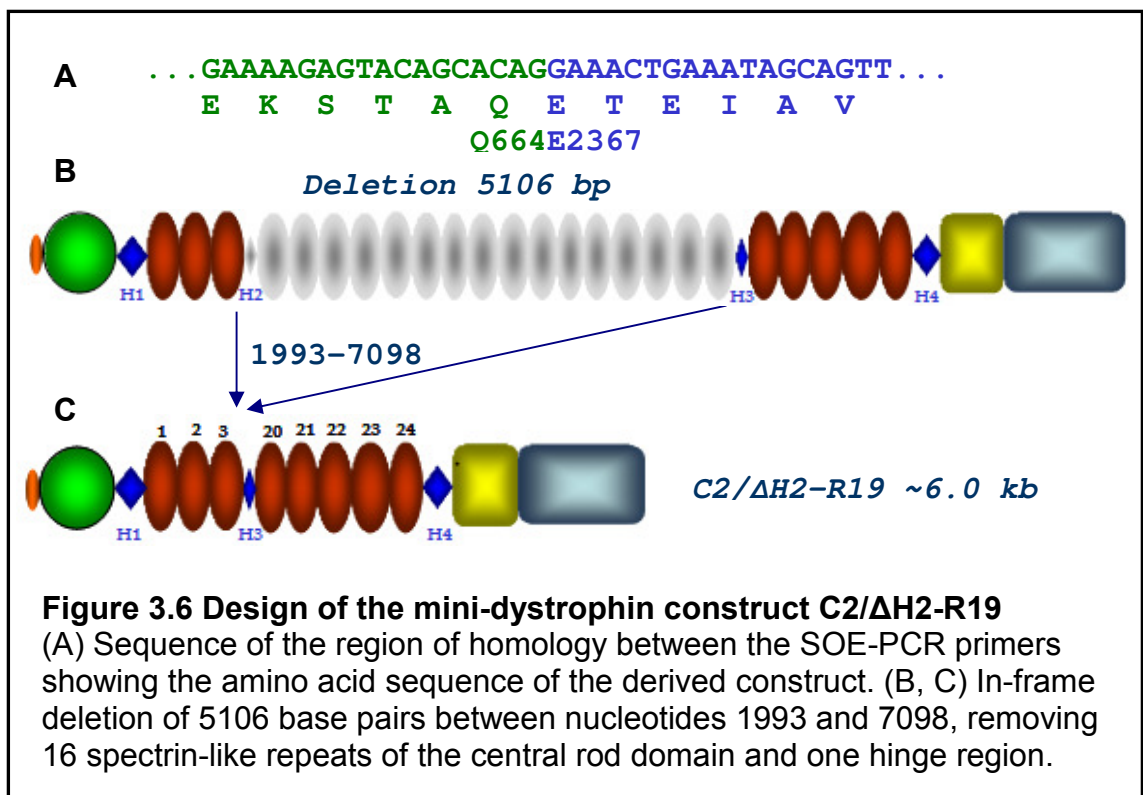


**Figure 3.6 Design of the mini-dystrophin construct C2/ $\Delta$ H2-R19**

(A) Sequence of the region of homology between the SOE-PCR primers showing the amino acid sequence of the derived construct. (B, C) In-frame deletion of 5106 base pairs between nucleotides 1993 and 7098, removing 16 spectrin-like repeats of the central rod domain and one hinge region.

### 3.4.3 SOE-PCR of mini-dystrophin C2/ $\Delta$ H2-R19

The C2/ $\Delta$ H2-R19 construct carries the major functional parts of dystrophin including the N-terminal actin-binding domain, cysteine rich domain and C-terminal region. This construct was generated from the full-length dystrophin cDNA using SOE-PCR primers C1/C2-F1-*Clal* and C2-R1 to amplify the left fragment and C2-F2 and C1/C2-R2-*NgoMIV* to amplify the right fragment (Figure 3.7A), resulting in 378 bp and 1391 bp products (Figure 3.7B). Primers C2-R1 and C2-F2 contained mutually homologous sequences on each 3' end to enable the two fragments to be combined in a second PCR step (SOE-PCR), creating a 1769 bp product (Figure 3.7C).

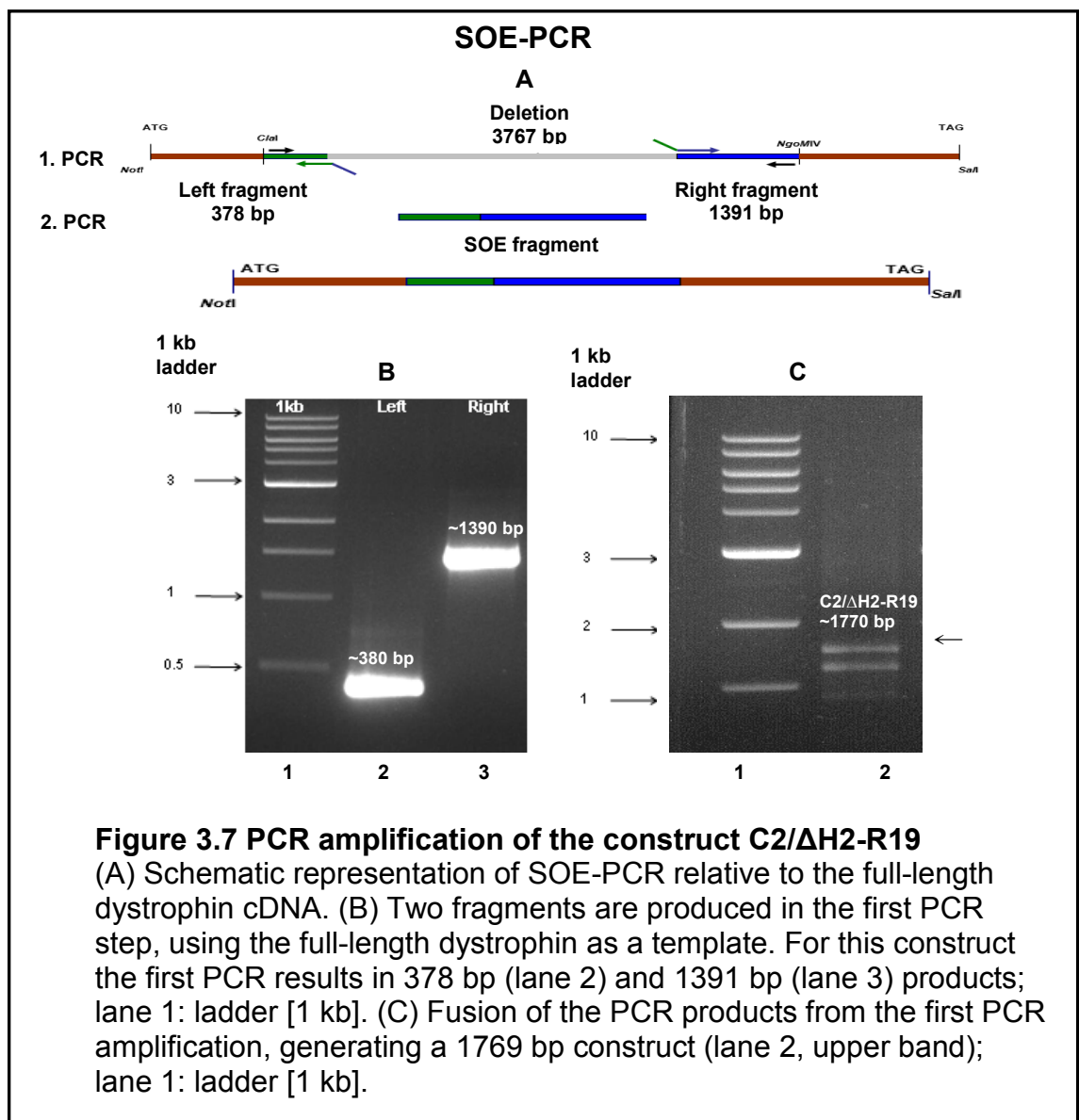
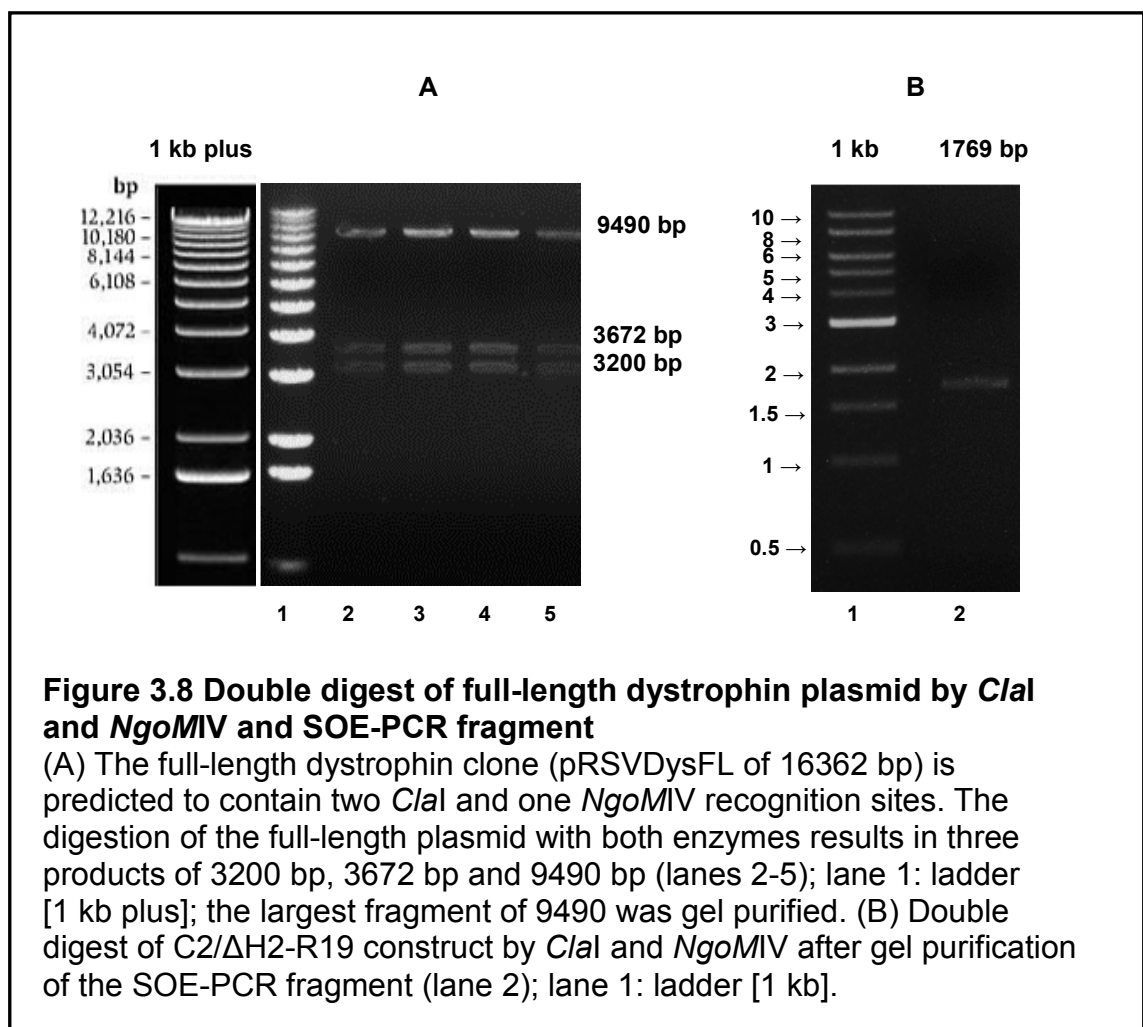


**Figure 3.7 PCR amplification of the construct C2/ $\Delta$ H2-R19**

(A) Schematic representation of SOE-PCR relative to the full-length dystrophin cDNA. (B) Two fragments are produced in the first PCR step, using the full-length dystrophin as a template. For this construct the first PCR results in 378 bp (lane 2) and 1391 bp (lane 3) products; lane 1: ladder [1 kb]. (C) Fusion of the PCR products from the first PCR amplification, generating a 1769 bp construct (lane 2, upper band); lane 1: ladder [1 kb].

### 3.4.4 Introducing SOE-PCR product into pRSVDysFL

The SOE fragment and the full-length dystrophin were digested with *ClaI* and *NgoMIV*. Digestion of the full-length dystrophin resulted in three products of 3200 bp, 3672 bp and 9490 bp (Figure 3.8A). The largest product of 9490 bp was gel purified for ligation. The SOE-PCR fragment of 1769 bp was digested with the same enzymes, gel purified (Figure 3.8B) and ligated with the 9490 bp fragment of the full-length dystrophin. The ligation was used to transform XL10-Gold ultracompetent cells. The resulting clones were picked, grown up in liquid culture overnight and the plasmids purified for characterisation and further experiments (sections 2.3.2 and 2.3.3).



### 3.5 Characterisation of the mini-dystrophin constructs

#### 3.5.1 Verification of the C2/ $\Delta$ H2-R19 insert and vector by digestion

First, restriction analysis was performed to test different clones. Plasmids were purified and digested with the appropriate restriction enzymes and compared to full-length dystrophin. Usually a double digest was performed alongside a single digest to compare the insert size with the linearised plasmid. Since the dystrophin cDNA was cloned using *NotI* and *SaII*, a single digest was usually performed with *NotI* and a double digest with *NotI* and *SaII*. The single digest for the construct C2/ $\Delta$ H2-R19 resulted in a product of >10 kb, consistent with the predicted size of 11095 bp (Figure 3.9A). The vector size after double digest was ~4.3 kb, consistent with the predicted 4313 bp and the insert of ~7 kb consistent with the predicted 6943 bp (including 5' and 3' UTR) (Figure 3.9B).

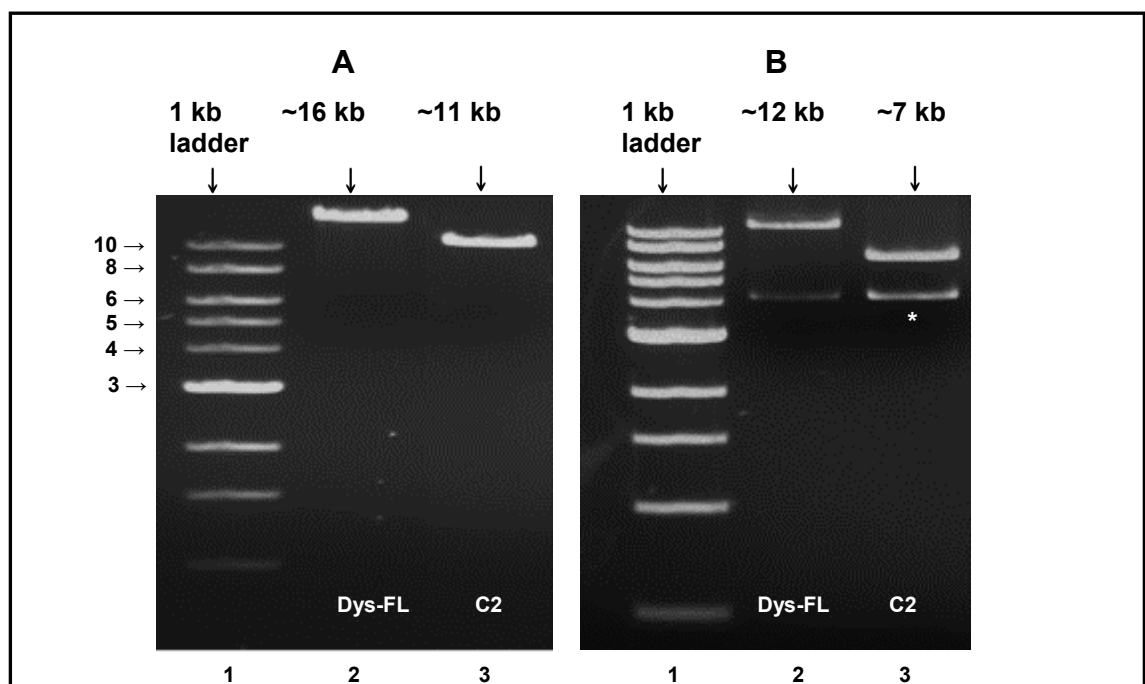
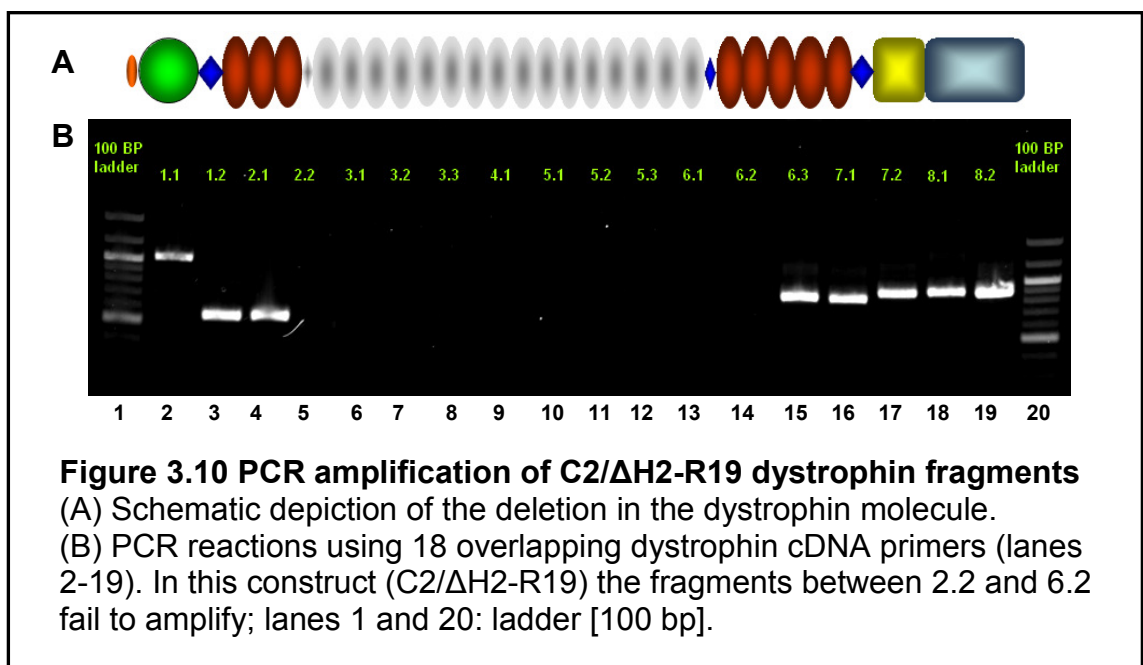


**Figure 3.9 Digestion of C2/ $\Delta$ H2-R19 compared to the full-length dystrophin**

(A) The clones of the full-length dystrophin (lane 2) and C2/ $\Delta$ H2-R19 (lane 3) were digested with *NotI* to linearise the plasmids; lane 1: ladder [1 kb]. (B) Double digest of full-length dystrophin (lane 2) and C2/ $\Delta$ H2-R19 (lane 3) with *SaII* and *NotI*. The asterisk denotes the vector (~4.3 kb); lane 1: ladder [1 kb].

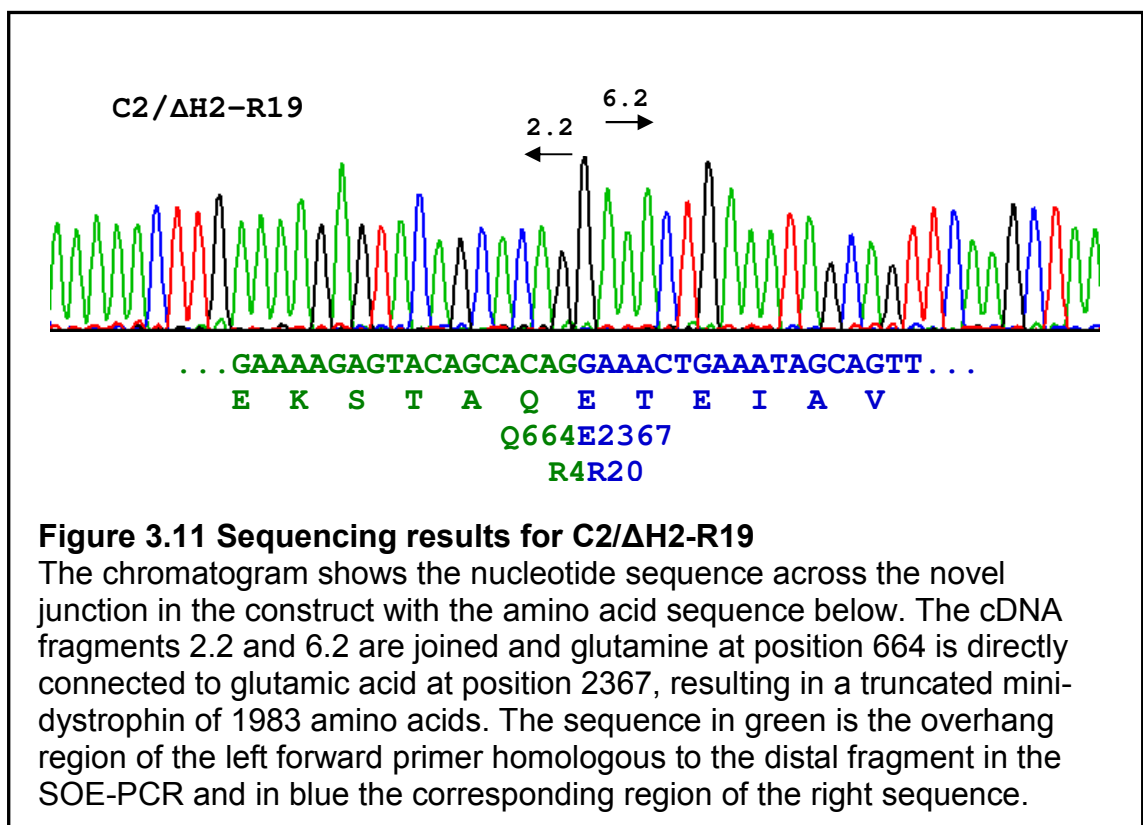
### 3.5.2 Verification of the deletion in C2/ $\Delta$ H2-R19 by PCR

The second method for verification of the deleted sequence and the insert of the mini-dystrophins was PCR amplification using 18 overlapping dystrophin cDNA primers showing differences and identities between the amplified sequences and the full-length dystrophin PCR products (Figure 3.2). In this example, the mini-dystrophin C2/ $\Delta$ H2-R19 deleted for nucleotides 1993-7098 of the wild type dystrophin, results in the absence of fragments 2.2-6.2 (Figure 3.10B). cDNA amplification offers a fast and sensitive technique for confirmation of the engineered deletions in mini-dystrophin constructs prior to complete sequencing and further characterisation.



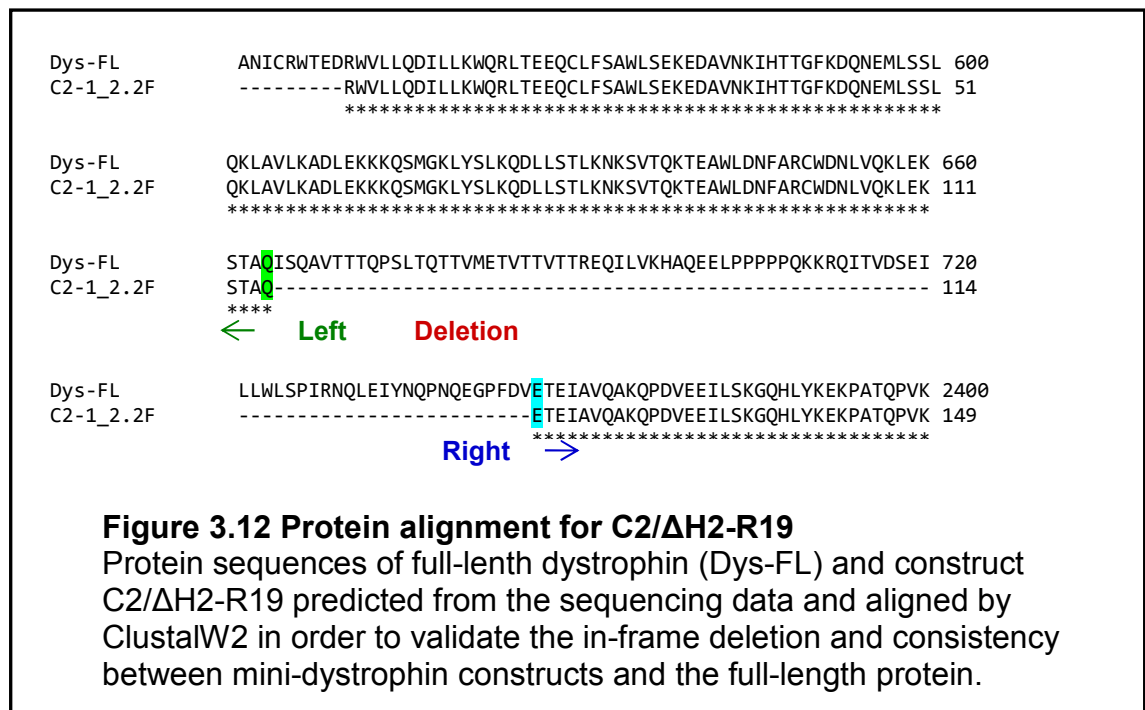
### 3.5.3 Verification of the insert C2/ $\Delta$ H2-R19 and sequencing results

In parallel, the mini-dystrophins were sequenced for verification of the inserts and reading frame. The sequencing results of individual constructs confirmed the absence of the deleted region and a reading frame which connected the glutamine at position 664 directly to the glutamic acid at position 2367 as predicted. As expected the overhang primer (blue: forward primer of the right fragment; green: overhang sequence, complementary to the reverse primer of the left fragment) were identified that were designed to join the left and right fragments together. The chromatogram below shows that the cDNA fragments 2.2 and 6.2 were joined, resulting in a truncated mini-dystrophin (Figure 3.11).



### 3.5.4 Verification of the reading frame of C2/ $\Delta$ H2-R19

To further confirm that the sequence was as predicted, protein sequences were aligned using ClustalW2, validating in-frame deletions relative to specific protein domains and the consistency between mini-dystrophin constructs and the full-length dystrophin. The protein alignment below (Figure 3.12) illustrates two predicted parts of dystrophin sequence separated by a deletion in the construct C2/ $\Delta$ H2-R19. Individual constructs were generated and characterised by being fully sequenced in the same way as described for the construct C2/ $\Delta$ H2-R19. The entire coding sequence for this construct can be found as an example in appendix D.



### **3.5.5 Subcloning of C2/ $\Delta$ H2-R19 into expression vector pCMV-Tag2**

Dystrophin mini-genes were subcloned into the expression vector pCMV-Tag2 in the *NofI* and *SaII* sites (section 2.3.1), removing and replacing the FLAG sequence immediately following the CMV promoter with the construct sequence (Figure 3.13D). The end of the plasmid including the cloning sites was sequenced to confirm the insertion of the constructs into the expression vector. This cloning step placed the mini-dystrophin construct under the control of the cytomegalovirus (CMV) promoter.

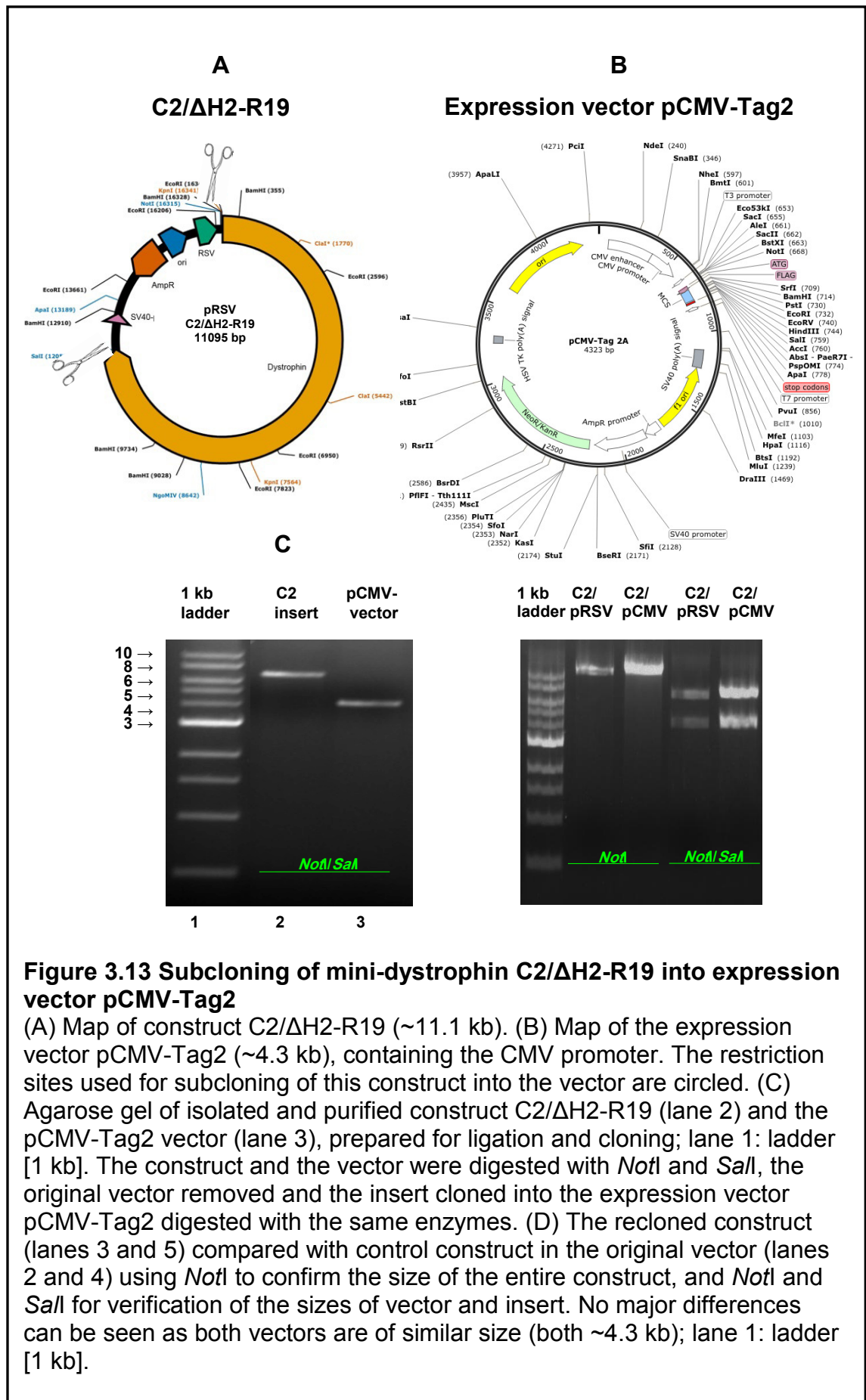
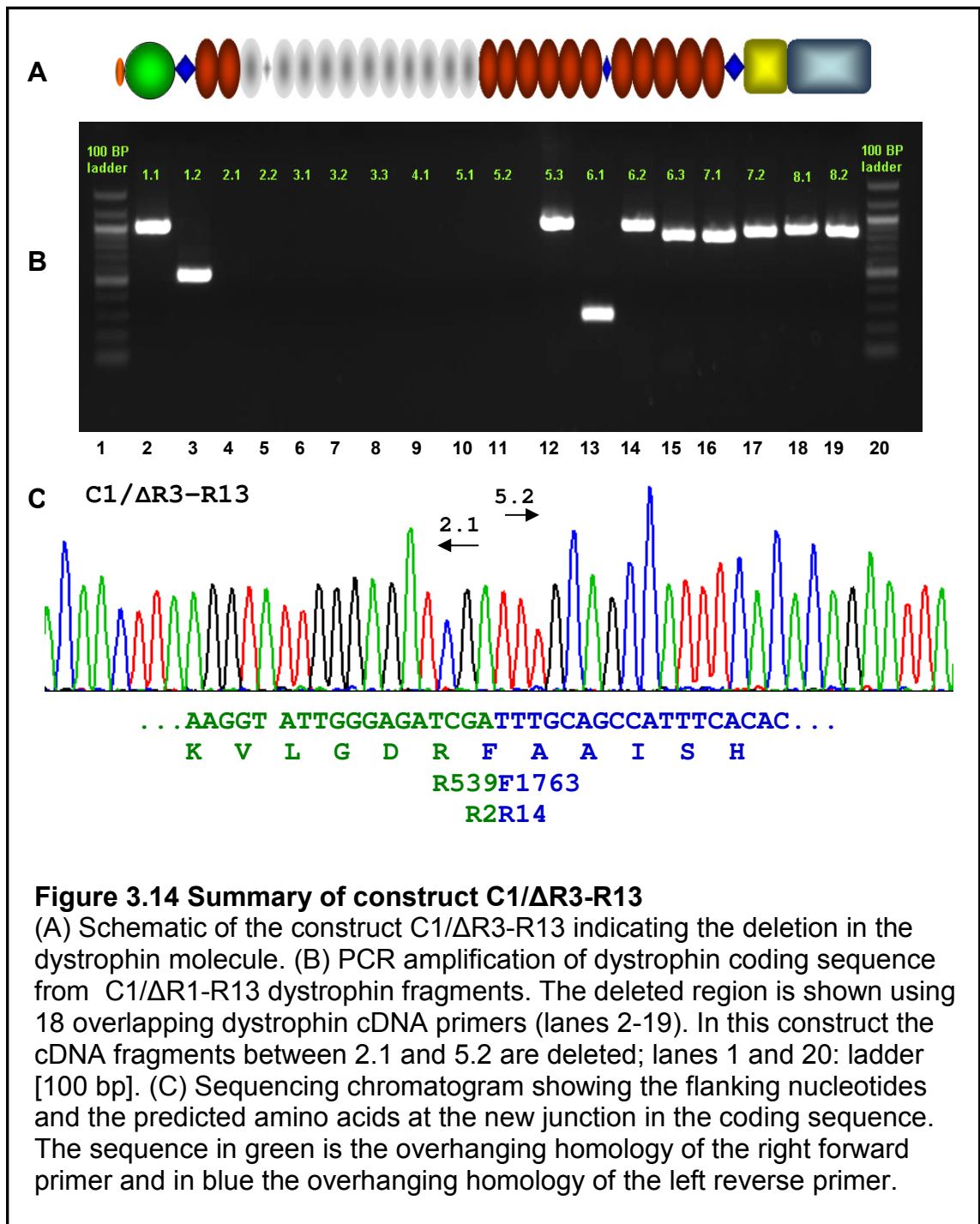


**Figure 3.13 Subcloning of mini-dystrophin C2/ΔH2-R19 into expression vector pCMV-Tag2**

(A) Map of construct C2/ΔH2-R19 (~11.1 kb). (B) Map of the expression vector pCMV-Tag2 (~4.3 kb), containing the CMV promoter. The restriction sites used for subcloning of this construct into the vector are circled. (C) Agarose gel of isolated and purified construct C2/ΔH2-R19 (lane 2) and the pCMV-Tag2 vector (lane 3), prepared for ligation and cloning; lane 1: ladder [1 kb]. The construct and the vector were digested with *NotI* and *SalI*, the original vector removed and the insert cloned into the expression vector pCMV-Tag2 digested with the same enzymes. (D) The re-cloned construct (lanes 3 and 5) compared with control construct in the original vector (lanes 2 and 4) using *NotI* to confirm the size of the entire construct, and *NotI* and *SalI* for verification of the sizes of vector and insert. No major differences can be seen as both vectors are of similar size (both ~4.3 kb); lane 1: ladder [1 kb].

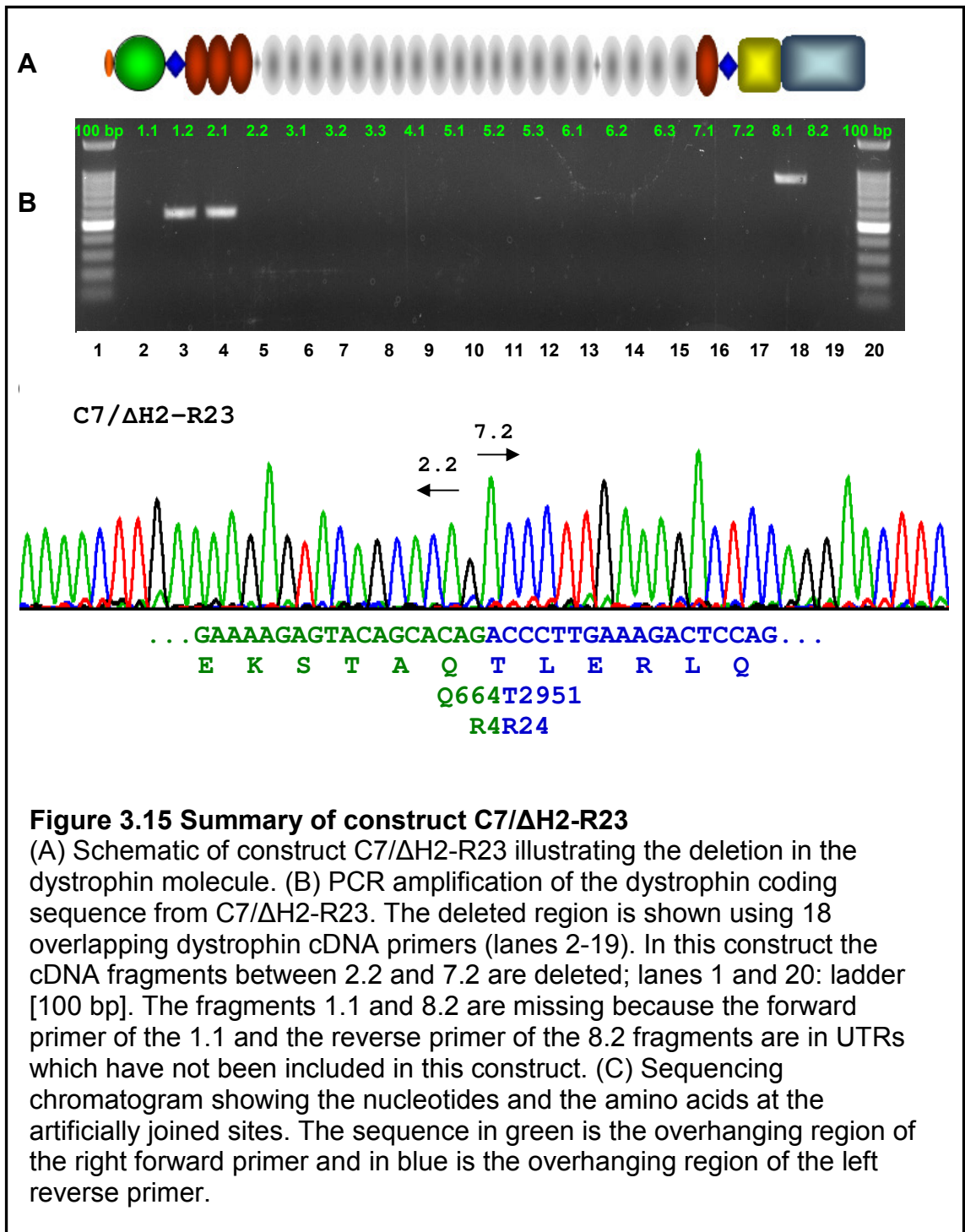
### 3.5.6 ***Summary of C1/ $\Delta$ R3-R13 construction and characterisation***

Construct C1/ $\Delta$ R3-R13 was designed to maintain the most functional parts of the dystrophin molecule, while being within the packaging capacity of lentiviral vectors. This construct represents a novel mini-dystrophin maintaining the rod domain nNOS-binding site (repeats 16 and 17). It was predicted that the constructs carrying this part of the protein would lead to nNOS restoration and normalise its localisation at the sarcolemma. This construct carries a deletion in the rod domain including hinge 2 and repeats 3-13 (11 repeats), resulting in a truncated dystrophin protein predicted to be 284 kDa. The corresponding truncation on the transcript level is an internal deletion of 3671 bases between nucleotide 1619 and 5290, connecting arginine at position 539 to phenylalanine at position 1763 (Figure 3.14C). The insert for this construct was generated using SOE-PCR primers C1/C2-F1-*ClaI* and C1-R1 to amplify the left fragment and C1-F2 and C1/C2-R2-*NgoMIV* for the right fragment resulting in 537 bp and 2572 bp products. In a second PCR step (SOE-PCR) these products were fused together generating a 3109 bp construct containing recognition sites for *ClaI* and *NgoMIV*. The construct was cloned back into the full-length dystrophin plasmid by removing the sequence between the same restriction sites and replacing it with the synthetic sequence resulting in a final dystrophin coding sequence size of 7389 bp.



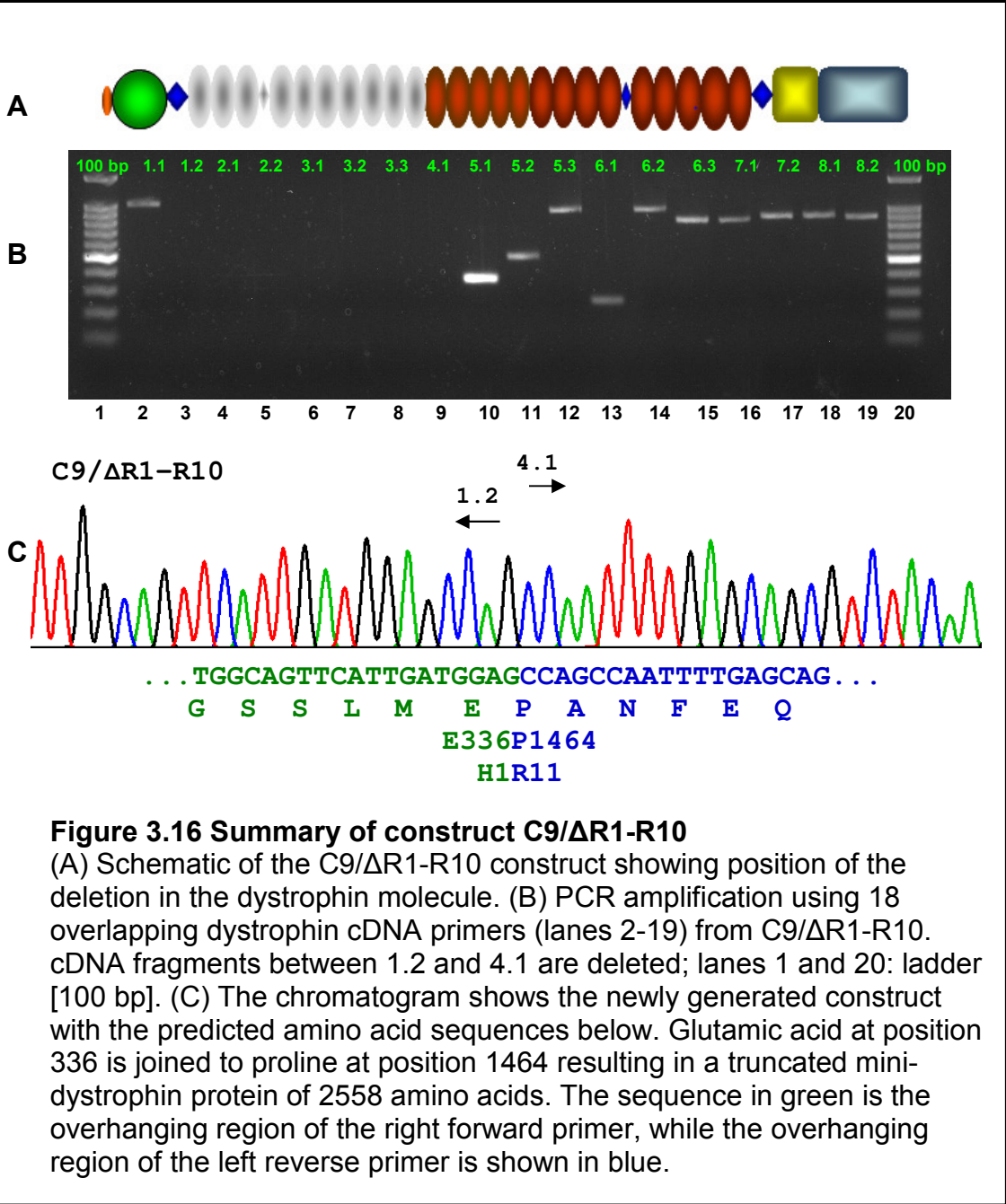
### **3.5.7 Summary of C7/ $\Delta$ H2-R23 construction and characterisation**

Construct C7/ $\Delta$ H2-R23 carries a large deletion in the rod domain including hinge 2 and 3 (2 hinges) and repeats 4-23 (20 repeats) resulting in a truncated dystrophin protein of 163 kDa. The corresponding truncation on the transcript level is an internal deletion of 6800 bases between nucleotide 1993 and 8793, connecting glutamine at position 664 to threonine at position 2951 (Figure 3.15C). The construct is the smallest dystrophin mini-gene and was derived from the C1/ $\Delta$ R3-R13 using SOE-PCR. The primers C7-F1-*Not*I and C7-R1 were used to amplify the left PCR product of 1992 bp, and C7-F2 and C7-R2-*Apa*I to amplify of the right fragment of 2265 bp. The two fragments were joined to form a construct of 4275 bp. Through an unexpected mutation event in the bacteria the *Not*I site was found to be missing one cytosine (GCGGCCGC was mutated to GGGCCGC). However the construct remained unaffected since the adjacent recognition site *Sac*II could be used for cloning and further experiments. Although the *Sac*II site has an internal restriction site in the dystrophin cDNA, this was removed from the transcript as part of the internal deletion.



### 3.5.8 Summary of C9/ $\Delta$ R1-R10 construction and characterisation

To further study an additional portion of the rod domain and further optimise our constructs, the second actin-binding domain (ABD2) in the rod region (repeats 11-15) was retained in construct C9/ $\Delta$ R1-R10 (~7.7 kb). This construct encompasses a deletion of the rod domain repeats 1-10 and maintains actin-binding domain of the rod region (ABD2) in addition to N- and C-terminal domains, a similar deletion as in construct C1/ $\Delta$ R3-13, hence providing a useful comparison. This region of dystrophin interacts with lipid bilayers and binds more strongly to the membrane lipids which could stabilise, maintain and support the membrane attachment (Sarkis *et al.*, 2011). This construct harbours a deletion in the central rod domain including hinge 2 and repeats 1-10 (10 repeats) resulting in a predicted dystrophin protein of 300 kDa. The internal deletion removes 3380 base pairs between nucleotides 1009 and 4389, joining glutamic acid at position 336 to proline at position 1464 (Figure 3.16C). Using the same technique as previously described, SOE-PCR primers including unique restriction sites for this construct (*KasI* and *ClaI*) were used to create a SOE-PCR fragment of 1780 bp from the full-length dystrophin cDNA. The primers C9-F1-*KasI* and C9-R1 were used to amplify an 874 bp fragment, and C9-F2 and C9-R2-*ClaI* a 906 bp fragment. The SOE-PCR derived construct was ligated into the *KasI* and *ClaI* sites of full-length dystrophin. The size of this mini-dystrophin was 7677 bp.



Construct	Vector	Cloning sites	Insert size ATG-stop	1. Deletion (bp)	2. Deletion (bp)	Deletion (Repeat and Hinge)	number of amino acids	1. AA deletion	2. AA deletion	MW (kDa)
pRSVDysFL	pRSV-DysFL	<i>NotI/SalI</i>	11058 bp (~11.1 kb)	∅	∅	∅	3686	∅	∅	427
C1/ΔR3-R13	pCMV2-Tag2A	<i>NotI/SalI</i>	7389 bp (~7.4 kb)	1619-5290 (3671 bp)	∅	R3-R13 (11R & 1H)	2462	539-1763	∅	284
C2/ΔH2-R19	pCMV2-Tag2A	<i>NotI/SalI</i>	5952 bp (~6.0 kb)	1993-7098 (5106 bp)	∅	H2-R19 (16R & 1H)	1983	664-2367	∅	222
C7/ΔH2-R23	pCMV2-Tag2A	<i>SacII/ApaI</i>	4257 bp (~4.3 kb)	1993-8793 (6800 bp)	∅	H2-R23 (20R & 2H)	1418	664-2951	∅	163
C9/ΔR1-R10	pCMV2-Tag2A	<i>NotI/SalI</i>	7677 bp (~7.7 kb)	1009-4389 (3380 bp)	∅	R1-R10 (10R & 1H)	2558	336-1464	∅	300
C10/ΔR3-R13-ΔCT	pCMV2-Tag2A	<i>NotI/SalI</i>	6942 bp (~6.9 kb)	1619-5290 (3671 bp)	10610-11055 (445 bp)	R3-R13 (11R & 1H & CT)	2314	539-1763	2313-3685	268
C11/ΔR3-R13-ΔCT-synt	pCMV2-Tag2A	<i>NotI/SalI</i>	6558 bp (~6.6 kb)	1619-5290 (3671 bp)	10225-11055 (830 bp)	R3-R13 (11R & 1H & CT)	2186	539-1763	2185-3685	254

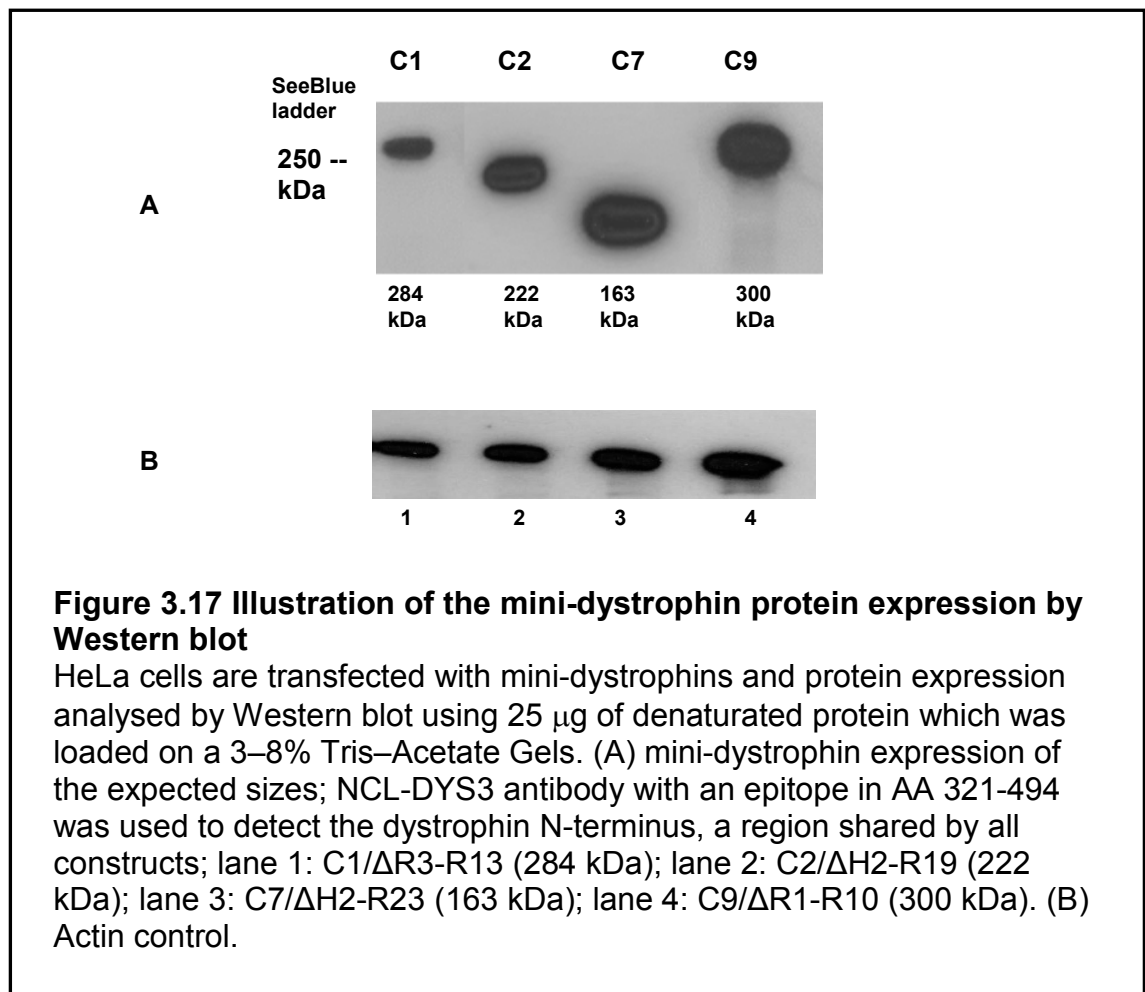
**Table 3.1 Summary of the mini-dystrophin constructs**

Abbreviations: R: repeat; H: hinge; AA: amino acid; bp: base pair; kb: kilo base; kDa: kilo Dalton; Δ: deletion; MW: molecular weight.

### 3.6 Cell transfection and protein expression of mini-dystrophin constructs

#### 3.6.1 Transfection into HeLa cells and Western blotting

To test whether the constructs were able to express the mini-dystrophins in a cell culture system, HeLa cells were grown and transfected (section 2.4.11). Transfected cell pellets were harvested, lysed with sample buffer and loaded on a PAGE gel and the sizes and expression levels of the dystrophin constructs determined by Western blot (section 2.5) using a monoclonal antibody specific for N-terminus of dystrophin (NCL-DYS3). All constructs expressed mini-dystrophins (Figure 3.17) and the observed bands correlated with the predicted size of the mini-dystrophin proteins.



### 3.7 Discussion

In this chapter a series of 4.3-7.7 kb truncated dystrophin constructs with in-frame deletions of the dystrophin rod domain have been generated and their genetic sequences and reading frame validated. This approach offered the opportunity to explore some novel deletions in the dystrophin protein that have not been observed in BMD or DMD patients or not generated and tested by other research groups.

SOE-PCR is an effective procedure providing spliced DNA for cloning purposes, however the technique proved to be challenging for dystrophin construction due abundance of restriction sites in the cDNA sequence, since there are only 33 restriction sites (NM\_004006 restriction map) that are absent within the dystrophin sequence which could also possibly lead to cleavage of the vector during cloning procedure. Moreover, some restriction sites such as *ClaI* were subject to dam methylation which required the regrowth of the cDNA template in dam negative bacteria. It was also not always possible to efficiently achieve the appropriate conditions for successful amplification of the large fragments. The PCR conditions were improved by designing smaller PCR fragments. This method has been previously used for generation of micro-dystrophin constructs (Clemens *et al.*, 1995; Jorgensen *et al.*, 2009). Although this technique required an intermediate cloning step of the constructs into original vectors before subcloning into expression vectors, the method proved to be an adequate system for generating overlapping sequences and exact location of deleted regions in any part of dystrophin cDNA. It was also sometimes difficult to amplify the overhang sequence in the second PCR reaction, since residual products from the first PCR could compete with the overlap fragments resulting in the amplification of undesirable individual fragments making the isolation of products difficult. Interestingly, the overlap extension was considerably enhanced when only 10-15 cycles were used for amplification. All constructs showed in-frame deletions with 100% identity to the full-length dystrophin, suggesting that this method is a reliable technique to introduce deletions for DMD construct generation.

Transient mini-dystrophin expression in HeLa cells was achieved following transfection of the plasmids, confirming protein expression and approximate size of the mini-dystrophins in live cells. In general, mini-dystrophins with larger deletions were associated with higher expression levels in HeLa cells, possibly reflecting greater transfection efficiency of smaller constructs. However, this finding was not consistent across all experiments, since the expression of C9/ $\Delta$ R1-R10 construct was almost as high as the shortest construct in some experiments, suggesting that protein expression *in vitro* is not exclusively determined by size of the constructs, or deletions and inclusion of individual repeats such as ABD2 in larger C9/ $\Delta$ R1-R10 may have played a role in higher expression compared to C1/ $\Delta$ R3-R13. On the other hand, different expression levels in HeLa cells could have been random, and as a result of inconsistency in transfection efficiency across repeated experiments using the same conditions and transfection method. These data suggest that expression level of plasmids in cell culture does not necessarily correlate with a higher or less functionality of mini-dystrophins and is rather a rapid method to confirm protein expression from constructs.

Dystrophin has a large untranslated 3' sequence which has been suggested to contribute to mRNA stability and removal of this region has been shown to lead in lower transfection efficiency of truncated dystrophins in C2C12 and COS cells (Clemens *et al.*, 1995). However, the construct C7/ $\Delta$ H2-R23 with a complete deletion of this region showed dystrophin expression in almost all experiments, suggesting that the 3' deletion does not affect protein expression in this cell culture system, and that this portion of the molecule can be removed to provide additional space for dystrophin coding sequence. The identification of functional portions of the rod domain is required when designing therapeutic dystrophin constructs. Further studies are required to assess the novel constructs and explore the role of different deletions and whether or not there is a correlation between the construct size and function *in vivo*. It has been proposed that all of the spectrin-like repeats might be necessary to withstand and convey the high force that is developed in skeletal muscle during contraction (Sweeney and Barton, 2000), suggesting that truncated versions carrying a large portion of the rod domain may be more beneficial than those with large rod domain deletions.

## Chapter 4 *In vitro* characterisation and assessment of mini-dystrophin constructs

### 4.1 Introduction

Cell culture and transfection are useful tools for *in vitro* study of exogenous gene expression and cellular mechanism, enabling functional testing of transgene localisation to specific regions in cells. Although cell culture models do not necessarily imitate the *in vivo* environment and cannot replace animal models, they allow fast and cost-effective testing of therapeutic strategies prior to *in vivo* studies. Depending on experimental questions, there are several cell models that can be used for delivery of engineered truncated dystrophin constructs in cell culture. Non-myogenic cell lines such as HeLa- or HEK cells are appropriate for transient transfection of constructs into cells, in order to observe gene expression, whereas myogenic dystrophin-deficient cell lines are required to be able to explore cellular localisation and functionality of therapeutic dystrophins. In this work two different types of immortalised myoblast lines originating from mouse and human were used. The mdx-immorto lines carry an immortalising oncogene, the simian virus 40 large tumour antigen, allowing infinite proliferation and growth of cells (Jat *et al.*, 1991; Morgan *et al.*, 1994). The main drawback of using mdx-immorto myoblasts is their low transfection efficiency. For this reason, immortalised DMD-derived myoblasts were generated using the E6E7 gene region from human papillomavirus, showing extended proliferative life span and potential to differentiate (Lochmuller *et al.*, 1999). Furthermore, dystrophic human myoblast lines derived from patient biopsies provide the most appropriate cell culture model to evaluate therapeutic interventions under their natural genetic conditions (Mamchaoui *et al.*, 2011). Lentiviral vectors have been shown to enhance transfection efficiency of micro-dystrophins into myoblasts resulting in long-term expression and integration of viral genomes into target cells (Shunchang *et al.*, 2008; Kimura *et al.*, 2010). In this chapter, the feasibility of performing lentiviral transduction as an alternative method to introduce mini-dystrophins into myoblasts will be explored.

## 4.2 Aims

Transient transfection of mdx-immorto myoblasts to confirm the cellular localisation of expressed mini-dystrophins.

Optimisation of transfection and differentiation protocols for mdx-immorto cells.

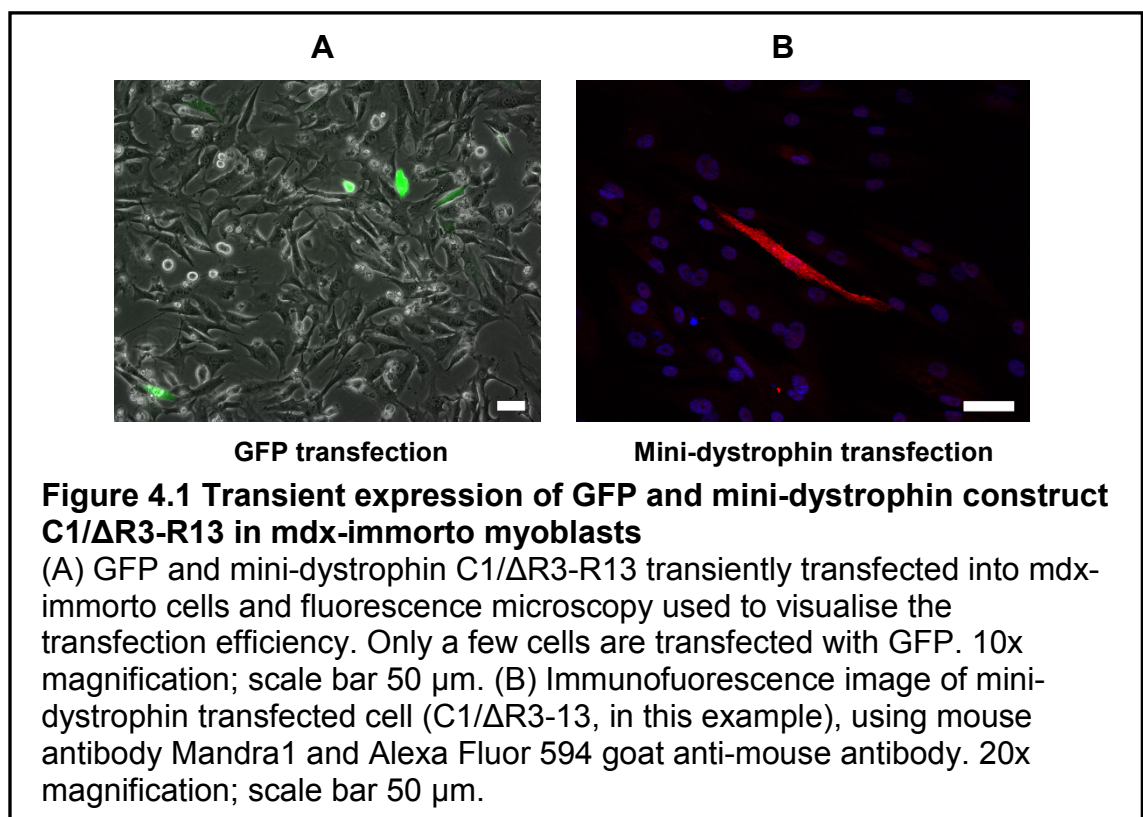
Investigation of stable transfection of mdx-immorto myoblasts with mini-dystrophin constructs for further *in vitro* functional tests.

Identification and establishment of a dystrophin-deficient cell line as a cell model system.

Exploration of the ability of lentivirus to transduce dystrophin-deficient myoblasts, successfully integrate the viral genome into cells and induce dystrophin expression in transduced myoblasts.

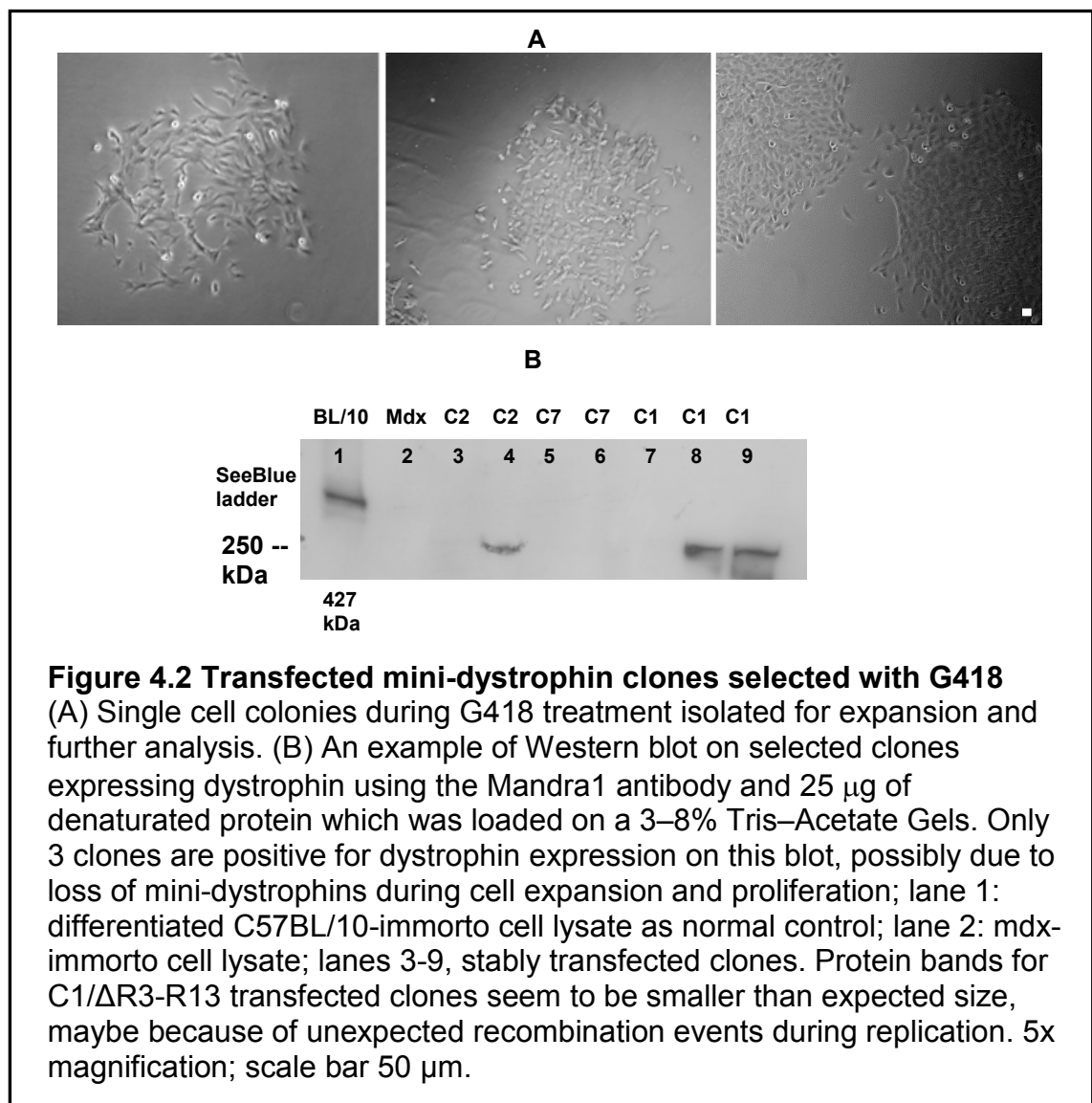
### 4.3 Transient transfection of mini-dystrophins and their cellular localisation

To investigate protein expression in cultured myoblasts and to examine the localisation of the mini-dystrophin constructs, mdx-immorto cells were transfected with plasmids carrying mini-dystrophins, followed by immunofluorescence microscopy. At day 1, cells were transfected with different mini-dystrophin constructs and a GFP plasmid as control. 3 days post transfection, myoblasts were fixed and stained with the anti-dystrophin antibody Mandra1. Despite repeated attempts only poor transfection efficiency in both the GFP as well as mini-dystrophin transfected cells was obtained, indicating that the plasmids, including the GFP control, were inefficiently transfected (Figure 4.1). The number of transfected cells was insufficient for differentiation into myotubes for further functional characterisation experiments such as inducing cell damage by osmotic shock. As an alternative to transient transfection, stable transfection was undertaken to circumvent this problem.



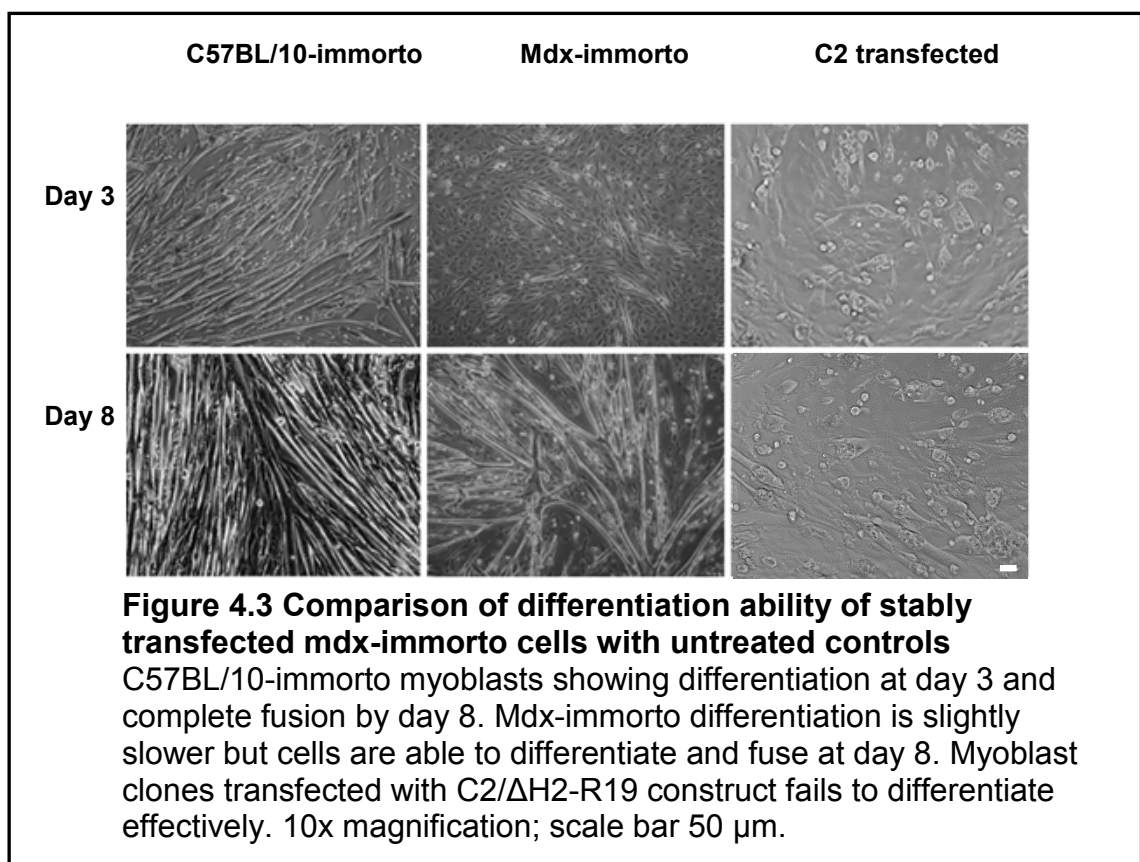
#### 4.3.1 *Stable transfection of mdx-immorto myoblasts with mini-dystrophin constructs*

Using the neomycin resistance of the mini-dystrophin constructs, stably transfected mdx-immorto cells were selected after G418 treatment (Figure 4.2A). The selection conditions for this cell type, including the optimal cell density and the level of G418 to maintain stably transfected clones (section 2.4.15) were determined in advance to prevent the growth of untransfected cells. 400 µg/ml G418 was used for ~30% confluent cells in 6-well plates and resistant clones were selected, expanded and analysed for expression of the mini-dystrophins by Western blot (Figure 4.2B). 140 resistant clones were screened, however only seven myoblast clones that expressed dystrophin were found, indicating inefficient integration of the mini-dystrophin carrying plasmids in the genome of cells.



#### 4.3.2 Differentiation ability of stably transfected myoblasts

Differentiation of stably transfected clones into myotubes is required for a number of *in vitro* functional tests and for comparison of the protective effect of different mini-dystrophins on membrane stability. C57BL/10-immorto and mdx-immorto cells were used as wild type and non-transfected dystrophic controls, respectively. After 3 days of differentiation, myotube formation was observed in the wild type control with complete and unified differentiation after 8 days. Similar results were found in mdx-immorto control with a slightly later onset in differentiation and lower numbers of fused cells. Differentiation of the stably transfected cell lines resulted in some multinucleated, round cells that were not able to further differentiate. Despite repeated attempts to achieve an improved rate of differentiation, none of the stably transfected clones could be differentiated to a comparable state to that observed in control cell lines (Figure 4.3).



#### 4.4 Establishment of an immortalised DMD human myoblast line

In order to explore whether an alternative dystrophin-deficient cell line would provide a more suitable cell model for the *in vitro* experiments, an immortalised DMD human cell line with an extended life span was established. A muscle biopsy obtained in the course of a clinical trial from a Duchenne patient (aged 10 years at biopsy) with a deletion in exon 52 had been processed in the MRC-CNMD Biobank in Newcastle. The myoblasts were infected at ~30% confluence with a retrovirus expressing the E6E7 region from human papillomavirus type 16 (Lochmuller *et al.*, 1999) and the integration of the virus was confirmed by selection of colonies for G418 (Geneticin) resistance for at least 14 days. The G418-resistant clones were cultured for several weeks without significant change to their proliferative potential. The immortalisation was also performed on myoblasts from a healthy donor to serve as normal control. To determine the purity of the immortalised myoblasts, cells were stained with an antibody against the myoblast marker desmin. The staining showed a pure population of proliferative myoblasts as well as myotubes at day 4 after seeding (Figure 4.4).

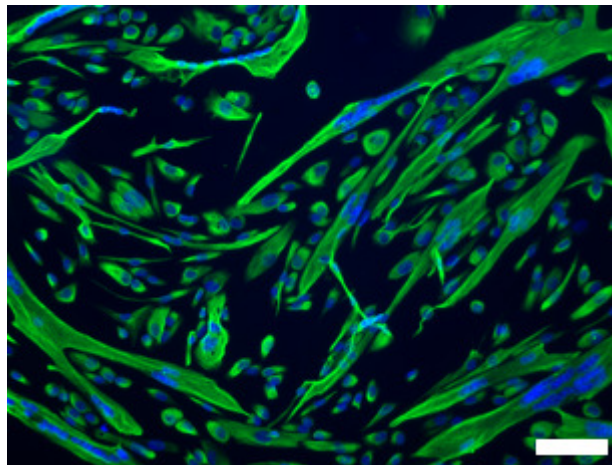
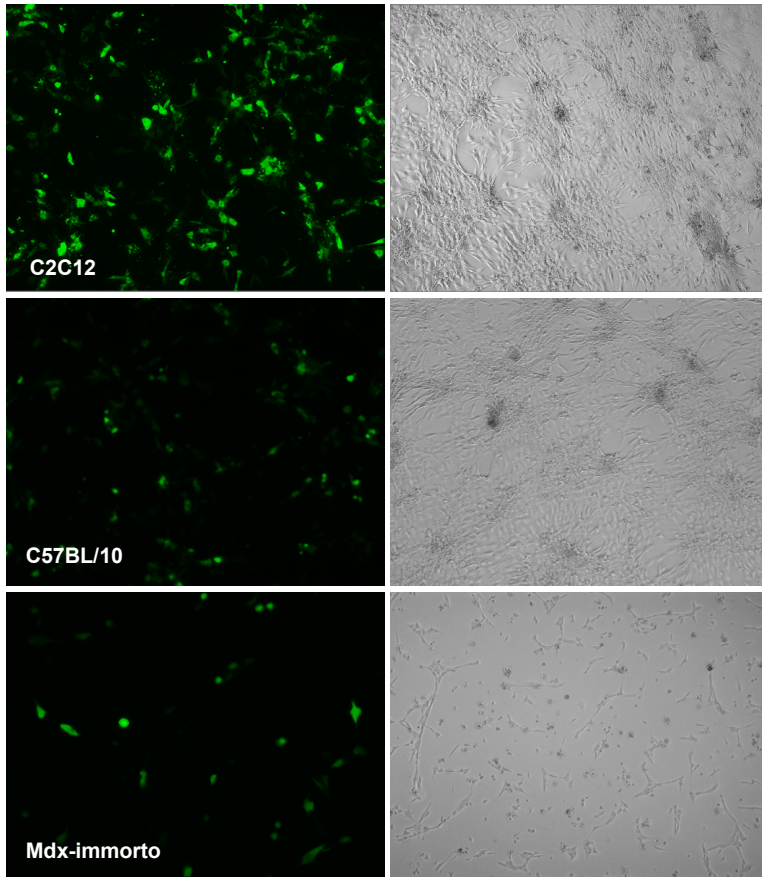


**Figure 4.4 Desmin staining on immortalised DMD human cell line**  
Mouse anti-desmin antibody and Alexa Fluor 488 goat anti-mouse antibody is used to test the purity of the immortalised DMD human myoblast line. Myoblasts and myotubes are positive for desmin staining (green) and nuclei is stained with DAPI (blue). 20x magnification; scale bar 50  $\mu\text{m}$ .

#### **4.4.1 *Comparison of transfection efficiency in mouse and human cell lines***

Efficiency of transfection was compared in several immortalised myoblasts cell lines available to define the optimal cell line for these experiments. Cells were grown to 70-90% confluence and transfected with a control GFP expressing construct using the Amaxa Nucleofector, followed by analysis by fluorescence microscopy and FACS. The aim was to determine the most suitable cell line for transfection. The mouse myoblast cell lines included C2C12, dystrophin-deficient mdx-immorto and C57BL/10-immorto as a normal control. The human cells included the newly immortalised DMD human and the normal control myoblasts.

**Mouse cell lines**



**Human cell lines**

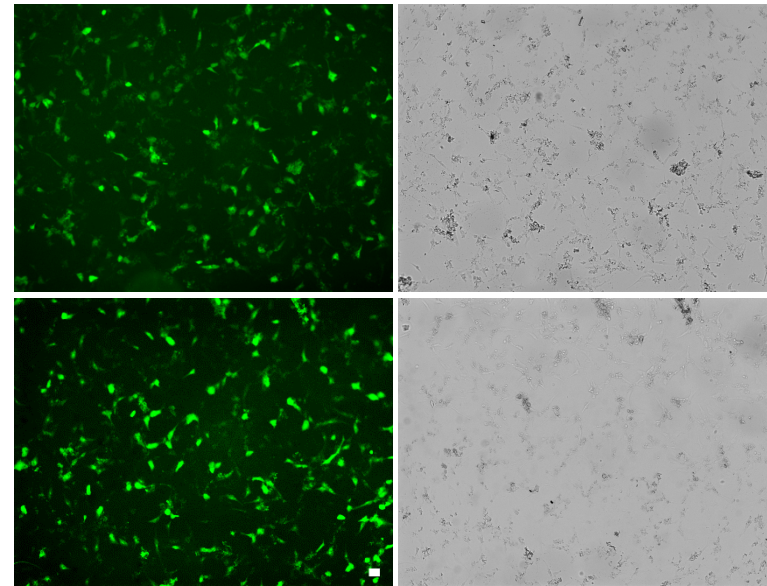
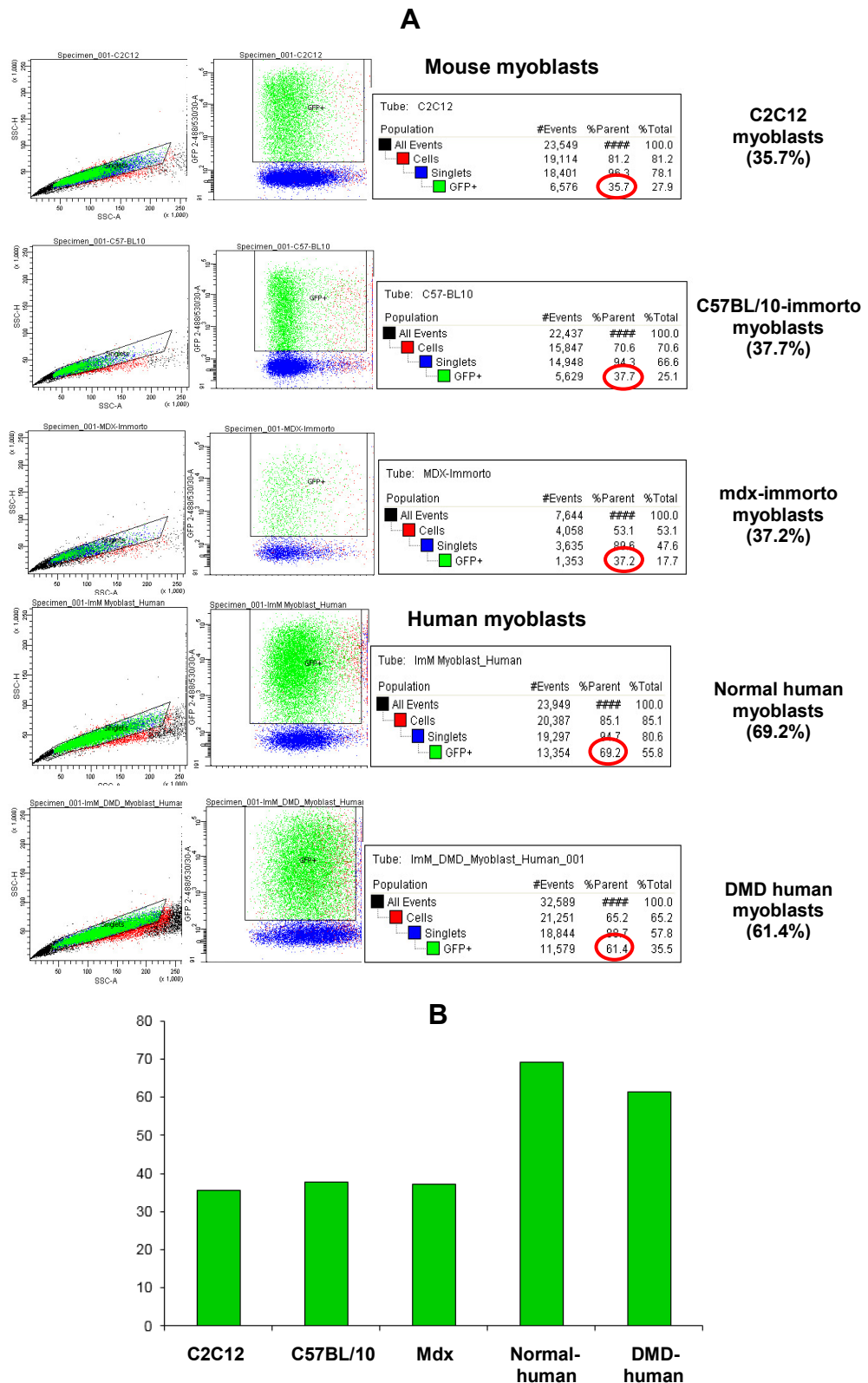


**Figure 4.5 Comparison of transfection efficiency in different myoblast lines**

Mouse cell lines (C2C12, C57/BL10-immorto and mdx-immorto) and human cell lines (immortalised DMD and normal human myoblasts) transfected with a control GFP construct. Cell culture images at 5x magnification; scale bar 50  $\mu$ m.

#### **4.4.2 FACS analysis of transfection in different cell lines**

To obtain quantitative results on the transfection efficiency in myoblasts, FACS analysis 24 hours following transfection was undertaken. Only surviving, adherent myoblasts were collected. The detached and dead cells were not considered. In each group 20,000 cells were counted (except the mdx-immorto cell line, as only 4058 cells could be harvested in total). The transfection rate was 35.7% in C2C12, 37.7% in C57/BL10-immorto, 37.2% in mdx-immorto, 69.2% in immortalised, normal human myoblasts and 61.4% in immortalised DMD human myoblasts (Figure 4.6).



Specimen\_001-InM Myoblast\_Human

Specimen\_001-InM Myoblast\_Human

**Normal human myoblasts (69.2%)**

Specimen\_001-InM\_DMD\_Myoblast\_Human

Specimen\_001-InM\_DMD\_Myoblast\_Human

**DMD human myoblasts (61.4%)**

**B**

Cell Type	Percentage of GFP+ Cells
C2C12	35.7%
C57BL/10	37.7%
Mdx	37.2%
Normal-human	69.2%
DMD-human	61.4%

**Figure 4.6 Flow cytometric results of mouse and human myoblasts transfected with a GFP control construct following Amaxa nucleofection**

(A) Scatter plots showing GFP positive cells (green) after transfection. (B) Bar chart presents the percentage rate of GFP positive cells for each cell type. Human myoblast lines show higher transfection efficiency than mouse myoblasts.

#### **4.4.3 *Choice of the best transfection method and transfectants***

In order to evaluate and compare the transfection efficacy of several lipofection reagents to that of the nucleofection system, immortalised DMD human myoblasts were transfected with a GFP plasmid using several different available lipofection reagents including Lipofectamine 2000, NanoJuice and FuGene HD and compared to nucleofection using the Amaxa system. Nucleofection proved to be less toxic and more efficient at delivering DNA into the cells as determined by cell viability that was estimated by observations of attached GFP positive cells in cell culture. Lipofectamine 2000, NanoJuice and FuGene were essentially equivalent in terms of toxicity and very low in efficiency. In general, the Amaxa nucleofection system seems to be superior to lipofection systems for this cell line (Figure 4.7).

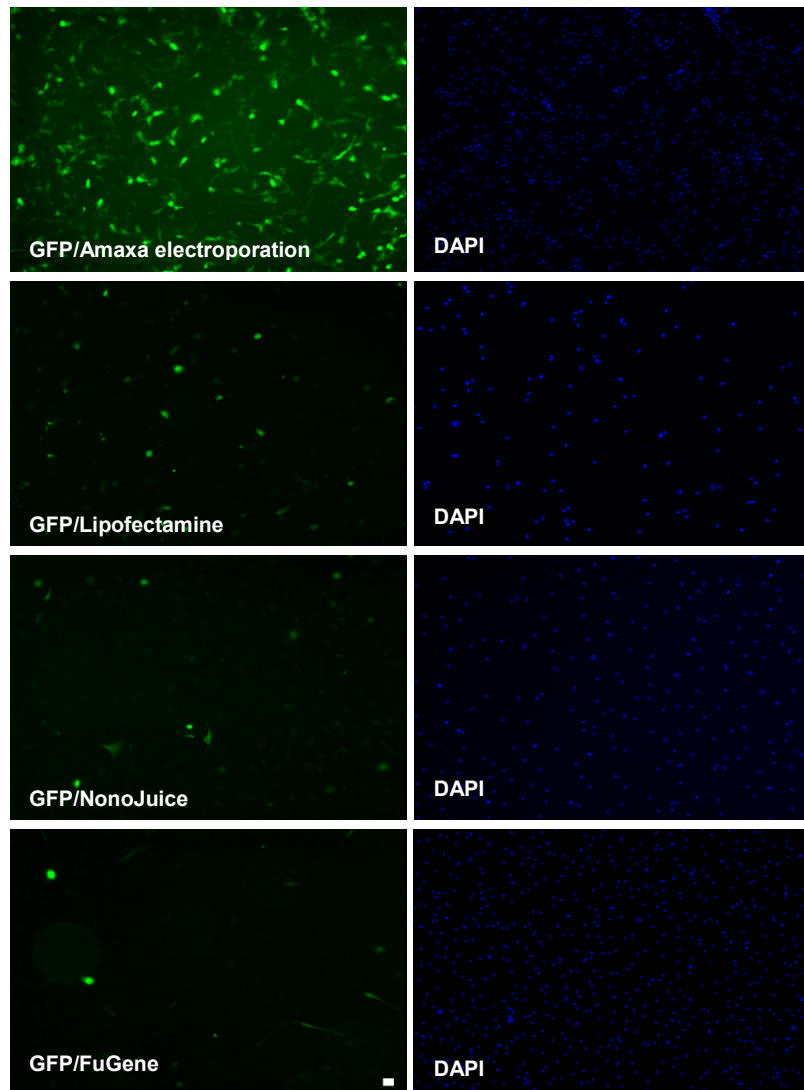
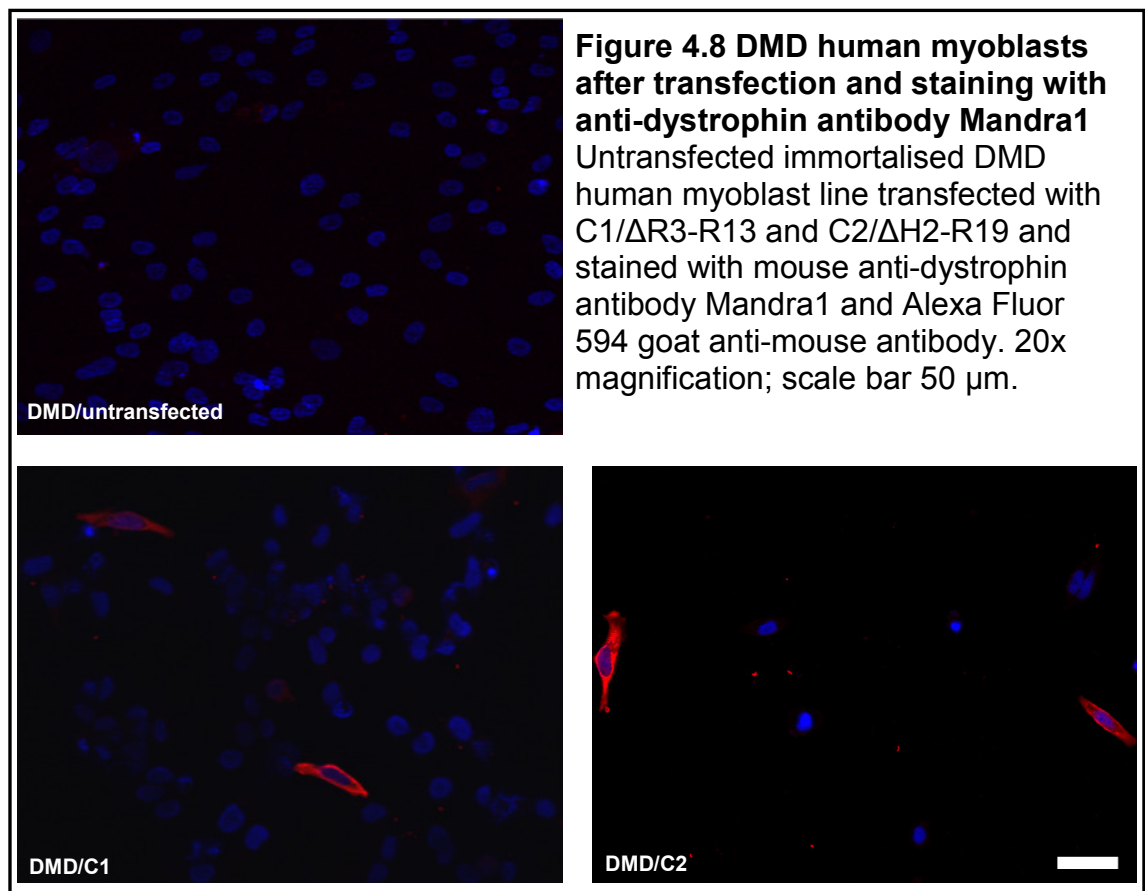


**Figure 4.7 Comparison of transfection efficiency of several lipofection reagents with nucleofection on DMD human myoblasts in cell culture**  
 Fluorescence microscope images of immortalised human DMD myoblast line transfected with a GFP control plasmid using various lipofection reagents or nucleofection. The highest efficiency was achieved using Amaxa nucleofection, as judged by attached cells. 5x magnification; scale bar 50  $\mu$ m.

## 4.5 Immunofluorescence results

### 4.5.1 *Transient transfection of DMD human myoblasts*

Transfection of immortalised DMD human myoblasts was carried out with mini-dystrophin constructs and GFP plasmid as a control, using the Amaxa nucleofection procedure, in order to define the localisation of dystrophin in the muscle fibre membrane after staining with anti-dystrophin antibodies. Following staining with Mandra1 (abcam), which has an epitope in the C-terminal region of dystrophin, fluorescence microscopy was used to identify transfected cells. Despite repeated attempts only low levels of transfection were observed, a level comparable to that obtained for the mouse myoblasts. Since, the GFP transfection had shown (Figure 4.7) a high transfection efficiency of approximately 60%, consistent with the previously described FACS analysis, it was concluded that the transfection efficiency was largely dependent on the construct used and not necessarily on the cell line (Figure 4.8).



## **4.6 Improving gene transfer efficiency using viral transduction**

### **4.6.1 *Introduction to design of replication incompetent lentiviral vectors***

In order to provide a more efficient and reliable mini-dystrophin transfection protocol, the mini-dystrophin constructs were first inserted into viral vector backbones to allow the use of lentiviral vectors (LVs) for expressing mini-dystrophin constructs in muscle cells.

Lentiviral vectors can transduce both dividing and non-dividing cells and have a relatively large transgene carrying capacity, and are therefore highly attractive as a gene delivery system (Talbot *et al.*, 2010). The third generation lentiviral vectors are based on HIV-1 and carry an almost complete deletion in the U3 region of the HIV 3' LTR which contains viral enhancer and promoter in addition to removal of all essential packaging and replication genes, improving biosafety (Follenzi and Naldini, 2002) (Figure 4.9). The constructs used for lentivirus production are maintained in the form of bacterial plasmids and can be transfected into mammalian cells to produce replication-defective viral stocks.

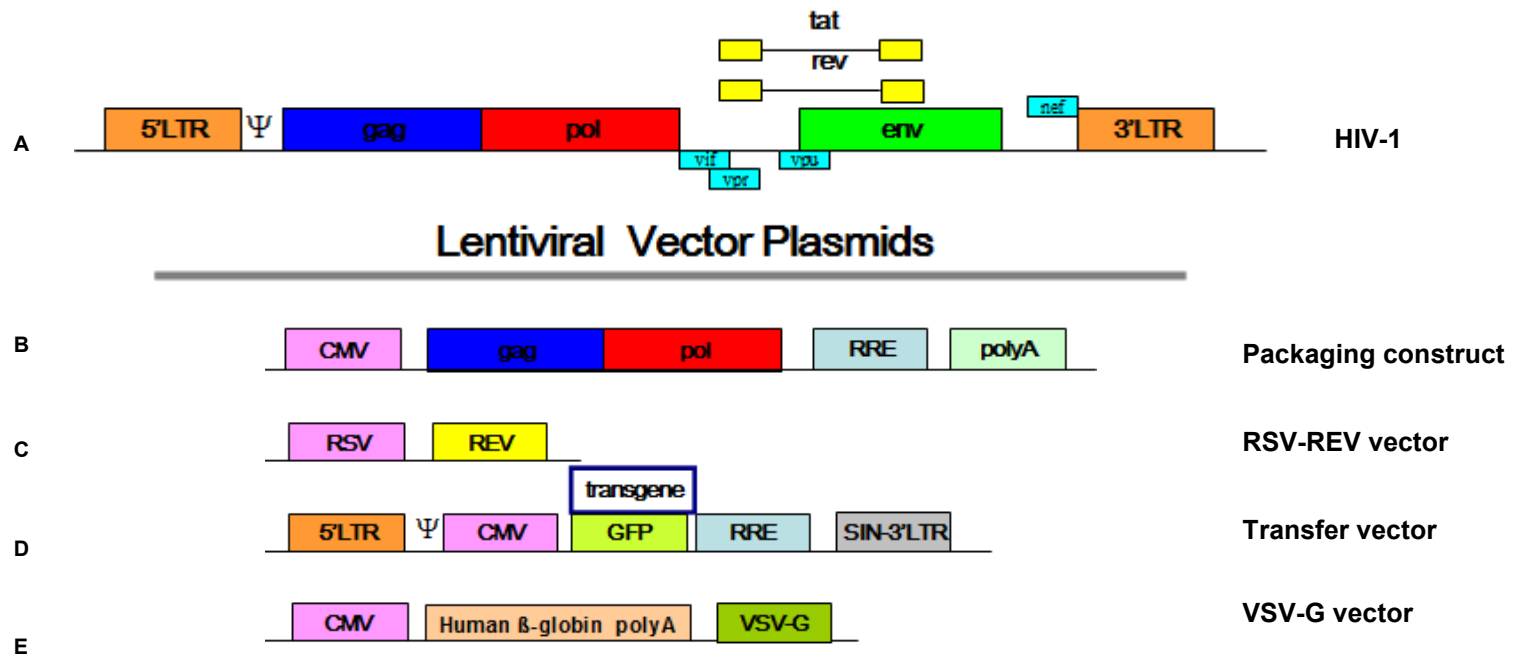


**Figure 4.9 Schematic drawing of the four constructs required to generate VSV-pseudotyped third generation HIV-1 derived lentiviral vectors**

(A) HIV-1 virus including structural (gag, pol and env), regulatory (tat and rev) and accessory (nef, vif, vpr and vpu) viral elements (B) The conditional packaging construct expressing the gag and pol genes driven by the CMV promoter. (C) Construct RSV-REV, expressing the REV cDNA from the RSV promoter. (D) The self-inactivating (SIN) transfer construct containing HIV cis-acting sequences and inactivating LTR in the transfer vector to prevent the virus from activating, containing an expression cassette for the transgene (in this case GFP), which can be replaced with the gene of interest and is driven by an internal promoter. (E) A construct encoding a heterologous envelope to pseudotype the vector, coding for the protein G of the vesicular stomatitis virus under the control of CMV promoter to replace the envelope protein of the virus. Illustration adapted from Follenzi and Naldini 2002. Abbreviations: gag: group antigen; pol: reverse transcriptase; env: envelope protein; LTR: long terminal repeat; tat: transcriptional transactivator; rev: RNA-binding protein; nef: negative factor.

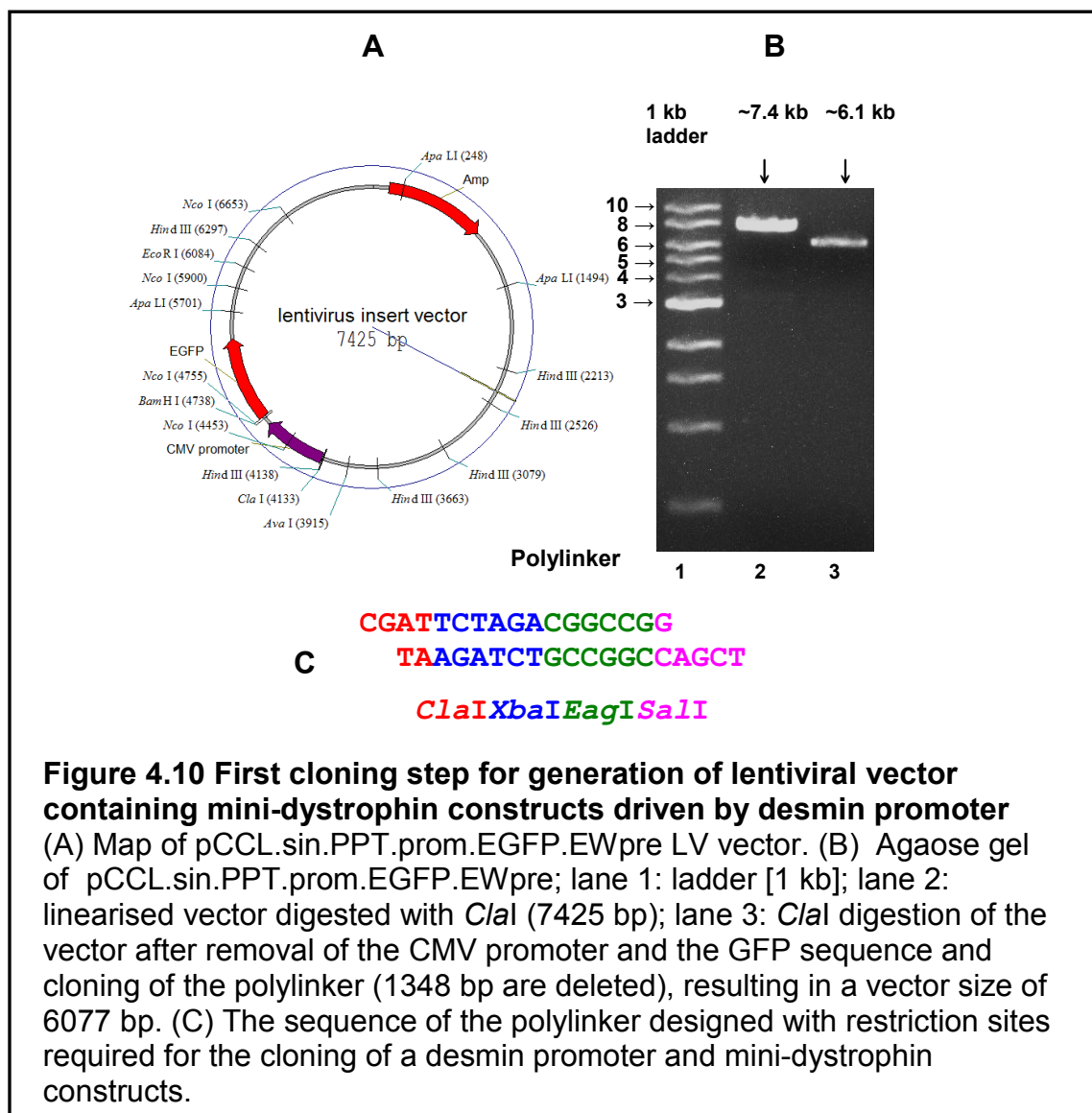
## 4.7 Lentiviral transduction

### 4.7.1 *Subcloning of selected constructs into a lentiviral vector*

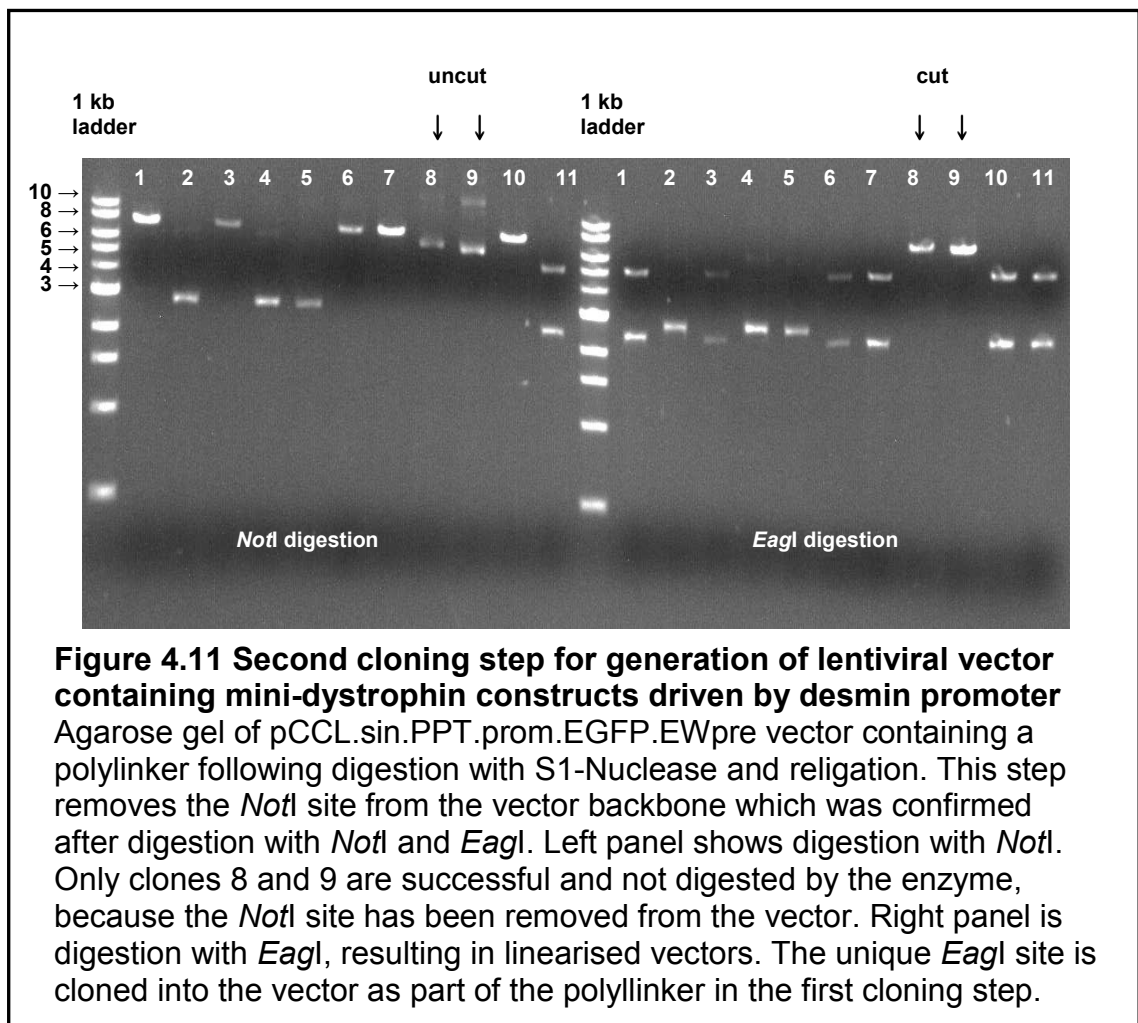
In order to produce viral particles for transduction, two of the mini-dystrophins were cloned into the pCCL.sin.PPT.prom.EGFP.EWpre lentiviral vector backbone to provide packaging signals which direct the construct into the packaged virus particles. The four previously described plasmids (Figure 4.9) (Follenzi and Naldini, 2002) and a plasmid (~7.7 kb) containing a desmin promoter (kindly provided by Professor Jenny Morgan, Dubowitz Neuromuscular Centre, Institute of Child Health, UCL, London) were used to investigate the behaviour of a muscle specific promoter in the new vector system. The construct C1/ $\Delta$ R3-R13 (~7.4 kb) and the C2/ $\Delta$ H2-R19 (~6.0 kb) were selected for this experiment in order to compare the transduction efficiency of lentivirus using two constructs of different sizes. In addition, these constructs offered a comparison for nNOS restoration between a constructs that contain the rod domain nNOS-binding site (C1/ $\Delta$ R3-R13) and a construct that is deleted for this region (C2/ $\Delta$ H2-R19).

#### 4.7.2 Generation of lentivirus containing mini-dystrophin constructs driven by desmin promoter

Three different vectors were used for this approach in multiple cloning steps. The lentiviral transfer vector pCCL.sin.PPT.prom.EGFP.EWpre, a vector carrying the desmin promoter (MA 884) and the expression vector PCMV-Tag2/C1/ $\Delta$ R3-R13 or pCMV-Tag2/C2/ $\Delta$ H2-R19, carrying the constructs. In the first step the vector was digested with *Cla*I and *Sa*II to remove the GFP and the CMV promoter, whereby the *Not*I site in the multiple cloning site, located next to the *Sa*II site was removed as part of the deleted sequence. In this step 1348 bp were deleted from the vector. A polylinker containing *Cla*I, *Xba*I, *Eag*I and *Sa*II was cloned into the digested lentiviral transfer vector to allow cloning of the desmin promoter and the mini-dystrophin constructs in multiple cloning steps (Figure 4.10).



The resulting plasmids were then cut with *NotI* and treated with S1-Nuclease, an enzyme that removes single stranded tails from DNA to create blunt-ended molecules. This step resulted in the removal of the *NotI* recognition site from the vector backbone. The vector was then self-ligated and purified for the next cloning step. The removal of both *NotI* sites was confirmed after digestion with *NotI* and *EagI*. Plasmids without *NotI* sites remained undigested but linearised with *EagI* which was cloned into the vector as part of the polylinker (Figure 4.11; lanes 8 and 9).



In the third step the self-ligated vector (~6.1 kb) and the desmin plasmid (~7.7 kb) were digested with *Cla*I and *Xba*I to allow the cloning of the desmin promoter in the vector (~1.8 kb) (Figure 4.12).

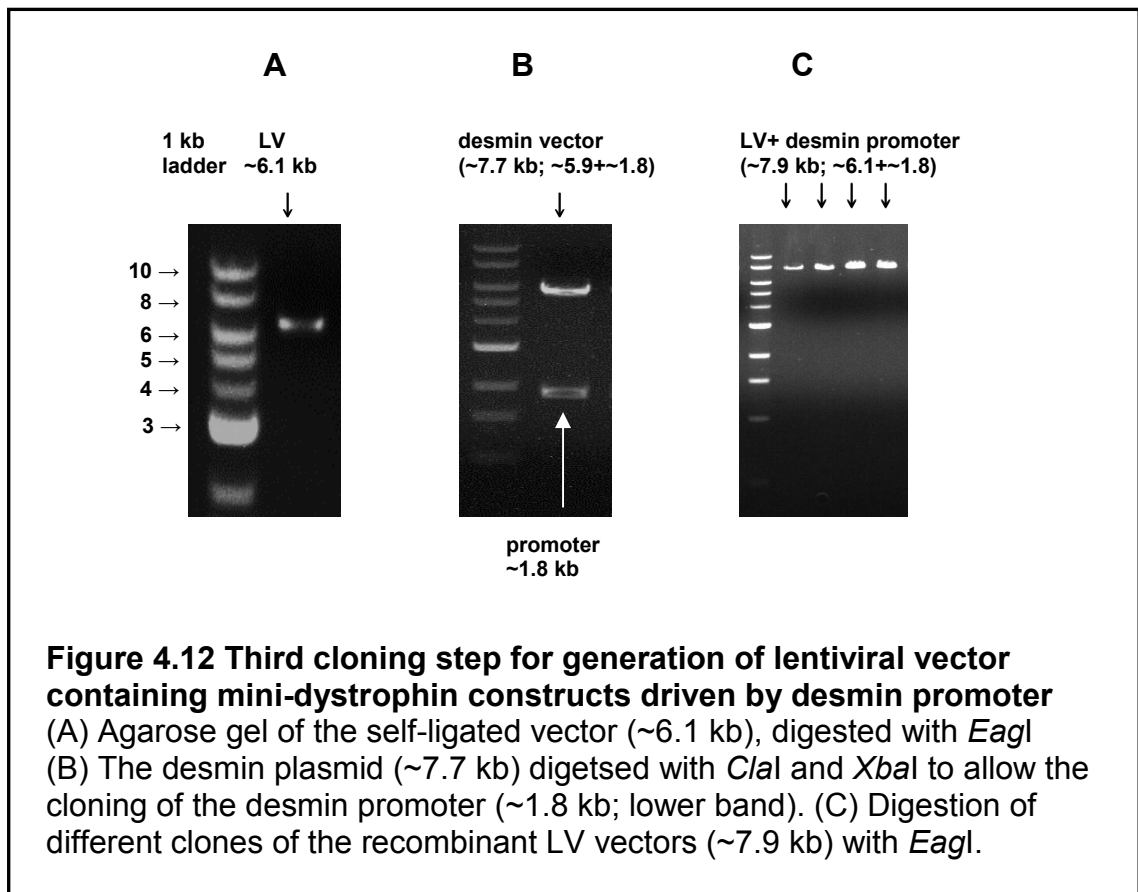
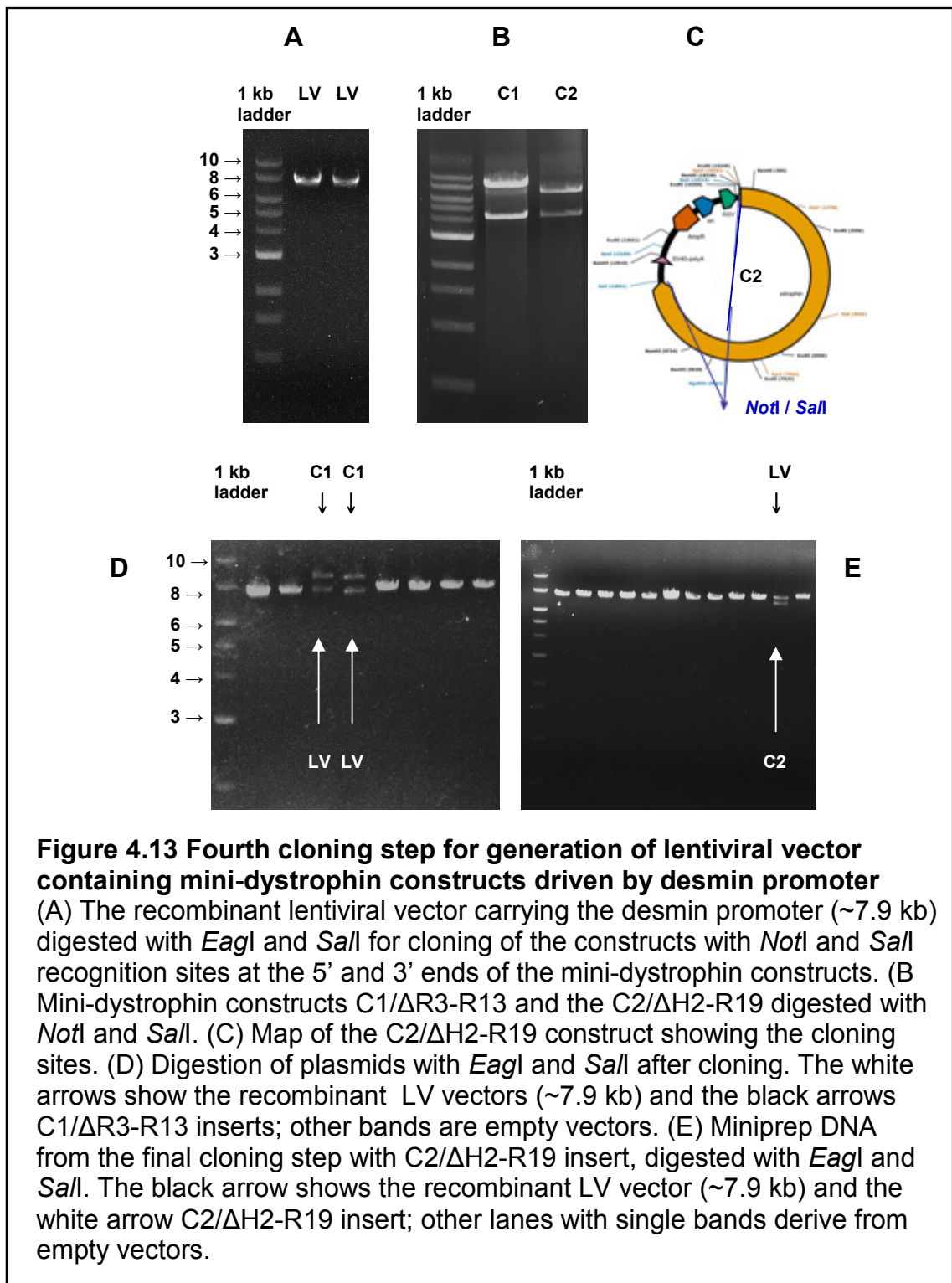


**Figure 4.12 Third cloning step for generation of lentiviral vector containing mini-dystrophin constructs driven by desmin promoter**  
(A) Agarose gel of the self-ligated vector (~6.1 kb), digested with *Eag*I  
(B) The desmin plasmid (~7.7 kb) digested with *Cla*I and *Xba*I to allow the cloning of the desmin promoter (~1.8 kb; lower band). (C) Digestion of different clones of the recombinant LV vectors (~7.9 kb) with *Eag*I.

The recombinant lentiviral vector containing the desmin promoter (~7.9 kb) was then digested with *EagI* and *SalI* (Figure 4.13A) to facilitate the cloning of the constructs with unique *NotI* and *SalI* recognition sites at the 5' and 3' ends of the mini-gene constructs (Figure 4.13B). The resulting plasmids were digested with *NotI* and *SalI* for verification of the insert. The final lentiviral vectors containing mini-dystrophins were sequenced for verification of the desmin sequence and the cloning sites.



## 4.8 Production of VSV-G lentivirus

Lentiviruses with a VSV-G envelope can infect most mammalian cells, therefore all work must be performed at containment level 2, according to local institution guidelines. The four plasmids (Figure 4.9) were transfected into the packaging cell line HEK-293T to create the infectious viral particles (Figure 4.14). The transfer constructs carried the mini-dystrophins C1/ $\Delta$ R3-R13 and C2/ $\Delta$ H2-R19, driven by the desmin promoter or the GFP construct under control of the same promoter; the latter was used as a control. The virus supernatant was collected 20, 30 and 48 hours after transduction.

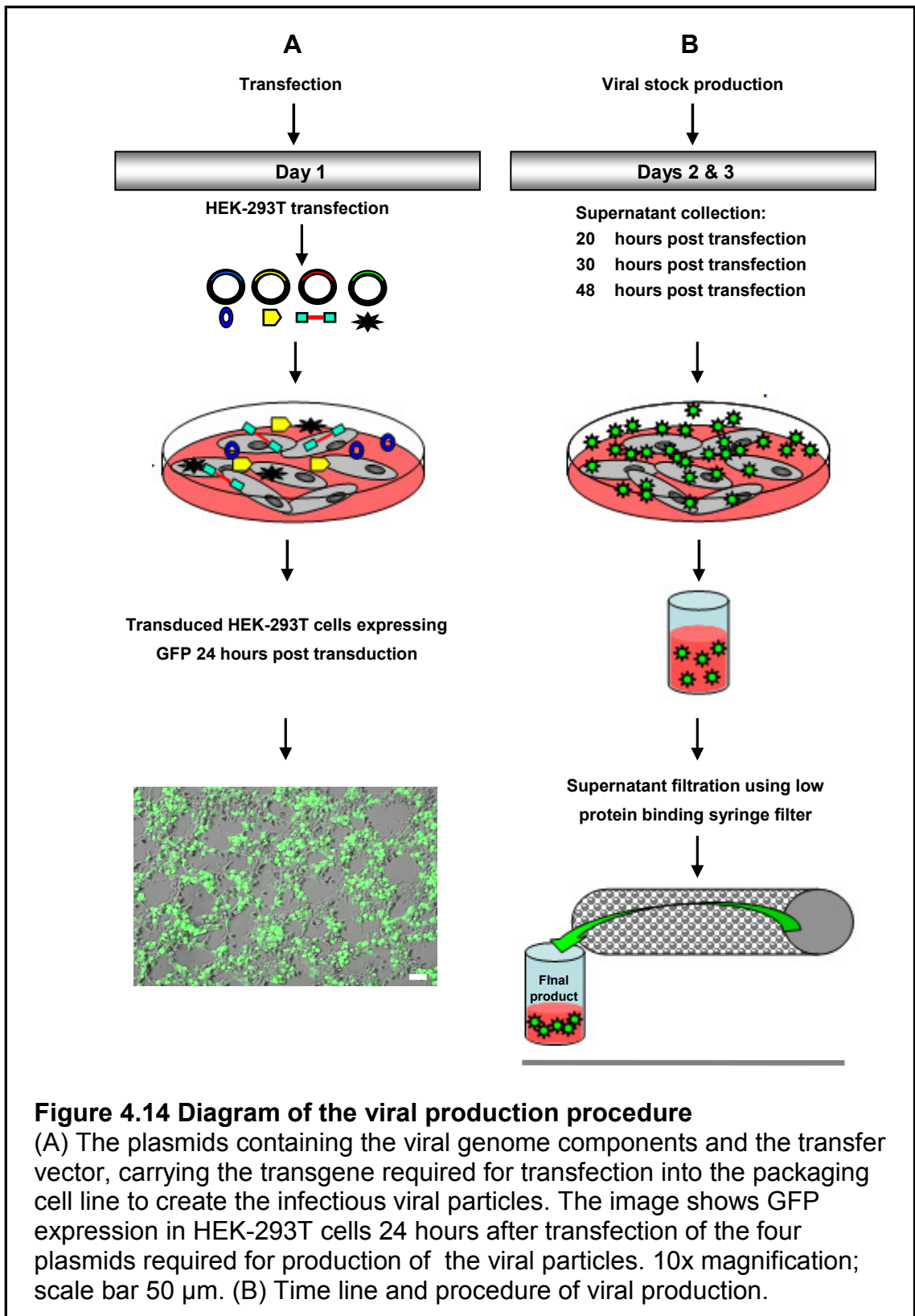


**Figure 4.14 Diagram of the viral production procedure**

(A) The plasmids containing the viral genome components and the transfer vector, carrying the transgene required for transfection into the packaging cell line to create the infectious viral particles. The image shows GFP expression in HEK-293T cells 24 hours after transfection of the four plasmids required for production of the viral particles. 10x magnification; scale bar 50  $\mu$ m. (B) Time line and procedure of viral production.

## 4.9 Myoblasts transduction

### 4.9.1 *GFP transduction and expression results*

Human DMD myoblasts were grown to ~50% confluence and transduced with the virus expressing GFP. Fluorescence microscopy images were taken 24 hours later, showing GFP expression and the infection of the vast majority of the myoblasts (>99%) (Figure 4.15).

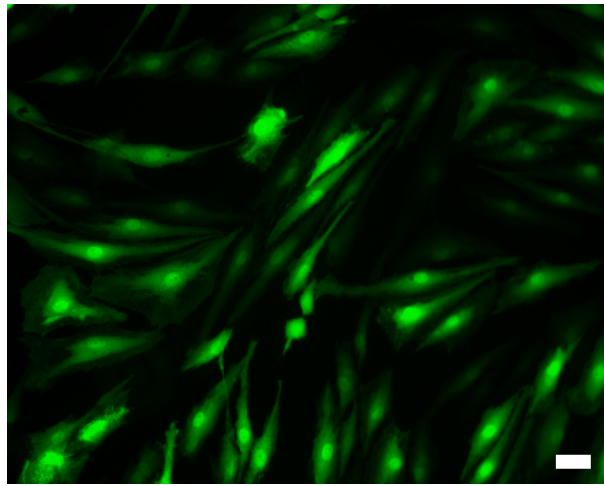


**Figure 4.15 Myoblast transduction using lentivirus**  
Fluorescence microscope image of myoblasts transduced with the virus stock expressing GFP 24 hours after transduction. 20x magnification; scale bar 50  $\mu$ m.

### 4.9.2 *Staining results of DMD human myoblasts after transduction with viral particles carrying mini-dystrophins*

DMD human myoblasts were grown at ~50% confluence and transduced with viruses carrying the mini-dystrophins C1/ $\Delta$ R3-R13 and C2/ $\Delta$ H2-R19. Cells were stained with anti-dystrophin antibody Mandra1, 72 hours after transduction. The results showed the infection of nearly all cells. A large proportion of the staining displayed membrane localisation of the dystrophin to the sarcolemma in the infected cells (Figure 4.16).

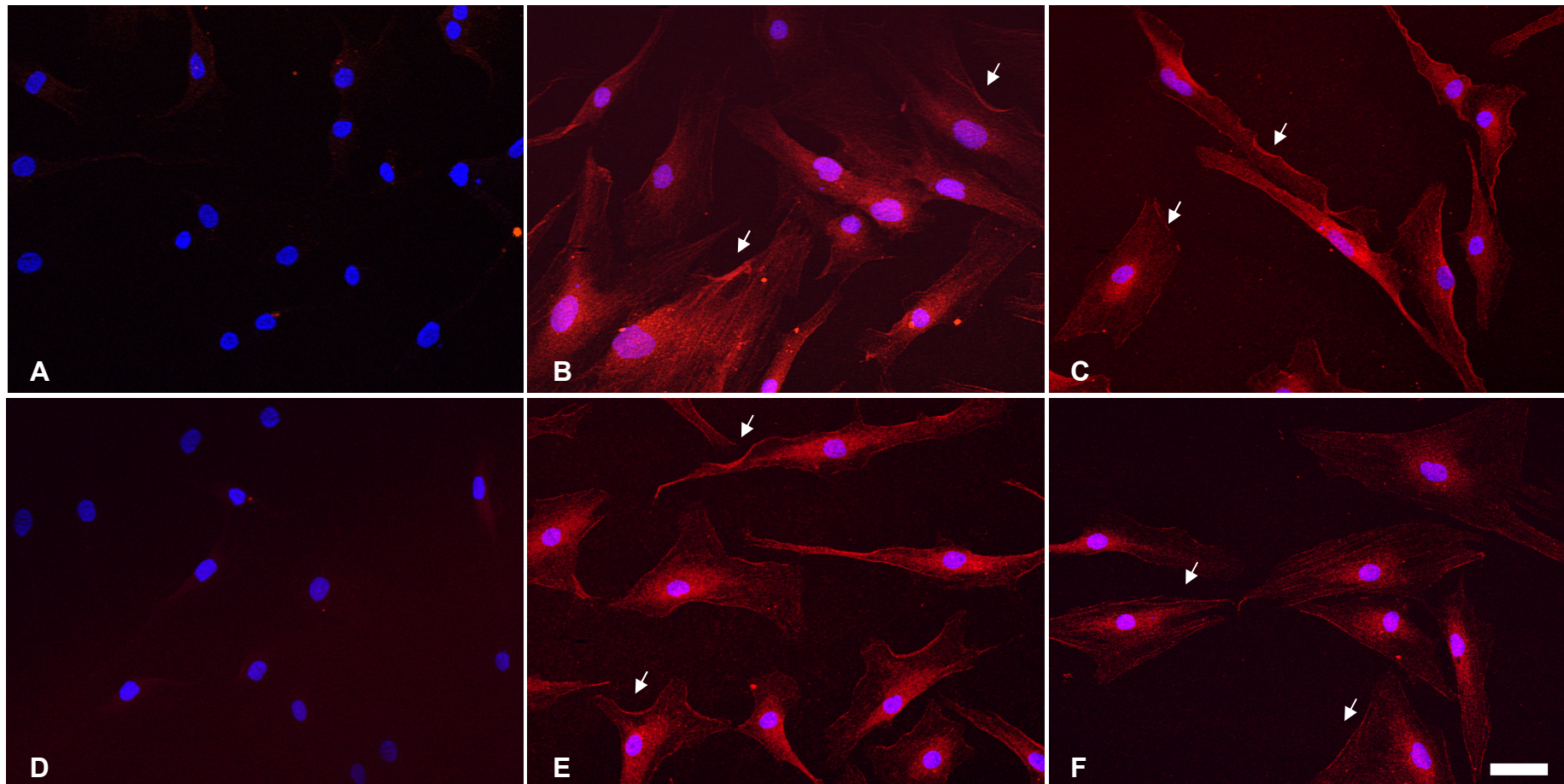


**Figure 4.16 Immunofluorescence following transduction of DMD human myoblasts with lentivirus carrying mini-dystrophins** (A, D) untransduced DMD myoblasts, (B, C) DMD myoblasts transduced with lentivirus carrying C1/ $\Delta$ R13-R13. (E, F) DMD human myoblasts transduced with lentivirus carrying C2/ $\Delta$ H2-R19. The staining was performed using mouse anti-dystrophin antibody Mandra1 and Alexa Fluor 594 goat anti-mouse. White arrows indicate membrane localisation of the mini-dystrophins. 20x magnification; scale bar 50  $\mu$ m.

#### 4.10 Discussion

In contrast to mini-dystrophin expression in HeLa cells in chapter 3, myoblast transfection with mini-dystrophins proved to be challenging. One limiting factor was low transfection efficiency and insufficient expression of mini-dystrophins in transfected dystrophin-deficient myoblasts. Only seven of the 140 stably transfected mdx-immorto clones expressed dystrophin by Western blot, although only those cells which had integrated the resistance gene of the vector should be able to survive selection. These results indicate inefficient integration of the mini-dystrophins carrying plasmids in cells, probably due to loss of the transgene during cell replication. Some results showed smaller bands in Western blot than expected, indicating that the constructs had rearranged during integration, deleting the mini-dystrophins. Transfected nucleic acids in cells can be lost through different processes such as cell division, and transfection efficiency and sustainable expression largely depends on cell type (Kim and Eberwine, 2010).

It has been reported that mdx-immorto cells were successfully transfected in order to express micro-dystrophins *in vitro* (Jorgensen *et al.*, 2009), suggesting that this cell type may be efficiently used for integration of small micro-dystrophins but did not allow the integration of the larger constructs that were generated in this project. One factor influencing DNA transfection efficiency is the size of the plasmids (Campeau *et al.*, 2001; Molnar *et al.*, 2004) and efficient transfection of large plasmid DNA may only be possible using viral vectors (Campeau *et al.*, 2001).

Another hurdle that limited the use of functional assays *in vitro* was lack of differentiation ability of the few stably transfected and isolated cell lines relative to untransfected mdx-immorto myoblasts. Ideally, a cell model for dystrophin restoration studies should not only offer a high transfection rate but also possess the ability to form myotubes, since dystrophin is only expressed in differentiated myotubes (Denetclaw *et al.*, 1993). In addition, many *in vitro* experiments using myoblasts and transfection of a therapeutic gene require the formation of mature myotubes to evaluate and quantify the impact of transfected genes on late onset proteins. For instance assessment of CK activity after

induced stress is dependent on a high and reproducible differentiation state of the cells which is consistent between the experimental and control lines, since CK is an enzyme that is produced only in mature myofibres (Valdes and Jortani, 1999; Tai *et al.*, 2011). Comparing CK release in myotube cultures which are not at the same stage of differentiation could produce strongly biased results simply due to the different levels of CK expression between the myotubes.

It was hoped that the use of immortalised myoblasts from a DMD patient might lead to sufficient amounts and proper subsarcolemmal localisation of dystrophin to offer an alternative cell model. Transient transfection of immortalised human myoblasts using a GFP plasmid presented up to two-fold transfection efficiency relative to mouse cell lines, suggesting that the dystrophin-deficient DMD human myoblast cell model had more favourable transfection characteristics. However no significant dystrophin expression was observed after staining and efficient transfection of the mini-dystrophin plasmids was not achieved in this cell line. FACS analysis data showed transfection efficiency of approximately 60% with GFP plasmid in DMD human myoblasts, suggesting that that the GFP transfection data did not correlate with the transfection of cells with mini-dystrophins and the transfection efficiency was largely dependent on the construct used. One possible explanation is that the constructs were too large to be expressed sufficiently in any of the myoblast lines. These data confirm that transfection efficiency of plasmid cDNA is proportional to the size of transfected DNA molecule (Campeau *et al.*, 2001), and suggest that the large size of mini-dystrophin plasmids could be the dominant factor resulting in the low transfection efficiency in both mouse and human cell lines.

Although transfection is generally a powerful tool for study of transgenes in cells, each transfection method has its disadvantages, can be harmful, toxic and affect nucleic acid delivery to cells depending on the cell type (Kim and Eberwine, 2010). These findings suggest that transfection itself might have caused damage to myoblasts and impaired their differentiation potential. Furthermore, stable transfection could not be considered for DMD human myoblasts, since this cell line was already transformed and selected with G418 during the immortalisation procedure. In addition, DMD human cells had only extended lifespan and may not have survived during the long procedure of

stable transfection. It was concluded that transfection of myoblasts using plasmid constructs, either transient or stable, was difficult to achieve and that a different strategy was necessary to obtain localisation data on the constructs in cell culture.

To address the low transfection capability of the constructs, lentiviral vectors were used to explore their feasibility to efficiently introducing DNA constructs into myoblasts. Several studies have shown that viral vectors increase transfection in a variety of cells and tissues (Odom *et al.*, 2007; Macsai *et al.*, 2012; Sun *et al.*, 2012). Lentiviral vectors were chosen since these vectors have a large packaging capacity and are suitable for the large constructs generated in this work. In addition, lentivirus can infect both dividing and non-dividing cells, independently of their proliferation status (Follenzi and Naldini, 2002), suggesting that differentiated myotubes could be used for transduction in future functional assays to circumvent the low differentiation potential of myoblasts after transfection.

A pilot study with viral transduction by cloning two of the constructs into lentiviral vectors was initiated. Upon transduction a rapid uptake of GFP control in HEK-293T and transduction of the same transgene in myoblasts after 48 hours was observed. The immunofluorescence results of dystrophin expression in myoblasts showed this method to be successful and have potential for future *in vitro* experiments. However, the expression showed not only subsarcolemmal but also cytoplasmic localisation of dystrophin. Studies have shown that dystrophin in skeletal muscle is detected in the cytoplasm at early stages which during maturation increasingly localises to the sarcolemma (Kobayashi *et al.*, 1995). It has also been reported that during transfection the majority of DNA is introduced to the nucleus during mitosis and reformation of nuclear membrane (Campeau *et al.*, 2001). This could explain the incomplete migration of dystrophin to the sarcolemma (Figure 4.16) due to the short period between transduction and analysis. The preliminary viral work described in this chapter provides a basis for the efficient transfer of large plasmids into human myoblasts to facilitate *in vitro* studies as a precursor to using these constructs in gene therapy experiments.

Future work will involve differentiation and transduction of DMD human myotubes with lentivirus carrying mini-dystrophin constructs and evaluation of their ability to restore membrane stability by measuring CK release and cell survival after osmotic shock treatment of transfected cells. If successful, this experiment could be used as a standard method for *in vitro* characterisation of future micro- and mini-dystrophin constructs.

## Chapter 5 Expression of mini-dystrophin constructs in mdx mouse muscle

### 5.1 Introduction

Viral vector mediated gene delivery as a therapy for Duchenne muscular dystrophy requires functional mini-genes that can express and restore dystrophin in dystrophic muscle. However, the functional nature of different mini-genes remains to be defined. DMD is primarily caused by the loss of dystrophin protein (Hoffman *et al.*, 1987a) which forms a link between cytoskeletal elements and extracellular matrix that protects muscle from contraction-induced injury (Ervasti and Sonnemann, 2008). Clearly, there is a direct relationship between dystrophin expression and disease severity in DMD (Nicholson *et al.*, 1993). Most DMD patients show very little or no dystrophin protein in muscle fibres, whereas patients with BMD have reduced but partially functional dystrophin (Monaco *et al.*, 1988; Hrdlicka *et al.*, 2002). Clinical correlations in DMD and BMD patients indicate that internally deleted dystrophin has the potential to convey clinical benefits in DMD patients (Anthony *et al.*, 2011). In order to determine the functionality of truncated dystrophin constructs and their therapeutic potential to ameliorate disease severity in DMD, it is essential to characterise the consequences of internal deletions in animal models. The mdx mouse is the most frequently used animal models for DMD preclinical studies. A wide range of physiological and histological parameters have been used to assess the therapeutic interventions in mdx mouse (Willmann *et al.*, 2012). For characterisation of the mini-dystrophins that were generated in this study, direct injection of plasmid DNA in adult mdx muscles followed by electroporation was used (Molnar *et al.*, 2004). This chapter will focus particularly on the effect of construct expression in the *tibialis anterior* (TA) muscle of dystrophic mdx mice and aims to quantify the outcome with respect to pathology-relevant morphometric parameters including expression intensity, number of internal nuclei, muscle fibre diameter and size distribution. A detailed comparison of cryosectioned injected muscles was performed to explore the extent to which different parts of the dystrophin molecule are required or dispensable for function. This initial assessment will determine the overall

suitability of different constructs for cloning into lentiviral vectors and gene delivery to skeletal muscle.

## **5.2 Aims**

To examine whether the mini-dystrophins are able to restore dystrophin expression after injection and electroporation of naked plasmids into mdx mouse muscles.

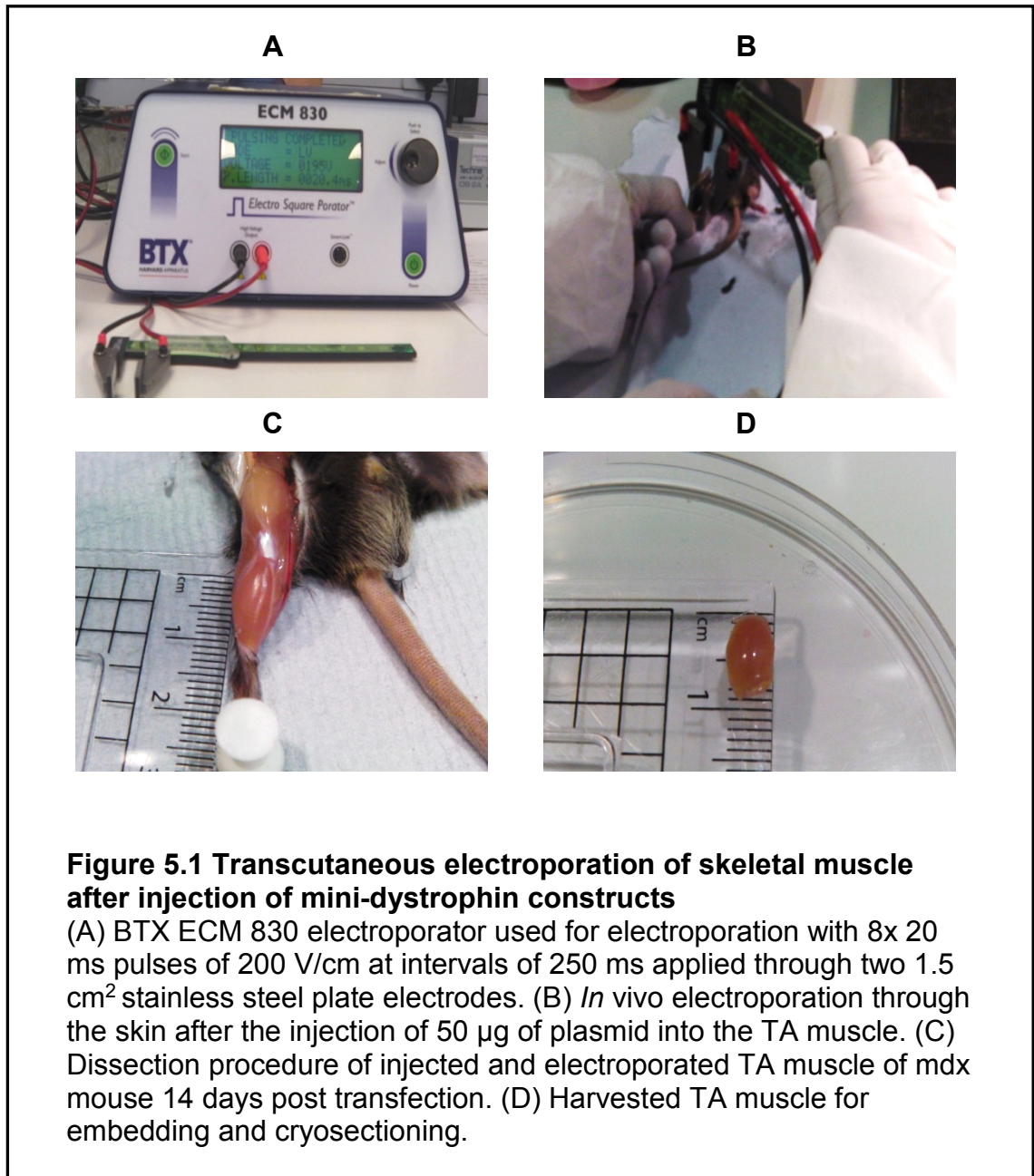
To test whether mini-dystrophin expression would lead to recruitment of other DGC proteins such as the sarcoglycan complex to the sarcolemma.

To assess the relative expression levels of different constructs in the context of dystrophic muscle.

To evaluate the relative change in morphometric parameters of fibres transfected with different constructs including measurement of muscle fibre diameter and analysis of the size distribution.

### 5.3 Intramuscular injection and electroporation of mini-dystrophins into mdx mouse muscle

To evaluate the functional characteristics of the mini-dystrophin constructs *in vivo*, the newly generated mini-dystrophin plasmids were injected and immediately electroporated into 12 week old TA muscle of mdx mice (n=8) (Figure 5.1).



#### 5.4 Analysis of mini-dystrophin expression and localisation in electroporated mdx muscles

In these experiments 14 week old male wild type and untreated male mdx mice were used as controls (n=4 in each group). Dystrophin expression after electroporation of mini-dystrophin constructs was detected on serial sections using the NCL-DYS2 dystrophin antibody and compared to control mice. In wild type mice, there was an equal and uniform dystrophin expression in nearly all fibres (Figure 5.2). In order to calculate the number of revertant fibres, a systematic study of the revertant fibres in age-matched mdx mice was required to estimate the number of such fibres in muscles transfected with mini-dystrophin constructs. This was because the dystrophin antibody (NCL-DYS2) that were used for dystrophin detection, recognised revertant fibres. Revertant fibres occur in 50% of DMD patients (Hoffman *et al.*, 1990; Nicholson *et al.*, 1990; Fanin *et al.*, 1992) as well as in the mdx mouse (Koenig *et al.*, 1987; Grounds *et al.*, 2008) and in the golden retriever dystrophic dog (Schatzberg *et al.*, 1998). Revertant fibres are thought to be the result of spontaneous alternative splicing or exon skipping leading to expression of internally deleted smaller isoforms (Schatzberg *et al.*, 1998). A clear interpretation of these pre-existing fibres in treated muscle is required for dystrophin quantification and evaluation of the efficiency of therapeutic interventions. The number of revertant fibres in mdx TA muscles varied between 2 and 12 per section. All four constructs that were used for the experiment produced dystrophin and were localised at the muscle fibre membrane, confirming the expression of mini-dystrophins at the correct cellular localisation in mdx muscle (Figure 5.2). However the number of transfected myofibres ranged from 35-198 per section (Figure 5.3). The use of dual immunohistochemistry staining for dystrophin and laminin allowed dystrophin quantification relative to laminin, providing an internal control across different samples and experiments (Figure 5.3). To assess expression levels of mini-dystrophins, the number of dystrophin positive fibres was first counted. Between 7 and 8 TA muscles were analysed in each group and 1560-2580 muscle fibres per section were used to calculate the percentage of positive fibres relative to the entire muscle cross section (Figure 5.3; Table 5.1).

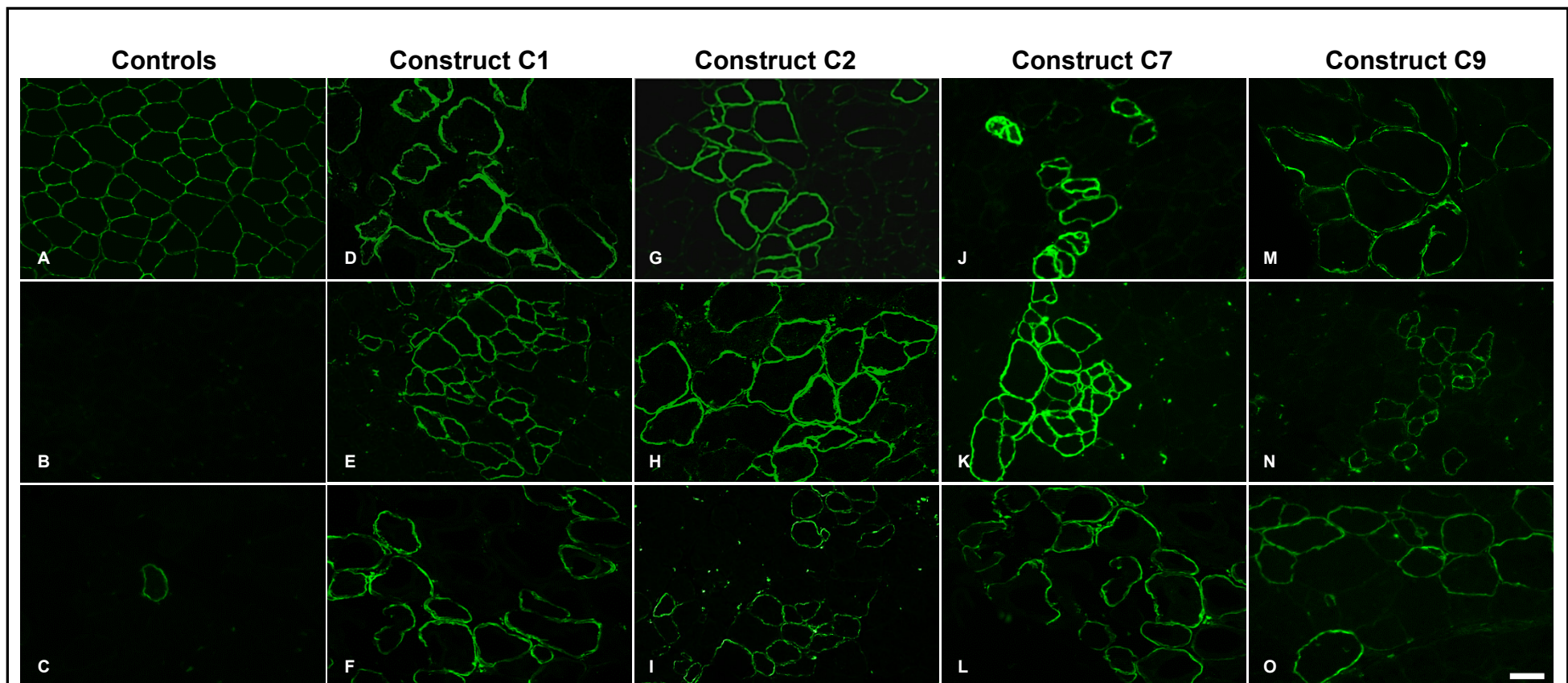
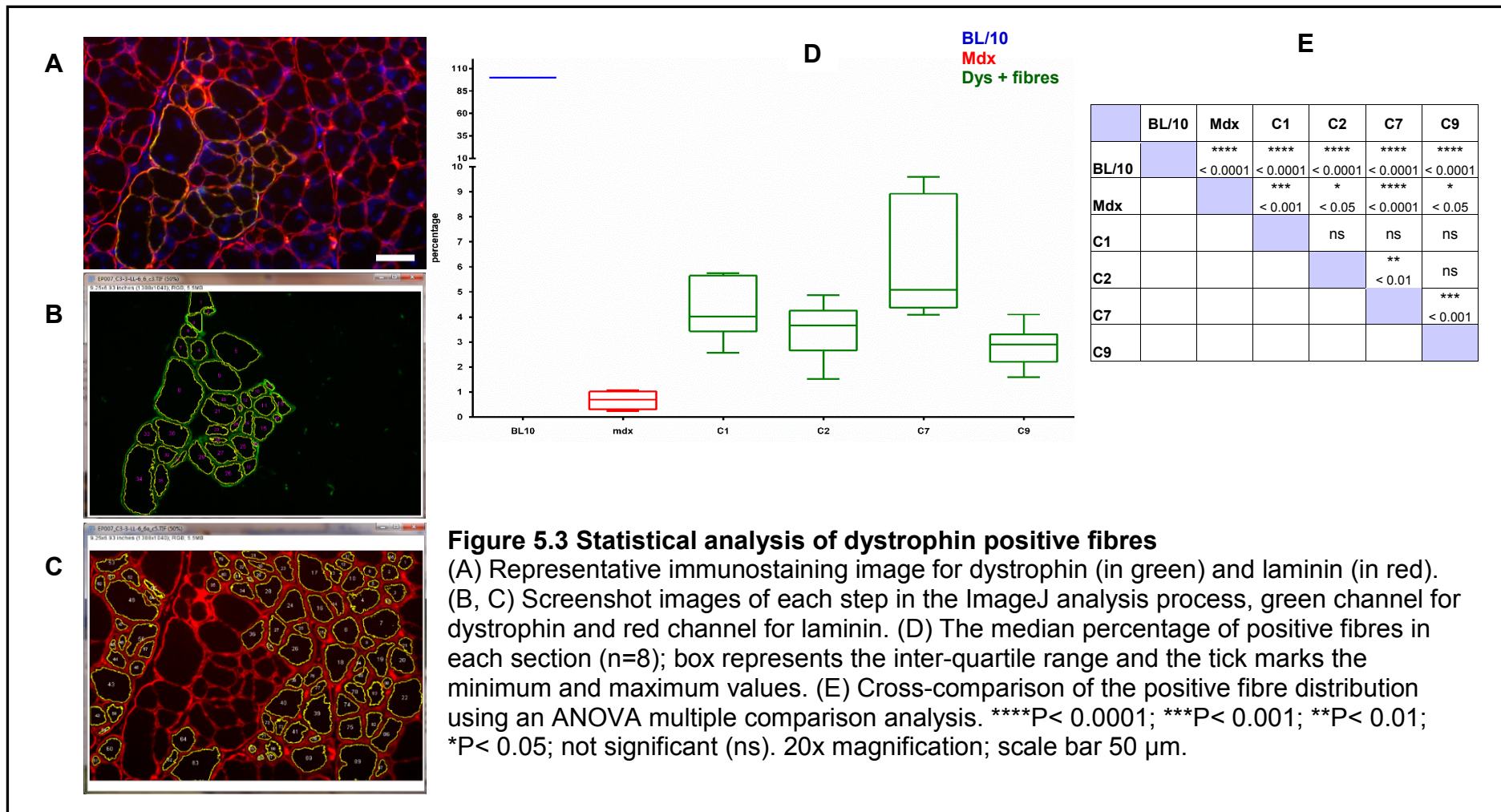


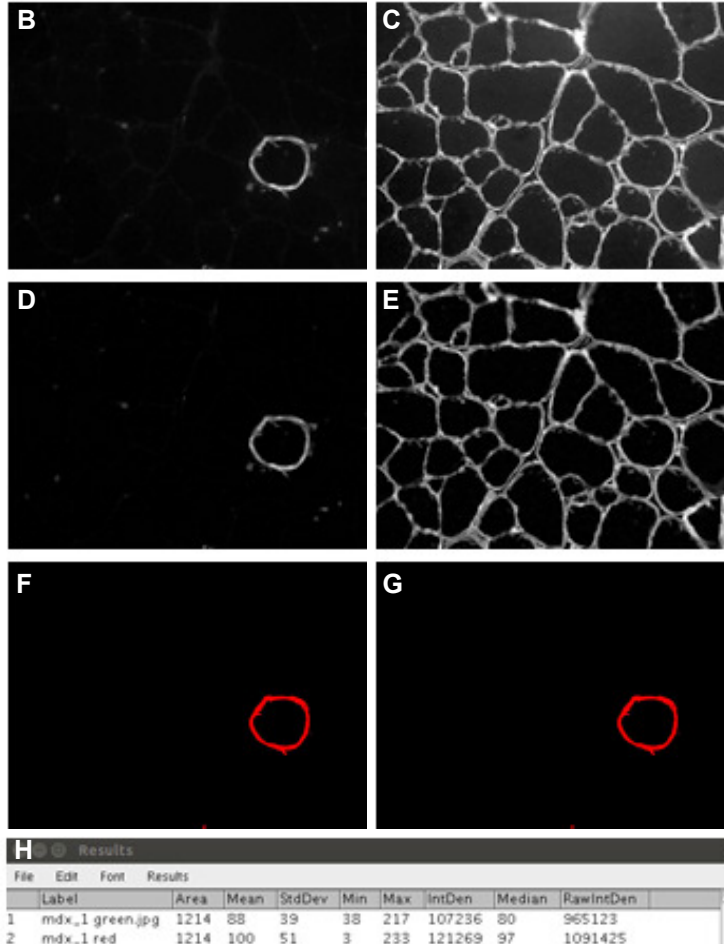
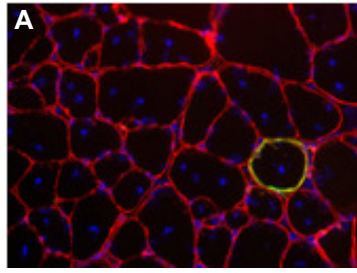
**Figure 5.2 Dystrophin expression in mdx mouse muscles electroporated with mini-dystrophin constructs**

Typical immunofluorescence images of mouse muscle sections stained with anti-dystrophin mouse antibody NCL-DYS2 and direct labelling using Zenon Alexa Fluor 488. (A) Control C57BL/10; (B, C) non-electroporated mdx mouse muscle; (D, E, F) mdx mouse muscle electroporated with construct C1/ΔR3-R13; (G, H, I) mdx mouse muscle electroporated with construct C2/ΔH2-R19; (J, K, L) mdx mouse muscle electroporated with construct C7/ΔH2-R23; (M, N, O); mdx mouse muscle electroporated with construct C9/ΔR1-R10. 20x magnification; scale bar 50 μm.



## 5.5 Analysis of dystrophin expression intensity

In view of relatively low percentage of dystrophin positive fibres, it was not possible to perform a semi-quantitative analysis using Western blot to quantify the amount of dystrophin in electroporated muscles. In order to get an idea of how much dystrophin was expressed, the intensity of immunofluorescence staining on cryosections was measured. Images of muscle sections were opened in ImageJ, the channels split into green, stained for dystrophin and red, stained for laminin as a control. Background was reduced (Figure 5.4) and the green channel was used to identify dystrophin positive fibres. A threshold was selected to create a mask, in order to measure the region of the selected area (dystrophin expressing fibres). The red channel was used to measure the intensity of the same selected region to normalise the dystrophin value relative to laminin which should be constant between fibres and experiments. Several parameters were measured for each section including area, min/max intensity, mean, standard deviation and median. The median value was chosen to reflect the average dystrophin expression intensity per selection. For comparison of sections with different numbers of dystrophin positive fibres and consideration of unavoidable technical variations (antibody batches, sample preparation and microscope light properties) in staining intensities, a ratio of dystrophin and laminin staining was calculated (median intensity green divided by median intensity red) and presented in box plots (Figure 5.5). No significant differences between constructs, or between constructs and revertant fibres, or positive controls was observed. However, the range of dystrophin expression from the constructs showed wider variability.



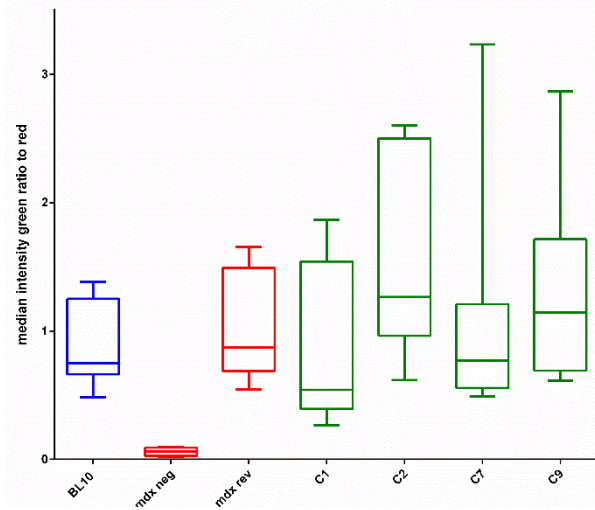
**H** Results

Label	Area	Mean	StdDev	Min	Max	IntDen	Median	RawIntDen
1 mdx_1 green.jpg	1214	88	39	38	217	107236	80	965123
2 mdx_1 red	1214	100	51	3	233	121269	97	1091425

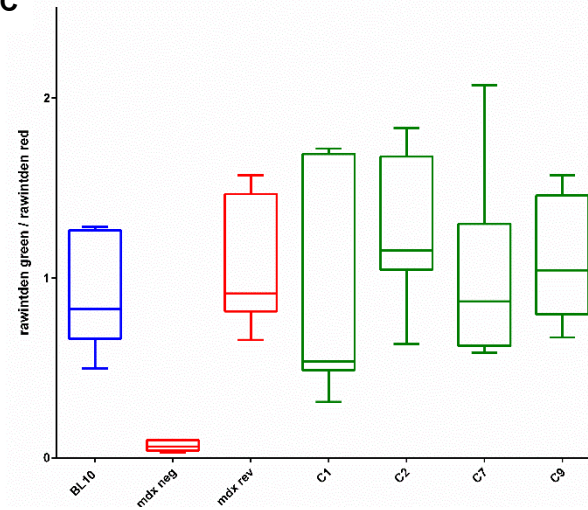
**Figure 5.4 Semi-quantitative measurement of dystrophin expression intensity**

(A) Representative immunofluorescence image of an untreated muscle with a revertant fibre opened in ImageJ analysis process. (B) The image is split into channels for dystrophin and (C) for laminin staining. (D, E) Background staining is reduced and subtracted for both channels. (F) The green channel is used to identify dystrophin positive fibre and a threshold is adjusted to create a mask. (G) The red channel is used to measure the intensity of the same selected area as the normalisation value. (H) Screenshot of the parameters that were taken for calculation of the intensity.

**A**



**C**



**B**

	BL/10	Mdx	Mdx rev	C1	C2	C7	C9
BL/10		** <0.01	ns	ns	ns	ns	ns
Mdx			*** <0.001	* <0.05	**** <0.0001	** <0.01	**** <0.0001
Mdx rev				ns	ns	ns	ns
C1					ns	ns	ns
C2						ns	ns
C7							ns
C9							

**D**

	BL/10	Mdx	Mdx rev	C1	C2	C7	C9
BL/10		* <0.05	ns	ns	ns	ns	ns
Mdx			** <0.01	* <0.05	*** <0.001	** <0.01	** <0.01
Mdx rev				ns	ns	ns	ns
C1					ns	ns	ns
C2						ns	ns
C7							ns
C9							

**Figure 5.5 Statistical analysis of dystrophin expression intensity**

(A) Ratios of median intensity values (n=8) of dystrophin normalised to laminin.

(B) Cross-comparison of the median intensity ratios of dystrophin and laminin, using an ANOVA multiple comparison analysis.

(C) Ratios of median RawIntDen values of dystrophin normalised to laminin.

(D) ANOVA multiple comparison of median RawIntDen ratios of dystrophin and laminin. \*\*\*\*P< 0.0001; \*\*\*P< 0.001; \*\*P< 0.01; \*P< 0.05; not significant (ns).

## **5.6 Correlation between dystrophin expression, internal nuclei and myofibre size**

One of the pathologic changes in dystrophic muscle is ongoing cycles of degeneration and regeneration of muscle fibres. This process is characterised by an increased rate of internally located nuclei and an abnormal distribution of myofibre size, with a large proportion of small regenerating fibres (Carnwath and Shotton, 1987; Coulton *et al.*, 1988; Pastoret and Sebille, 1995). A decreased number of internal nuclei and a mitigation of the heterogeneity in myofibre size are considered as improvements in dystrophic muscle and proposed as standard targets for experimental readouts (Cavalcanti *et al.*, 2011). In order to compare the relative functionality of different mini-dystrophin constructs on these outcome measures, quantitative assessment of muscle fibre size variation and distribution of internal nuclei in mini-dystrophin expressing fibres was undertaken. Different protocols have been developed and published for standardised assessment of functional and histological parameters (Briguet *et al.*, 2004; Grounds *et al.*, 2008; Taylor *et al.*, 2012). In this study, procedures in accordance with Treat-NMD protocols (Willmann *et al.*, 2012), available at <http://www.treat-nmd.eu/research/preclinical/dmd-sops/> with some modifications such as the choice and use of the software were adapted.

### **5.6.1 Evaluation of internal nuclei**

For determination of the proportion of internal nuclei in control muscles, overlapping images of H&E stained muscle at 10x magnification were acquired and assembled into one picture, allowing the analysis of 1800-4400 muscle fibres (Figure 5.6). Fibres containing internal nuclei were counted manually and expressed as the percentage of the nuclei in control muscles (Table 5.1).

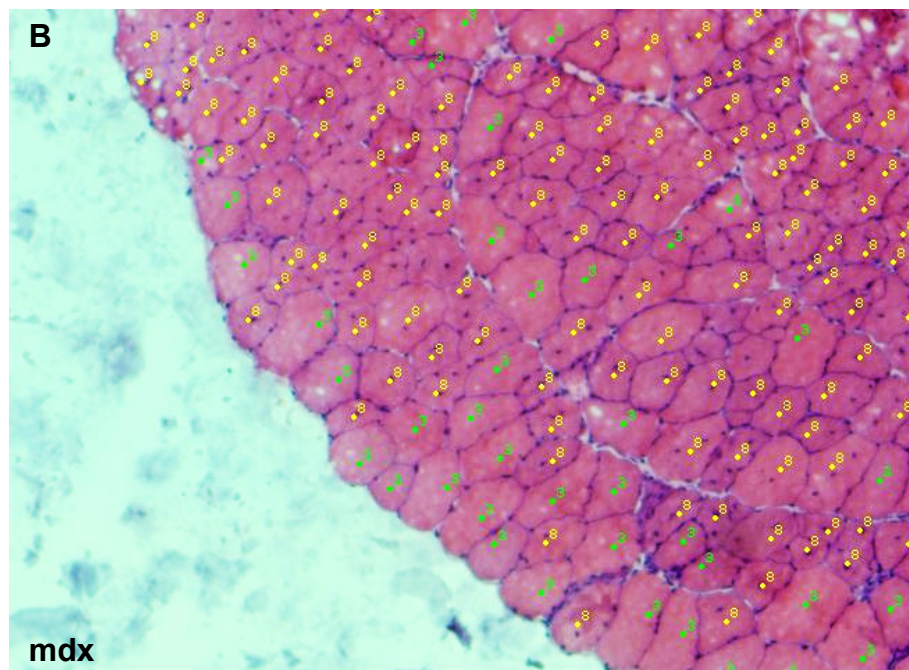
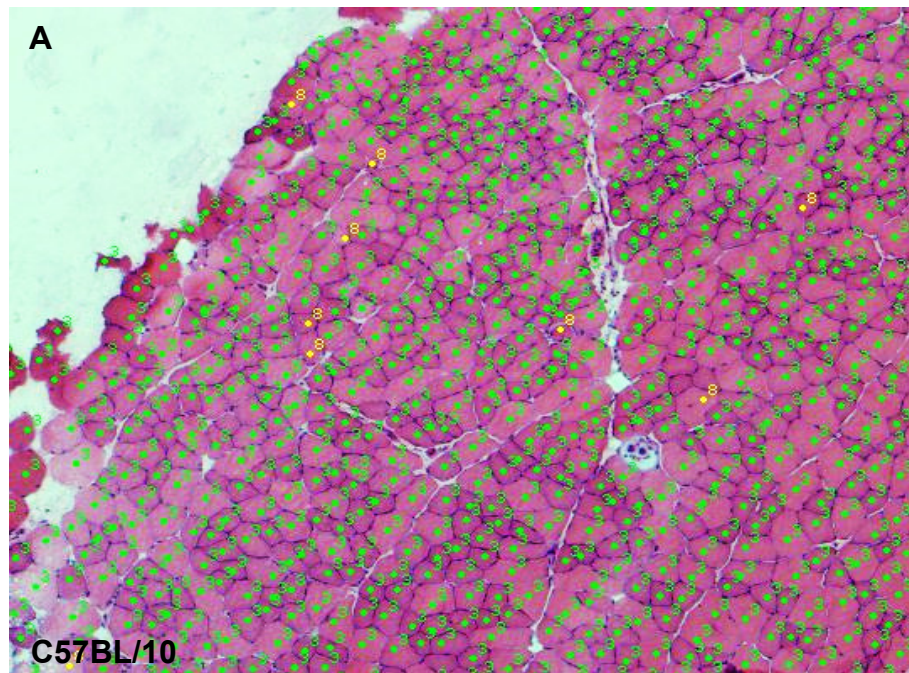


**Figure 5.6 Analysis of internalised nuclei in muscle fibres**

Images of H&E stained TA muscle sections for evaluation of the proportion of internal nuclei using ImageJ. Overlapping images from the entire muscle section are analysed. The fibres containing internally located nuclei are labelled as 8, those without internal nuclei as 3 (arbitrary numbers). (A) Wild type control C57BL/10; (B) mdx control.

Proportions of internally located nuclei in muscle fibres expressing mini-dystrophins were compared to those of dystrophin negative fibres on the same muscle sections (Figure 5.7). Dual immunostaining for dystrophin and laminin was also performed to distinguish between positive and negative fibres. At least 50 images for each construct were analysed. Each image encompassed between 25 and 120 fibres and each analysis used a total of between 1800 and 4400 muscle fibres. The number of internal nuclei in mini-dystrophin positive mdx muscles was reduced compared to untreated mdx muscles. It was also observed that dystrophin negative fibres with peripheral nuclei occurred more frequently where surrounded by dystrophin positive fibres compared with those ones without direct contact with dystrophin positive fibres. Dystrophin negative fibres in the injected muscles also showed a reduction in internal nuclei in comparison to uninjected mdx. However, dystrophin positive fibres showed considerably less internal nuclei compared to dystrophin negative fibres (Figure 5.8A). In C1/ $\Delta$ R3-R13 the fibres with internal nuclei was reduced to ~48% (55% in negative fibres), in C2/ $\Delta$ H2-R19 to ~57% (68% in negative fibres), in C7/ $\Delta$ H2-R23 to ~49% (49% in negative fibres) and in C9/ $\Delta$ R1-R10 to 51% (58% in negative fibres) (Table 5.1).

<i>strain</i>	<i>construct</i>	<i>dystrophin positive fibres (%)</i>	<i>internal nuclei in dystrophin positive fibres (%)</i>	<i>internal nuclei in dystrophin negative fibres (%)</i>
<i>BL/10 (n=4)</i>	----	100	1.7	N/A
<i>mdx (n=4)</i>	----	0.7	79	85
<i>mdx (n=8)</i>	C1	4.3	48	56
<i>mdx (n=8)</i>	C2	3.5	57	68
<i>mdx (n=8)</i>	C7	6.1	49	49
<i>mdx (n=8)</i>	C9	2.9	51	58

**Table 5.1 Median percentage of dystrophin positive fibres and proportion of internal nuclei in electroporated muscles**

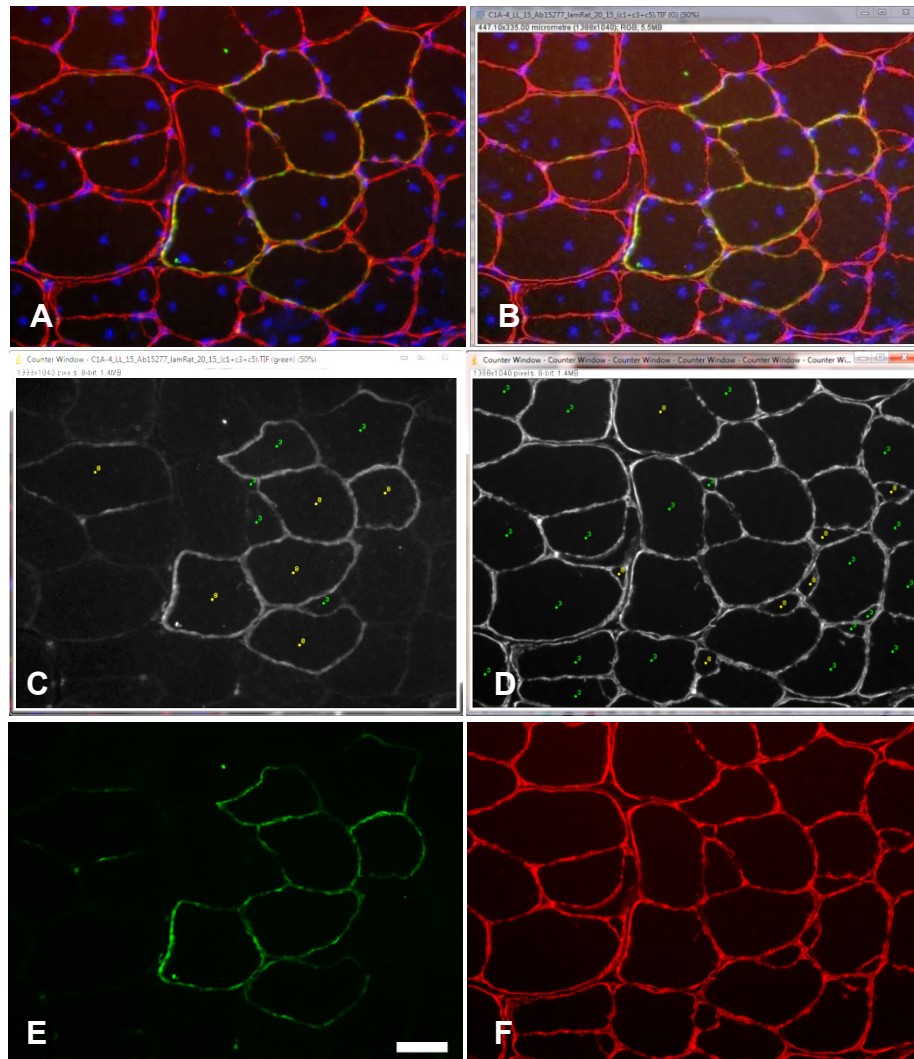
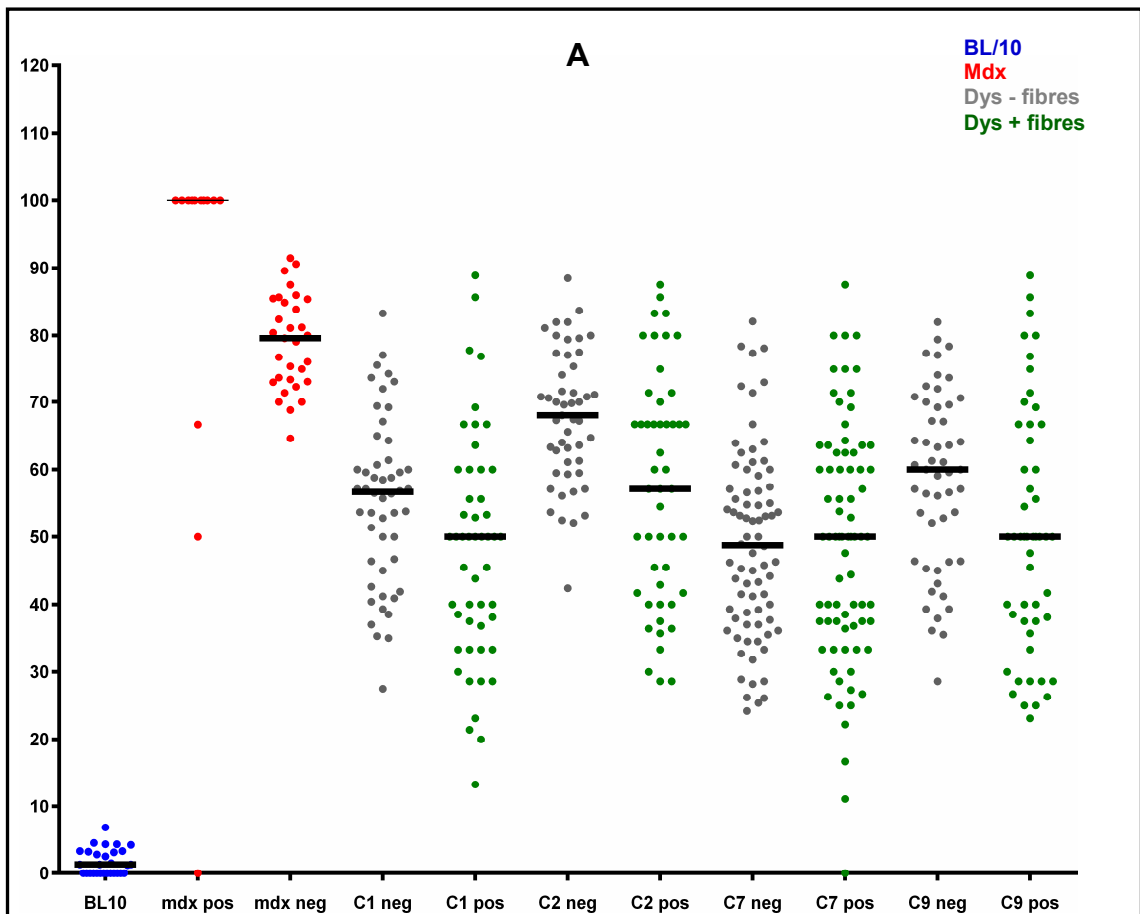


**Figure 5.7 Determination of internal nuclei in mini-dystrophin expressing fibres**

Dual immunostaining of dystrophin and laminin showing the localisation of nuclei in fibres that show dystrophin expression and localisation and those without sarcolemmal dystrophin expression on the sections of electroporated muscle. (A) The merged image of dystrophin, laminin and nuclear staining (green for dystrophin, red for laminin and blue for nuclei stained with DAPI). (B) Image opened in ImageJ; (C, D) different channels are split to distinguish between positive and negative fibres. Fibres with internal nuclei are highlighted with yellow (8) and those without internal nuclei with green (3) (arbitrary numbers). (E, F) The original channels are used for confirmation. 20x magnification; scale bar 50  $\mu\text{m}$ .



**B**

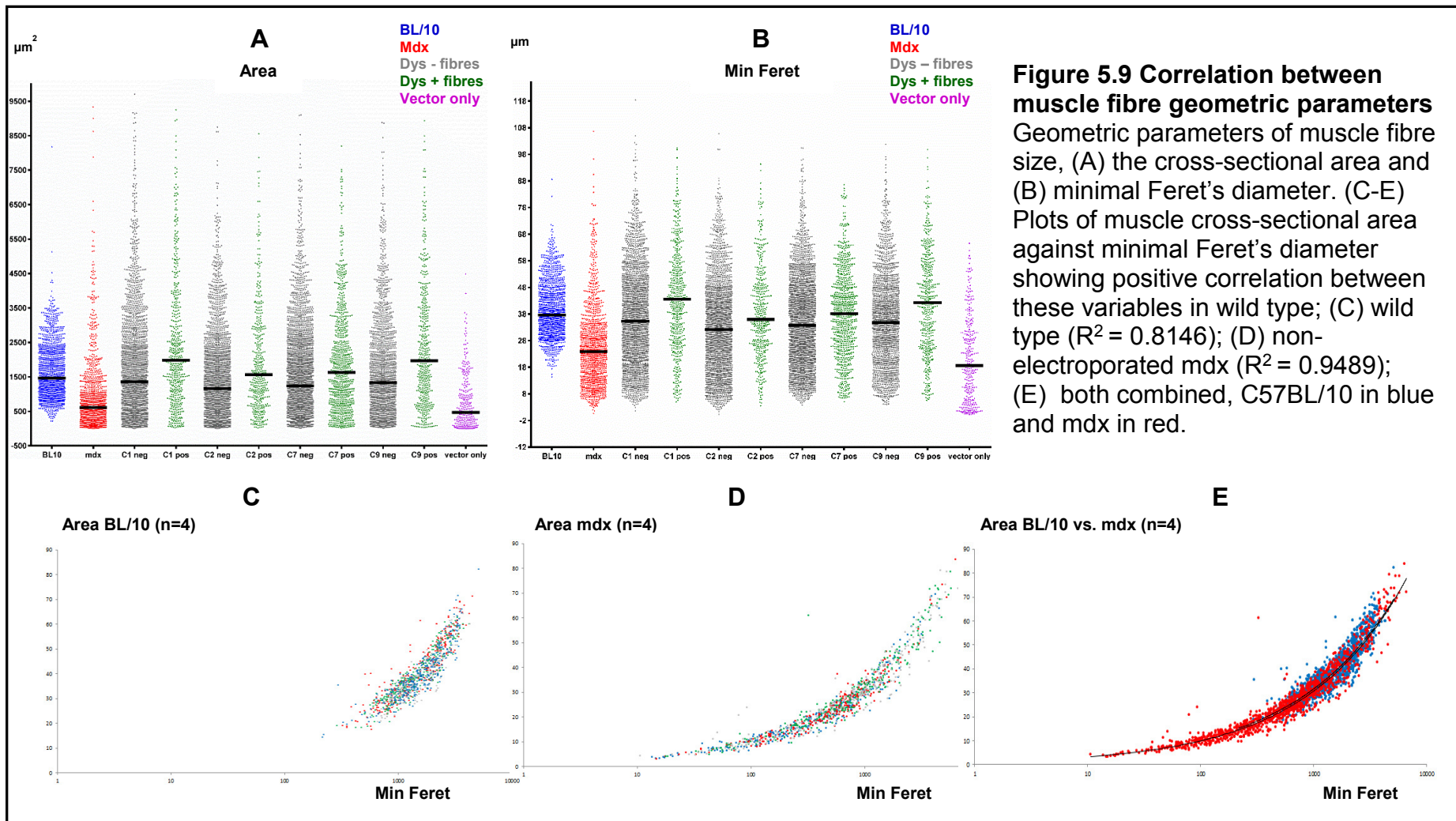
	BL/10	Mdx	C1 neg	C1 pos	C2 neg	C2 pos	C7 neg	C7 pos	C9 neg	C9 pos
BL/10		**** < 0.0001								
Mdx			**** < 0.0001	**** < 0.0001	** < 0.01	**** < 0.0001				
C1 neg				ns	** < 0.01	ns	ns	ns	ns	ns
C1 pos					**** < 0.0001	** < 0.01	ns	ns	ns	* < 0.05
C2 neg						* < 0.05	**** < 0.0001	**** < 0.0001	ns	**** < 0.0001
C2 pos							ns	ns	ns	ns
C7 neg								ns	* < 0.05	ns
C7 pos									ns	ns
C9 neg										ns
C9 pos										

**Figure 5.8 Distribution of internal nuclei in mini-dystrophin positive electroperated fibres**

(A) Each dot represents the percentage of internal nuclei in muscle fibres from one image containing 25-120 fibres. (B) Statistical analysis of internalised nuclei distribution by ANOVA. \*\*\*\*P < 0.0001; \*\*\*P < 0.001; \*\*P < 0.01; \*P < 0.05; not significant (ns).

### **5.6.2 *Quantitative determination of myofibre size***

To provide baseline values for the quantitative measurement of muscle fibre size and variability in mini-dystrophin expressing muscle fibres the muscle fibre size distribution of C57BL/10 wild type mice and mdx TA muscles was assessed. 1250 muscle fibres were measured for wild type and mdx control and between 2300 and 4400 muscle fibres for mini-dystrophin electroporated muscles. For evaluation of myofibre size, sections were stained for dystrophin and laminin (section 2.6.5). Pixel values were converted into  $\mu\text{m}^2$  using a scaling factor determined from the microscope before measurement. Using ImageJ different channels were split and the boundaries of individual muscle fibres were identified and selected semi-automatically then manually checked. After identification of regions of interest two geometric parameters for muscle fibre size determination were calculated including the entire cross-sectional area and the minimal Feret's diameter. Linear correlation performed with the paired observations indicated strong relationship between the two parameters (Figure 5.9). Therefore only one parameter (area) was used for quantification and statistical analysis.



Analysis of muscle fibre morphometrics showed an abnormal distribution and higher variability of mdx muscle fibre size distribution when compared to wild type mouse muscle. In mini-dystrophin expressing fibres a high number of both small and extremely large fibres was found, as observed in untreated mdx fibres. However the median values of transfected fibres showed a tendency towards wild type values when compared to mdx (Figure 5.9; Figure 5.10). The median values for the wild type muscles showed a range between 218 and 8174  $\mu\text{m}^2$ , in the mdx muscle between 3 and 9336  $\mu\text{m}^2$ , in C1/ $\Delta$ R3-R13 transfected muscles between 26 and 13827  $\mu\text{m}^2$ , in C2/ $\Delta$ H2-R19 between 23 and 8553  $\mu\text{m}^2$ , in C7/ $\Delta$ H2-R23 between 21 and 8200  $\mu\text{m}^2$  and in C9/ $\Delta$ R1-R10 between 35 and 8937  $\mu\text{m}^2$  (Table 5.2). These results suggest that the mini-dystrophin expression leads to improvement of morphological parameters which characterise the pathology of mdx dystrophic muscle. Fibre size distribution was illustrated as percentage of muscle fibre cross-sectional area in histograms (Figure 5.11). Muscle fibres were grouped in 100  $\mu\text{m}^2$  intervals by relative frequency. Mdx cross-sectional area showed variable proportions of small and large muscle fibres with a shift towards the smaller fibre sizes compared to wild type C57BL/10. The electroporated muscles with mini-dystrophin constructs seemed to retain the shift to smaller fibres as in untreated mdx, but also showed larger fibres within fibre size range in control muscle C57BL/10.

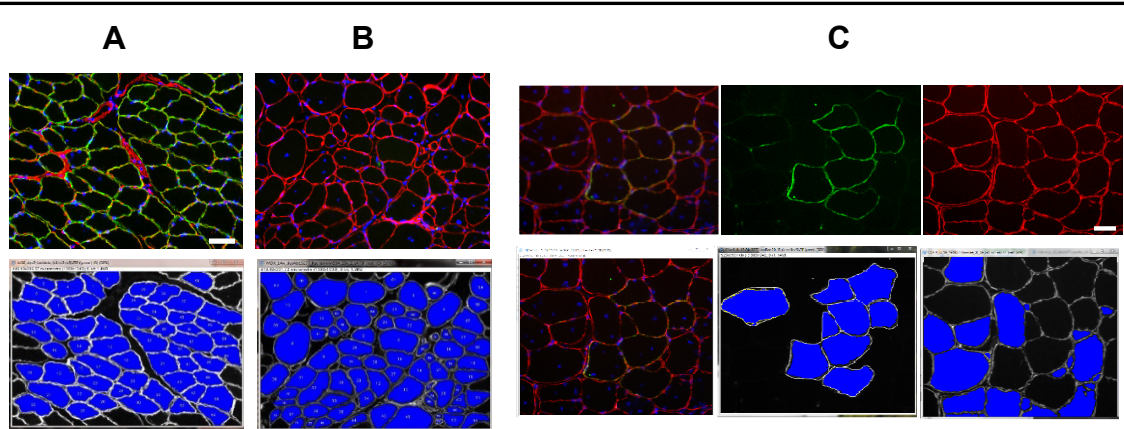
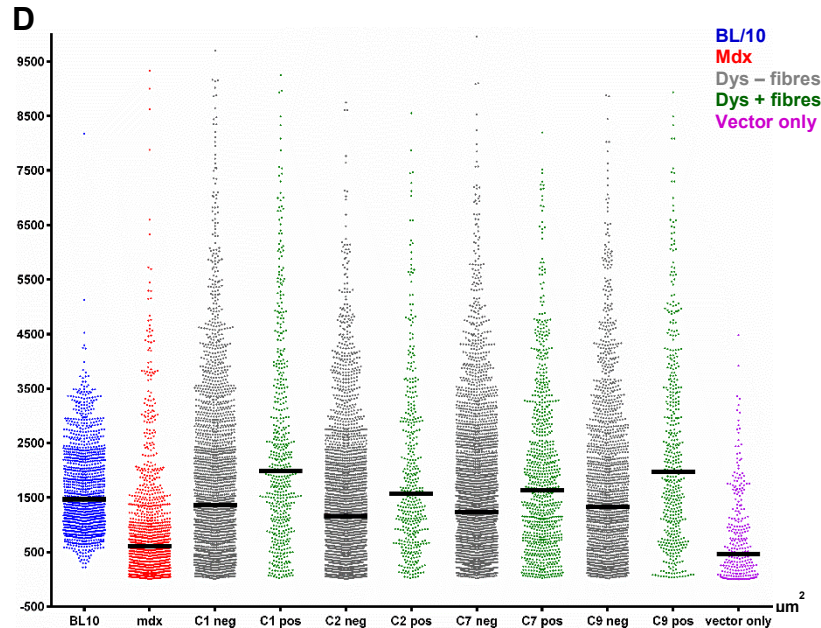


**Figure 5.10 Morphometric quantification of muscle fibre size and statistical analysis of transfected fibres**

Illustration of muscle fibre size measurement in (A) wild type muscle C57BL/10, (B) mdx and (C) electroperated muscle. 20x magnification; scale bar 50 µm. (D) Graphic presentation of the muscle fiber size distribution. (E) Size distribution data assessed for statistical significance using ANOVA multiple comparison between mini-dystrophin electroperated mdx and wild type mouse muscle. \*\*\*\*P < 0.0001; \*\*\*P < 0.001; \*\*P < 0.01; \*P < 0.05; not significant (ns).



**E**

Area	BL/10	Mdx	C1 neg	C1 pos	C2 neg	C2 pos	C7 neg	C7 pos	C9 neg	C9 pos	Vector
BL/10		****	****	*	****	ns	****	ns	****	**	****
Mdx			****	****	****	****	****	****	****	****	ns
C1 neg				< 0.0001	< 0.0001	< 0.05	< 0.01	< 0.01	ns	< 0.0001	< 0.0001
C1 pos					****	*	****	**	****	ns	****
C2 neg						****	ns	****	****	****	****
C2 pos							****	ns	**	ns	< 0.0001
C7 neg								****	ns	****	****
C7 pos									< 0.001	< 0.05	< 0.0001
C9 neg										****	****
C9 pos											< 0.0001
Vector											

<i>Area</i>	<i>BL/10</i>	<i>Mdx</i>	<i>C1 neg</i>	<i>C1 pos</i>	<i>C2 neg</i>	<i>C2 pos</i>	<i>C7 neg</i>	<i>C7 pos</i>	<i>C9 neg</i>	<i>C9 pos</i>	<i>Vector only</i>
<i>Number of values</i>	1250	1250	2328	511	2523	417	3292	813	1775	458	312
<i>Median</i>	<b>1467</b>	<b>608</b>	<b>1359</b>	<b>1982</b>	<b>1160</b>	<b>1568</b>	<b>1238</b>	<b>1631</b>	<b>1327</b>	<b>1975</b>	<b>465</b>
<i>Minimum</i>	218	3	5	26	7	23	18	21	14	35	2
<i>25% Percentile</i>	1036	238	579	1065	506	842	590	765	588	931	84
<i>75% Percentile</i>	2209	1150	2488	3508	2037	2900	2105	2839	2403	3508	1124
<i>Maximum</i>	8174	9336	12178	13827	10428	8553	13268	8200	11716	8937	4482
<i>Mean</i>	1663	934	1790	2486	1470	2019	1558	1972	1712	2403	753
<i>Standard deviation</i>	813	1103	1608	1991	1294	1619	1344	1555	1498	1847	827

**Table 5.2 Descriptive statistics of muscle fibre size distribution (area)**

This table shows the values of the cross-sectional area measurements. All values are given in  $\mu\text{m}^2$ . Measurements are performed in dystrophin positive as well as in dystrophin negative fibres from mini-dystrophin electroporated mouse muscles.

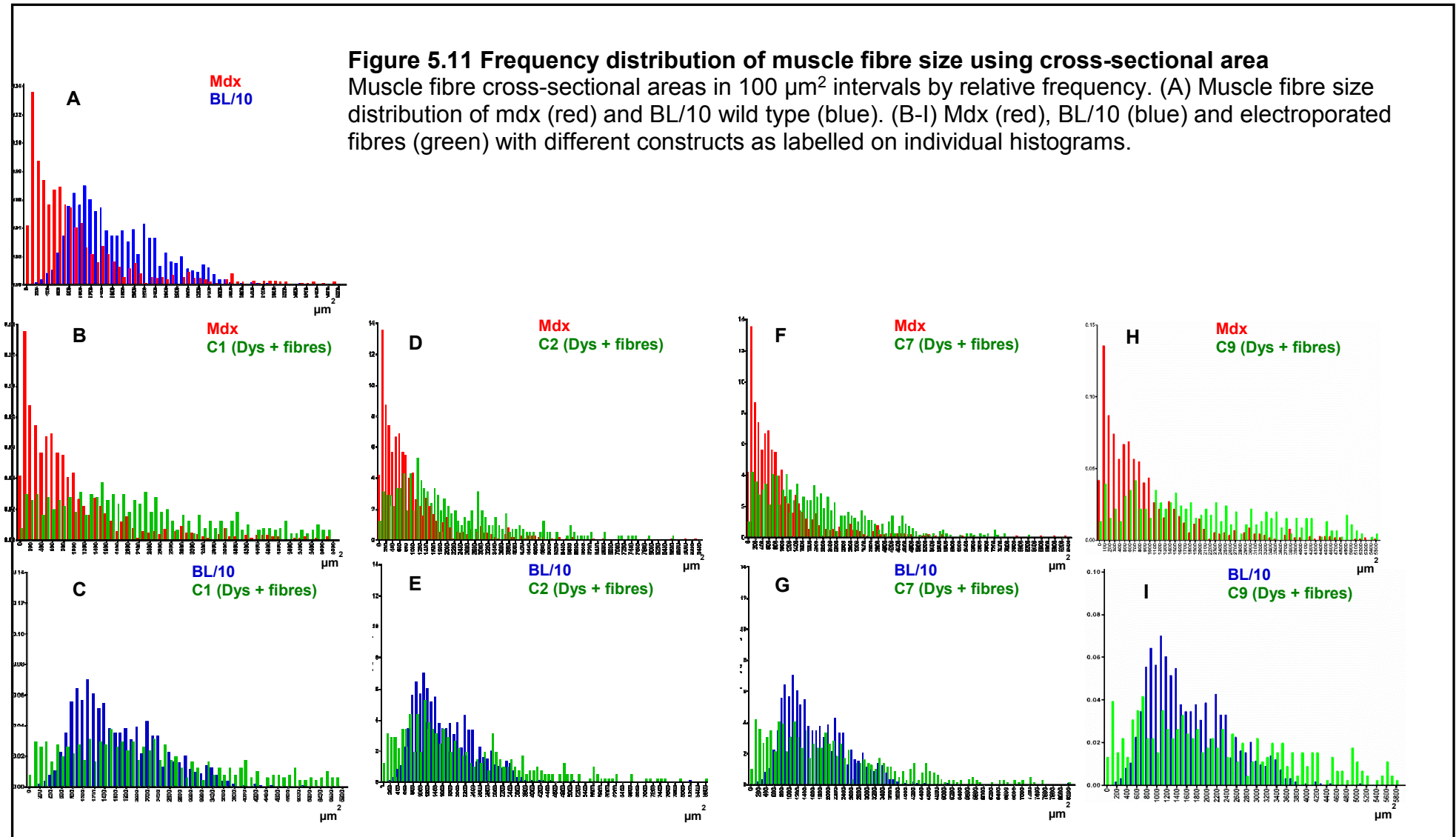
<i>Minimal Feret</i>	<i>BL/10</i>	<i>Mdx</i>	<i>C1 neg</i>	<i>C1 pos</i>	<i>C2 neg</i>	<i>C2 pos</i>	<i>C7 neg</i>	<i>C7 pos</i>	<i>C9 neg</i>	<i>C9 pos</i>	<i>Vector only</i>
<i>Number of values</i>	1250	1250	2328	511	2523	417	3292	813	1775	458	312
<i>Median</i>	<b>38</b>	<b>24</b>	<b>35</b>	<b>32</b>	<b>35</b>	<b>34</b>	<b>34</b>	<b>38</b>	<b>35</b>	<b>42</b>	<b>19</b>
<i>Minimum</i>	14	0.7	1.5	5	0.3	3.5	3.8	5	4	7	0.3
<i>25% Percentile</i>	32	15	23	30	21	26	23	26	23	27	6
<i>75% Percentile</i>	46	33	48	56	43	49	44	49	47	56	32
<i>Maximum</i>	87	107	335	337	106	94	125	87	335	337	65
<i>Mean</i>	40	26	37	44	33	39	36	38	36	43	21
<i>Standard deviation</i>	11	15	19	23	17	18	15	17	19	24	16

**Table 5.3 Descriptive statistics of muscle fibre size distribution (minimal Feret)**

This table shows the values of the cross-sectional minimal Feret's diameter. All values are given in  $\mu\text{m}$ . Measurements were performed in dystrophin positive as well as in dystrophin negative fibres from mini-dystrophin electroporated mouse muscles.

### Figure 5.11 Frequency distribution of muscle fibre size using cross-sectional area

Muscle fibre cross-sectional areas in  $100 \mu\text{m}^2$  intervals by relative frequency. (A) Muscle fibre size distribution of mdx (red) and BL/10 wild type (blue). (B-I) Mdx (red), BL/10 (blue) and electroporated fibres (green) with different constructs as labelled on individual histograms.



## 5.7 Effect of mini-dystrophin constructs on DGC proteins

### 5.7.1 *Gamma-sarcoglycan restoration*

In the absence of dystrophin, DGC proteins are reduced and therefore restoration of these proteins is a requirement for a mini-dystrophin to be considered functional (Turk *et al.*, 2005). In order to examine the localisation of the mini-dystrophin constructs and their effect on sarcoglycan complex restoration, dual immunofluorescence staining was used with antibodies directed against mini-dystrophin C-terminus and  $\gamma$ -sarcoglycan. In wild type fibres, dystrophin and  $\gamma$ -sarcoglycan were detected at the correct location in all fibres, whereas in mdx muscles both antibodies were only found in the myofibre membrane of revertant fibres. All four constructs showed co-localisation of  $\gamma$ -sarcoglycan at the sarcolemma of dystrophin expressing fibres in muscles (Figure 5.12). These data suggest that the mini-dystrophins are capable of restoring the link between dystrophin and the DGC.

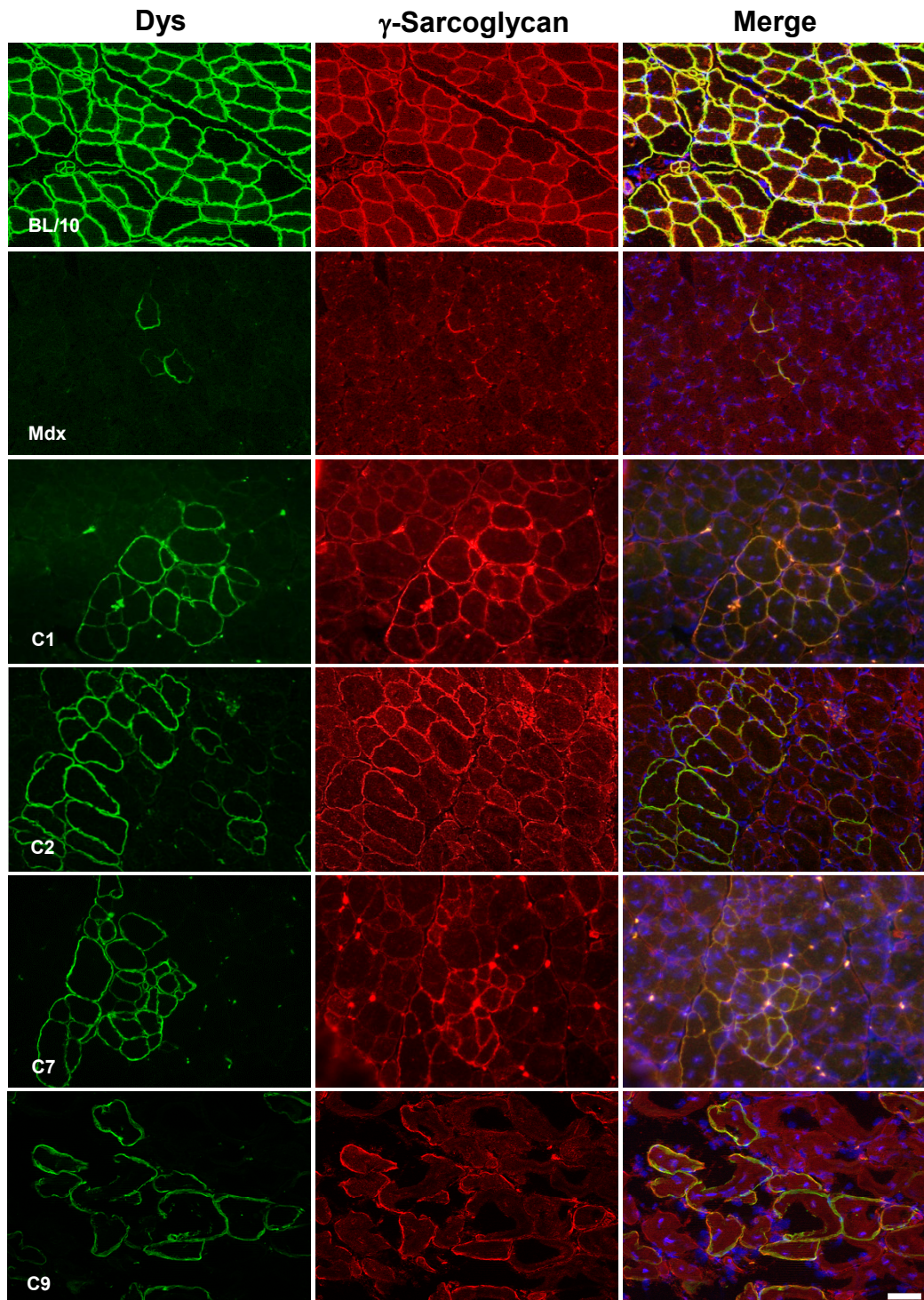


**Figure 5.12 Dystrophin and  $\gamma$ -sarcoglycan expression in electroporated muscle**

Immunofluorescence analysis of TA muscles from mice electroporated with mini-dystrophins compared to control sections of wild type muscles and untreated mdx. Samples were stained for dystrophin with mouse anti-dystrophin NCL-DYS2 and direct labelling with Zenon Alexa Fluor 488 (green) and for  $\gamma$ -sarcoglycan with rabbit anti- $\gamma$ -sarcoglycan and rat anti-rabbit (red). 20x magnification; scale bar 50  $\mu$ m.

### **5.7.2 nNOS stabilisation at the sarcolemma**

Studies have shown that dystrophin rod repeats 16 and 17 are capable of stabilising nNOS at the sarcolemma (Lai *et al.*, 2009a; Lai *et al.*, 2013). The following experiment was performed to test the hypothesis that mini-dystrophin molecules containing the rod domain nNOS-binding site (C1/ $\Delta$ R3-R13 and C9/ $\Delta$ R1-R10) would enhance nNOS localisation to the sarcolemma, compared to the mini-dystrophin constructs lacking these regions (C2/ $\Delta$ H2-R19 and C7/ $\Delta$ H2-R23). Dual immunostaining on muscle sections with antibodies directed against the dystrophin C-terminus and nNOS was performed. Both proteins were expressed at the muscle fibre membrane in wild type control and in revertant fibres of mdx sections. The majority of fibres in electroporated muscles expressing mini-dystrophins C1/ $\Delta$ R3-R13 and C9/ $\Delta$ R1-R10 increased nNOS expression at the sarcolemma whereas fibres of muscles electroporated with C2/ $\Delta$ H2-R19 and C7/ $\Delta$ H2-R23 were negative for nNOS staining (Figure 5.13).

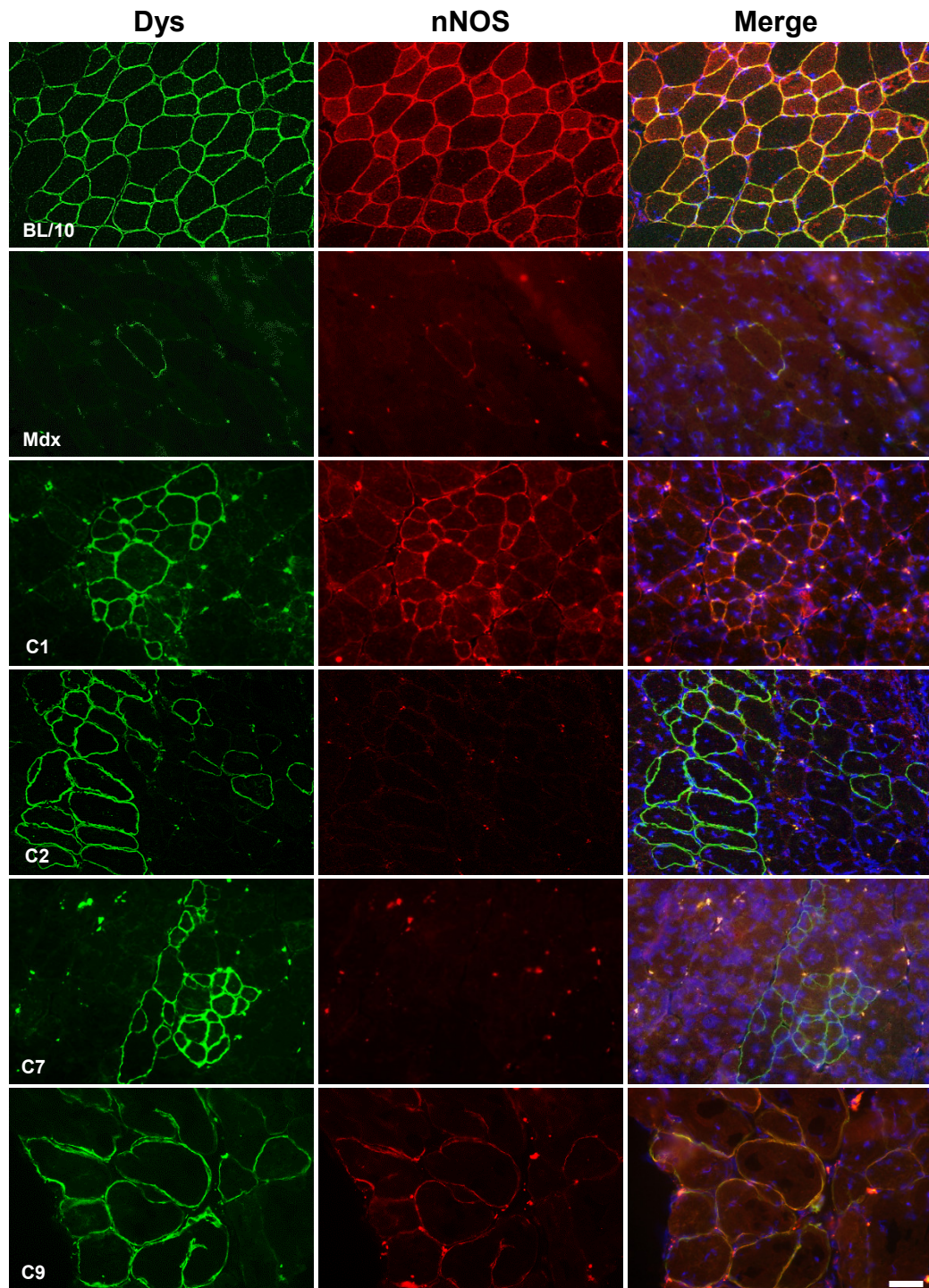


**Figure 5.13 Dystrophin and nNOS expression in electroporated muscle**  
 Representative images of dystrophin and nNOS co-expression in muscle electroporated with different constructs. TA muscle sections were stained with mouse anti-dystrophin NCL-DYS2 directed against the dystrophin C-terminus and direct labelling with Zenon Alexa Fluor 488 (green) and against nNOS with rabbit anti-nNOS and rat anti-rabbit Alexa Fluor 594 (red), predominantly observed in C1/ $\Delta$ R3-R13 and C9/ $\Delta$ R1-R10 carrying rod domain nNOS-binding site. Both proteins were expressed at the muscle fibre membrane in wild type control and in revertant fibres of mdx sections. 20x magnification; scale bar 50  $\mu$ m.

## 5.8 Discussion

With several potential therapeutic approaches aiming at dystrophin restoration and finding the best treatment option for DMD patients, there is a continuous need for optimisation and standardisation of the current research strategies. In this chapter functional analysis of the mini-dystrophin constructs was conducted in order to test their ability to express dystrophin and restore dystrophin-associated proteins such as sarcoglycans to the sarcolemma.

Four mini-dystrophin constructs were successfully tested and expressed in dystrophic mdx muscle using injection and electroporation. Although not all fibres displayed dystrophin expression (as expected for this method), the mini-dystrophin expression resulted in some morphological benefits. Studies on dystrophin restoration therapies suggest a certain level (30%) of induced dystrophin expression is required to achieve clinical benefits (Neri *et al.*, 2007). However recent studies describe that even low levels of dystrophin expression can lead to slower disease progression in the dko mouse model (Li *et al.*, 2010a; van Putten *et al.*, 2011; van Putten *et al.*, 2013). It has been shown that mice that expressed <4% of wild type dystrophin levels had prolonged life span and improved functional performance. Dystrophin levels between 4-15% improved functional performance and survival (van Putten *et al.*, 2011). One reason for the low level of dystrophin could be due to the fact that naked plasmid delivery using local injection results in low uptake of plasmid, since the most injected plasmid remains extracellular (Cappelletti *et al.*, 2003). Although, electroporation-associated gene transfer was a useful tool for studying histopathological changes after mini-dystrophin expression in mdx muscle, the method displayed significant discrepancies between experiments even if the same conditions were applied using the same plasmid DNA. For instance, the number of positive fibres or the number of replicates needed to achieve acceptable results showed enormous variability. Furthermore the number of positive fibres varied considerably in muscles expressing different constructs, possibly depending on their size. C7/ $\Delta$ H2-R23, the smallest construct showed the highest number of transfected fibres and the lowest repeated attempts of injection and electroporation, whereas the largest construct C9/ $\Delta$ R1-R10 showed sufficient results only through repeated experiments. These results are

consistent with those observed in studies on myoblasts which have shown that size of constructs significantly influences the transfection efficiency and reduces the transgene expression *in vitro* (Campeau *et al.*, 2001; Yin *et al.*, 2005). A different group that investigated factors affecting plasmid-based gene transfer combined with electroporation *in vivo*, have also provided data on low transfection ability of large plasmids of ~9 kb when compared with smaller constructs of ~3.5 kb (Molnar *et al.*, 2004). Nonetheless, all examined sections showed significant levels of expression compared to untreated mdx and the number of mini-dystrophin expressing fibres was substantially greater than revertant fibres.

Confirmed expression levels of C7/ $\Delta$ H2-R23 were also consistent with high level dystrophin expression in HeLa cells as shown in chapter 3, indicating that the lack of 3' UTR does not affect the mini-dystrophin expression *in vivo*. This is an important finding, since removal of the 3' UTR from larger constructs would reduce the size without affecting gene expression which yet again may improve dystrophin expression for future studies.

Most studies consider internal nucleation as an endpoint to evaluate correlation between dystrophin expression and pathological improvements. In this study, morphological analysis on numbers of internal nuclei showed mdx mice were clearly distinguishable from wild type (79% compared to 1.7%). Despite the invasive electroporation method and massive muscle damage as a consequence of application of electric pulses to the injected muscles, mini-dystrophin expressing fibres showed reduced numbers of internal nuclei, while dystrophin negative fibres displayed a higher percentage of internally located nuclei, indicating that this feature of dystrophic pathology was decreased in electroporated muscles, possibly by fewer cycles of degeneration and regeneration. Another reason could be due to incomplete detection of low levels of dystrophin in treated muscles or loss of expression in fibres that might have triggered this protective effect. These data suggest that positive fibres may provide additional stability for negative fibres and protect muscle against myofibre degeneration and regeneration assuming that internal nucleation is a measure of past regenerative activity. Statistical analysis showed that all constructs were significantly different from untreated mdx ( $P < 0.0001$ ) but also

from wild type control ( $P < 0.0001$ ), suggesting that they had almost the same effect as in wild type using internal nuclei as an indicator for dystrophic pathology, yet far from the values observed in the wild type control. Since the onset of the dystrophic changes in mdx muscle starts at ~3 weeks age (Grounds *et al.*, 2008), it would probably be more favourable to start the treatment in younger mice to assess the pathological changes and the efficacy of treatment, before the onset of degenerative and regenerative cycles.

Dystrophic muscle is marked by prevalence of small fibres in the course of the disease (Massa *et al.*, 1997). Animals in treated groups showed to some extent an increase in muscle fibre size compared to untreated mdx with a tendency toward the size range observed in wild type controls. Morphometric analyses of muscles in different groups suggest that C7/ $\Delta$ H2-R23 had a more pronounced effect on the myofibre diameter. Remarkably, there was an increase in myofibre size of some electroporated fibres of the treated groups in excess of that observed in wild type and mdx controls, perhaps manifesting muscle fibre hypertrophy as a side effect of electroporation. In wild type the median value of myofibres was  $1467/\mu\text{m}^2$ , a value that was almost double that in mdx animals which showed a cross-sectional area of  $608/\mu\text{m}^2$  (Figure 5.10; Figure 5.11). In addition muscle fibre measurements per unit area demonstrated a reduction in the number of small fibres in all treated groups compared to mdx animals, reflecting a decrease in muscle fibre degeneration and fewer smaller myofibres, probably representing regenerating fibres (Table 5.2). Muscle fibre size in muscles electroporated with empty vector revealed smaller fibres compared to untreated mdx indicating that the electroporation had negative consequences in the absence of dystrophin delivery (Figure 5.9), suggesting that restoration of fibre sizes in the positive fibres was associated with expression of mini-dystrophins.

As for internal nuclei, muscle fibre size of electroporated muscles displayed significant differences when compared to untreated mdx ( $P < 0.0001$ ), however comparing the P-values with the wild type control, variable levels of significance were observed (C1/ $\Delta$ R3-R13,  $P < 0.05$ ; C9/ $\Delta$ R1-R10,  $P < 0.01$ ). Only constructs C2/ $\Delta$ H2-R19 and C7/ $\Delta$ H2-R23 showed no significance compared to fibre size range of normal control, suggesting that these construct

may have more prominent effects on muscle fibre size, unless this occurrence is a coincidence. However this assumption is debatable, since these data are from only a few hundreds positive fibres, which may not be enough for a credible and convincing assessment.

Expression intensity measurements of mini-dystrophins on immunofluorescence cryosections with different constructs showed some differences when compared with one another, but these were not statistically significant from each other or from mdx revertant fibres. The ratios of median intensity values (dystrophin to laminin) (Figure 5.5A) were taken as the average amount of dystrophin within the selection, or as the sum of the grey values (RawIntDen) reflecting the total amount of dystrophin within the selection (Figure 5.5C), respectively. These measurements were also used in a different group to show the close relationship between both parameters (Taylor *et al.*, 2012). The dystrophin expression amount in untreated mdx mice was significantly different, compared to wild type mice. Muscle sections of untreated mdx mice expressing revertant fibres were assessed as a separate group which clearly demonstrated that dystrophin expression in revertant fibres was similar to the wild type group. Dystrophin expression levels from different constructs displayed a high variance, however dystrophin expression was consistently higher than untreated mdx mice and in the range of values obtained in wild type controls. These variations could also be observed in other publications (Arechavala-Gomez *et al.*, 2010; Anthony *et al.*, 2011; Taylor *et al.*, 2012). Initially, Arechavala-Gomez *et al.* demonstrated a difference in dystrophin expression between DMD, BMD and female carriers by selection of ten random areas on a cryosection using the maximum value (at the sarcolemma) minus a minimum value (representing regions within the cytoplasm as background). A ratio was calculated using dystrophin levels on control sections. In addition, they used  $\alpha$ -sarcoglycan,  $\beta$ -dystroglycan and utrophin staining and measured the intensity of these proteins. In contrast to our work, no internal standard was used. To compare the expression intensity in sections of female carriers, they selected 100 regions of interest in strong and weak labelled fibres. All pixels within the selected region (dystrophin positive fibres) were measured to get values of dystrophin expression in areas where dystrophin at different levels was expressed. The same procedure for intensity measurement was used by Anthony *et al.* for

quantitative assessment of dystrophin levels in BMD patients that were grouped by deletions. In addition they used Western blot analysis in BMD patients with different dystrophin mutations and found comparable expression levels using both techniques. Expression intensity values were quantified in control muscles and normalised to  $\beta$ -spectrin expression (Anthony *et al.*, 2011). Taylor *et al.* used a similar method as that in our study using spectrin and dystrophin co-staining as an internal control. As in our study, they also used a mask for identification of regions of interest with the difference that they selected the entire section. The use of immunofluorescence intensity measurements, may help to understand the relationship between low dystrophin expression levels and clinical benefit in gene therapy strategies, however whether dystrophin expression just over the lowest expression ranges correlates to improvement in muscle function remains to be elucidated (Taylor *et al.*, 2012). Therefore, immunofluorescence intensity on cryosections of skeletal muscle for dystrophin quantification should be approached with caution, since the method is at best only semi-quantitative and should not be used as an absolute outcome measure for gene therapy experiments and diagnostic procedures (Taylor *et al.*, 2012).

In addition to histopathological assessment, the ability of mini-dystrophins to restore other members of DGC to the sarcolemma was examined. Our data provided evidence for  $\gamma$ -sarcoglycan restoration in treated mice using different mini-dystrophin constructs.  $\gamma$ -sarcoglycan co-expression at the muscle fibre membrane was observed in almost all fibres that were positive for dystrophin which remained consistent throughout repeated experiments using different constructs indicating that the mini-dystrophins are equally capable of interacting with other muscle proteins and restore function of the DGC. It is known that dystrophin absence in the dystrophic muscles leads to abnormal localisation and reduced levels of several other DGC proteins at the sarcolemma (Turk *et al.*, 2005). Immunohistochemistry on sarcoglycans is being used as a standard outcome measure in a variety of DMD preclinical studies in animal models as well as a diagnostic marker in clinical trials (Cirak *et al.*, 2011; Cirak *et al.*, 2012). Recruitment of sarcoglycan subunits is considered as evidence for DGC restoration. However, one should bear in mind that DGC restoration is not necessarily an indication for dystrophin functionality, since studies on transgenic

Dp71 expressing mice have been shown to result in DGC restoration but fails to prevent muscle dystrophy (Cox *et al.*, 1994; Greenberg *et al.*, 1994).

Immunohistochemistry on nNOS resulted in nNOS restoration and the ability of two constructs to restore nNOS to the sarcolemma. In previous studies, it was thought that the dystrophin C-terminal domain is responsible for nNOS expression at the sarcolemma (Brenman *et al.*, 1996; Tochio *et al.*, 1999; Adams *et al.*, 2001), suggesting that truncated versions of dystrophin with an intact C-terminal domain should restore sarcolemmal nNOS expression. However none of the miniaturised dystrophins with large internal rod domain deletions that were used in experimental studies seemed to be able to recruit nNOS expression to the sarcolemma (Chao *et al.*, 1996; Crawford *et al.*, 2000; Wells *et al.*, 2003). It was hypothesised that the constructs C1/ $\Delta$ R3-R13 and C9/ $\Delta$ R1-R10 carrying the rod domain nNOS binding-site should recruit nNOS to the sarcolemma, while the constructs missing these regions were not supposed to display subcellular localisation of this protein in dystrophin positive fibres. This prediction was confirmed in repeated experiments, however nNOS expression was occasionally observed in fibres that were treated with constructs lacking this region, probably due to presence of revertant fibres. It has been suggested that the use of mdx52 knockout mouse could be considered as an alternative option to overcome this issue, since no revertant fibres are present in this strain, due to loss of other shorter isoforms (Araki *et al.*, 1997; Grounds *et al.*, 2008).

No correlation between nNOS restoration and any of the other parameters was found, since percentage of internal nuclei and increase in muscle fibre size were statistically equivalent using any of the constructs. It would be interesting to monitor nNOS expression in long-term studies and compare the expression pattern in different time points after injection to assess the effect of mini-dystrophins on nNOS expression over a longer time period. Although C9/ $\Delta$ R1-R10 nNOS expression was also confirmed by immunostaining, but this construct required multiple injection attempts, indicating that it was much more difficult to be stably expressed *in vivo*. In addition, the feasibility of accommodating this construct in a suitable viral vector might be more challenging due to its larger size of ~7.7 kb. The role of the ABD2 in this

construct has not been explored yet and future physiological studies may address the importance of this region.

In the present study it was only possible to demonstrate expression and localisation of mini-dystrophins. A range of additional functional tests have been reported to monitor dystrophin restoration and assess the impact of interventions on the disease progression in the mdx mouse, including the degree of fibrotic, necrotic (Briguet *et al.*, 2004) and leaky myofibres using dyes or proteins that can enter or exit muscle fibres through damaged sarcolemma (Straub *et al.*, 1997), measurement of blood biomarkers such as muscle creatine kinase (Zatz *et al.*, 1991), immunological testing (Yokota *et al.*, 2006), whole body imaging (MRI) (Pasquesi *et al.*, 2006), *In vivo* measurement of whole body function and muscle strength in mouse (van Putten *et al.*, 2011; van Putten *et al.*, 2012; van Putten *et al.*, 2013; van Putten *et al.*, 2014). However, each of these quantification methods would require a whole body administration of mini-dystrophins to be able to overcome the limitations of local injection and to circumvent the adverse effect of electroporation. Nevertheless, the use of electroporation as a screening tool has several advantages including large insert capacity, relative cost-effectiveness, lack of viral vector-mediated toxicity and the possibility for testing candidate genes before use of viral vectors. Furthermore, repeated administration is possible without concerns about immunological reaction, which is a major issue when using viral vectors (McMahon *et al.*, 2001; Molnar *et al.*, 2004).

Another important factor is the choice of the most appropriate promoter which could sustain high transgene expression with long-term efficiency. It has been shown that use of the muscle specific desmin promoter produced significantly greater expression compared to other muscle specific promoters such as MCK (Talbot *et al.*, 2010).

Due to lack of physiological studies and low dystrophin expression it is too early to assess which construct is the optimal mini-dystrophin construct. Although morphological analyses on different constructs displayed some significant differences when they were compared to untreated mdx muscles, a major

divergence was not demonstrated when compared with one another. Undoubtedly, each construct has its advantages and disadvantages.

Construct C1/ $\Delta$ R3-R13 has been designed to maintain the most functional part of the dystrophin including the rod domain nNOS-binding site and part of the ABD2 (repeats 14 and 15), while maintaining a size within the packaging capacity of lentiviral vectors. This construct represents a novel mini-dystrophin and could be the most favourable construct, since it restores both  $\gamma$ -sarcoglycan and nNOS expression, and showed also sarcolemmal localisation in DMD myoblasts.

The C2/ $\Delta$ H2-R19 construct carries the major functional domain of dystrophin including the N-terminal actin-binding part, cysteine rich domain and C-terminal region. Repeats 16 and 17 were deleted to be able to create a useful comparison between this mini-gene and the constructs that carry this region. Moreover this construct resembles a Becker-like deletion from mildly affected BMD patients (England *et al.*, 1990). Other groups have also developed and tested a similar construct using dual AAV vectors (Lai *et al.*, 2005; Odom *et al.*, 2011) or generated transgenic mouse lines expressing this mini-gene, indicating full functionality of the transgene and overall improvement in phenotype (Harper *et al.*, 2002; Banks *et al.*, 2007). A major advantage of this construct is its smaller size (~6.0 kb) when compared to C1/ $\Delta$ R3-R13 and C9/ $\Delta$ R1-R10 in this study, keeping in mind that the nNOS-binding site is missing due to the large deletion in central rod domain. Taken together this construct could be used as a control to monitor the ability of the other constructs with a well-established mini-dystrophin which also displays a mild Becker muscular dystrophy deletion.

Construct C7/ $\Delta$ H2-R23 could be considered as a potential candidate for AAV-mediated gene therapy. This construct appeared to be more advantageous in terms of higher expression levels *in vitro* and *in vivo*. However, since the construct is deleted for most of the rod domain, it will not restore nNOS to the sarcolemma.

On the basis of these observations the construct C1/ $\Delta$ R3-R13 seems to be superior compared to other mini-dystrophins in this project, therefore this

construct is predicted to be the optimal mini-dystrophin construct at this stage. Future studies will use this mini-gene, alongside two other constructs C10/ $\Delta$ R3-R13- $\Delta$ CT and C11/ $\Delta$ R3-R13- $\Delta$ CT-synt (recently generated; Table 3.1) to evaluate whether or not reduced size of this construct is beneficial. Apart from lentiviral vectors, the use of dual AAV vectors could be an alternative option for gene delivery of these mini-genes in dystrophic muscle. In a recent study, it has been shown that intravenous injection of dual AAV vectors expressing a mini-dystrophin of ~6.0 kb resulted in 30-50% dystrophin positive fibres leading to improvement of histopathology and increased muscle force (Zhang *et al.*, 2013). Many hurdles remain, such as wide spread delivery of the constructs, yet this study provided reliable data on some functional benefits of novel mini-dystrophin constructs for preclinical studies.

## Chapter 6 General discussion and future directions

Since identification of the dystrophin protein and its molecular sequence, numerous genetic strategies have been developed showing encouraging results in animal models with potential to treat Duchenne muscular dystrophy patients. A variety of approaches have been moving from basic studies in animal models to early phase clinical trials and show great promise to defeat DMD; however none of these therapeutic options have reached the level of treatment and cure. Therefore, optimisation and refinement of the individual methods and ongoing research remains one of the most important efforts to achieve long-term therapeutic benefits.

The work presented in this thesis has been conducted to contribute to DMD gene replacement therapy with the main focus on constructs designed to take the maximum advantage of the cloning capacity of lentiviral vectors. So far, most studies have been restricted to characterisation and study of smaller micro-dystrophin genes due to consideration of the limited packaging capacity of AAV vectors (<5 kb). Studying and characterisation of larger constructs that are as close as possible to the full-length dystrophin is useful for future gene replacement studies.

Currently, several genetic therapeutic approaches are in development, aiming at dystrophin restoration, including stop codon readthrough, exon skipping and gene replacement therapy using truncated versions of dystrophin (Fairclough *et al.*, 2013). Exon skipping using AONs is the most promising strategy for treatment of DMD and has shown great promise in preclinical studies. Most mutations found in DMD patients are frame-shifting deletions of one or several exons that alter the translational reading frame and therefore fail to express dystrophin in muscle (Monaco *et al.*, 1988; Muntoni *et al.*, 2003). Skipping of one or more exons by binding a short synthetic RNA sequence (AON) to block sequences promoting splicing results in a shorter but partially functional dystrophin (Nowak and Davies, 2004). Although this method is not applicable to all DMD patients due to the heterogeneity of DMD mutations and would need to be a personalised therapy, the majority of patients (~80%) would theoretically benefit from this treatment and skipping of exon 51 (currently in clinical trials)

could be applied to ~13% of DMD patients (Aartsma-Rus *et al.*, 2009). Therapeutic efficacy of AONs has been demonstrated in various experimental studies in animal models including mdx and cxmd (canine X-linked muscular dystrophy) (Yokota *et al.*, 2009; Aartsma-Rus *et al.*, 2010; Tanganyika-de Winter *et al.*, 2012; Yokota *et al.*, 2012). However some of the recent clinical trials using AONs failed to demonstrate significant improvement in the 6-minute walk test (6MWT) outcome measure compared to placebo, while some studies reported a high level of dystrophin expression (Mendell *et al.*, 2013; Flanigan *et al.*, 2014). In addition, in the drisapersen trial low platelets and kidney toxicity was found in some patients (Flanigan *et al.*, 2014). These results have raised doubts whether the 6MWT is a reliable outcome measure as a clinical endpoint and as to whether or not the clinical efficacy of treatments is directly linked with dystrophin expression (Lu *et al.*, 2014). Nonetheless, the correlation between dystrophin expression and clinical condition cannot be ignored since the lack of dystrophin results in DMD and reduced expression to the milder BMD (Wilton *et al.*, 2014). Extensive studies are required to optimise exon skipping strategy and demonstrate clinical benefits for DMD patients.

Another approach for DMD gene therapy is delivery of a functional copy of dystrophin to dystrophic muscle (Chamberlain, 2002; Blankinship *et al.*, 2006). Adeno-associated virus (AAV)-based vectors are the most commonly used vectors (Athanasopoulos *et al.*, 2011) and have facilitated gene transfer of micro-dystrophins showing safe and long-term dystrophin expression with significant functional improvement in animal models. The potential advantage of gene replacement therapy over exon skipping is that the same treatment can theoretically be applied to all patients, irrespective of their mutation (Tremblay and Frederickson, 2011). Advantages of using rAAV-based vectors include their non-pathogenic nature (Sun *et al.*, 2003; Okada and Takeda, 2013), their production at high titres (Wright, 2008) and long-term expression in animal models (Schultz and Chamberlain, 2008). However these vectors have several drawbacks including the inability to integrate into the host genome resulting in the lack of heritable characteristics that can be passed on and repopulate newly formed muscle (Chamberlain, 2002; Blankinship *et al.*, 2006) and the small size of gene that can be inserted (<5 kb) (Lai *et al.*, 2010; Yuan *et al.*, 2011). To date engineered micro-dystrophins that have been used in experimental models

have deletions in a large portion of the rod domain but contain the minimal essential regions of the dystrophin molecule (Phelps *et al.*, 1995; Cadenas *et al.*, 2002; Fabb *et al.*, 2002; Watchko *et al.*, 2002; Foster *et al.*, 2007; Jorgensen *et al.*, 2009; Wang *et al.*, 2009a; Koo *et al.*, 2011) to bypass the packaging limitations of AAV vectors (<5 kb) (Lai *et al.*, 2010; Yuan *et al.*, 2011) which has restricted the application of larger and possibly more favourable constructs that could carry additional regions of the dystrophin molecule.

With advanced viral technology and increasing knowledge about the functional domains in dystrophin, researchers have realised that the concept of rod domain dispensability needs to be reconsidered due to data that have been published on spectrin-like repeats interacting with other cell components, including signalling molecules (Afanasiev *et al.*, 2009; Lai *et al.*, 2013), membrane lipids and other cytoskeletal elements (Sarkis *et al.*, 2011). Mini-dystrophins in this project have been designed to be packaged into lentiviral vectors. Lentiviral vectors carry a considerably larger DNA insert (~10 kb) (Xiao *et al.*, 2000; Kumar *et al.*, 2001) compared to AAV vectors and have been considered as the potential delivery system for this project to allow use of less highly truncated mini-dystrophins, given our eventual aim of correcting dystrophin deficiency in stem cells.

Lentiviral vectors can efficiently infect dividing and non-dividing cells including satellite cells and stem cells (Kimura *et al.*, 2010), can integrate into the host genome and provide long-term, heritable gene expression. Lentiviral vectors have been shown to transduce myogenic stem cells as well as myofibres in dystrophic muscle and successfully express micro-dystrophins. Expression was maintained for at least two years and supported by stable transduced satellite cells that were able to regenerate dystrophin expressing myofibres *in vivo* (Kimura *et al.*, 2010). Drawbacks with lentiviral vectors include possible gene silencing or mutagenesis due to the site at which the virus inserts into the host genome (Ciuffi, 2008). However, the development of third generation lentiviruses and advances in vector design with physiological promoters and cell-specific envelope proteins (Follenzi and Naldini, 2002) and incorporation of non-viral regulatory elements are likely to address these shortcomings to a significant extent (Bonci *et al.*, 2003).

The first clinical trial for gene replacement therapy using intramuscular injections of an AAV recombinant vector carrying a mini-dystrophin into the biceps of six DMD patients at the Nationwide Children's Hospital Ohio did not result in clinical benefits due to mini-dystrophin specific T-cell immune response (Mendell *et al.*, 2010) which poses new challenges for dystrophin gene therapy. More importantly, none of the patients displayed significant levels of mini-dystrophin expression ( $\Delta$ D3990; encoding the N-terminus, cysteine-rich domain, H1, H3, H4, 5 spectrin-like repeats including R1-R2 and R22-R24 (Mendell *et al.*, 2010). This leads to the question whether the therapeutic transgene was capable of restoring dystrophin in patients and did not lack some functional parts of dystrophin.

To answer this question, one could speculate that one of the reasons for insufficient dystrophin expression in this clinical trial might have been due to removal of the C-terminus of the mini-dystrophin, given that the truncated C-terminus  $\Delta$ D3990 (exon 70-79) has never been reported in a BMD patient (<http://www.dmd.nl/>). Truncated dystrophins with deletion of the C-terminus have been shown to be functional in animal models (Phelps *et al.*, 1995; Gregorevic *et al.*, 2006; Yue *et al.*, 2006), but this does not necessarily mean that this part is dispensable for a functional protein in man. In addition, repeats 20 and 21 were deleted in the mini-gene  $\Delta$ D3990 and H3 directly joined to repeat 22, a composition that is not similar to natural structure of dystrophin molecule. Harper *et al.* studied the dystrophin structural domains and identified several factors important for function of the truncated dystrophin molecule including the phasing of the rod domain repeats. Organisation of the rod domain spectrin-like repeats plays a critical role in supporting dystrophin function and the repeats should be arranged in a way that do not differ from the natural dystrophin organisation (Harper *et al.*, 2002). Mini-dystrophins that were generated in this study have addressed several limitations of the mini-gene  $\Delta$ D3990. In addition to an intact C-terminus, they all carry only one internal deletion and maintain consecutive repeats without disruption, and precisely follow the native composition as in full-length dystrophin. Studies on BMD patients have shown that deletions of different parts of the rod domain are associated with different levels of dystrophin expression. For instance, dystrophin expression levels in patients with a deletion of exon 51 endpoint are

higher than patients ending with exon 53 deletions (Anthony *et al.*, 2011), suggesting that dystrophin expression depends on the extent and location of the deleted region and resulting disruption in the functional domains, such as spectrin-like repeats, could be important factors that have not been identified as yet (Wilton *et al.*, 2014). Based on the data from the gene therapy clinical trial, these considerations might be critical for mini-dystrophin functionality. At least one construct (C7/ $\Delta$ H2-R23; ~4.3 kb) with a similar size to the mini-dystrophin that was used for the clinical trial ( $\Delta$ D3990) could be more advantageous, since it has only one internal deletion, phased repeats and additionally retains the entire C-terminal region which is preserved in most mildly affected BMD patients. Due to its smaller size compared to other mini-dystrophins, this construct could be considered as a potential candidate for AAV-mediated gene therapy.

In addition to considerations for design and construction of optimised and functional dystrophin proteins, some of which have been addressed in this project, it is critical to provide data on the outcome measures for evaluation of therapeutic efficacy. There are several challenges for dystrophin quantification which are common to all genetic therapeutic strategies, including the low amount of dystrophin protein which accounts for only 0.002% of total muscle protein (Hoffman *et al.*, 1987), its large size of 427 kDa (Watkins *et al.*, 1988) and the presence of revertant fibres in DMD patients and the mdx mouse (Crawford *et al.*, 2001; Pigozzo *et al.*, 2013). In recent years several studies have been published reporting techniques for dystrophin quantification in treated DMD patients and the mdx mouse. Semi-quantitative methods to detect dystrophin include Western blot (Anderson and Davison, 1999) and immunohistochemistry (Arechavala-Gomez *et al.*, 2010a; Anthony *et al.*, 2011; Taylor *et al.*, 2012; Pertl *et al.*, 2013), whereas alternative methods such as mass spectrometry (Brown *et al.*, 2012), reverse protein arrays (Escher *et al.*, 2010) and ELISA (Ishikawa *et al.*, 1996) allow absolute quantification of the protein.

Most studies measure morphological changes in biopsies from patients or treated animals. For interpretation of morphological changes, it was crucial to include age-matched controls which allowed a reliable comparison of dystrophin

expressing fibres compared to untreated controls. Clearly, one of the main reasons for low levels of dystrophin expression in muscle was the local administration of the mini-dystrophins and therefore the limited distribution in dystrophic muscle. Because the number of dystrophin expressing fibres was not as high as hoped, the presence of revertant fibres was strictly defined in control muscles, in order to avoid any possibility that revertant fibres could lead to misinterpretation of the frequency of dystrophin positivity. Since dystrophin restoration is the end point for most therapeutic approaches (Arechavala-Gomez *et al.*, 2010b; Lu *et al.*, 2014), a pre-assessment of the frequency of revertant fibres prior to treatment is absolutely crucial. Since the onset of the dystrophic changes in mdx muscle starts at ~3 weeks age (Grounds *et al.*, 2008), it would probably be more favourable to start the treatment in younger mice to assess the pathological changes and the efficacy of treatment, before the onset of degenerative and regenerative cycles; however one should bear in mind that this does not reflect the human situation as treatment may not be feasible before the onset of degeneration.

The pathological mechanism in dystrophin-deficient muscle is characterised by myofibres that have gone through rounds of degeneration and regeneration. Internally located nuclei and variability in muscle fibre size are two characteristic features diagnostic for this process (Willmann *et al.*, 2012) and can provide evidence for disease progression or efficacy of therapeutic approaches if resulting in improvement of muscle pathology. In this study, despite the low level of dystrophin expression in treated animals, there was a significant reduction of internally located nuclei in treated muscles, more pronounced in dystrophin-positive, but also apparent in dystrophin-negative muscle fibres. However, this should be taken with caution since the low number of dystrophin positive fibres may not have been substantial enough for an unequivocal interpretation of these parameters. Nonetheless, dystrophin negative fibres in treated muscles showed reduction of internally located nuclei, perhaps a bystander effect from the positive effect of mini-dystrophins in injected muscles which may be due to general reduction in inflammation (Porter *et al.*, 2002), slower cycles of necrosis and regeneration (Coulton *et al.*, 1988) or the effect of dystrophin below the detection range in immunohistochemical analysis (Dunant *et al.*, 2003).

Standard protocols and improvement of conventional detection methods are required for accurate evaluation of therapeutic interventions worldwide to avoid repeated efforts (Willmann *et al.*, 2012). For instance, semi-quantitative expression intensity measurement has been developed in two different laboratories (Arechavala-Gomez *et al.*, 2010a; Taylor *et al.*, 2012) and recognised as a standard protocol for assessment of muscle biopsies undergoing clinical trials (Kinali *et al.*, 2009; Cirak *et al.*, 2011; Finkel *et al.*, 2013). Expression intensity in combination with Western blot should be used for analysis of treated muscle to determine the correlation between the levels of expression intensities in both detection methods. However, dystrophin detection using Western blot would require a minimum expression of 10% in treated muscle (Lu *et al.*, 2014). Drawbacks of this methods include requirement for a muscle biopsy from patient during treatment and ideally prior to treatment in order to compare the effectiveness of therapeutic interventions on a “per-patient” level rather than cumulatively for the entire cohort (Lu *et al.*, 2014). Repeated muscle biopsies are invasive for patients, especially because most patients are at young ages. For these reasons alternative quantification methods should be considered to reflect the therapeutic outcome including serum biomarkers which provide a useful tool for monitoring disease progression (’t Hoen *et al.*, 2011; Martin *et al.*, 2014). However the potential of such biomarkers as alternative markers for dystrophin or disease progression has not been validated yet. Furthermore, it is questionable whether these biomarkers can distinguish between endogenous and therapeutic dystrophin (Wilton *et al.*, 2014).

A major issue for all DMD gene therapy approaches is that the treatment efficacy depends on the degree of disease progression, fibrotic tissue replacement and the number of intact fibres (Chamberlain, 1997; Meregalli *et al.*, 2008). In a recent exon skipping study it was shown that the treatment significantly improved the phenotype in young dko mice and extended life span, however even a high level of dystrophin expression failed to prevent disease progression in older, more disease progressed mice (Wu *et al.*, 2014), suggesting that a successful therapy requires regenerating, myogenic muscle mass not lost prior to treatment. Although regeneration in DMD patients and dystrophin-deficient animal models is supported by activation of satellite cells,

this self-repair capacity is limited resulting in loss of muscle strength over time (Collins *et al.*, 2005; Sacco *et al.*, 2008). Moreover, these regenerated muscle fibres are still dystrophin-deficient in DMD patients and therefore continue to degenerate (Luz *et al.*, 2002). A possible treatment option is transplantation of stem cells to introduce the missing dystrophin gene to muscle fibres (Wang *et al.*, 2009b). Transplants from a healthy donor to repair and regenerate muscle fibres would result in dystrophin protein production. However, the use of heterologous stem cells would need lifelong immunosuppression of the treated patient (Benchaouir *et al.*, 2008; Chamberlain, 2013).

A potential therapy is a combination of autologous stem cells and viral vectors to introduce the missing dystrophin gene and the lost muscle mass to muscle fibres (Wang *et al.*, 2009b). This approach may have more efficacy for patients in later stages of the disease (Seto *et al.*, 2014). Genetic correction of autologous stem cells has been successfully demonstrated as a therapeutic option in animal models (Davies and Grounds, 2007; Benchaouir *et al.*, 2008; Wang *et al.*, 2009a). This approach would need the choice of the best stem cell that has both myogenic potential and can give rise to the muscle fibres (Parker *et al.*, 2009; Meng *et al.*, 2014). Although satellite cells can functionally reconstitute the satellite cell pool, they have only a very local effect after direct intramuscular injection and lose their regenerative capacity following expansion in tissue culture, limiting their practicality (Montarras *et al.*, 2005). Alternative stem cells include muscle-derived stem cells including CD133<sup>+</sup> bone marrow and blood cells, vessel cells such as pericytes and their progeny mesoangioblasts (Skuk *et al.*, 2014), and patient-derived iPSC (Dick *et al.*, 2013).

Mini-dystrophins that were produced in this study have already been used in a combined gene- and cell therapy research within a collaborative project with encouraging results (Morgan and Muntoni, unpublished data). In this project, lentivirally-transduced stem cells (pericytes), carrying mini-dystrophins C1/ $\Delta$ R3-13, C2/ $\Delta$ H2-R19 and C7/ $\Delta$ H2-R23 were injected into dystrophin-deficient mice. First, GFP tagged mini-dystrophins were transduced into DMD pericytes and dystrophin expressing cells were sorted and transplanted into dystrophin-deficient mice. One month after transplantation human DMD pericytes

expressing spectrin and dystrophin fibres were formed. Cells were able to successfully differentiate and fuse with existing fibres. These encouraging results may help to pave the way for future preclinical studies using mini-dystrophins. Challenges when using this method include a potential risk for an immune response against viral proteins expressed by the vectors required for genetic correction, activation of oncogenes and insertional mutagenesis and administration route to obtain dystrophin restoration in all muscle fibres including heart (Okada and Takeda, 2013). The latter is one of the major difficulties for any *ex vivo* treatment strategy. Accumulation of cells in non-muscle tissues such as the lung which has been shown after treatment of dystrophic dog with mesoangioblasts could also be a serious issue (Sampaolesi *et al.*, 2006).

It is encouraging that studies in DMD gene therapy may also be useful in treatment of other diseases. A recent publication suggested that dystrophin may have anti-metastatic features in cancer and act as a tumour suppressor suggesting that molecular therapies that are in development for muscular dystrophies may also have relevance in the treatment of cancer (Wang *et al.*, 2014).

## Future directions

The long-term goal of this study is to contribute to the development of a clinical trial using autologous stem cells encoding a functional mini-dystrophin. Although expression of mini-dystrophins has shown improvements in histopathology of the mdx mouse, it is still unclear how they will affect disease pathology when administered systemically.

Prospective studies will involve measurable outcomes from physiological studies, utilising lentiviral vectors and systemic delivery, which would be expected to result in higher and long-term transgene expression. Monitoring dystrophin expression over time may provide data on expression stability and additional histopathology-relevant parameters, including evaluation of macrophage infiltrations, fibrosis and necrotic area and would enable us to assess their long-term potential to improve muscle function and delay disease progression. The investigation could be extended to a combined gene- and cell therapy approach.

Meanwhile, collaborative studies have harnessed the mini-dystrophins in combination with stem cell and lentiviral technology to transplant dystrophin expressing human cells in the mdx dystrophic mouse. It has been proposed to use mini-dystrophin expressing stem cells for treatment of a small hand muscle in a selected cohort of older DMD patients by local delivery to provide proof-of-principle for safety and functionality. This will enable us to determine whether or not the mini-dystrophins could be used as potential candidates for human clinical trials (Professor Francesco Muntoni; personal communication).

Future studies will particularly focus on studying the long-term expression of mini-dystrophins and the mechanism of nNOS relocalisation in dystrophic pathogenesis. In addition, it is important to focus on optimising a vector system that can package larger dystrophin transgenes rather than shortening the dystrophin molecule. Finally, in order to compare efficacy in these preclinical studies, it is essential to put efforts in implementation of standardised operating procedures for dystrophin quantification based on collaborations worldwide.

## Appendix A

Fragment	Primer name	Primer sequence (5'-3')	Product size
1.1	1 F	ACTCAGA TCTGGGAGGC AATTA	nt. 64 -1032 969 bp
	1.1 R	TCTTTAGTCACTTTAGGTGGCC	
1.2	1.2 F	GATGTTGATACCACCTATCCAG	nt. 893- 1445 bp 553
	1.2 R	GTAGAATATTACCAACCCGGCCC	
2.1	2 F	TGTA AACGACGCGCCAGTATGGAT TTGACAGCCC	nt. 1393- 1952 bp 549
	2.1 R	GGCACTGTTCTTCAGTAAGACG	
2.2	2.2 F	AGGTATTGGGAGATCGATGG	nt. 1845- 2347 bp 503
	2.2 R	CTCTTGAGCATGCTTTACCAG	
3.1	3 F	CAGCCATCACTAACACAGAC	nt. 2261- 2886 bp 626
	3.1 R	GATAGCCGGTTGACTTCATC	
3.2	3.2 F	TGAAAATCCAACCCACCACC	nt. 2802- 3522 bp 721
	3.2 R	AGTCTGCACTGTTTCAGCTGC	
3.3	3.3 F	TTTCTGAAGGAGGAATGGCC	nt. 3452- 4155 bp 704
	3.3 R	TCAGAGTTTCTCAGCTCCG	
4.1	4 F	GGAGAAAGCAAACAAGTGGC	nt. 4069- 5019 bp 951
	4.1 R	ATATCTGTAGCTGCCAGCC	
5.1	5 F	GAAATTGTCCCGTAAGATGCG	nt. 4954- 5319 bp 366
	5.1 R	GTGATGTGGTCCACATTCTGG	
5.2	5.2 F	GGAATACCAGAAACACATGG	nt. 5269- 5780 bp 512
	5.2 R	CCTCTCTTTCTCTCATCTG	
5.3	5.3 F	GGGTGAATCTGAAAGAGGAAG	nt. 5655- 6615 bp 961
	5.3 R	TCAGCTTCTGTTAGCCACTG	
6.1	6 F	AAATGTACAAGGACCGACAAGG	nt. 6513- 6778 bp 266
	6.1 R	GGCATCTGTTTTGAGGATTGC	
6.2	6.2 F	TCCTGAGAATTGGGAACATGCT	nt. 6640- 7598 bp 959
	6.2 R	TAGTAACCACAGTTGTGTAC	
6.3	6.3 F	GGA CTGACCACTATTGGAG	nt. 7532- 8380 bp 849
	6.3 R	GGCAGTTGTTTCAGCTTCTGTA	
7.1	7 F	GGCTGCTTTGGAAGAACTC	nt. 8287- 9061 bp 834
	7.1 R	GATCCCTTGATCACCTCAGCTTGG	
7.2	7.2 F	AATGTCACTCGCTTCTACGAAA	nt. 8939- 9821 bp 883
	7.2 R	TCCCTGTTTCGTCCTGATC	
8.1	8 F	CAATTTGGTCAACGTCCCTC	nt. 9742- 10636 bp 895
	8.1 R	GCTCTCATTAGGAGAGATGC	
8.2	8.2 F	TTCTGGCCAGTAGATTCTGC	nt. 10487- 11357 bp 871
	8.2 R	GATACTAAGGACTCCATCGC	

### Sequences of the oligonucleotides used for cDNA synthesis and PCR

The nomenclature refers to the cDNA sequence position of oligonucleotides; adapted from Rinninsland *et al.*, 1992

## Appendix B

Primer name	Sequence (5'-3')	Restriction site	Application
C1/C2-F1- <i>Clal</i>	ATTGGGAGATCGATGGGCAAACATCTGTA	<i>Clal</i>	Construct
C1-R1	CATCATCGTTTCTTCACGGACAGTGTGAAT ATCCACAGTAATCTGCCTCTTCTTTGGG	-	Construct
C1-F2	CCCCAAAAGAAGAGGCAGATTACTGTGGAT ATTCACACTGTCCGTGAAGAAACGATGATG	-	Construct
C1/C2-R2- <i>NgoMIV</i>	GTGCCTGCCGGCTTAATTCATCATCTTT	<i>NgoMIV</i>	Construct
C2-R1	CGGTTGTTTAGCTTGAAGTCTATTTTCAGTTTC CTGTGCTGTACTCTTTTCAAGTTTTTGGACTAAATTAT	-	Construct
C2-F2	ATAATTTAGTCCAAAACTTGAAAAGAGTACAGC ACAGGAAACTGAAATAGCAGTTCAAGCTAAACAACG	-	Construct
C7 Left-R	TCCGTGGCCTCTTGAAGTTCCTGGAGTCTTTCAAGGGTC TGTGCTGTACTCTTTTCAAGTTTTTGGACTAAATTAT	-	Construct
C7 right-R	ATAATTTAGTCCAAAACTTGAAAAGAGTACAGCACAGAC CCTTGAAAGACTCCAGGAACTTCAAGAGGCCACGGA	-	Construct
C9-F1- <i>KasI</i>	GGATGGGAGGCGCCTCCTAGACCTCCTC	<i>KasI</i>	Construct
C9-R1	TTGTAGACGCTGCTCAAAATTGGCTGGCTCCATCAATGA ACTGCCAAATGACTTGTCT	-	Construct
C9-F2	AGACAAGTCATTTGGCAGTTCATTGATGGAGCCAGCCAA TTTTGAGCAGCGTCTACAA	-	Construct
C9-R2- <i>Clal</i>	CTGCAAATCGATGGTTGAGCTCTGAGATTT	<i>Clal</i>	Construct
8.3F	AGGACACAAGCACAGGGTTAGA	-	Dystrophin cDNA primer
1.0R	CTTAGAAAATTGTGCATTTACC	-	Dystrophin cDNA primer
T7	TAATACGACTCACTATAGGG	-	Universal primer
DysT1-4/2 F-vec	AGAGGCCAAA GTGAATGGCA CAAC	-	RSV-Vector
DysT1-4/2 R-vec	GGTTCTCAAT ATGCTGCTTC CCAA	-	RSV-Vector
Dys- Forward 3'	CCACCACACCAAATGACTACTACACA	-	RSV-Vector
Dys- Reverse 5'	ATACGCAGGAAAGAACATGTGAGCA	-	RSV-Vector
3rd-Dys- Forward	CCACACAGGCATAGAGTGTCTGCTA	-	RSV-Vector
3rd-Dys- Rev	GGCACCTATCTCAGCGATCTGTCTA	-	RSV-Vector
4 <sup>th</sup> -Dys- Forward	TATCCAAAACAGCCTTGTGGTCAGT	-	RSV-Vector
4 <sup>th</sup> -Dys- Reverse	GTGAGCAAAAACAGGAAGGCCAAAAT	-	RSV-Vector

### Primers for mini-dystrophin constructs and vectors

## Appendix C

Antibody	Name	Description	Application In this study	Target	Source	Order information
Anti-dystrophin	Mandra1	Mouse monoclonal	WB, ICC	AA 3558-3684 (C-terminus)	abcam	Ab7164
Anti-dystrophin	Ab15277	Rabbit polyclonal	IHC	Rod domain residues 1400 and 1505	abcam	ab15277
Anti-dystrophin	NCL-DYS1	Mouse monoclonal	WB	AA 1181-1388 (rod domain)	Leica biosystems	DYS1-CE-S
Anti-dystrophin	NCL-DYS2	Mouse monoclonal	IHC	AA 3669- 3685 (C-terminus)	Leica biosystems	DYS2-CE-S
Anti-dystrophin	NCL-DYS3	Mouse monoclonal	IHC	AA 321-494 (N- terminus)	Leica biosystems	DYS3-CE-S
Anti-actin	Anti-Actin	Rabbit polyclonal	WB	----	Sigma-Aldrich	A2066
Anti-laminin	Anti-Laminin	Rat monoclonal	WB	----	Sigma-Aldrich	L0663
Anti-desmin	Anti-Desmin	Mouse monoclonal	ICC	----	Dako	M0760
Anti-nNOS	nNOS Rabbit Antibody	Rabbit polyclonal	IHC	----	Life technologies	617000
Anti-gamma sarcoglycan	Anti-GSGC	Rabbit polyclonal	IHC	----	Proteintech Europe	18102-1-AP
Anti-laminin	Anti-Laminin	Rabbit polyclonal	IHC	----	Sigma-Aldrich	L9393

### Antibodies used in this project

## Appendix D

### The entire coding sequence from C2/ $\Delta$ H2-R19 as an example (5952 bp)

1           **ATG**CTTTGGTGGGAAGAAGTAGAGGACTGTTATGAAAAGAGAAGATGTTCAAAAAGAAAACA  
1           M L W W E E V E D C Y E R E D V Q K K T

61           TTCACAAAATGGGTAAATGCACAATTTTCTAAGTTTGGGAAGCAGCATATTGAGAACCTC  
21           F T K W V N A Q F S K F G K Q H I E N L

121          TTCAGTGACCTACAGGATGGGAGGCGCCTCCTAGACCTCCTCGAAGGCCTGACAGGGCAA  
41           F S D L Q D G R R L L D L L E G L T G Q

181          AAACTGCCAAAAGAAAAAGGATCCACAAGAGTTCATGCCCTGAACAATGTCAACAAGGCA  
61           K L P K E K G S T R V H A L N N V N K A

241          CTGCGGGTTTTGCAGAACAATAATGTTGATTTAGTGAATATTGGAAGTACTGACATCGTA  
81           L R V L Q N N N V D L V N I G S T D I V

301          GATGGAAATCATAAACTGACTCTTGGTTTTGATTTGGAATATAATCCTCCACTGGCAGGTC  
101          D G N H K L T L G L I W N I I L H W Q V

361          AAAAATGTAATGAAAAATATCATGGCTGGATTGCAACAAACCAACAGTGAAAAGATTCTC  
121          K N V M K N I M A G L Q Q T N S E K I L

421          CTGAGCTGGGTCCGACAATCAACTCGTAATTATCCACAGGTTAATGTAATCAACTTCACC  
141          L S W V R Q S T R N Y P Q V N V I N F T

481          ACCAGCTGGTCTGATGGCCTGGCTTTGAATGCTCTCATCCATAGTCATAGGCCAGACCTA  
161          T S W S D G L A L N A L I H S H R P D L

541          TTTACTGGAATAGTGTGGTTTGCCAGCAGTCAGCCACACAACGACTGGAACATGCATTC  
181          F D W N S V V C Q Q S A T Q R L E H A F

601          AACATCGCCAGATATCAATTAGGCATAGAGAACTACTCGATCCTGAAGATGTTGATACC  
201          N I A R Y Q L G I E K L L D P E D V D T

661          ACCTATCCAGATAAGAAGTCCATCTTAATGTACATCACATCACTCTTCCAAGTTTTGCCT  
221          T Y P D K K S I L M Y I T S L F Q V L P

721          CAACAAGTGAGCATTGAAGCCATCCAGGAAGTGAAAATGTTGCCAAGGCCACCTAAAGTG  
241          Q Q V S I E A I Q E V E M L P R P P K V

781          ACTAAAGAAGAACATTTTCAGTTACATCATCAAATGCACTATTCTCAACAGATCACGGTC  
261          T K E E H F Q L H H Q M H Y S Q Q I T V

841          AGTCTAGCACAGGGATATGAGAGAACTTCTTCCCCTAAGCCTCGATTCAAGAGCTATGCC  
281          S L A Q G Y E R T S S P K P R F K S Y A

901          TACACACAGGCTGCTTATGTCACCACCTCTGACCCTACACGGAGCCATTTCTTTCACAG  
301          Y T Q A A Y V T T S D P T R S P F P S Q

961          CATTTGGAAGCTCCTGAAGACAAGTCATTTGGCAGTTCATTGATGGAGAGTGAAGTAAAC  
321          H L E A P E D K S F G S S L M E S E V N

1021         CTGGACCGTTATCAAACAGCTTTAGAAGAAGTATTATCGTGGCTTCTTTCTGCTGAGGAC  
341          L D R Y Q T A L E E V L S W L L S A E D

1081         ACATTGCAAGCACAAAGGAGAGATTTCTAATGATGTGGAAGTGGTGAAGACCAGTTTCAT  
361          T L Q A Q G E I S N D V E V V K D Q F H

1141         ACTCATGAGGGGTACATGATGGATTTGACAGCCCATCAGGGCCGGTTGGTAATATTCTA  
381          T H E G Y M M D L T A H Q G R V G N I L

1201 CAATTGGGAAGTAAGCTGATTGGAACAGGAAAAATTATCAGAAGATGAAGAACTGAAGTA  
401 Q L G S K L I G T G K L S E D E E T E V  
  
1261 CAAGAGCAGATGAATCTCCTAAATTCAAGATGGGAATGCCTCAGGGTAGCTAGCATGGAA  
421 Q E Q M N L L N S R W E C L R V A S M E  
  
1321 AAACAAAGCAATTTACATAGAGTTTTAATGGATCTCCAGAATCAGAACTGAAAGAGTTG  
441 K Q S N L H R V L M D L Q N Q K L K E L  
  
1381 AATGACTGGCTAACAAAAACAGAAGAAAGAACAAGGAAAAATGGAGGAAGAGCCTCTTGGA  
461 N D W L T K T E E R T R K M E E E P L G  
  
1441 CCTGATCTTGAAGACCTAAAACGCCAAGTACAACAACATAAGGTGCTTCAAGAAGATCTA  
481 P D L E D L K R Q V Q Q H K V L Q E D L  
  
1501 GAACAAGAACAAGTCAGGGTCAATTCTCTCACTCACATGGTGGTGGTAGTTGATGAATCT  
501 E Q E Q V R V N S L T H M V V V V D E S  
  
1561 AGTGGAGATCACGCAACTGCTGCTTTGGAAGAACAACCTTAAGGTATTGGGAGATCGATGG  
521 S G D H A T A A L E E Q L K V L G D R W  
  
1621 GCAAACATCTGTAGATGGACAGAAGACCGCTGGGTTCTTTTACAAGACATCCTTCTCAA  
541 A N I C R W T E D R W V L L Q D I L L K  
  
1681 TGGCAACGTCTTACTGAAGAACAGTGCCTTTTTAGTGCATGGCTTTCAGAAAAAGAAGAT  
561 W Q R L T E E Q C L F S A W L S E K E D  
  
1741 GCAGTGAACAAGATTCACACAACCTGGCTTTAAAGATCAAAATGAAATGTTATCAAGTCTT  
581 A V N K I H T T G F K D Q N E M L S S L  
  
1801 CAAAACTGGCCGTTTTAAAAGCGGATCTAGAAAAGAAAAAGCAATCCATGGGCAAACCTG  
601 Q K L A V L K A D L E K K K Q S M G K L  
  
1861 TATTCACTCAAACAAGATCTTCTTTCAACACTGAAGAATAAGTCAGTGACCCAGAAGACG  
621 Y S L K Q D L L S T L K N K S V T Q K T  
  
1921 GAAGCATGGCTGGATAACTTTGCCCGGTGTTGGGATAATTTAGTCCAAAACTT**GAAAAG**  
641 E A W L D N F A R C W D N L V Q K L **E K**  
  
(Deletion)  
1981 **AGTACAGCACAGGAAACTGAAATAGCAGTT**CAAGCTAAACAACCGGATGTGGAAGAGATT  
661 **S T A Q E T E I A V** Q A K Q P D V E E I  
  
Left Right  
2041 TTGTCTAAAGGGCAGCATTGTGACAAGGAAAAACCAGCCACTCAGCCAGTGAAGAGGAAG  
681 L S K G Q H L Y K E K P A T Q P V K R K  
  
2101 TTAGAAGATCTGAGCTCTGAGTGGAAAGGCGGTAAACCGTTTACTTCAAGAGCTGAGGGCA  
701 L E D L S S E W K A V N R L L Q E L R A  
  
2161 AAGCAGCCTGACCTAGCTCCTGGACTGACCACTATTGGAGCCTCTCCTACTCAGACTGTT  
721 K Q P D L A P G L T T I G A S P T Q T V  
  
2221 ACTCTGGTGACACAACCTGTGGTTACTAAGGAAACTGCCATCTCCAAACTAGAAATGCCA  
741 T L V T Q P V V T K E T A I S K L E M P  
  
2281 TCTTCCTTGATGTTGGAGGTACCTGCTCTGGCAGATTTCAACCGGGCTTGGACAGAACTT  
761 S S L M L E V P A L A D F N R A W T E L  
  
2341 ACCGACTGGCTTTCTCTGCTTGATCAAGTTATAAAATCACAGAGGGTGATGGTGGGTGAC  
781 T D W L S L L D Q V I K S Q R V M V G D  
  
2401 CTTGAGGATATCAACGAGATGATCATCAAGCAGAAGGCAACAATGCAGGATTTGGAACAG  
801 L E D I N E M I I K Q K A T M Q D L E Q

2461 AGGCGTCCCCAGTTGGAAGAACTCATTACCGCTGCCCAAAATTTGAAAAACAAGACCAGC  
 821 R R P Q L E E L I T A A Q N L K N K T S  
  
 2521 AATCAAGAGGCTAGAACAAATCATTACGGATCGAATTGAAAGAATTCAGAATCAGTGGGAT  
 841 N Q E A R T I I T D R I E R I Q N Q W D  
  
 2581 GAAGTACAAGAACACCTTCAGAACC GGAGGCAACAGTTGAATGAAATGTTAAAGGATTCA  
 861 E V Q E H L Q N R R Q Q L N E M L K D S  
  
 2641 ACACAATGGCTGGAAGCTAAGGAAGAAGCTGAGCAGGTCTTAGGACAGGCCAGAGCCAAG  
 881 T Q W L E A K E E A E Q V L G Q A R A K  
  
 2701 CTTGAGTCATGGAAGGAGGGTCCCTATACAGTAGATGCAATCCAAAAGAAAATCACAGAA  
 901 L E S W K E G P Y T V D A I Q K K I T E  
  
 2761 ACCAAGCAGTTGGCCAAAGACCTCCGCCAGTGGCAGACAAAATGTAGATGTGGCAAATGAC  
 921 T K Q L A K D L R Q W Q T N V D V A N D  
  
 2821 TTGGCCCTGAAACTTCTCCGGGATTATTCTGCAGATGATACCAGAAAAGTCCACATGATA  
 941 L A L K L L R D Y S A D D T R K V H M I  
  
 2881 ACAGAGAATATCAATGCCTCTTGGAGAAGCATTCAAAAAGGGTGAGTGAGCGAGAGGCT  
 961 T E N I N A S W R S I H K R V S E R E A  
  
 2941 GCTTTGGAAGAAACTCATAGATTACTGCAACAGTTCCTCCCTGGACCTGGAAAAGTTTCTT  
 981 A L E E T H R L L Q Q F P L D L E K F L  
  
 3001 GCCTGGCTTACAGAAGCTGAAACAACCTGCCAATGTCTTACAGGATGCTACCCGTAAGGAA  
 1001 A W L T E A E T T A N V L Q D A T R K E  
  
 3061 AGGCTCCTAGAAGACTCCAAGGGAGTAAAAGAGCTGATGAAACAATGGCAAGACCTCCAA  
 1021 R L L E D S K G V K E L M K Q W Q D L Q  
  
 3121 GGTGAAATTGAAGCTCACACAGATGTTTATCACAACTGGATGAAAACAGCCAAAAAATC  
 1041 G E I E A H T D V Y H N L D E N S Q K I  
  
 3181 CTGAGATCCCTGGAAGGTTCCGATGATGCAGTCCTGTTACAAAAGACGTTTGGATAACATG  
 1061 L R S L E G S D D A V L L Q R R L D N M  
  
 3241 AACTTCAAGTGGAGTGAACCTCGGAAAAAGTCTCTCAACATTAGGTCCCGTTTGGAAAGCC  
 1081 N F K W S E L R K K S L N I R S R L E A  
  
 3301 AGTTCTGACCAGTGGAAAGCGTCTGCACCTTTCTCTGCAGGAACTTCTGGTGTGGCTACAG  
 1101 S S D Q W K R L H L S L Q E L L V W L Q  
  
 3361 CTGAAAGAGGATGAATTAAGCCGGCAGGCACCTATTGGAGGCGACTTTCCAGCAGTTCCAG  
 1121 L K E D E L S R Q A P I G G D F P A V Q  
  
 3421 AAGCAGAACGATGTACATAGGGCCTTCAAGAGGGAATTGAAAACCTAAAGAACCTGTAATC  
 1141 K Q N D V H R A F K R E L K T K E P V I  
  
 3481 ATGAGTACTCTTGAGACTGTACGAATATTTCTGACAGAGCAGCCTTTGGAAAGGACTAGAG  
 1161 M S T L E T V R I F L T E Q P L E G L E  
  
 3541 AAACCTACCAGGAGCCCAGAGAGCTGCCTCCTGAGGAGAGAGCCCAGAATGTCACTCGG  
 1181 K L Y Q E P R E L P P E E R A Q N V T R  
  
 3601 CTTCTACGAAAGCAGGCTGAGGAGGTCAATACTGAGTGGGAAAAATGAACTGCACCTCC  
 1201 L L R K Q A E E V N T E W E K L N L H S  
  
 3661 GCTGACTGGCAGAGAAAAATAGATGAGACCTTGAAGACTCCAGGAACTTCAAGAGGCC  
 1221 A D W Q R K I D E T L E R L Q E L Q E A  
  
 3721 ACGGATGAGCTGGACCTCAAGCTGCGCAAGCTGAGGTGATCAAGGGATCCTGGCAGCCC

1241 T D E L D L K L R Q A E V I K G S W Q P  
3781 GTGGGCGATCTCCTCATTGACTCTCTCCAAGATCACCTCGAGAAAAGTCAAGGCACTTCGA  
1261 V G D L L I D S L Q D H L E K V K A L R  
3841 GGAGAAATTGCGCCTCTGAAAGAGAACGTGAGCCACGTCAATGACCTTGCTCGCCAGCTT  
1281 G E I A P L K E N V S H V N D L A R Q L  
3901 ACCACTTTGGGCATTGACTCTCACCGTATAACCTCAGCACTCTGGAAGACCTGAACACC  
1301 T T L G I Q L S P Y N L S T L E D L N T  
3961 AGATGGAAGCTTCTGCAGGTGGCCGTCGAGGACCGAGTCAGGCAGCTGCATGAAGCCCAC  
1321 R W K L L Q V A V E D R V R Q L H E A H  
4021 AGGGACTTTGGTCCAGCATCTCAGCACTTTCTTTCCACGTCTGTCCAGGGTCCCTGGGAG  
1341 R D F G P A S Q H F L S T S V Q G P W E  
4081 AGAGCCATCTCGCCAAAACAAAGTGCCCTACTATATCAACCACGAGACTCAAACAACCTTGC  
1361 R A I S P N K V P Y Y I N H E T Q T T C  
4141 TGGGACCATCCCAAAATGACAGAGCTCTACCAGTCTTTAGCTGACCTGAATAATGTCAGA  
1381 W D H P K M T E L Y Q S L A D L N N V R  
4201 TTCTCAGCTTATAGGACTGCCATGAAACTCCGAAGACTGCAGAAGGCCCTTTGCTTGGAT  
1401 F S A Y R T A M K L R R L Q K A L C L D  
4261 CTCTTGAGCCTGTGACGTGCATGTGATGCCTTGGACCAGCACAACTCAAGCAAAATGAC  
1421 L L S L S A A C D A L D Q H N L K Q N D  
4321 CAGCCCATGGATATCCTGCAGATTATTAATTGTTTGACCACTATTTATGACCGCCTGGAG  
1441 Q P M D I L Q I I N C L T T I Y D R L E  
4381 CAAGAGCACAAACAATTTGGTCAACGTCCCTCTCTGCGTGGATATGTGTCTGAACTGGCTG  
1461 Q E H N N L V N V P L C V D M C L N W L  
4441 CTGAATGTTTATGATACGGGACGAACAGGGAGGATCCGTGTCCTGTCTTTTAAACTGGC  
1481 L N V Y D T G R T G R I R V L S F K T G  
4501 ATCATTTCCTGTGTAAAGCACATTTGGAAGACAAGTACAGATACCTTTTCAAGCAAGTG  
1501 I I S L C K A H L E D K Y R Y L F K Q V  
4561 GCAAGTTCAACAGGATTTTGTGACCAGCGCAGGCTGGGCCTCCTTCTGCATGATTCTATC  
1521 A S S T G F C D Q R R L G L L L H D S I  
4621 CAAATTCCAAGACAGTTGGGTGAAGTTGCATCCTTTGGGGGCAGTAACATTGAGCCAAGT  
1541 Q I P R Q L G E V A S F G G S N I E P S  
4681 GTCCGGAGCTGCTTCCAATTTGCTAATAATAAGCCAGAGATCGAAGCGGCCCTCTTCTTA  
1561 V R S C F Q F A N N K P E I E A A L F L  
4741 GACTGGATGAGACTGGAACCCAGTCCATGGTGTGGCTGCCCGTCCCTGCACAGAGTGGCT  
1581 D W M R L E P Q S M V W L P V L H R V A  
4801 GCTGCAGAACTGCCAAGCATCAGGCCAAATGTAACATCTGCAAAGAGTGTCCAATCATT  
1601 A A E T A K H Q A K C N I C K E C P I I  
4861 GGATTCAGGTACAGGAGTCTAAAGCACTTTAATTATGACATCTGCCAAAGCTGCTTTTTT  
1621 G F R Y R S L K H F N Y D I C Q S C F F  
4921 TCTGGTTCGAGTTGCAAAAAGGCCATAAAATGCACTATCCCATGGTGGAAATATTGCACTCCG  
1641 S G R V A K G H K M H Y P M V E Y C T P  
4981 ACTACATCAGGAGAAGATGTTTCGAGACTTTGCCAAGGTACTAAAAACAAATTTCGAAC

1661 T T S G E D V R D F A K V L K N K F R T  
 5041 AAAAGGTATTTTGCGAAGCATCCCCGAATGGGCTACCTGCCAGTGCAGACTGTCTTAGAG  
 1681 K R Y F A K H P R M G Y L P V Q T V L E  
 5101 GGGGACAACATGGAAACTCCCGTTACTCTGATCAACTTCTGGCCAGTAGATTCTGCGCCT  
 1701 G D N M E T P V T L I N F W P V D S A P  
 5161 GCCTCGTCCCTCAGCTTTCACACGATGATACTCATTACGCATTGAACATTATGCTAGC  
 1721 A S S P Q L S H D D T H S R I E H Y A S  
 5221 AGGCTAGCAGAAATGGAAAACAGCAATGGATCTTATCTAAATGATAGCATCTCTCCTAAT  
 1741 R L A E M E N S N G S Y L N D S I S P N  
 5281 GAGAGCATAGATGATGAACATTTGTTAATCCAGCATTACTGCCAAAGTTTGAACCAGGAC  
 1761 E S I D D E H L L I Q H Y C Q S L N Q D  
 5341 TCCCCCTGAGCCAGCCTCGTAGTCCTGCCAGATCTTGATTTCTTAGAGAGTGAGGAA  
 1781 S P L S Q P R S P A Q I L I S L E S E E  
 5401 AGAGGGGAGCTAGAGAGAATCCTAGCAGATCTTGAGGAAGAAAACAGGAATCTGCAAGCA  
 1801 R G E L E R I L A D L E E E N R N L Q A  
 5461 GAATATGACCGTCTAAAGCAGCAGCACGAACATAAAGGCCGTGCCCACTGCCGTCCCCT  
 1821 E Y D R L K Q Q H E H K G L S P L P S P  
 5521 CCTGAAATGATGCCACCTCTCCCCAGAGTCCCCGGGATGCTGAGCTCATTGCTGAGGCC  
 1841 P E M M P T S P Q S P R D A E L I A E A  
 5581 AAGCTACTGCGTCAACACAAAGGCCCGCTGGAAGCCAGGATGCAAATCCTGGAAGACCAC  
 1861 K L L R Q H K G R L E A R M Q I L E D H  
 5641 AATAAACAGCTGGAGTCACAGTTACACAGGCTAAGGCAGCTGCTGGAGCAACCCAGGCA  
 1881 N K Q L E S Q L H R L R Q L L E Q P Q A  
 5701 GAGGCCAAAGTGAATGGCACAACGGTGTCTCTCTTCTACCTCTCTACAGAGGTCCGAC  
 1901 E A K V N G T T V S S P S T S L Q R S D  
 5761 AGCAGTCAGCCTATGCTGCTCCGAGTGGTTGGCAGTCAAACCTCGGACTCCATGGGTGAG  
 1921 S S Q P M L L R V V G S Q T S D S M G E  
 5821 GAAGATCTTCTCAGTCTCCCCAGGACACAAGCACAGGGTTAGAGGAGGTGATGGAGCAA  
 1941 E D L L S P P Q D T S T G L E E V M E Q  
 5881 CTCAACAACCTCCTTCCCTAGTTCAAGAGGAAGAAAATACCCCTGGAAAGCCAATGAGAGAG  
 1961 L N N S F P S S R G R N T P G K P M R E  
 5941 GACACAATG**TAG**

## References

- 't Hoen, P.A.C., Nadarajah, V.D., van Putten, M., Chaouch, A., Garrood, P., Straub, V., Ginjaar, H.B., Aartsma-Rus, A.M., van Ommen, G.J.B., den Dunnen, J.T. and Lochmuller, H. (2011) 'Serum matrix metalloproteinase-9 (MMP-9) as a biomarker for monitoring Duchenne muscular dystrophy (DMD) disease progression', *Neuromuscular Disorders*, 21(9-10), pp. 656-656.
- Aartsma-Rus, A., Kaman, W.E., Weij, R., den Dunnen, J.T., van Ommen, G.J. and van Deutekom, J.C. (2006) 'Exploring the frontiers of therapeutic exon skipping for Duchenne muscular dystrophy by double targeting within one or multiple exons', *Mol Ther*, 14(3), pp. 401-7.
- Aartsma-Rus, A., Fokkema, I., Verschuuren, J., Ginjaar, I., van Deutekom, J., van Ommen, G.J. and den Dunnen, J.T. (2009) 'Theoretic applicability of antisense-mediated exon skipping for Duchenne muscular dystrophy mutations', *Hum Mutat*, 30(3), pp. 293-9.
- Aartsma-Rus, A., Houlleberghs, H., van Deutekom, J.C.T., van Ommen, G.J.B. and 't Hoen, P.A.C. (2010) 'Exonic Sequences Provide Better Targets for Antisense Oligonucleotides Than Splice Site Sequences in the Modulation of Duchenne Muscular Dystrophy Splicing', *Oligonucleotides*, 20(2), pp. 69-77.
- Acsadi, G., Dickson, G., Love, D.R., Jani, A., Walsh, F.S., Gurusinghe, A., Wolff, J.A. and Davies, K.E. (1991) 'Human dystrophin expression in mdx mice after intramuscular injection of DNA constructs', *Nature*, 352(6338), pp. 815-8.
- Adams, M.E., Mueller, H.A. and Froehner, S.C. (2001) 'In vivo requirement of the alpha-syntrophin PDZ domain for the sarcolemmal localization of nNOS and aquaporin-4', *J Cell Biol*, 155(1), pp. 113-22.
- Akbar, M.T., Lundberg, A.M., Liu, K., Vidyadaran, S., Wells, K.E., Dolatshad, H., Wynn, S., Wells, D.J., Latchman, D.S. and de Belleruche, J. (2003) 'The neuroprotective effects of heat shock protein 27 overexpression in transgenic

animals against kainate-induced seizures and hippocampal cell death', *J Biol Chem*, 278(22), pp. 19956-65.

Alberts, B., Johnson, A., Lewis, J., Raff, M., Roberts, K., Walter, P. (2008) *Molecular Biology of the Cell*. New York: Garland Science.

Anderson, L.V.B. and Davison, K. (1999) 'Multiplex Western blotting system for the analysis of muscular dystrophy proteins', *American Journal of Pathology*, 154(4), pp. 1017-1022.

Annexstad, E.J., Lund-Petersen, I. and Rasmussen, M. (2014) 'Duchenne muscular dystrophy', *Tidsskr Nor Laegeforen*, 134(14), pp. 1361-1364.

Anthony, K., Cirak, S., Torelli, S., Tasca, G., Feng, L., Arechavala-Gomez, V., Armaroli, A., Guglieri, M., Straathof, C.S., Verschuuren, J.J., Aartsma-Rus, A., Helderman-van den Enden, P., Bushby, K., Straub, V., Sewry, C., Ferlini, A., Ricci, E., Morgan, J.E. and Muntoni, F. (2011) 'Dystrophin quantification and clinical correlations in Becker muscular dystrophy: implications for clinical trials', *Brain*, 134(Pt 12), pp. 3547-59.

Araki, E., Nakamura, K., Nakao, K., Kameya, S., Kobayashi, O., Nonaka, I., Kobayashi, T. and Katsuki, M. (1997) 'Targeted disruption of exon 52 in the mouse dystrophin gene induced muscle Degeneration similar to that observed in Duchenne muscular dystrophy', *Biochemical and Biophysical Research Communications*, 238(2), pp. 492-497.

Arechavala-Gomez, V., Kinali, M., Feng, L., Brown, S.C., Sewry, C., Morgan, J.E. and Muntoni, F. (2010a) 'Immunohistological intensity measurements as a tool to assess sarcolemma-associated protein expression', *Neuropathol Appl Neurobiol*, 36(4), pp. 265-74.

Arechavala-Gomez, V., Kinali, M., Feng, L., Guglieri, M., Edge, G., Main, M., Hunt, D., Lehovsky, J., Straub, V., Bushby, K., Sewry, C.A., Morgan, J.E. and Muntoni, F. (2010b) 'Revertant fibres and dystrophin traces in Duchenne

muscular dystrophy: Implication for clinical trials', *Neuromuscular Disorders*, 20(5), pp. 295-301.

Athanasopoulos, T., Foster, H., Foster, K. and Dickson, G. (2011) 'Codon optimization of the microdystrophin gene for Duchene muscular dystrophy gene therapy', *Methods Mol Biol*, 709, pp. 21-37.

Bagshaw (1982) *Outline studies in biology muscle contraction*. Chapman and Hall, New York.

Banks, G.B., Gregorevic, P., Allen, J.M., Finn, E.E. and Chamberlain, J.S. (2007) 'Functional capacity of dystrophins carrying deletions in the N-terminal actin-binding domain', *Hum Mol Genet*, 16(17), pp. 2105-13.

Banks, G.B., Judge, L.M., Allen, J.M. and Chamberlain, J.S. (2010) 'The polyproline site in hinge 2 influences the functional capacity of truncated dystrophins', *PLoS Genet*, 6(5), p. e1000958.

Barton-Davis, E.R., Cordier, L., Shoturma, D.I., Leland, S.E. and Sweeney, H.L. (1999) 'Aminoglycoside antibiotics restore dystrophin function to skeletal muscles of mdx mice', *J Clin Invest*, 104(4), pp. 375-81.

Becker, P.E. and Kiener, F. (1955) '[A new x-chromosomal muscular dystrophy]', *Arch Psychiatr Nervenkr Z Gesamte Neurol Psychiatr*, 193(4), pp. 427-48.

Benchouir, R., Meregalli, M., Farini, A., Belicchi, M., Battistelli, M., Bresolin, N., Torrente, Y., D'Antona, G., Bottinelli, R. and Garcia, L. (2008) 'Restoration of human dystrophin following transplantation of exon-skipping-engineered DMD patient stem cells into dystrophic mice', *M S-Medecine Sciences*, 24(1), pp. 99-101.

Berger, J., Berger, S., Hall, T.E., Lieschke, G.J. and Currie, P.D. (2010) 'Dystrophin-deficient zebrafish feature aspects of the Duchenne muscular dystrophy pathology', *Neuromuscular Disorders*, 20(12), pp. 826-832.

Bies, R.D., Caskey, C.T. and Fenwick, R. (1992) 'An Intact Cysteine-Rich Domain Is Required for Dystrophin Function', *Journal of Clinical Investigation*, 90(2), pp. 666-672.

Blake, D.J., Weir, A., Newey, S.E. and Davies, K.E. (2002) 'Function and genetics of dystrophin and dystrophin-related proteins in muscle', *Physiol Rev*, 82(2), pp. 291-329.

Blankinship, M.J., Gregorevic, P. and Chamberlain, J.S. (2006) 'Gene therapy strategies for Duchenne muscular dystrophy utilizing recombinant adeno-associated virus vectors', *Molecular Therapy*, 13(2), pp. 241-249.

Bonci, D., Cittadini, A., Latronico, M.V., Borello, U., Aycocock, J.K., Drusco, A., Innocenzi, A., Follenzi, A., Lavitrano, M., Monti, M.G., Ross, J., Jr., Naldini, L., Peschle, C., Cossu, G. and Condorelli, G. (2003) 'Advanced' generation lentiviruses as efficient vectors for cardiomyocyte gene transduction in vitro and in vivo', *Gene Ther*, 10(8), pp. 630-6.

Brenman, J.E., Chao, D.S., Xia, H., Aldape, K. and Brecht, D.S. (1995) 'Nitric oxide synthase complexed with dystrophin and absent from skeletal muscle sarcolemma in Duchenne muscular dystrophy', *Cell*, 82(5), pp. 743-52.

Brenman, J.E., Christopherson, K.S., Craven, S.E., McGee, A.W. and Brecht, D.S. (1996) 'Cloning and characterization of postsynaptic density 93, a nitric oxide synthase interacting protein', *J Neurosci*, 16(23), pp. 7407-15.

Briguet, A., Courdier-Fruh, I., Foster, M., Meier, T. and Magyar, J.P. (2004) 'Histological parameters for the quantitative assessment of muscular dystrophy in the mdx-mouse', *Neuromuscul Disord*, 14(10), pp. 675-82.

Brinkmeyer-Langford, C. and Kornegay, J.N. (2013) 'Comparative Genomics of X-linked Muscular Dystrophies: The Golden Retriever Model', *Curr Genomics*, 14(5), pp. 330-42.

Brockington, M., Yuva, Y., Prandini, P., Brown, S.C., Torelli, S., Benson, M.A., Herrmann, R., Anderson, L.V.B., Bashir, R., Burgunder, J.M., Fallet, S., Romero, N., Fardeau, M., Straub, V., Storey, G., Pollitt, C., Richard, I., Sewry, C.A., Bushby, K., Voit, T., Blake, D.J. and Muntoni, F. (2001) 'Mutations in the fukutin-related protein gene (FKRP) identify limb girdle muscular dystrophy 2I as a milder allelic variant of congenital muscular dystrophy MDC1C', *Human Molecular Genetics*, 10(25), pp. 2851-2859.

Brown, K.J., Marathi, R., Fiorillo, A.A., Ciccimaro, E.F., Sharma, S., Rowlands, D.S., Rayavarapu, S., Nagaraju, K., Hoffman, E.P. and Hathout, Y. (2012) 'Accurate Quantitation of Dystrophin Protein in Human Skeletal Muscle Using Mass Spectrometry', *J Bioanal Biomed*, Suppl 7.

Bulfield, G., Siller, W.G., Wight, P.A. and Moore, K.J. (1984) 'X chromosome-linked muscular dystrophy (mdx) in the mouse', *Proc Natl Acad Sci U S A*, 81(4), pp. 1189-92.

Bushby, K.M., Appleton, R., Anderson, L.V., Welch, J.L., Kelly, P. and Gardner-Medwin, D. (1995) 'Deletion status and intellectual impairment in Duchenne muscular dystrophy', *Dev Med Child Neurol*, 37(3), pp. 260-9.

Bushby, K., Chiu, Y.H., Hornsey, M.A., Klinge, L., Jorgensen, L.H., Laval, S.H., Charlton, R., Barresi, R., Straub, V. and Lochmuller, H. (2009) 'Attenuated muscle regeneration is a key factor in dysferlin-deficient muscular dystrophy', *Human Molecular Genetics*, 18(11), pp. 1976-1989.

Bushby, K., Finkel, R. and Birnkrant, D.J. (2010a) 'Diagnosis and management of Duchenne muscular dystrophy, part 2: implementation of multidisciplinary care (vol 9, pg 177, 2010)', *Lancet Neurology*, 9(3), pp. 237-237.

Bushby, K., Finkel, R., Birnkrant, D.J., Case, L.E., Clemens, P.R., Cripe, L., Kaul, A., Kinnett, K., McDonald, C., Pandya, S., Poysky, J., Shapiro, F., Tomezsko, J. and Constantin, C. (2010b) 'Diagnosis and management of Duchenne muscular dystrophy, part 1: diagnosis, and pharmacological and psychosocial management', *Lancet Neurol*, 9(1), pp. 77-93.

Bushby, K., Finkel, R., Wong, B., Barohn, R., Campbell, C., Comi, G.P., Connolly, A.M., Day, J.W., Flanigan, K.M., Goemans, N., Jones, K.J., Mercuri, E., Quinlivan, R., Renfroe, J.B., Russman, B., Ryan, M.M., Tulinius, M., Voit, T., Moore, S.A., Lee Sweeney, H., Abresch, R.T., Coleman, K.L., Eagle, M., Florence, J., Gappmaier, E., Glanzman, A.M., Henricson, E., Barth, J., Elfring, G.L., Reha, A., Spiegel, R.J., O'Donnell M, W., Peltz, S.W., McDonald, C.M. and Ptc124-Gd-007-Dmd Study, G. (2014) 'Ataluren treatment of patients with nonsense mutation dystrophinopathy', *Muscle Nerve*, 50(4), pp. 477-87.

Cadenas, S., Echtay, K.S., Harper, J.A., Jekabsons, M.B., Buckingham, J.A., Grau, E., Abuin, A., Chapman, H., Clapham, J.C. and Brand, M.D. (2002) 'The basal proton conductance of skeletal muscle mitochondria from transgenic mice overexpressing or lacking uncoupling protein-3', *J Biol Chem*, 277(4), pp.2773-8.

Campeau, P., Chapdelaine, P., Seigneurin-Venin, S., Massie, B. and Tremblay, J.P. (2001) 'Transfection of large plasmids in primary human myoblasts', *Gene Therapy*, 8(18), pp. 1387-1394.

Cappelletti, M., Zampaglione, I., Rizzuto, G., Ciliberto, G., La Monica, N. and Fattori, E. (2003) 'Gene electro-transfer improves transduction by modifying the fate of intramuscular DNA', *J Gene Med*, 5(4), pp. 324-32.

Carnwath, J.W. and Shotton, D.M. (1987) 'Muscular dystrophy in the mdx mouse: histopathology of the soleus and extensor digitorum longus muscles', *J Neurol Sci*, 80(1), pp. 39-54.

Carsana, A., Frisso, G., Tremolaterra, M.R., Lanzillo, R., Vitale, D.F., Santoro, L. and Salvatore, F. (2005) 'Analysis of dystrophin gene deletions indicates that the hinge III region of the protein correlates with disease severity', *Annals of Human Genetics*, 69, pp. 253-259.

Carter, B.J. (2005) 'Adeno-associated virus vectors in clinical trials', *Hum Gene Ther*, 16(5), pp. 541-50.

Cavalcanti, G.M., Oliveira, A.D.B., Assis, T.D., Chimelli, L.M.C., de Medeiros, P.L. and da Mota, D.L. (2011) 'Histochemistry and Morphometric Analysis of Muscle Fibers from Patients with Duchenne Muscular Dystrophy (DMD)', *International Journal of Morphology*, 29(3), pp. 934-938.

Ceafalan, L.C., Popescu, B.O. and Hinescu, M.E. (2014) 'Cellular players in skeletal muscle regeneration', *Biomed Res Int*, 2014, p. 957014.

Chakkalakal, J.V., Thompson, J., Parks, R.J. and Jasmin, B.J. (2005) 'Molecular, cellular, and pharmacological therapies for Duchenne/Becker muscular dystrophies', *Faseb Journal*, 19(8), pp. 880-891.

Chamberlain, J.S. (1997) 'Dystrophin levels required for genetic correction of Duchenne muscular dystrophy', *Basic and Applied Myology*, 7(3-4), pp. 251-255.

Chamberlain, J.S. (2002) 'Gene therapy of muscular dystrophy', *Hum Mol Genet*, 11(20), pp. 2355-62.

Chamberlain, J.S., Metzger, J., Reyes, M., Townsend, D. and Faulkner, J.A. (2007) 'Dystrophin-deficient mdx mice display a reduced life span and are susceptible to spontaneous rhabdomyosarcoma', *FASEB J*, 21(9), pp. 2195-204.

Chamberlain, J.S. (2013) 'Removing the Immune Response From Muscular Dystrophy Research', *Molecular Therapy*, 21(10), pp. 1821-1822.

Chang, W.J., Iannaccone, S.T., Lau, K.S., Masters, B.S., McCabe, T.J., McMillan, K., Padre, R.C., Spencer, M.J., Tidball, J.G. and Stull, J.T. (1996) 'Neuronal nitric oxide synthase and dystrophin-deficient muscular dystrophy', *Proc Natl Acad Sci U S A*, 93(17), pp. 9142-7.

Chao, D.S., Silvagno, F. and Bredt, D.S. (1998) 'Muscular dystrophy in mdx mice despite lack of neuronal nitric oxide synthase', *Journal of Neurochemistry*, 71(2), pp. 784-789.

Charge, S.B. and Rudnicki, M.A. (2004) 'Cellular and molecular regulation of muscle regeneration', *Physiol Rev*, 84(1), pp. 209-38.

Cirak, S., Arechavala-Gomez, V., Guglieri, M., Feng, L., Torelli, S., Anthony, K., Abbs, S., Garralda, M.E., Bourke, J., Wells, D.J., Dickson, G., Wood, M.J., Wilton, S.D., Straub, V., Kole, R., Shrewsbury, S.B., Sewry, C., Morgan, J.E., Bushby, K. and Muntoni, F. (2011) 'Exon skipping and dystrophin restoration in patients with Duchenne muscular dystrophy after systemic phosphorodiamidate morpholino oligomer treatment: an open-label, phase 2, dose-escalation study', *Lancet*, 378(9791), pp. 595-605.

Cirak, S., Feng, L., Anthony, K., Arechavala-Gomez, V., Torelli, S., Sewry, C., Morgan, J.E. and Muntoni, F. (2012) 'Restoration of the dystrophin-associated glycoprotein complex after exon skipping therapy in Duchenne muscular dystrophy', *Mol Ther*, 20(2), pp. 462-7.

Ciuffi, A. (2008) 'Mechanisms Governing Lentivirus Integration Site Selection', *Current Gene Therapy*, 8(6), pp. 419-429.

Clemens, P.R., Krause, T.L., Chan, S., Korb, K.E., Graham, F.L. and Caskey, C.T. (1995) 'Recombinant Truncated Dystrophin Minigenes - Construction, Expression, and Adenoviral Delivery', *Human Gene Therapy*, 6(11), pp. 1477-1485.

Collins, C.A. and Morgan, J.E. (2003) 'Duchenne's muscular dystrophy: animal models used to investigate pathogenesis and develop therapeutic strategies', *International Journal of Experimental Pathology*, 84(4), pp. 165-172.

Collins, C.A., Olsen, I., Zammit, P.S., Heslop, L., Petrie, A., Partridge, T.A. and Morgan, J.E. (2005) 'Stem cell function, self-renewal, and behavioral heterogeneity of cells from the adult muscle satellite cell niche', *Cell*, 122(2), pp. 289-301.

Corrado, K., Rafael, J.A., Mills, P.L., Cole, N.M., Faulkner, J.A., Wang, K. and Chamberlain, J.S. (1996) 'Transgenic mdx mice expressing dystrophin with a

deletion in the actin-binding domain display a "mild becker" phenotype', *Journal of Cell Biology*, 134(4), pp. 873-884.

Cossu, G. and Sampaolesi, M. (2007) 'New therapies for Duchenne muscular dystrophy: challenges, prospects and clinical trials', *Trends Mol Med*, 13(12), pp. 520-6.

Coulton, G.R., Morgan, J.E., Partridge, T.A. and Sloper, J.C. (1988) 'The mdx mouse skeletal muscle myopathy: I. A histological, morphometric and biochemical investigation', *Neuropathol Appl Neurobiol*, 14(1), pp. 53-70.

Cox, G.A., Sunada, Y., Campbell, K.P. and Chamberlain, J.S. (1994) 'Dp71 can restore the dystrophin-associated glycoprotein complex in muscle but fails to prevent dystrophy', *Nat Genet*, 8(4), pp. 333-9.

Crawford, G.E., Lu, Q.L., Partridge, T.A. and Chamberlain, J.S. (2001) 'Suppression of revertant fibers in mdx mice by expression of a functional dystrophin', *Hum Mol Genet*, 10(24), pp. 2745-50.

Crosbie, R.H., Straub, V., Yun, H.Y., Lee, J.C., Rafael, J.A., Chamberlain, J.S., Dawson, V.L., Dawson, T.M. and Campbell, K.P. (1998) 'mdx muscle pathology is independent of nNOS perturbation', *Human Molecular Genetics*, 7(5), pp. 823-829.

Culligan, K.G., Mackey, A.J., Finn, D.M., Maguire, P.B. and Ohlendieck, K. (1998) 'Role of dystrophin isoforms and associated proteins in muscular dystrophy (review)', *Int J Mol Med*, 2(6), pp. 639-48.

Davies, K.E. and Grounds, M.D. (2007) 'Modified patient stem cells as prelude to autologous treatment of muscular dystrophy', *Cell Stem Cell*, 1(6), pp. 595-596.

Deconinck, A.E., Rafael, J.A., Skinner, J.A., Brown, S.C., Potter, A.C., Metzinger, L., Watt, D.J., Dickson, J.G., Tinsley, J.M. and Davies, K.E. (1997)

'Utrophin-dystrophin-deficient mice as a model for Duchenne muscular dystrophy', *Cell*, 90(4), pp. 717-727.

Dellavalle, A., Sampaolesi, M., Tonlorenzi, R., Tagliafico, E., Sacchetti, B., Perani, L., Innocenzi, A., Galvez, B.G., Messina, G., Morosetti, R., Li, S., Belicchi, M., Peretti, G., Chamberlain, J.S., Wright, W.E., Torrente, Y., Ferrari, S., Bianco, P. and Cossu, G. (2007) 'Pericytes of human skeletal muscle are myogenic precursors distinct from satellite cells', *Nat Cell Biol*, 9(3), pp. 255-67.

Den Dunnen, J.T., Grootsholten, P.M., Bakker, E., Blonden, L.A.J., Ginjaar, H.B., Wapenaar, M.C., Vanpaassen, H.M.B., Vanbroeckhoven, C., Pearson, P.L. and Vanommen, G.J.B. (1989) 'Topography of the Duchenne Muscular-Dystrophy (Dmd) Gene - Fige and Cdna Analysis of 194 Cases Reveals 115 Deletions and 13 Duplications', *American Journal of Human Genetics*, 45(6), pp. 835-847.

Denetclaw, W.F., Jr., Bi, G., Pham, D.V. and Steinhardt, R.A. (1993) 'Heterokaryon myotubes with normal mouse and Duchenne nuclei exhibit sarcolemmal dystrophin staining and efficient intracellular free calcium control', *Mol Biol Cell*, 4(9), pp. 963-72.

Dent, K.M., Dunn, D.M., von Niederhausern, A.C., Aoyagi, A.T., Kerr, L., Bromberg, M.B., Hart, K.J., Tuohy, T., White, S., den Dunnen, J.T., Weiss, R.B. and Flanigan, K.M. (2005) 'Improved molecular diagnosis of dystrophinopathies in an unselected clinical cohort', *American Journal of Medical Genetics Part A*, 134A(3), pp. 295-298.

Dick, E., Matsa, E., Bispham, J., Reza, M., Guglieri, M., Staniforth, A., Watson, S., Kumari, R., Lochmuller, H., Young, L., Darling, D. and Denning, C. (2011) 'Two new protocols to enhance the production and isolation of human induced pluripotent stem cell lines', *Stem Cell Res*, 6(2), pp. 158-67.

Dick, E., Kalra, S., Anderson, D., George, V., Ritso, M., Laval, S.H., Barresi, R., Aartsma-Rus, A., Lochmuller, H. and Denning, C. (2013) 'Exon Skipping and Gene Transfer Restore Dystrophin Expression in Human Induced Pluripotent

Stem Cells-Cardiomyocytes Harboring DMD Mutations', *Stem Cells and Development*, 22(20), pp. 2714-2724.

Dickson, G., Roberts, M.L., Wells, D.J. and Fabb, S.A. (2002) 'Recombinant micro-genes and dystrophin viral vectors', *Neuromuscul Disord*, 12 Suppl 1, pp. S40-4.

Dubowitz, V. (1978) 'Muscle disorders in childhood', *Major Probl Clin Pediatr*, 16, pp. iii-xiii, 1-282.

Dunant, P., Larochelle, N., Thirion, C., Stucka, R., Ursu, D., Petrof, B.J., Wolf, E. and Lochmuller, H. (2003) 'Expression of dystrophin driven by the 1.35-kb MCK promoter ameliorates muscular dystrophy in fast, but not in slow muscles of transgenic mdx mice', *Mol Ther*, 8(1), pp. 80-9.

Durbeej, M. and Campbell, K.P. (2002) 'Muscular dystrophies involving the dystrophin-glycoprotein complex: an overview of current mouse models', *Current Opinion in Genetics & Development*, 12(3), pp. 349-361.

Eisenberg, B.R. (1985). *Adaptability of ultrastructure in the mammalian muscle*. The Journal of Experimental Biology: Design and Performance of Muscular Systems. The Company of Biologists Limited. Cambridge, Great Britain. 115:55-68.

Emery, A.E. (1993) 'Duchenne muscular dystrophy--Meryon's disease', *Neuromuscul Disord*, 3(4), pp. 263-6.

Emery, A.E. (2002a) 'The muscular dystrophies', *Lancet*, 359(9307), pp. 687-95.

Emery, A.E. (2002b) 'Muscular dystrophy into the new millennium', *Neuromuscul Disord*, 12(4), pp. 343-9.

England, S.B., Nicholson, L.V., Johnson, M.A., Forrest, S.M., Love, D.R., Zubrzycka-Gaarn, E.E., Bulman, D.E., Harris, J.B. and Davies, K.E. (1990)

'Very mild muscular dystrophy associated with the deletion of 46% of dystrophin', *Nature*, 343(6254), pp. 180-2.

Ervasti, J.M. (2007) 'Dystrophin, its interactions with other proteins, and implications for muscular dystrophy', *Biochimica Et Biophysica Acta-Molecular Basis of Disease*, 1772(2), pp. 108-117.

Ervasti, J.M. and Sonnemann, K.J. (2008) 'Biology of the striated muscle dystrophin-glycoprotein complex', *Int Rev Cytol*, 265, pp. 191-225.

Escher, C., Lochmuller, H., Fischer, D., Frank, S., Reimann, J., Walter, M.C., Ehrat, M., Ruegg, M.A. and Gyax, D. (2010) 'Reverse protein arrays as novel approach in muscular dystrophies', *Neuromuscular Disorders*, 20(5), pp.302-309.

Fabb, S.A., Wells, D.J., Serpente, P. and Dickson, G. (2002) 'Adeno-associated virus vector gene transfer and sarcolemmal expression of a 144 kDa micro-dystrophin effectively restores the dystrophin-associated protein complex and inhibits myofibre degeneration in nude/mdx mice', *Human Molecular Genetics*, 11(7), pp. 733-741.

Fairclough, R.J., Wood, M.J. and Davies, K.E. (2013) 'Therapy for Duchenne muscular dystrophy: renewed optimism from genetic approaches', *Nat Rev Genet*, 14(6), pp. 373-8.

Fanin, M., Danieli, G.A., Vitiello, L., Senter, L. and Angelini, C. (1992) 'Prevalence of dystrophin-positive fibers in 85 Duchenne muscular dystrophy patients', *Neuromuscul Disord*, 2(1), pp. 41-5.

Ferrari, G., Cusella-De Angelis, G., Coletta, M., Paolucci, E., Stornaiuolo, A., Cossu, G. and Mavilio, F. (1998) 'Muscle regeneration by bone marrow derived myogenic progenitors', *Science*, 279(5356), pp. 1528-1530.

Finkel, R.S., Flanigan, K.M., Wong, B., Bonnemann, C., Sampson, J., Sweeney, H.L., Reha, A., Northcutt, V.J., Elfring, G., Barth, J. and Peltz, S.W. (2013)

'Phase 2a Study of Ataluren-Mediated Dystrophin Production in Patients with Nonsense Mutation Duchenne Muscular Dystrophy', *Plos One*, 8(12).

Flanigan, K.M., von Niederhausern, A., Dunn, D.M., Alder, J., Mendell, J.R. and Weiss, R.B. (2003) 'Rapid direct sequence analysis of the dystrophin gene', *American Journal of Human Genetics*, 72(4), pp. 931-939.

Flanigan, K.M., Campbell, K., Viollet, L., Wang, W., Gomez, A.M., Walker, C.M. and Mendell, J.R. (2013) 'Anti-dystrophin T cell responses in Duchenne muscular dystrophy: prevalence and a glucocorticoid treatment effect', *Hum Gene Ther*, 24(9), pp. 797-806.

Flanigan, K.M., Voit, T., Rosales, X.Q., Servais, L., Kraus, J.E., Wardell, C., Morgan, A., Dorricott, S., Nakielny, J., Quarcoo, N., Liefwaard, L., Drury, T., Champion, G. and Wright, P. (2014) 'Pharmacokinetics and safety of single doses of drisapersen in non-ambulant subjects with Duchenne muscular dystrophy: results of a double-blind randomized clinical trial', *Neuromuscul Disord*, 24(1), pp. 16-24.

Flisikowska, T., Kind, A. and Schnieke, A. (2014) 'Genetically modified pigs to model human diseases', *Journal of Applied Genetics*, 55(1), pp. 53-64.

Folker, E.S. and Baylies, M.K. (2013) 'Nuclear positioning in muscle development and disease', *Front Physiol*, 4, p. 363.

Follenzi, A. and Naldini, L. (2002) 'Generation of HIV-1 derived lentiviral vectors', *Methods Enzymol*, 346, pp. 454-65.

Foster, H., Sharp, P., Trollet, C., Athanasopoulos, T., Graham, I., Foster, K., Wells, D. and Dickson, G. (2007) 'Codon optimization of microdystrophin results in improvements in expression and physiological outcome in the mdx mouse following AAV8 gene transfer', *Human Gene Therapy*, 18(10), pp. 1078-1078.

Friedrich, O., Both, M., Gillis, J.M., Chamberlain, J.S. and Fink, R.H. (2004) 'Mini-dystrophin restores L-type calcium currents in skeletal muscle of transgenic mdx mice', *J Physiol*, 555(Pt 1), pp. 251-65.

Ghosh, S.S., Gopinath, P. and Ramesh, A. (2006) 'Adenoviral vectors: a promising tool for gene therapy', *Appl Biochem Biotechnol*, 133(1), pp. 9-29.

Ghosh, A., Yue, Y., Long, C., Bostick, B. and Duan, D. (2007) 'Efficient whole-body transduction with trans-splicing adeno-associated viral vectors', *Mol Ther*, 15(4), pp. 750-5.

Goyenvalle, A., Seto, J.T., Davies, K.E. and Chamberlain, J. (2011) 'Therapeutic approaches to muscular dystrophy', *Hum Mol Genet*, 20(R1), pp. R69-78.

Greenberg, D.S., Sunada, Y., Campbell, K.P., Yaffe, D. and Nudel, U. (1994) 'Exogenous Dp71 restores the levels of dystrophin associated proteins but does not alleviate muscle damage in mdx mice', *Nat Genet*, 8(4), pp. 340-4.

Gregorevic, P., Blankinship, M.J., Allen, J.M., Crawford, R.W., Meuse, L., Miller, D.G., Russell, D.W. and Chamberlain, J.S. (2004) 'Systemic delivery of genes to striated muscles using adeno-associated viral vectors', *Nature Medicine*, 10(8), pp. 828-834.

Gregorevic, P., Allen, J.M., Minami, E., Blankinship, M.J., Haraguchi, M., Meuse, L., Finn, E., Adams, M.E., Froehner, S.C., Murry, C.E. and Chamberlain, J.S. (2006) 'rAAV6-microdystrophin preserves muscle function and extends lifespan in severely dystrophic mice', *Nat Med*, 12(7), pp. 787-9.

Gregorevic, P., Schultz, B.R., Allen, J.M., Halldorson, J.B., Blankinship, M.J., Meznarich, N.A., Kuhr, C.S., Doremus, C., Finn, E., Liggitt, D. and Chamberlain, J.S. (2009) 'Evaluation of vascular delivery methodologies to enhance rAAV6-mediated gene transfer to canine striated musculature', *Mol Ther*, 17(8), pp. 1427-33.

Grounds, M.D., Radley, H.G., Lynch, G.S., Nagaraju, K. and De Luca, A. (2008) 'Towards developing standard operating procedures for pre-clinical testing in

the mdx mouse model of Duchenne muscular dystrophy', *Neurobiol Dis*, 31(1), pp. 1-19.

Hagen, G.H., F. Keller, G. Leutert, K. Schippel und W.Schmidt (1998) *Histologie*. Verlag Wissenschaftliche Skripten.

Harper, S.Q., Hauser, M.A., DelloRusso, C., Duan, D., Crawford, R.W., Phelps, S.F., Harper, H.A., Robinson, A.S., Engelhardt, J.F., Brooks, S.V. and Chamberlain, J.S. (2002) 'Modular flexibility of dystrophin: implications for gene therapy of Duchenne muscular dystrophy', *Nat Med*, 8(3), pp. 253-61.

Hartigan-O'Connor, D. and Chamberlain, J.S. (2000) 'Developments in gene therapy for muscular dystrophy', *Microsc Res Tech*, 48(3-4), pp. 223-38.

Helbling-Leclerc, A., Topaloglu, H., Tome, F.M., Sewry, C., Gyapay, G., Naom, I., Muntoni, F., Dubowitz, V., Barois, A., Estournet, B. and et al. (1995) 'Readjusting the localization of merosin (laminin alpha 2-chain) deficient congenital muscular dystrophy locus on chromosome 6q2', *C R Acad Sci III*, 318(12), pp. 1245-52.

Heydemann, A. and McNally, E.M. (2007) 'Consequences of disrupting the dystrophin-sarcoglycan complex in cardiac and skeletal myopathy', *Trends Cardiovasc Med*, 17(2), pp. 55-9.

Hoffman, E.P., Brown, R.H., Jr. and Kunkel, L.M. (1987a) 'Dystrophin: the protein product of the Duchenne muscular dystrophy locus', *Cell*, 51(6), pp. 919-28.

Hoffman, E.P., Knudson, C.M., Campbell, K.P. and Kunkel, L.M. (1987b) 'Subcellular fractionation of dystrophin to the triads of skeletal muscle', *Nature*, 330(6150), pp. 754-8.

Hoffman, E.P., Morgan, J.E., Watkins, S.C. and Partridge, T.A. (1990) 'Somatic reversion/suppression of the mouse mdx phenotype in vivo', *J Neurol Sci*, 99(1), pp. 9-25.

- Hoffman, E.P. and Dressman, D. (2001) 'Molecular pathophysiology and targeted therapeutics for muscular dystrophy', *Trends Pharmacol Sci*, 22(9), pp. 465-70.
- Hollinger, K., Yang, C.X., Montz, R.E., Nonneman, D., Ross, J.W. and Selsby, J.T. (2014) 'Dystrophin insufficiency causes selective muscle histopathology and loss of dystrophin-glycoprotein complex assembly in pig skeletal muscle', *Faseb Journal*, 28(4), pp. 1600-1609.
- Hrdlicka, I., Zadina, J., Siskova, V., Gregor, A., Srbova, A., Santava, A. and Kantorova, E. (2002) 'Correlation of genotypes and phenotypes in patients with Duchenne and Becker muscular dystrophy caused by deletions in the dystrophin gene', *Ceska a Slovenska Neurologie a Neurochirurgie*, 65(2), pp. 85-91.
- Huang, P.L., Dawson, T.M., Brettt, D.S., Snyder, S.H. and Fishman, M.C. (1993) 'Targeted Disruption of the Neuronal Nitric-Oxide Synthase Gene', *Cell*, 75(7), pp. 1273-1286.
- Ibraghimov-Beskrovnaya, O., Ervasti, J.M., Leveille, C.J., Slaughter, C.A., Sernett, S.W. and Campbell, K.P. (1992) 'Primary structure of dystrophin-associated glycoproteins linking dystrophin to the extracellular matrix', *Nature*, 355(6362), pp. 696-702.
- Isaac, C., Wright, A., Usas, A., Li, H., Tang, Y., Mu, X., Greco, N., Dong, Q., Vo, N., Kang, J., Wang, B. and Huard, J. (2013) 'Dystrophin and utrophin "double knockout" dystrophic mice exhibit a spectrum of degenerative musculoskeletal abnormalities', *J Orthop Res*, 31(3), pp. 343-9.
- Ishikawa, A. (1983) *Fine structure of skeletal muscle*. New York: Plenum Press.
- Ishikawa, Y., Ishikawa, Y. and Minami, R. (1996) 'Quantitative estimation of dystrophin protein: A sensitive and convenient "two-antibody sandwich" ELISA', *Tohoku Journal of Experimental Medicine*, 180(1), pp. 57-63.

Jarmin, S., Kymalainen, H., Popplewell, L. and Dickson, G. (2014) 'New developments in the use of gene therapy to treat Duchenne muscular dystrophy', *Expert Opinion on Biological Therapy*, 14(2), pp. 209-230.

Jat, P.S., Noble, M.D., Ataliotis, P., Tanaka, Y., Yannoutsos, N., Larsen, L. and Kioussis, D. (1991) 'Direct derivation of conditionally immortal cell lines from an H-2Kb-tsA58 transgenic mouse', *Proc Natl Acad Sci U S A*, 88(12), pp. 5096-100.

Johnson, E.K., Li, B., Yoon, J.H., Flanigan, K.M., Martin, P.T., Ervasti, J. and Montanaro, F. (2013) 'Identification of new dystroglycan complexes in skeletal muscle', *PLoS One*, 8(8), p. e73224.

Jorgensen, L.H., Larochelle, N., Orlopp, K., Dunant, P., Dudley, R.W., Stucka, R., Thirion, C., Walter, M.C., Laval, S.H. and Lochmuller, H. (2009) 'Efficient and fast functional screening of microdystrophin constructs in vivo and in vitro for therapy of duchenne muscular dystrophy', *Hum Gene Ther*, 20(6), pp. 641-50.

Khurana, T.S., Watkins, S.C., Chafey, P., Chelly, J., Tome, F.M., Fardeau, M., Kaplan, J.C. and Kunkel, L.M. (1991) 'Immunolocalization and developmental expression of dystrophin related protein in skeletal muscle', *Neuromuscul Disord*, 1(3), pp. 185-94.

Kim, T.K. and Eberwine, J.H. (2010) 'Mammalian cell transfection: the present and the future', *Anal Bioanal Chem*, 397(8), pp. 3173-8.

Kimura, E., Li, S., Gregorevic, P., Fall, B.M. and Chamberlain, J.S. (2010) 'Dystrophin Delivery to Muscles of mdx Mice Using Lentiviral Vectors Leads to Myogenic Progenitor Targeting and Stable Gene Expression', *Molecular Therapy*, 18(1), pp. 206-213.

Kinali, M., Arechavala-Gomez, V., Feng, L., Cirak, S., Hunt, D., Adkin, C., Guglieri, M., Ashton, E., Abbs, S., Nihoyannopoulos, P., Garralda, M.E., Rutherford, M., McCulley, C., Popplewell, L., Graham, I.R., Dickson, G., Wood,

M.J., Wells, D.J., Wilton, S.D., Kole, R., Straub, V., Bushby, K., Sewry, C., Morgan, J.E. and Muntoni, F. (2009) 'Local restoration of dystrophin expression with the morpholino oligomer AVI-4658 in Duchenne muscular dystrophy: a single-blind, placebo-controlled, dose-escalation, proof-of-concept study', *Lancet Neurol*, 8(10), pp. 918-28.

Kingston, H.M., Sarfarazi, M., Thomas, N.S. and Harper, P.S. (1984) 'Localisation of the Becker muscular dystrophy gene on the short arm of the X chromosome by linkage to cloned DNA sequences', *Human Genetics*, 67(1), pp. 6-17.

Klymiuk, N., Blutke, A., Graf, A., Krause, S., Burkhardt, K., Wuensch, A., Krebs, S., Kessler, B., Zakhartchenko, V., Kurome, M., Kemter, E., Nagashima, H., Schoser, B., Herbach, N., Blum, H., Wanke, R., Aartsma-Rus, A., Thirion, C., Lochmuller, H., Walter, M.C. and Wolf, E. (2013) 'Dystrophin-deficient pigs provide new insights into the hierarchy of physiological derangements of dystrophic muscle', *Human Molecular Genetics*, 22(21), pp. 4368-4382.

Kobayashi, T., Ohno, S., Park-Matsumoto, Y.C., Kameda, N. and Baba, T. (1995) 'Developmental studies of dystrophin and other cytoskeletal proteins in cultured muscle cells', *Microsc Res Tech*, 30(6), pp. 437-57.

Koenig, M., Hoffman, E.P., Bertelson, C.J., Monaco, A.P., Feener, C. and Kunkel, L.M. (1987) 'Complete cloning of the Duchenne muscular dystrophy (DMD) cDNA and preliminary genomic organization of the DMD gene in normal and affected individuals', *Cell*, 50(3), pp. 509-17.

Koenig, M., Monaco, A.P. and Kunkel, L.M. (1988) 'The complete sequence of dystrophin predicts a rod-shaped cytoskeletal protein', *Cell*, 53(2), pp. 219-28.

Koenig, M., Beggs, A.H., Moyer, M., Scherpf, S., Heindrich, K., Bettecken, T., Meng, G., Muller, C.R., Lindlof, M., Kaariainen, H. and et al. (1989) 'The molecular basis for Duchenne versus Becker muscular dystrophy: correlation of severity with type of deletion', *American Journal of Human Genetics*, 45(4), pp. 498-506.

Koo, T., Okada, T., Athanasopoulos, T., Foster, H., Takeda, S. and Dickson, G. (2011) 'Long-term functional adeno-associated virus-microdystrophin expression in the dystrophic CXMDj dog', *Journal of Gene Medicine*, 13(9), pp. 497-506.

Kornegay, J.N., Childers, M.K., Bogan, D.J., Bogan, J.R., Nghiem, P., Wang, J., Fan, Z., Howard, J.F., Jr., Schatzberg, S.J., Dow, J.L., Grange, R.W., Styner, M.A., Hoffman, E.P. and Wagner, K.R. (2012) 'The paradox of muscle hypertrophy in muscular dystrophy', *Phys Med Rehabil Clin N Am*, 23(1), pp. 149-72, xii.

Kuang, S., Kuroda, K., Le Grand, F. and Rudnicki, M.A. (2007) 'Asymmetric self-renewal and commitment of satellite stem cells in muscle', *Cell*, 129(5), pp. 999-1010.

Kumar, M., Keller, B., Makalou, N. and Sutton, R.E. (2001) 'Systematic determination of the packaging limit of lentiviral vectors', *Hum Gene Ther*, 12(15), pp. 1893-905.

Kunkel, L.M., Beggs, A.H. and Hoffman, E.P. (1989) 'Molecular genetics of Duchenne and Becker muscular dystrophy: emphasis on improved diagnosis', *Clin Chem*, 35(7 Suppl), pp. B21-4.

Lai, Y., Yue, Y.P., Liu, M.J., Ghosh, A., Engelhardt, J.F., Chamberlain, J.S. and Duan, D.S. (2005) 'Efficient in vivo gene expression by trans-splicing adeno-associated viral vectors', *Nature Biotechnology*, 23(11), pp. 1435-1439.

Lai, Y., Thomas, G.D., Yue, Y., Yang, H.T., Li, D., Long, C., Judge, L., Bostick, B., Chamberlain, J.S., Terjung, R.L. and Duan, D. (2009a) 'Dystrophins carrying spectrin-like repeats 16 and 17 anchor nNOS to the sarcolemma and enhance exercise performance in a mouse model of muscular dystrophy', *J Clin Invest*, 119(3), pp. 624-35.

Lai, Y., Thomas, G.D., Yue, Y.P., Yang, H.T., Li, D.J., Long, C., Bostick, B., Terjung, R.L. and Duan, D.S. (2009b) 'A Novel Mini-Dystrophin Gene Recruits nNOS to the Sarcolemma and Improves Vascular Perfusion and Exercise Performance in mdx Mice', *Molecular Therapy*, 17, pp. S359-S359.

Lai, Y., Yue, Y. and Duan, D. (2010) 'Evidence for the failure of adeno-associated virus serotype 5 to package a viral genome  $\geq 8.2$  kb', *Mol Ther*, 18(1), pp. 75-9.

Lai, Y., Zhao, J., Yue, Y. and Duan, D. (2013) ' $\alpha 2$  and  $\alpha 3$  helices of dystrophin R16 and R17 frame a microdomain in the  $\alpha 1$  helix of dystrophin R17 for neuronal NOS binding', *Proc Natl Acad Sci U S A*, 110(2), pp. 525-30.

Lalic, T., Vossen, R.H., Coffa, J., Schouten, J.P., Guc-Scekic, M., Radivojevic, D., Djuricic, M., Breuning, M.H., White, S.J. and den Dunnen, J.T. (2005) 'Deletion and duplication screening in the DMD gene using MLPA', *European Journal of Human Genetics*, 13(11), pp. 1231-1234.

Lambert, M., Chafey, P., Hugnot, J.P., Koulakoff, A., Berwald-Netter, Y., Billard, C., Morris, G.E., Kahn, A., Kaplan, J.C. and Gilgenkrantz, H. (1993) 'Expression of the transcripts initiated in the 62nd intron of the dystrophin gene', *Neuromuscul Disord*, 3(5-6), pp. 519-24.

Lander, E.S., Linton, L.M., Birren, B., Nusbaum, C., Zody, M.C., Baldwin, J., Devon, K., Dewar, K., Doyle, M., FitzHugh, W., Funke, R., Gage, D., Harris, K., Heaford, A., Howland, J., Kann, L., Lehoczky, J., LeVine, R., McEwan, P., McKernan, K., Meldrim, J., Mesirov, J.P., Miranda, C., Morris, W., Naylor, J., Raymond, C., Rosetti, M., Santos, R., Sheridan, A., Sougnez, C., Stange-Thomann, N., Stojanovic, N., Subramanian, A., Wyman, D., Rogers, J., Sulston, J., Ainscough, R., Beck, S., Bentley, D., Burton, J., Clee, C., Carter, N., Coulson, A., Deadman, R., Deloukas, P., Dunham, A., Dunham, I., Durbin, R., French, L., Grafham, D., Gregory, S., Hubbard, T., Humphray, S., Hunt, A., Jones, M., Lloyd, C., McMurray, A., Matthews, L., Mercer, S., Milne, S., Mullikin, J.C., Mungall, A., Plumb, R., Ross, M., Shownkeen, R., Sims, S., Waterston, R.H., Wilson, R.K., Hillier, L.W., McPherson, J.D., Marra, M.A., Mardis, E.R., Fulton,

L.A., Chinwalla, A.T., Pepin, K.H., Gish, W.R., Chissoe, S.L., Wendl, M.C., Delehaunty, K.D., Miner, T.L., Delehaunty, A., Kramer, J.B., Cook, L.L., Fulton, R.S., Johnson, D.L., Minx, P.J., Clifton, S.W., Hawkins, T., Branscomb, E., Predki, P., Richardson, P., Wenning, S., Slezak, T., Doggett, N., Cheng, J.F., Olsen, A., Lucas, S., Elkin, C., Uberbacher, E., Frazier, M., et al. (2001) 'Initial sequencing and analysis of the human genome', *Nature*, 409(6822), pp. 860-921.

Lane, R.J., Robinow, M. and Roses, A.D. (1983) 'The genetic status of mothers of isolated cases of Duchenne muscular dystrophy', *Journal of Medical Genetics*, 20(1), pp. 1-11.

Lapidos, K.A., Kakkar, R. and McNally, E.M. (2004) 'The dystrophin glycoprotein complex: signaling strength and integrity for the sarcolemma', *Circ Res*, 94(8), pp. 1023-31.

Le Rumeur, E., Winder, S.J. and Hubert, J.F. (2010) 'Dystrophin: more than just the sum of its parts', *Biochim Biophys Acta*, 1804(9), pp. 1713-22.

Lederfein, D., Levy, Z., Augier, N., Mornet, D., Morris, G., Fuchs, O., Yaffe, D. and Nudel, U. (1992) 'A 71-Kilodalton Protein Is a Major Product of the Duchenne Muscular-Dystrophy Gene in Brain and Other Nonmuscle Tissues', *Proceedings of the National Academy of Sciences of the United States of America*, 89(12), pp. 5346-5350.

Li, D., Yue, Y. and Duan, D. (2010a) 'Marginal level dystrophin expression improves clinical outcome in a strain of dystrophin/utrophin double knockout mice', *PLoS One*, 5(12), p. e15286.

Li, D.J., Bareja, A., Judge, L., Yue, Y.P., Lai, Y., Fairclough, R., Davies, K.E., Chamberlain, J.S. and Duan, D.S. (2010b) 'Sarcolemmal nNOS anchoring reveals a qualitative difference between dystrophin and utrophin', *Journal of Cell Science*, 123(12), pp. 2007-2012.

- Li, D., Yue, Y., Lai, Y., Hakim, C.H. and Duan, D. (2011) 'Nitrosative stress elicited by nNOSmicro delocalization inhibits muscle force in dystrophin-null mice', *J Pathol*, 223(1), pp. 88-98.
- Lim, L.E. and Campbell, K.P. (1998) 'The sarcoglycan complex in limb-girdle muscular dystrophy', *Curr Opin Neurol*, 11(5), pp. 443-52.
- Lochmuller, H., Johns, T. and Shoubbridge, E.A. (1999) 'Expression of the E6 and E7 genes of human papillomavirus (HPV16) extends the life span of human myoblasts', *Exp Cell Res*, 248(1), pp. 186-93.
- Loeb (1986). *Electromyography for Experimentalists*. Chicago; University of Chicago Press.
- Love, D.R., England, S.B., Speer, A., Marsden, R.F., Bloomfield, J.F., Roche, A.L., Cross, G.S., Mountford, R.C., Smith, T.J. and Davies, K.E. (1991a) 'Sequences of junction fragments in the deletion-prone region of the dystrophin gene', *Genomics*, 10(1), pp. 57-67.
- Love, D.R., Flint, T.J., Genet, S.A., Middletonprice, H.R. and Davies, K.E. (1991b) 'Becker Muscular-Dystrophy Patient with a Large Intragenic Dystrophin Deletion - Implications for Functional Minigenes and Gene-Therapy', *Journal of Medical Genetics*, 28(12), pp. 860-864.
- Lu, Q.L., Cirak, S. and Partridge, T. (2014) 'What Can We Learn From Clinical Trials of Exon Skipping for DMD?', *Molecular Therapy-Nucleic Acids*, 3.
- Luz, M.A.M., Marques, M.J. and Neto, H.S. (2002) 'Impaired regeneration of dystrophin-deficient muscle fibers is caused by exhaustion of myogenic cells', *Brazilian Journal of Medical and Biological Research*, 35(6), pp. 691-695.
- Macasai, C.E., Derrick-Roberts, A.L., Ding, X., Zarrinkalam, K.H., McIntyre, C., Anderson, P.H., Anson, D.S. and Byers, S. (2012) 'Skeletal response to lentiviral mediated gene therapy in a mouse model of MPS VII', *Mol Genet Metab*, 106(2), pp. 202-13.

Malik, V., Rodino-Klapac, L.R., Viollet, L., Wall, C., King, W., Al-Dahhak, R., Lewis, S., Shilling, C.J., Kota, J., Serrano-Munuera, C., Hayes, J., Mahan, J.D., Campbell, K.J., Banwell, B., Dasouki, M., Watts, V., Sivakumar, K., Bien-Willner, R., Flanigan, K.M., Sahenk, Z., Barohn, R.J., Walker, C.M. and Mendell, J.R. (2010) 'Gentamicin-Induced Readthrough of Stop Codons in Duchenne Muscular Dystrophy', *Annals of Neurology*, 67(6), pp. 771-780.

Mamchaoui, K., Trollet, C., Bigot, A., Negroni, E., Chaouch, S., Wolff, A., Kandalla, P.K., Marie, S., Di Santo, J., St Guily, J.L., Muntoni, F., Kim, J., Philippi, S., Spuler, S., Levy, N., Blumen, S.C., Voit, T., Wright, W.E., Aamiri, A., Butler-Browne, G. and Mouly, V. (2011) 'Immortalized pathological human myoblasts: towards a universal tool for the study of neuromuscular disorders', *Skelet Muscle*, 1, p. 34.

Mann, C.J., Honeyman, K., Cheng, A.J., Ly, T., Lloyd, F., Fletcher, S., Morgan, J.E., Partridge, T.A. and Wilton, S.D. (2001) 'Antisense-induced exon skipping and synthesis of dystrophin in the mdx mouse', *Proc Natl Acad Sci U S A*, 98(1), pp. 42-7.

Manzur, A.Y., Kinali, M. and Muntoni, F. (2008) 'Update on the management of Duchenne muscular dystrophy', *Arch Dis Child*, 93(11), pp. 986-90.

Martin, F.C., Hiller, M., Spitali, P., Oonk, S., Dalebout, H., Palmblad, M., Chaouch, A., Guglieri, M., Straub, V., Lochmuller, H., Niks, E.H., Verschuuren, J.J.G.M., Aartsma-Rus, A., Deelder, A.M., van der Burgt, Y.E.M. and 't Hoen, P.A.C. (2014) 'Fibronectin is a serum biomarker for Duchenne muscular dystrophy', *Proteomics Clinical Applications*, 8(3-4), pp. 269-278.

Massa, R., Silvestri, G., Zeng, Y.C., Martorana, A., Sancesario, G. and Bernardi, G. (1997) 'Muscle regeneration in mdx mice: Resistance to repeated necrosis is compatible with myofiber maturity', *Basic and Applied Myology*, 7(6), pp. 387-394.

McMahon, J.M., Signori, E., Wells, K.E., Fazio, V.M. and Wells, D.J. (2001) 'Optimisation of electrotransfer of plasmid into skeletal muscle by pretreatment with hyaluronidase - increased expression with reduced muscle damage', *Gene Therapy*, 8(16), pp. 1264-1270.

Mendell, J.R., Campbell, K., Rodino-Klapac, L., Sahenk, Z., Shilling, C., Lewis, S., Bowles, D., Gray, S., Li, C., Galloway, G., Malik, V., Coley, B., Clark, K.R., Li, J., Xiao, X., Samulski, J., McPhee, S.W., Samulski, R.J. and Walker, C.M. (2010) 'Dystrophin immunity in Duchenne's muscular dystrophy', *N Engl J Med*, 363(15), pp. 1429-37.

Mendell, J.R., Shilling, C., Leslie, N.D., Flanigan, K.M., al-Dahhak, R., Gastier-Foster, J., Kneile, K., Dunn, D.M., Duval, B., Aoyagi, A., Hamil, C., Mahmoud, M., Roush, K., Bird, L., Rankin, C., Lilly, H., Street, N., Chandrasekar, R. and Weiss, R.B. (2012) 'Evidence-based path to newborn screening for Duchenne muscular dystrophy', *Ann Neurol*, 71(3), pp. 304-13.

Mendell, J.R., Rodino-Klapac, L.R., Sahenk, Z., Roush, K., Bird, L., Lowes, L.P., Alfano, L., Gomez, A.M., Lewis, S., Kota, J., Malik, V., Shontz, K., Walker, C.M., Flanigan, K.M., Corridore, M., Kean, J.R., Allen, H.D., Shilling, C., Melia, K.R., Sazani, P., Saoud, J.B., Kaye, E.M. and Eteplirsen Study, G. (2013) 'Eteplirsen for the treatment of Duchenne muscular dystrophy', *Ann Neurol*, 74(5), pp. 637-47.

Meng, X., Deng, C.S., Wang, Q.X., Wang, T.X. and Liu, W.X. (2012) '[Expression and significance of pericytes and TGF-beta in infantile parotid hemangioma]', *Shanghai Kou Qiang Yi Xue*, 21(6), pp. 687-90.

Meng, J., Chun, S., Asfahani, R., Lochmuller, H., Muntoni, F. and Morgan, J. (2014) 'Human skeletal muscle-derived CD133(+) cells form functional satellite cells after intramuscular transplantation in immunodeficient host mice', *Mol Ther*, 22(5), pp. 1008-17.

Mercuri, E. and Muntoni, F. (2013) 'Muscular dystrophies', *Lancet*, 381(9869), pp. 845-60.

Meregalli, M., Farini, A. and Torrente, Y. (2008) 'Combining stem cells and exon skipping strategy to treat muscular dystrophy', *Expert Opinion on Biological Therapy*, 8(8), pp. 1051-1061.

Mirza, A., Sagathevan, M., Sahni, N., Choi, L. and Menhart, N. (2010) 'A biophysical map of the dystrophin rod', *Biochim Biophys Acta*, 1804(9), pp. 1796-809.

Mitropant, C., Fletcher, S. and Wilton, S.D. (2009) 'Personalised genetic intervention for Duchenne muscular dystrophy: antisense oligomers and exon skipping', *Curr Mol Pharmacol*, 2(1), pp. 110-21.

Molnar, M.J., Gilbert, R., Lu, Y., Liu, A.B., Guo, A., Larochelle, N., Orlopp, K., Lochmuller, H., Petrof, B.J., Nalbantoglu, J. and Karpati, G. (2004) 'Factors influencing the efficacy, longevity, and safety of electroporation-assisted plasmid-based gene transfer into mouse muscles', *Mol Ther*, 10(3), pp. 447-55.

Monaco, A.P., Neve, R.L., Collettifeneer, C., Bertelson, C.J., Kurnit, D.M. and Kunkel, L.M. (1986) 'Isolation of Candidate Cdnas for Portions of the Duchenne Muscular-Dystrophy Gene', *Nature*, 323(6089), pp. 646-650.

Monaco, A.P., Bertelson, C.J., Liechti-Gallati, S., Moser, H. and Kunkel, L.M. (1988) 'An Explanation for the Phenotypic Differences between Patients Bearing Partial Deletions of the DMD Locus', *Genomics*, 2(1), pp. 90-95.

Monaco, A.P. (1989) 'Dystrophin, the protein product of the Duchenne/Becker muscular dystrophy gene', *Trends Biochem Sci*, 14(10), pp. 412-5.

Montarras, D., Morgan, J., Collins, C., Relaix, F., Zaffran, S., Cumano, A., Partridge, T. and Buckingham, M. (2005) 'Direct isolation of satellite cells for skeletal muscle regeneration', *Science*, 309(5743), pp. 2064-2067.

Moore, S.A., Saito, F., Chen, J.G., Michele, D.E., Henry, M.D., Messing, A., Cohn, R.D., Ross-Barta, S.E., Westra, S., Williamson, R.A., Hoshi, T. and

- Campbell, K.P. (2002) 'Deletion of brain dystroglycan recapitulates aspects of congenital muscular dystrophy', *Nature*, 418(6896), pp. 422-425.
- Moore, C.J. and Winder, S.J. (2010) 'Dystroglycan versatility in cell adhesion: a tale of multiple motifs', *Cell Commun Signal*, 8, p. 3.
- Morgan, J.E., Beauchamp, J.R., Pagel, C.N., Peckham, M., Ataliotis, P., Jat, P.S., Noble, M.D., Farmer, K. and Partridge, T.A. (1994) 'Myogenic cell lines derived from transgenic mice carrying a thermolabile T antigen: a model system for the derivation of tissue-specific and mutation-specific cell lines', *Dev Biol*, 162(2), pp. 486-98.
- Moyle, L.A. and Zammit, P.S. (2014) 'Isolation, culture and immunostaining of skeletal muscle fibres to study myogenic progression in satellite cells', *Methods Mol Biol*, 1210, pp. 63-78.
- Muir, L.A. and Chamberlain, J.S. (2009) 'Emerging strategies for cell and gene therapy of the muscular dystrophies', *Expert Rev Mol Med*, 11, p. e18.
- Muntoni, F., Torelli, S. and Ferlini, A. (2003) 'Dystrophin and mutations: one gene, several proteins, multiple phenotypes', *Lancet Neurology*, 2(12), pp. 731-740.
- Muntoni, F. and Voit, T. (2004) 'The congenital muscular dystrophies in 2004: a century of exciting progress', *Neuromuscular Disorders*, 14(10), pp. 635-649.
- Nakamura, A. and Takeda, S. (2011) 'Mammalian Models of Duchenne Muscular Dystrophy: Pathological Characteristics and Therapeutic Applications', *Journal of Biomedicine and Biotechnology*.
- Naldini, L., Blomer, U., Gallay, P., Ory, D., Mulligan, R., Gage, F.H., Verma, I.M. and Trono, D. (1996) 'In vivo gene delivery and stable transduction of nondividing cells by a lentiviral vector', *Science*, 272(5259), pp. 263-7.

Nawrotzki, R., Loh, N.Y., Ruegg, M.A., Davies, K.E. and Blake, D.J. (1998) 'Characterisation of alpha-dystrobrevin in muscle', *J Cell Sci*, 111 ( Pt 17), pp. 2595-605.

Neri, M., Torelli, S., Brown, S., Ugo, I., Sabatelli, P., Merlini, L., Spitali, P., Rimessi, P., Gualandi, F., Sewry, C., Ferlini, A. and Muntoni, F. (2007) 'Dystrophin levels as low as 30% are sufficient to avoid muscular dystrophy in the human', *Neuromuscul Disord*, 17(11-12), pp. 913-8.

Nicholson, L.V., Johnson, M.A., Gardner-Medwin, D., Bhattacharya, S. and Harris, J.B. (1990) 'Heterogeneity of dystrophin expression in patients with Duchenne and Becker muscular dystrophy', *Acta Neuropathol*, 80(3), pp. 239-50.

Nicholson, L.V., Johnson, M.A., Bushby, K.M. and Gardner-Medwin, D. (1993) 'Functional significance of dystrophin positive fibres in Duchenne muscular dystrophy', *Arch Dis Child*, 68(5), pp. 632-6.

Nigro, V. (2003) 'Molecular bases of autosomal recessive limb-girdle muscular dystrophies', *Acta Myol*, 22(2), pp. 35-42.

Nowak, K.J. and Davies, K.E. (2004) 'Duchenne muscular dystrophy and dystrophin: pathogenesis and opportunities for treatment', *EMBO Rep*, 5(9), pp. 872-6.

Odom, G.L., Gregorevic, P. and Chamberlain, J.S. (2007) 'Viral-mediated gene therapy for the muscular dystrophies: successes, limitations and recent advances', *Biochim Biophys Acta*, 1772(2), pp. 243-62.

Odom, G.L., Gregorevic, P., Allen, J.M. and Chamberlain, J.S. (2011) 'Gene Therapy of mdx Mice With Large Truncated Dystrophins Generated by Recombination Using rAAV6', *Molecular Therapy*, 19(1), pp. 36-45.

Okada, T. and Takeda, S. (2013) 'Current Challenges and Future Directions in Recombinant AAV-Mediated Gene Therapy of Duchenne Muscular Dystrophy', *Pharmaceuticals (Basel)*, 6(7), pp. 813-36.

Park, K.S. and Oh, D. (2010) 'Gene therapy for muscular dystrophies: progress and challenges', *J Clin Neurol*, 6(3), pp. 111-6.

Parker, M.H., Kuhr, C., Wang, Z.J., Tapscott, S.J. and Storb, R. (2009) 'Hematopoietic Cell Transplantation Provides an Immune-tolerant Platform for Myoblast Transplantation in Dystrophic Dogs (vol 16, pg 1340, 2008)', *Molecular Therapy*, 17(2), pp. 396-396.

Pasquesi, J.J., Schlachter, S.C., Boppart, M.D., Chaney, E., Kaufman, S.J. and Boppart, S.A. (2006) 'In vivo detection of exercise-induced ultrastructural changes in genetically-altered murine skeletal muscle using polarization-sensitive optical coherence tomography', *Optics Express*, 14(4), pp. 1547-1556.

Passos-Bueno, M.R., Vainzof, M., Marie, S.K. and Zatz, M. (1994) 'Half the dystrophin gene is apparently enough for a mild clinical course: confirmation of its potential use for gene therapy', *Hum Mol Genet*, 3(6), pp. 919-22.

Pastoret, C. and Sebillé, A. (1995) 'Mdx Mice Show Progressive Weakness and Muscle Deterioration with Age', *Journal of the Neurological Sciences*, 129(2), pp. 97-105.

Peachey, L.E. (1985) *Excitation-contraction coupling: The link between the surface and the interior of a muscle cell*. Cambridge, Great Britain: Journal of Experimental Biology.

Perlingeiro, R.C.R., Darabi, R., Gehlbach, K., Bachoo, R.M., Kamath, S., Osawa, M., Kamm, K.E. and Kyba, M. (2008) 'Functional skeletal muscle regeneration from differentiating embryonic stem cells', *Nature Medicine*, 14(2), pp. 134-143.

- Pertl, C., Eblenkamp, M., Pertl, A., Pfeifer, S., Wintermantel, E., Lochmuller, H., Walter, M.C., Krause, S. and Thirion, C. (2013) 'A new web-based method for automated analysis of muscle histology', *Bmc Musculoskeletal Disorders*, 14.
- Phelps, S.F., Hauser, M.A., Cole, N.M., Rafael, J.A., Hinkle, R.T., Faulkner, J.A. and Chamberlain, J.S. (1995) 'Expression of full-length and truncated dystrophin mini-genes in transgenic mdx mice', *Hum Mol Genet*, 4(8), pp.1251-8.
- Pigozzo, S.R., Da Re, L., Romualdi, C., Mazzara, P.G., Galletta, E., Fletcher, S., Wilton, S.D. and Vitiello, L. (2013) 'Revertant fibers in the mdx murine model of Duchenne muscular dystrophy: an age- and muscle-related reappraisal', *PLoS One*, 8(8), p. e72147.
- Poon, E., Howman, E.V., Newey, S.E. and Davies, K.E. (2002) 'Association of syncoilin and desmin: linking intermediate filament proteins to the dystrophin-associated protein complex', *J Biol Chem*, 277(5), pp. 3433-9.
- Porter, J.D., Khanna, S., Kaminski, H.J., Rao, J.S., Merriam, A.P., Richmonds, C.R., Leahy, P., Li, J., Guo, W. and Andrade, F.H. (2002) 'A chronic inflammatory response dominates the skeletal muscle molecular signature in dystrophin-deficient mdx mice', *Hum Mol Genet*, 11(3), pp. 263-72.
- Price, F.D., Kuroda, K. and Rudnicki, M.A. (2007) 'Stem cell based therapies to treat muscular dystrophy', *Biochim Biophys Acta*, 1772(2), pp. 272-83.
- Prior, T.W. and Bridgeman, S.J. (2005) 'Experience and strategy for the molecular testing of Duchenne muscular dystrophy', *J Mol Diagn*, 7(3), pp. 317-26.
- Rafael, J.A., Cox, G.A., Corrado, K., Jung, D., Campbell, K.P. and Chamberlain, J.S. (1996) 'Forced expression of dystrophin deletion constructs reveals structure-function correlations', *J Cell Biol*, 134(1), pp. 93-102.

Rahimov, F. and Kunkel, L.M. (2013a) 'The cell biology of disease: cellular and molecular mechanisms underlying muscular dystrophy', *J Cell Biol*, 201(4), pp. 499-510.

Rahimov, F. and Kunkel, L.M. (2013b) 'Cellular and molecular mechanisms underlying muscular dystrophy', *Journal of Cell Biology*, 201(4), pp. 499-510.

Rando, T.A. (2001) 'The dystrophin-glycoprotein complex, cellular signaling, and the regulation of cell survival in the muscular dystrophies', *Muscle Nerve*, 24(12), pp. 1575-94.

Roberts, R.G., Gardner, R.J. and Bobrow, M. (1994) 'Searching for the 1 in 2,400,000 - a Review of Dystrophin Gene Point Mutations', *Human Mutation*, 4(1), pp. 1-11.

Rodino-Klapac, L.R., Janssen, P.M., Shontz, K.M., Canan, B., Montgomery, C.L., Griffin, D., Heller, K., Schmelzer, L., Handy, C., Clark, K.R., Sahenk, Z., Mendell, J.R. and Kaspar, B.K. (2013) 'Micro-dystrophin and follistatin co-delivery restores muscle function in aged DMD model', *Hum Mol Genet*, 22(24), pp. 4929-37.

Romitti, P., Puzhankara, S., Mathews, K., Zamba, G., Cunniff, C., Andrews, J., Matthews, D., James, K., Miller, L., Druschel, C., Fox, D., Pandya, S., Ciafaloni, E., Adams, M., Mandel, D., Street, N., Ouyang, L., Constantin, C. and Costa, P. (2009) 'Prevalence of Duchenne/Becker Muscular Dystrophy Among Males Aged 5-24 Years-Four States, 2007 (Reprinted from MMWR, vol 58, pg 1119-1122, 2009)', *Jama-Journal of the American Medical Association*, 302(23), pp. 2539-+.

Rybakova, I.N., Amann, K.J. and Ervasti, J.M. (1996) 'A new model for the interaction of dystrophin with F-actin', *J Cell Biol*, 135(3), pp. 661-72.

Sacco, A., Doyonnas, R., Kraft, P., Vitorovic, S. and Blau, H.M. (2008) 'Self-renewal and expansion of single transplanted muscle stem cells', *Nature*, 456(7221), pp. 502-6.

Sacco, A., Mourkioti, F., Tran, R., Choi, J., Llewellyn, M., Kraft, P., Shkreli, M., Delp, S., Pomerantz, J.H., Artandi, S.E. and Blau, H.M. (2010) 'Short telomeres and stem cell exhaustion model Duchenne muscular dystrophy in mdx/mTR mice', *Cell*, 143(7), pp. 1059-71.

Sadoulet-Puccio, H.M. and Kunkel, L.M. (1996) 'Dystrophin and its isoforms', *Brain Pathology*, 6(1), pp. 25-35.

Sampaolesi, M., Blot, S., D'Antona, G., Granger, N., Tonlorenzi, R., Innocenzi, A., Mognol, P., Thibaud, J.L., Galvez, B.G., Barthelemy, I., Perani, L., Mantero, S., Guttinger, M., Pansarasa, O., Rinaldi, C., Cusella De Angelis, M.G., Torrente, Y., Bordignon, C., Bottinelli, R. and Cossu, G. (2006) 'Mesoangioblast stem cells ameliorate muscle function in dystrophic dogs', *Nature*, 444(7119), pp. 574-9.

Sander, M., Chavoshan, B., Harris, S.A., Iannaccone, S.T., Stull, J.T., Thomas, G.D. and Victor, R.G. (2000) 'Functional muscle ischemia in neuronal nitric oxide synthase-deficient skeletal muscle of children with Duchenne muscular dystrophy', *Proc Natl Acad Sci U S A*, 97(25), pp. 13818-23.

Sandona, D. and Betto, R. (2009) 'Sarcoglycanopathies: molecular pathogenesis and therapeutic prospects', *Expert Rev Mol Med*, 11, p. e28.

Sarkis, J., Hubert, J.F., Legrand, B., Robert, E., Cheron, A., Jardin, J., Hitti, E., Le Rumeur, E. and Vie, V. (2011) 'Spectrin-like repeats 11-15 of human dystrophin show adaptations to a lipidic environment', *J Biol Chem*, 286(35), pp. 30481-91.

Schatzberg, S.J., Anderson, L.V., Wilton, S.D., Kornegay, J.N., Mann, C.J., Solomon, G.G. and Sharp, N.J. (1998) 'Alternative dystrophin gene transcripts in golden retriever muscular dystrophy', *Muscle Nerve*, 21(8), pp. 991-8.

Schatzberg, S.J., Olby, N.J., Breen, M., Anderson, L.V., Langford, C.F., Dickens, H.F., Wilton, S.D., Zeiss, C.J., Binns, M.M., Kornegay, J.N., Morris, G.E. and

Sharp, N.J. (1999) 'Molecular analysis of a spontaneous dystrophin 'knockout' dog', *Neuromuscul Disord*, 9(5), pp. 289-95.

Schiebler, W.S., AND K. ZILLES ( 1999). *Anatomie*. Springer-Verlag.

Schultz, B.R. and Chamberlain, J.S. (2008) 'Recombinant adeno-associated virus transduction and integration', *Mol Ther*, 16(7), pp. 1189-99.

Scott, J.M., Li, S., Harper, S.Q., Welikson, R., Bourque, D., DelloRusso, C., Hauschka, S.D. and Chamberlain, J.S. (2002) 'Viral vectors for gene transfer of micro-, mini-, or full-length dystrophin', *Neuromuscul Disord*, 12 Suppl 1, pp. S23-9.

Seto, J.T., Bengtsson, N.E. and Chamberlain, J.S. (2014) 'Therapy of Genetic Disorders-Novel Therapies for Duchenne Muscular Dystrophy', *Curr Pediatr Rep*, 2(2), pp. 102-112.

Shimatsu, Y., Katagiri, K., Furuta, T., Nakura, M., Tanioka, Y., Yuasa, K., Tomohiro, M., Kornegay, J.N., Nonaka, I. and Takeda, S. (2003) 'Canine X-linked muscular dystrophy in Japan (CXMDJ)', *Exp Anim*, 52(2), pp. 93-7.

Shunchang, S., Haitao, C., Weidong, C., Jingbo, H. and Yunsheng, P. (2008) 'Expression of truncated dystrophin cDNAs mediated by a lentiviral vector', *Neurol India*, 56(1), pp. 52-6.

Sicinski, P., Geng, Y., Ryder-Cook, A.S., Barnard, E.A., Darlison, M.G. and Barnard, P.J. (1989) 'The molecular basis of muscular dystrophy in the mdx mouse: a point mutation', *Science*, 244(4912), pp. 1578-80.

Sinn, P.L., Sauter, S.L. and McCray, P.B., Jr. (2005) 'Gene therapy progress and prospects: development of improved lentiviral and retroviral vectors-design, biosafety, and production', *Gene Ther*, 12(14), pp. 1089-98.

Skuk, D., Goulet, M., Roy, B., Piette, V., Cote, C.H., Chapdelaine, P., Hogrel, J.Y., Paradis, M., Bouchard, J.P., Sylvain, M., Lachance, J.G. and Tremblay, J.P. (2007) 'First test of a "high-density injection" protocol for myogenic cell

transplantation throughout large volumes of muscles in a Duchenne muscular dystrophy patient: eighteen months follow-up', *Neuromuscul Disord*, 17(1), pp. 38-46.

Skuk, D., Goulet, M. and Tremblay, J.P. (2014) 'Intramuscular transplantation of myogenic cells in primates: importance of needle size, cell number, and injection volume', *Cell Transplant*, 23(1), pp. 13-25.

Stamler, J.S. and Meissner, G. (2001) 'Physiology of nitric oxide in skeletal muscle', *Physiol Rev*, 81(1), pp. 209-237.

Straub, V., Rafael, J.A., Chamberlain, J.S. and Campbell, K.P. (1997) 'Animal models for muscular dystrophy show different patterns of sarcolemmal disruption', *J Cell Biol*, 139(2), pp. 375-85.

Sun, H., Yang, F., Chu, W., Zhao, H., McMahon, C. and Li, C. (2012) 'Lentiviral-mediated RNAi knockdown of Cbfa1 gene inhibits endochondral ossification of antler stem cells in micromass culture', *PLoS One*, 7(10), p. e47367.

Sun, J.Y., Anand-Jawa, V., Chatterjee, S. and Wong, K.K. (2003) 'Immune responses to adeno-associated virus and its recombinant vectors', *Gene Ther*, 10(11), pp. 964-76.

Suzuki, A., Yoshida, M., Yamamoto, H. and Ozawa, E. (1992) 'Glycoprotein-Binding Site of Dystrophin Is Confined to the Cysteine-Rich Domain and the 1st-Half of the Carboxy-Terminal Domain', *Febs Letters*, 308(2), pp. 154-160.

Sweeney, H.L. and Barton, E.R. (2000) 'The dystrophin-associated glycoprotein complex: what parts can you do without?', *Proc Natl Acad Sci U S A*, 97(25), pp. 13464-6.

Tai, P.W., Fisher-Aylor, K.I., Himeda, C.L., Smith, C.L., Mackenzie, A.P., Heltterline, D.L., Angello, J.C., Welikson, R.E., Wold, B.J. and Hauschka, S.D. (2011) 'Differentiation and fiber type-specific activity of a muscle creatine kinase intronic enhancer', *Skelet Muscle*, 1, p. 25.

Talbot, G.E., Waddington, S.N., Bales, O., Tchen, R.C. and Antoniou, M.N. (2010) 'Desmin-regulated lentiviral vectors for skeletal muscle gene transfer', *Mol Ther*, 18(3), pp. 601-8.

Tanganyika-de Winter, C.L., Heemskerk, H., Karnaoukh, T.G., van Putten, M., de Kimpe, S.J., van Deutekom, J. and Aartsma-Rus, A. (2012) 'Long-term Exon Skipping Studies With 2'-O-Methyl Phosphorothioate Antisense Oligonucleotides in Dystrophic Mouse Models', *Mol Ther Nucleic Acids*, 1, p. e44.

Taylor, L.E., Kaminoh, Y.J., Rodesch, C.K. and Flanigan, K.M. (2012) 'Quantification of dystrophin immunofluorescence in dystrophinopathy muscle specimens', *Neuropathol Appl Neurobiol*, 38(6), pp. 591-601.

Tennyson, C.N., Dally, G.Y., Ray, P.N. and Worton, R.G. (1996) 'Expression of the dystrophin isoform Dp71 in differentiating human fetal myogenic cultures', *Hum Mol Genet*, 5(10), pp. 1559-66.

Thomas, G.D., Lai, Y. and Duan, D.S. (2009) 'Restoration of sarcolemmal nNOS is essential to normalize alpha-adrenoceptor control of muscle blood flow in transgenic mdx mice', *Faseb Journal*, 23.

Thomas, G.D., Sander, M., Lau, K.S., Huang, P.L., Stull, J.T. and Victor, R.G. (1998) 'Impaired metabolic modulation of alpha-adrenergic vasoconstriction in dystrophin-deficient skeletal muscle', *Proc Natl Acad Sci U S A*, 95(25), pp. 15090-5.

Thomas, G.D., Shaul, P.W., Yuhanna, I.S., Froehner, S.C. and Adams, M.E. (2003) 'Vasomodulation by skeletal muscle-derived nitric oxide requires alpha-syntrophin-mediated sarcolemmal localization of neuronal Nitric oxide synthase', *Circ Res*, 92(5), pp. 554-60.

Tinsley, J.M., Blake, D.J., Roche, A., Fairbrother, U., Riss, J., Byth, B.C., Knight, A.E., Kendrick-Jones, J., Suthers, G.K., Love, D.R. and et al. (1992) 'Primary structure of dystrophin-related protein', *Nature*, 360(6404), pp. 591-3.

Tinsley, J.M., Potter, A.C., Phelps, S.R., Fisher, R., Trickett, J.I. and Davies, K.E. (1996) 'Amelioration of the dystrophic phenotype of mdx mice using a truncated utrophin transgene', *Nature*, 384(6607), pp. 349-53.

Tochio, H., Zhang, Q., Mandal, P., Li, M. and Zhang, M. (1999) 'Solution structure of the extended neuronal nitric oxide synthase PDZ domain complexed with an associated peptide', *Nat Struct Biol*, 6(5), pp. 417-21.

Torrente, Y., Belicchi, M., Marchesi, C., Dantona, G., Cogiamanian, F., Pisati, F., Gavina, M., Giordano, R., Tonlorenzi, R., Fagiolari, G., Lamperti, C., Porretti, L., Lopa, R., Sampaolesi, M., Vicentini, L., Grimoldi, N., Tiberio, F., Songa, V., Baratta, P., Prella, A., Forzenigo, L., Guglieri, M., Pansarasa, O., Rinaldi, C., Mouly, V., Butler-Browne, G.S., Comi, G.P., Biondetti, P., Moggio, M., Gaini, S.M., Stocchetti, N., Priori, A., D'Angelo, M.G., Turconi, A., Bottinelli, R., Cossu, G., Rebull, P. and Bresolin, N. (2007) 'Autologous transplantation of muscle-derived CD133+ stem cells in Duchenne muscle patients', *Cell Transplant*, 16(6), pp. 563-77.

Townsend, D. (2014) 'Finding the sweet spot: assembly and glycosylation of the dystrophin-associated glycoprotein complex', *Anat Rec (Hoboken)*, 297(9), pp. 1694-705.

Tremblay, J.P. and Frederickson, R.M. (2011) 'Gene Transfer Using HACs: A Key Step Closer to Ex Vivo Gene Therapy Using Autologous Gene-Corrected Cells to Treat Muscular Dystrophy', *Molecular Therapy*, 19(12), pp. 2111-2113.

Turk, R., Sterrenburg, E., de Meijer, E.J., van Ommen, G.J., den Dunnen, J.T. and t Hoen, P.A. (2005) 'Muscle regeneration in dystrophin-deficient mdx mice studied by gene expression profiling', *BMC Genomics*, 6, p. 98.

Valdes, R., Jr. and Jortani, S.A. (1999) 'Standardizing utilization of biomarkers in diagnosis and management of acute cardiac syndromes', *Clin Chim Acta*, 284(2), pp. 135-40.

Valentine, B.A., Cooper, B.J., de Lahunta, A., O'Quinn, R. and Blue, J.T. (1988) 'Canine X-linked muscular dystrophy. An animal model of Duchenne muscular dystrophy: clinical studies', *J Neurol Sci*, 88(1-3), pp. 69-81.

van der Plas, M.C., Pilgram, G.S.K., Plomp, J.J., de Jong, A., Fradkin, L.G. and Noordermeer, J.N. (2006) 'Dystrophin is required for appropriate retrograde control of neurotransmitter release at the Drosophila neuromuscular junction', *Journal of Neuroscience*, 26(1), pp. 333-344.

van Essen, A.J., Busch, H.F., te Meerman, G.J. and ten Kate, L.P. (1992) 'Birth and population prevalence of Duchenne muscular dystrophy in The Netherlands', *Human Genetics*, 88(3), pp. 258-66.

van Putten, M., Hulsker, M.A., van Heiningen, S.H., Nadarajah, V.D., 't Hoen, P.A.C., van Ommen, G.J.B. and Aartsma-Rus, A.M. (2011) 'Low dystrophin levels improve life expectancy, phenotype and functional performance in the mdx/utrn  $-/-$  mouse', *Neuromuscular Disorders*, 21(9-10), pp. 648-648.

van Putten, M., Hulsker, M., Nadarajah, V.D., van Heiningen, S.H., van Huizen, E., van Iterson, M., Admiraal, P., Messemaker, T., den Dunnen, J.T., 't Hoen, P.A.C. and Aartsma-Rus, A. (2012) 'The Effects of Low Levels of Dystrophin on Mouse Muscle Function and Pathology', *Plos One*, 7(2).

van Putten, M., Hulsker, M., Young, C., Nadarajah, V.D., Heemskerk, H., van der Weerd, L., 't Hoen, P.A.C., van Ommen, G.J.B. and Aartsma-Rus, A.M. (2013) 'Low dystrophin levels increase survival and improve muscle pathology and function in dystrophin/utrophin double-knockout mice', *Faseb Journal*, 27(6), pp. 2484-2495.

van Putten, M., van der Pijl, E.M., Hulsker, M., Verhaart, I.E.C., Nadarajah, V.D., van der Weerd, L. and Aartsma-Rus, A. (2014) 'Low dystrophin levels in heart

can delay heart failure in mdx mice', *Journal of Molecular and Cellular Cardiology*, 69, pp. 17-23.

van Ruiten, H.J., Straub, V., Bushby, K. and Guglieri, M. (2014) 'Improving recognition of Duchenne muscular dystrophy: a retrospective case note review', *Arch Dis Child*.

Voermans, N.C., Bonnemann, C.G., Huijting, P.A., Hamel, B.C., van Kuppevelt, T.H., de Haan, A., Schalkwijk, J., van Engelen, B.G. and Jenniskens, G.J. (2008) 'Clinical and molecular overlap between myopathies and inherited connective tissue diseases', *Neuromuscular Disorders*, 18(11), pp. 843-856.

Vos, J.H., van der Linde-Sipman, J.S. and Goedegebuure, S.A. (1986) 'Dystrophy-like myopathy in the cat', *J Comp Pathol*, 96(3), pp. 335-41.

Wang, B., Li, J. and Xiao, X. (2000) 'Adeno-associated virus vector carrying human minidystrophin genes effectively ameliorates muscular dystrophy in mdx mouse model', *Proc Natl Acad Sci U S A*, 97(25), pp. 13714-9.

Wang, B., Li, J., Fu, F.H. and Xiao, X. (2009a) 'Systemic human minidystrophin gene transfer improves functions and life span of dystrophin and dystrophin/utrophin-deficient mice', *J Orthop Res*, 27(4), pp. 421-6.

Wang, Z., Chamberlain, J.S., Tapscott, S.J. and Storb, R. (2009b) 'Gene therapy in large animal models of muscular dystrophy', *ILAR J*, 50(2), pp. 187-98.

Wang, Y.X., Marino-Enriquez, A., Bennett, R.R., Zhu, M.J., Shen, Y.P., Eilers, G., Lee, J.C., Henze, J., Fletcher, B.S., Gu, Z.Z., Fox, E.A., Antonescu, C.R., Fletcher, C.D.M., Guo, X.Q., Raut, C.P., Demetri, G.D., van de Rijn, M., Ordog, T., Kunkel, L.M. and Fletcher, J.A. (2014) 'Dystrophin is a tumor suppressor in human cancers with myogenic programs', *Nature Genetics*, 46(6), pp. 601-606.

Warrington, K.H., Jr. and Herzog, R.W. (2006) 'Treatment of human disease by adeno-associated viral gene transfer', *Human Genetics*, 119(6), pp. 571-603.

Watchko, J.F., O'Day, J.L., Wang, B., Li, J. and Xiao, X. (2002) 'Functional recovery of dystrophic mouse (MDX) muscle after AAV-mini-dystrophin gene vector treatment', *Pediatric Research*, 51(4), pp. 225a-225a.

Watkins, S.C., Hoffman, E.P., Slayter, H.S. and Kunkel, L.M. (1988) 'Immunoelectron microscopic localization of dystrophin in myofibres', *Nature*, 333(6176), pp. 863-6.

Webster, C. and Blau, H.M. (1990) 'Accelerated age-related decline in replicative life-span of Duchenne muscular dystrophy myoblasts: implications for cell and gene therapy', *Somat Cell Mol Genet*, 16(6), pp. 557-65.

Welch, E.M., Barton, E.R., Zhuo, J., Tomizawa, Y., Friesen, W.J., Trifillis, P., Paushkin, S., Patel, M., Trotta, C.R., Hwang, S., Wilde, R.G., Karp, G., Takasugi, J., Chen, G., Jones, S., Ren, H., Moon, Y.C., Corson, D., Turpoff, A.A., Campbell, J.A., Conn, M.M., Khan, A., Almstead, N.G., Hedrick, J., Mollin, A., Risher, N., Weetall, M., Yeh, S., Branstrom, A.A., Colacino, J.M., Babiak, J., Ju, W.D., Hirawat, S., Northcutt, V.J., Miller, L.L., Spatrick, P., He, F., Kawana, M., Feng, H., Jacobson, A., Peltz, S.W. and Sweeney, H.L. (2007) 'PTC124 targets genetic disorders caused by nonsense mutations', *Nature*, 447(7140), pp. 87-91.

Wells, K.E., Fletcher, S., Mann, C.J., Wilton, S.D. and Wells, D.J. (2003) 'Enhanced in vivo delivery of antisense oligonucleotides to restore dystrophin expression in adult mdx mouse muscle', *FEBS Lett*, 552(2-3), pp. 145-9.

Willmann, R., De Luca, A., Benatar, M., Grounds, M., Dubach, J., Raymackers, J.M., Nagaraju, K. and Network, T.-N.N. (2012) 'Enhancing translation: guidelines for standard pre-clinical experiments in mdx mice', *Neuromuscul Disord*, 22(1), pp. 43-9.

Wilschanski, M., Miller, L.L., Shoseyov, D., Blau, H., Rivlin, J., Aviram, M., Cohen, M., Armoni, S., Yaakov, Y., Pugatsch, T., Cohen-Cymerknoh, M., Miller, N.L., Reha, A., Northcutt, V.J., Hirawat, S., Donnelly, K., Elfring, G.L.,

Ajayi, T. and Kerem, E. (2011) 'Chronic ataluren (PTC124) treatment of nonsense mutation cystic fibrosis', *Eur Respir J*, 38(1), pp. 59-69.

Wilton, S.D., Fletcher, S. and Flanigan, K.M. (2014) 'Dystrophin as a therapeutic biomarker: are we ignoring data from the past?', *Neuromuscul Disord*, 24(6), pp. 463-6.

Wright, J.F. (2008) 'Manufacturing and characterizing AAV-based vectors for use in clinical studies', *Gene Ther*, 15(11), pp. 840-8.

Wu, B., Cloer, C., Lu, P., Milazi, S., Shaban, M., Shah, S.N., Marston-Poe, L., Moulton, H.M. and Lu, Q.L. (2014) 'Exon skipping restores dystrophin expression, but fails to prevent disease progression in later stage dystrophic dko mice', *Gene Ther*, 21(9), pp. 785-93.

Xiao, X., Li, J., Tsao, Y.P., Dressman, D., Hoffman, E.P. and Watchko, J.F. (2000) 'Full functional rescue of a complete muscle (TA) in dystrophic hamsters by adeno-associated virus vector-directed gene therapy', *J Virol*, 74(3), pp. 1436-42.

Yatsenko, A.S., Kucherenko, M.M., Pantoja, M., Fischer, K.A., Madeoy, J., Deng, W.M., Schneider, M., Baumgartner, S., Akey, J., Shcherbata, H.R. and Ruohola-Baker, H. (2009) 'The conserved WW-domain binding sites in Dystroglycan C-terminus are essential but partially redundant for Dystroglycan function', *BMC Dev Biol*, 9, p. 18.

Yin, H., Moulton, H.M., Seow, Y., Boyd, C., Boutilier, J., Iverson, P. and Wood, M.J. (2008) 'Cell-penetrating peptide-conjugated antisense oligonucleotides restore systemic muscle and cardiac dystrophin expression and function', *Hum Mol Genet*, 17(24), pp. 3909-18.

Yin, W.X., Xiang, P. and Li, Q.L. (2005) 'Investigations of the effect of DNA size in transient transfection assay using dual luciferase system', *Analytical Biochemistry*, 346(2), pp. 289-294.

Yokota, T., Lu, Q.L., Morgan, J.E., Davies, K.E., Fisher, R., Takeda, S. and Partridge, T.A. (2006) 'Expansion of revertant fibers in dystrophic mdx muscles reflects activity of muscle precursor cells and serves as an index of muscle regeneration', *Journal of Cell Science*, 119(13), pp. 2679-2687.

Yokota, T., Lu, Q.L., Partridge, T., Kobayashi, M., Nakamura, A., Takeda, S. and Hoffman, E. (2009) 'Efficacy of systemic morpholino exon-skipping in Duchenne dystrophy dogs', *Ann Neurol*, 65(6), pp. 667-76.

Yokota, T., Nakamura, A., Nagata, T., Saito, T., Kobayashi, M., Aoki, Y., Echigoya, Y., Partridge, T., Hoffman, E.P. and Takeda, S. (2012) 'Extensive and prolonged restoration of dystrophin expression with vivo-morpholino-mediated multiple exon skipping in dystrophic dogs', *Nucleic Acid Ther*, 22(5), pp. 306-15.

Yoshida, Y. and Yamanaka, S. (2010) 'Recent stem cell advances: induced pluripotent stem cells for disease modeling and stem cell-based regeneration', *Circulation*, 122(1), pp. 80-7.

Yuan, Z., Qiao, C., Hu, P., Li, J. and Xiao, X. (2011) 'A versatile adeno-associated virus vector producer cell line method for scalable vector production of different serotypes', *Hum Gene Ther*, 22(5), pp. 613-24.

Yue, Y., Liu, M. and Duan, D. (2006) 'C-terminal-truncated microdystrophin recruits dystrobrevin and syntrophin to the dystrophin-associated glycoprotein complex and reduces muscular dystrophy in symptomatic utrophin/dystrophin double-knockout mice', *Mol Ther*, 14(1), pp. 79-87.

Zatz, M., Rapaport, D., Vainzof, M., Passosbueno, M.R., Bortolini, E.R., Pavanello, R.D.M. and Peres, C.A. (1991) 'Serum Creatine-Kinase (Ck) and Pyruvate-Kinase (Pk) Activities in Duchenne (Dmd) as Compared with Becker (Bmd) Muscular-Dystrophy', *Journal of the Neurological Sciences*, 102(2), pp. 190-196.

Zhang, Z., Zhang, P. and Hu, H. (2011) 'LARGE expression augments the glycosylation of glycoproteins in addition to alpha-dystroglycan conferring laminin binding', *PLoS One*, 6(4), p. e19080.

Zhang, Y.D., Yue, Y.P., Li, L., Hakim, C.H., Zhang, K.Q., Thomas, G.D. and Duan, D.S. (2013) 'Dual AAV therapy ameliorates exercise-induced muscle injury and functional ischemia in murine models of Duchenne muscular dystrophy', *Human Molecular Genetics*, 22(18), pp. 3720-3729.